Double-dynamic elastomers : combining dynamic chemistries in a repairable and recyclable material

Simon Mckie

UNIVERSITÉ DE STRASBOURG

ÉCOLE DOCTORALE 222

UPR 22

THÈSE

présentée par :

Simon McKIE

soutenue le : **27 octobre 2017**

pour obtenir le grade de : **Docteur de l'université de Strasbourg**

Discipline/ Spécialité : CHIMIE

DOUBLE-DYNAMIC ELASTOMERS: COMBINING DYNAMIC CHEMISTRIES IN A REPAIRABLE AND RECYCLABLE MATERIAL

THÈSE dirigée par :

M. GIUSEPPONE Nicolas Professeur, Université de Strasbourg, Strasbourg, France

RAPPORTEURS :

M. WALTHER Andreas Professeur, Albert-Ludwigs Universität Freiburg Freiburg, Allemagne

M. WOISEL Patrice Professeur, Université de Lille, Lille, France

---

AUTRES MEMBRES DU JURY :

M. GAUTHIER Christian Professeur, Université de Strasbourg, Strasbourg, France

M. PERRIN Rémi Docteur, Soprema, Strasbourg, France

Double-Dynamic Elastomers

Combining Dynamic Chemistries in a Repairable and Recyclable Material

Simon A. McKie

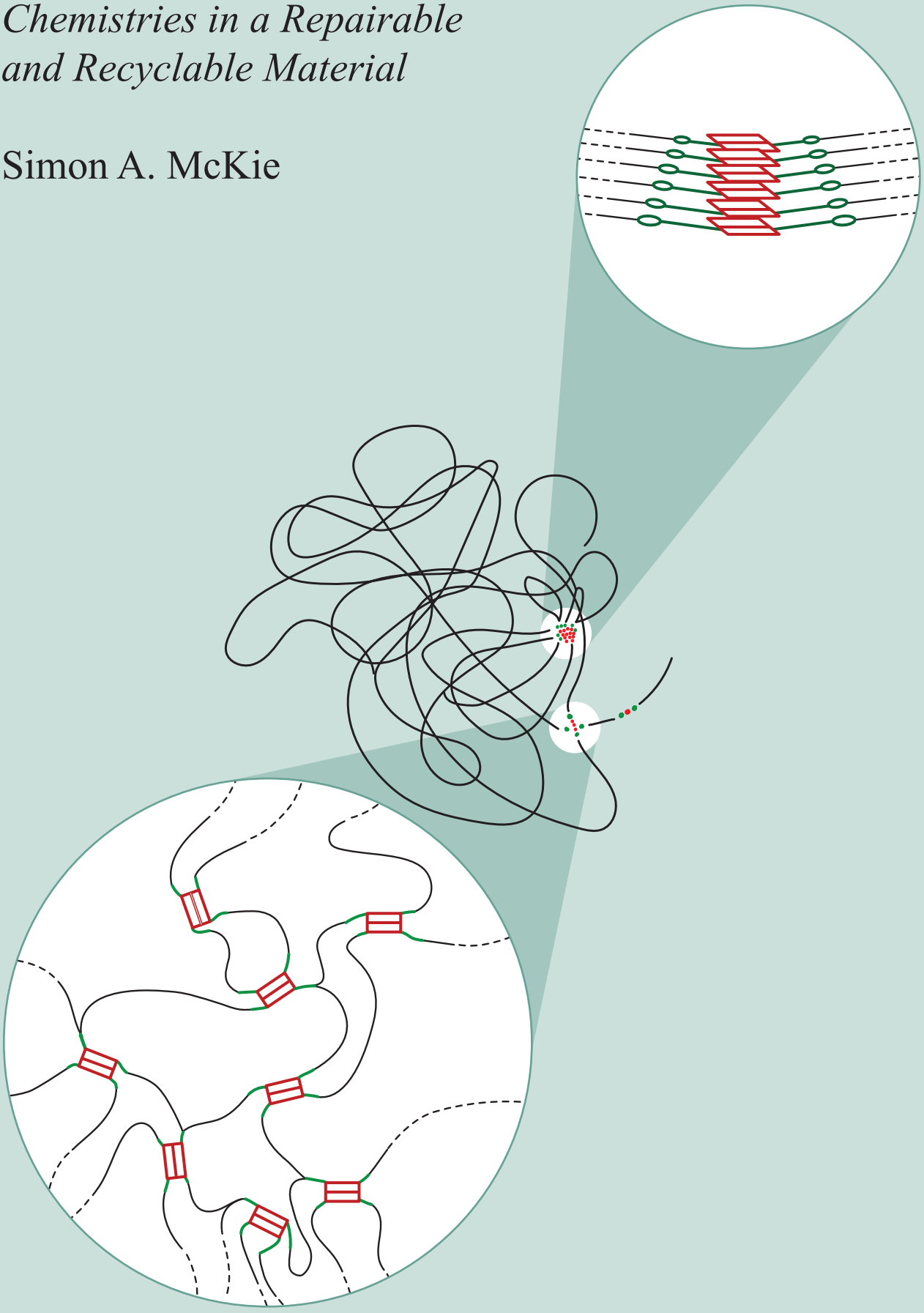

Double-Dynamic Elastomers

Combining Dynamic Chemistries in a Repairable and Recyclable Material

Simon A. McKie

Simon McKIE

DOUBLE-DYNAMIC ELASTOMERS

Résumé

Grâce à l'introduction de deux groupes chimiques dynamiques distincts dans un réseau de polymères élastomères, un matériau auto-cicatrisant et recyclable a été synthétisé et caractérisé. La polycondensation d'un polybutadiène polyamine avec une uréidopyrimidinone fonctionnalisée par deux aldéhydes, a abouti à un matériau élastique fort et extensible, composé de liaisons croisées d'imines ainsi que de dimères et d'agrégats d'uréidopyrimidinones. La caractérisation physique a montré que ce matériau à double dynamique présente un comportement caoutchouteux à température ambiante, tandis que, à des températures élevées, les chimies supramoléculaires et covalentes réversibles sont activées, ce qui entraîne des propriétés vitrimères. Pour étudier de plus près le rôle des deux fragments dynamiques, le comportement des matériaux uniquement réticulés par des interactions supramoléculaires a été exploré. Dans ces matériaux, le comportement caoutchouteux aux températures d'usage est à nouveau observé, tandis qu'un état visqueux est observé à des températures élevées. Dans tous les cas, les matériaux dynamiques se sont auto-cicatrisés lors de l'exposition à la chaleur et sont recyclables par hydrolyse acide.

Mots clés : Double-dynamique, Polymère, Supramoléculaire, Imine, Uréidopyrimidinone, Elastomère

Résumé en anglais

By the introduction of two distinct dynamic chemical groups into an elastomeric polymer network, a self-healing and soluble material was synthesised and characterised. The polycondensation of a polyamine polybutadiene with a novel dialdehyde-functionalised ureidopyrimidinone, resulted in a strong and stretchable elastic material, composed of imine cross-links as well as ureidopyrimidinone dimers and aggregates. Physical characterisation demonstrated that this double-dynamic material displays rubbery behaviour at ambient temperatures, while at elevated temperatures both supramolecular and reversible covalent chemistries are activated resulting in vitrimeric properties. To more closely investigate the role of both dynamic moieties, the behaviour of materials solely cross-linked by supramolecular interactions were studied. In these materials, rubbery behaviour at service temperatures is again observed, while viscous flow is observed at elevated temperatures. In all cases, the dynamic materials were self-healing on exposure to heat, and soluble by acid-catalysed hydrolysis.

Keywords: Double-Dynamic, Polymer, Supramolecular, Imine, Ureidopyrimidinone, Elastomer

“The best-laid schemes o’ mice an’ men
Gang aft agley,”

– To a Mouse by Robert Burns

Table of Contents

Abstract

Since the turn of the century, a field of research at the interface between thermoplastic and thermoset polymeric materials, aimed at obtaining recyclable cross-linked materials, has gained momentum. This field, Dynamic Covalent Networks (DCNs), uses stimulus-responsive dynamic chemical bonds to form polymeric networks, gaining the ability to easily change the physical behaviour of materials that had, until now, been viewed as unresponsive. Separately, but strongly related to DCNs, the targeted incorporation of supramolecular interactions into polymeric materials progressed in parallel. Similarly, these dynamic supramolecular moieties have been used to cross-link polymeric materials, resulting in materials with physical properties that can be changed on exposure to specific stimuli. The work in this thesis aims to create a double-dynamic cross-linked material containing both reversible covalent and non-covalent interacting groups; the incorporation of both reversible covalent and supramolecular chemistries plans to overcome the limited kinetic control observed in materials that contain just one dynamic chemical functionality.

In this first results chapter of this manuscript (chapter 2), this goal is approached by the formation of a main-chain supramolecular polymer. Synthesis and post-polymerisation functionalisation of an α,ω-alkyne-functionalised polyisoprene with an azide-functionalised ureidopyrimidinone derivative produced polymeric materials with little difference to the un-functionalised starting material.

In chapters 3 and 4, a different approach was taken, namely the polycondensation copolymerisation of an aldehyde-functionalised ureidopyrimidinone derivative with amine-functionalised polybutadiene. The catalyst-free polymerisation and cross-linking reaction yielded double-dynamic polyimine materials that were water-stable, soluble and self-healing. The presence of the elastic polybutadiene backbone resulted in materials that displayed rubbery behaviour between -30 to +70 ºC and a T_g at ~75 ºC. At room temperature, the material displayed a tensile strength of 14 MPa and an elongation at break exceeding 100%. The presence of the dynamic chemical functions within the double-dynamic materials gave self-healing properties of damaged materials in the bulk, as well as solubility in appropriate conditions.

In chapter 5, the formation of thermoplastic materials, based on the same polyimine polycondensation, was achieved from better-defined polybutadiene backbones. These materials displayed rubbery behaviour between a narrower temperature range (–10–+60 ºC), and a melting transition at temperatures above 100 ºC. On physical analysis, similar viscoelastic behaviour at room temperature was observed between thermoplastic and thermoset materials. The presence of the dynamic reversible imine and ureidopyrimidinone chemical groups again allowed for dissolution and self-healing of the materials, as well as a procedure for re-moulding dissolved material.

Acknowledgements

I would firstly like to give my sincerest thanks to Professor Nicolas Giuseppone, for accepting me into his group and allowing me to work on a new and inspiring project. My experience in his laboratory has given me the chance to explore new areas of chemistry, and discover the unforeseeable and dynamic nature of scientific research.

My deepest thanks go to Professor Pierre J. Lutz, for his patient and positive guidance at the beginnings of this project. His calm and collected approach to living anionic polymerisation, and research in general, has been a pleasure to work with and learn from.

I would like to thank Rémi Perrin for his inspiring vision concerning the industrial applicability of the work produced in this project.

My thanks also go to Professor Christian Gauthier for his supervision of the physical analysis conducted over the course of the project.

I express my gratitude to Doctor Emilie Moulin, for her well-organised and rigorous supervision for the duration of this project, as well during the editing of this manuscript.

I thank Georges Formon for his incredible help toward the physical characterisation and development of the thermoplastic materials. I'm sure you will have a successful future and Ph. D, and hope that this is the beginning of a bright friendship. Thank you to Dr Artem Osypenko for more things than I can write on this small page. I will cherish these past few years as a friend and colleague forever. Thank you to Dr Justin Foy for being there through the rough and the smooth, both in and out of the lab. Again, I look forward to many future years as friends. Thanks to Dr Sasha Koniev for his motivation and enthusiasm– я тебя уважаю. Thank you to Dr Antoine Goujon for our interesting conversations, both as lab neighbours and as friends. Thanks to Chris Reţe for his wit and wisdom as office neighbours and hiking partners. Thanks to Jean-Remy Collard-Itté for your help navigating the French language, and correcting my résumé. Thanks finally to all of the current and past members of the SAMS team, particularly Dr Susanne Schneider, Dr Joe Armao, Dr Valentina Garavini, Prof. Mounir Maaloum, Dr Gad Fuks, Odile Gavat, Dr Daniel Funeriu, Dr Qing Cao, Julie Lemoine, Damien Dattler, Flavio Picini, Mélodie Galerne, and Yali Zeng. Thank you also to Igor Dovgan and Stas Osypenko.

I'd like to thank Alexandre Collard for his enormous help with my training as a polymer chemist; Dr Leandro Jacomine, Dr Vincent Le Houerou and Dr Damien Favier for their incredible help in guiding me through the world or polymer engineering; and Dr Pascal Pichon

for his help with all things related to industry. Thank you to Michel Rawiso and Guillaume Fleith for their help with the X-ray scattering characterisation; as well as to Jean-Marc Strub and Bruno Vincent for their help with the Mass and DOSY characterisation, respectively, within this manuscript. Thanks to the platform of characterisation at the ICS, notably Dr Mélanie Legros and Catherine Foussat, and the administration of the ICS, particularly Odile Lemblé and Jean Marc , for guiding me through the 'mille-feuille' of French paperwork. Thank you to the people responsible for the running of the NMR facility at the ICS, especially Laurence Oswald and Emeric Wasielewski.

Thank you to my family: my Mum and Dad, Martin, Louise, Johnny, Grace and Rusty, for their unconditional support throughout this experience. Their guiding hands have helped me through the highest peaks and lowest troughs of life as a student.

Rikke, I can't thank you enough for your encouragement, patience and love over the past three years. I certainly wouldn't have been as successful in my work without your unquestioning support, everyday. I look forward to our future together, and to be able to call you 'doctor' too (because the title transfers over to you too, right?).

Thanks to Connie, Bjarne and Kasper for their constant encouragement and positivity over the past three years. Our conversations were helpful opportunities for calmness and reflection.

I would also like to thank my friends: John, Nick, Rory, Joe, Jimmy, Tagg, Aaron, Law and Darron, for their support and encouragement throughout my years as a student.

Finally, thank you to Professors Andreas Walther and Patrice Woisel for accepting to examine this work.

Abbreviations and Symbols

Å	ångström
ATR	attenuated total reflection
°C	degree celsius
CDI	carbonyldiimidazole
CuAAC	copper-catalyzed 1,3-dipolar azide-alkyne cycloaddition
δ	chemical shift
DABCO	1,4-diazabicyclo[2.2.2]octane
DBTDL	dibutyltin dilaurate
DCM	dichloromethane
DMF	dimethylformamide
DMSO	dimethylsulfoxide
DMTA	dynamic mechanical (thermal) analysis
DSC	differential scanning calorimetry
ε	strain
E	Young's modulus
E'	storage modulus
E''	loss modulus
E^*	complex modulus
E_a	activation energy
Equiv.	equivalent
ESI-MS	mass spectrometry with electrospray ionization
EtOH	ethanol
FTIR	fourier-transform infrared spectroscopy
GPC	gel permeation chromatography
h	hour
HDI	hexane-1,6-diisocyanate
HRMS	high resolution mass spectrometry
K	kelvin
MALDI-TOF	matrix-assisted laser desorption/ionization – time of
µL	microliter
µm	micrometer
mL	milliliter
µmol	micromole
mmol	millimole
M_n	number average molecular weight
MPa	megapascal
MS	mass spectrometry
Ms	mesityl

M_w	weight average molecular weight
N	newton
nm	nanometer
NMR	nuclear magnetic resonance
ppm	parts per million
PBD	polybutadiene
PDI	polydispersity index
PI	polyisoprene
PMDETA	N,N,N′,N″,N″-Pentamethyldiethylenetriamine
r.t.	room temperature
SAXS	small angle x-ray scattering
SEC	size exclusion chromatoraphy
σ	stress
τ^*	characteristic relaxation time
T	temperature
tan(δ)	tangent delta (phase angle)
TBAF	tetrabutylammonium fluoride
TBDPS	*tert*-butyldiphenylsilyl
TEA	triethylamine
TEM	transmission electron microscopy
TFA	trifluoroacetic acid
THF	tetrahydrofuran
TGA	thermogravimetric analysis
TLC	thin layer chromatography
UPLC	ultra performance liquid chromatography
UPy	ureidopyrimidinone
UV	ultra-violet
Vis	visible

Chapter 1: Synthetic Materials in the Modern World – From Polymer Pioneers and Pollution Problems to Plastic Progress

1.1 Introduction

1.1.1 General Plastics

Limitations of the Limitless

The turn of the 20th Century saw the development of what are now the most used man-made materials: plastics. From the first large-scale production of plastics, with Bakelite, shortly followed by Staudinger's controversial discovery of their covalent macromolecular composition,[1] to the present day, where over 300 million tonnes of plastics are produced on an annual basis,[2] plastics play an unparalleled role in our daily lives. The success of plastics in this modern world comes from their low cost (the vast majority of plastics are made from otherwise unused by-products of the petro-chemical industry) and their almost limitless range of physical forms, with which comes their use in limitless applications, from wrapping food to commercial flight*.[3] In fact, only a handful of applications come to mind when questioning the limits of synthetic plastics; resistance to very high temperatures are, as yet, unattainable due to the decomposition of the carbon-carbon bonds that constitute the polymer backbones, and their poor conductive properties limit their use as electrical and thermal conductors, although strong academic interest in metal-containing polymers is rapidly developing the field of electrically conductive polymers already.[4,5] There are, however, considerable problems that we face today caused by plastics, and drawbacks with their current day production and use, setting the scene in which the work in this thesis fits.

The limited sustainability of the production of polymers goes hand-in-hand with the non-renewable nature of the resource from which they are obtained: oil. Our absolute reliance on oil to produce plastics is clearly seen when observing the coupling of the price of plastics to the price of oil (Figure 1a).[6] Movement away from this reliance on oil, by producing plastics from other more sustainable resources, or by the regeneration of used materials by recycling down to the starting monomer, is a vision that is already in motion. A second and more pervasive problem associated with plastics is their polluting effect on lands and in seas. Public

* Polymer-based composites constitute half of the weight of Boeing's 787 Dreamliner.

pressure is mounting, and rightly so, on governments and industry to make more significant efforts to reduce plastic production, increase recycling infrastructure, and to remove plastic waste that already pollutes the worlds' oceans.[7,8] It is the robust and inert nature of plastics means that they are durable in use, but also durable in waste (Figure 1b), and with 25.8 million tonnes of post-consumer plastic ending up in the waste streams (from the EU28 + 2) in 2014 alone, this durability poses a significant ecological impact.[2,9] Again, the development of new methods and chemistries to enable efficient recycling of used plastic materials, that are currently unable to be recycled, is an area of wide interest.

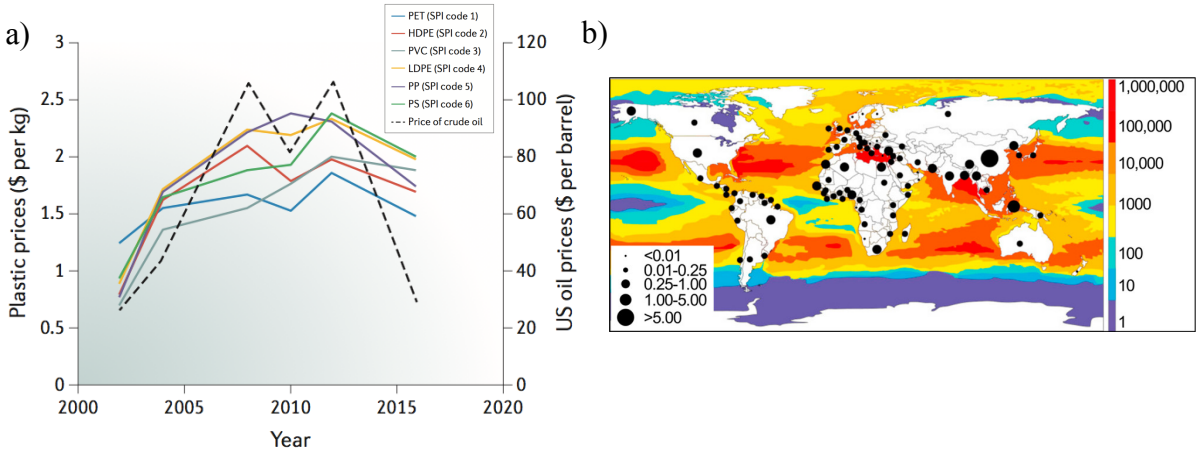

Figure 1 – a) Graph displaying the pairing of the price of crude oil to the price of 7 different commercial plastics;[6] b) Map depicting the prevelance of microplactics in oceans and seas of size >1 mm and <4.75 mm per m2. Black dots represent amount of plastics generated within 50 km of coastline in millions of mteric tons.[10]

The work in this thesis aimed to tackle the issue of the widespread disposal of elastomeric materials due to irreparable damage or our inability to recycle them with current-day technology. This was achieved by creating soluble elastomers that could be repaired by 'self-healing' (in the bulk) via the reversible exchange of covalent and non-covalent chemical bonds.

Polymer Morphologies

The physical properties of plastics are governed by their chemical constitution, and, by observing their chemical composition, may be categorised into two main groups: thermosets and thermoplastics.

Thermosets and thermoplastics share similarities, insofar as they are each composed of large macromolecular polymer chains that are interconnected in some way. Their differences lie in the way in which they are interconnected. The interactions between polymer chains in

thermoplastics are physical (van der Waals or chain entanglements), whereas these interactions in thermosets are chemical, and almost always irreversible (Figure 2a andFigure 2b). The physical outcome of this chemical difference is unmistakable. Thermoplastics, as their name suggests, transition from a solid to a melt state at elevated temperatures. Their melting is induced by the breaking of the *physical* bonds that hold the polymer strands together, which subsequently allows them to flow over one another in the melted state.[11] By contrast, the *chemical* bonds that hold polymer strands together in thermoset materials are considerably stronger in nature, and are not as easily broken by small increases in temperature.[5] As well as resistance to higher temperatures, thermosets tend to be considerably more resistant to physical stresses than thermoplastics due to structural reinforcement by the strong covalent cross-linking bonds that hold the polymer strands in place. The degree of functionalisation of the macromolecule is the sole chemical parameter that governs whether the resulting material will be thermoplastic or thermoset – macromolecules with a degree of functionality of two or below will be polymerised in a chain-extension fashion, whereas macromolecules with a degree of functionalisation above two will polymerise by simultaneous chain-extension and cross-linking, yielding thermosets (Figure 3).

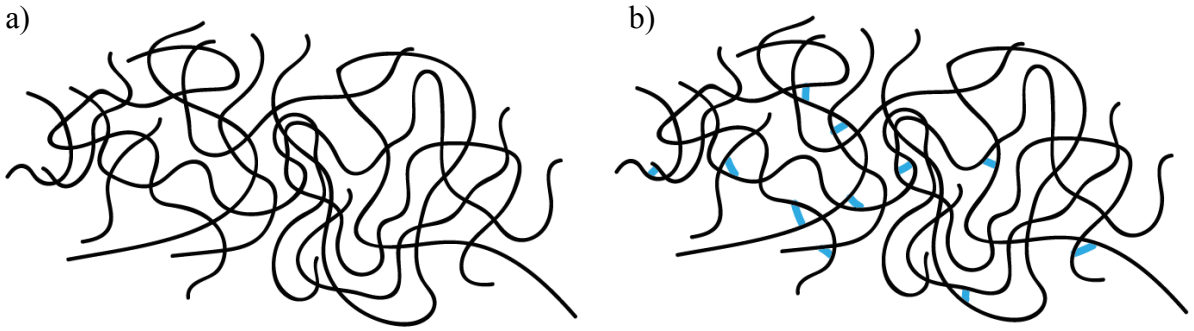

Figure 2 – a) Cartoon representation of the physical arrangement of polymer strands in thermoplastic materials; b) Cartoon representation of thermoset materials.

This difference, in the nature of the interactions between polymer chains, in thermoplastics and thermosets, is the focus of this work. As will be described later in this chapter, a new class of material, 'Vitrimers', takes the desirable thermal responsiveness of the former and the physical robustness of the latter, working as an intermediate between the two, by using reversible covalent bonds as cross-links between the polymer chains.[12]

Other chemical parameters also have a significant effect on the physical behaviours of plastic materials. When the macromolecule is flexible, with high degrees of freedom between the chemical bonds within the backbone, as is the case with polybutadiene and polyisoprene

(the polymeric backbones used in this work), more supple materials are produced. Decreasing the freedom with which the chemical bonds within the polymer backbone may move; introducing steric hindrance through the inclusion of bulky aromatic moieties results in stiffer materials.

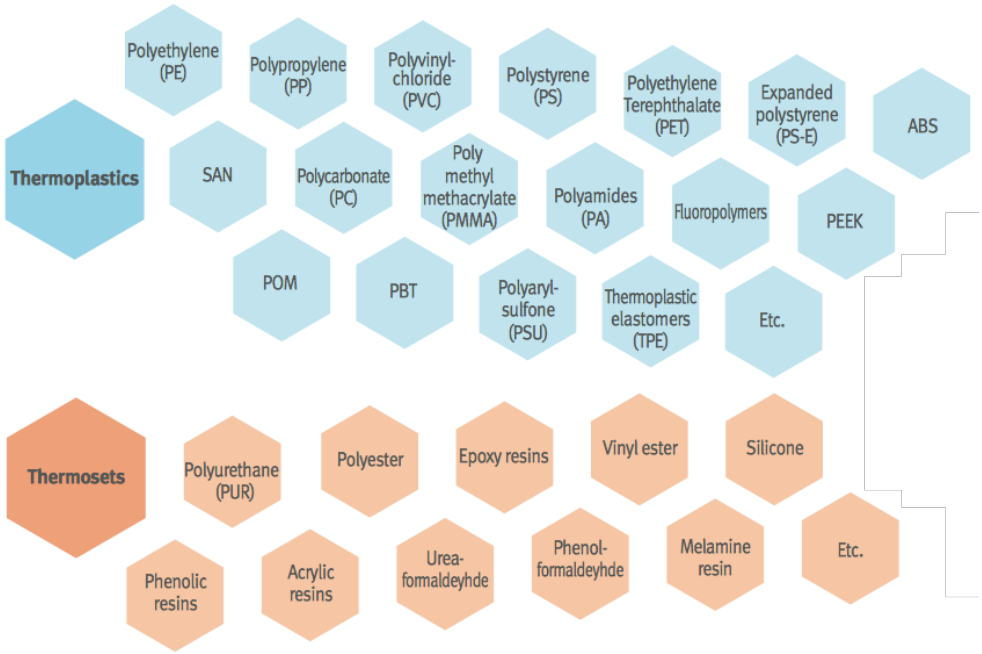

Figure 3 – Categorisation of some industrially-used plastics by thermoplastic and thermoset nature.[2]

If the polymerisation used to create the polymer strands introduces chemical functionalities that form non-covalent bonds (i.e. via van der Waals forces) with one another, aggregation between these chemical moieties may occur (Figure 4), resulting, again, in more physically robust materials. Polyamides, particularly the famous aromatic polyamide Kevlar®, and polyurethanes are common classes of material where this form of aggregation occurs, resulting in impressive improvement in physical resistance to stresses.[13]

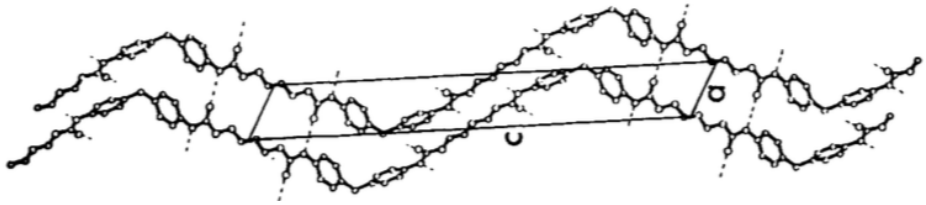

Figure 4 – ac projection of the model of the structure of methylene diphenyl diisocyanate (MDI)-butadiol hard segments.[14]

Current Challenges of Recycling Polymeric Materials

With the beneficial physical characteristics of thermoset materials (i.e. physical robustness and resistance to heat) comes their biggest drawback: thermoset materials cannot be easily recycled due to the irreversible nature of their chemical cross-links. By contrast, all thermoplastic materials may in theory be recycled in the melt or in solution; significant progress in industry-scale recycling infrastructure, predominantly for thermoplastic materials, is being made throughout the globe.[6] The unrecyclable nature of thermosets has resulted in a ranked hierarchy of waste-disposal solutions for all plastics (landfill, energy recovery, recycling, re-use, and prevention), from a European Commission directive,[15] and a push towards the innovation of new solutions, on both the physical and chemical reprocessing levels.[16]

As car tyres are a significant application for thermoset elastomeric materials, the development of new ideas for the re-use and recycling of used car tyres has been pursued by both industry and academia.[17–19] Physically grinding used tyres into small pieces or powders is the most common method to produce re-usable materials (although always for different applications to the virgin materials). The ground product has been used in roofing surfaces, as well as in composites surfacing roads and children's' playgrounds.[20] Re-use of tyre material in this fashion generates significant energy savings compared to the production of virgin materials used for these applications.

Chemical solutions to the recyclability problems of thermoset materials have brought about the most promising opportunities to produce new recyclable thermosets, as well as opportunities to recycle existing thermoset materials. As will be discussed in further detail in the next section of this chapter, thermoset materials based on reversible covalent cross-linking bonds may be selectively de-crosslinked and re-processed using similar heat or solution-based methods developed for thermoplastic materials.[6] Chemically recycling existing thermoset materials, by, for example, the breakage of carbon-sulfur or reduction of disulfide bonds in vulcanised rubber, may also be achieved chemically, by using thiol-based accelerators.[21] Chemical selectivity of breaking cross-linking bonds, while keeping the polymer backbone intact, is the biggest challenge faced when developing chemical methods for de-polymerisation of thermoset materials. De-vulcanisation by physically breaking cross-linking bonds, by swelling in super critical CO_2 is also a method of international interest, but suffers from the same issue of selectivity between backbone and cross-linking bonds.[19]

A final point to note concerns car tyres themselves, along with a vast amount of the thermoset materials used today, many materials that use thermoset materials are present as composite materials (mixtures of different materials), adding a significant layer of complexity to finding methods to chemically recycle them.[22–24]

1.1.2 Polyurethanes

Unlike any other class of polymer, polyurethanes can display plastic, elastomeric or thermoset behaviours depending on their chemical composition. This ability to produce such a wide range of physically differing materials, with a relatively modular approach to their chemical functionality, resulted in the global consumption of materials based on polyurethane to amount to 14 million tonnes in 2011 alone.[2] For this reason, the production and recycling of polyurethanes will be used as a benchmark, against which the performance of the materials produced in this project will be measured.

Synthesis

All industrially-produced polyurethanes are formed from the polyaddition of poly-isocyanates and polyols (Scheme 1). The properties of the resulting polyurethanes are dependent on the degree of functionality of the reagents, the chemical nature of the hard and soft blocks, and the chemical and physical interactions between or within hard and soft-block (micro-phase separation).[25]

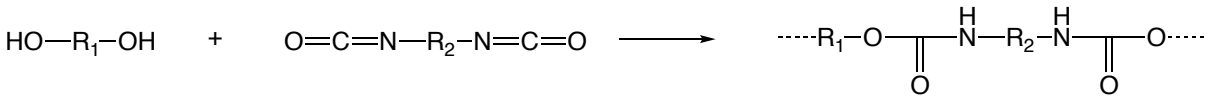

Scheme 1 – Formation of polyurethanes from diisocyanate and diol.

As described earlier, the degree of functionality of the reagents plays a key role in determining whether the produced polyurethane will be thermoset or thermoplastic: degrees of functionality of two or below, will produce the former; any degree of functionalisation above two in one or more reagents will produce the latter. Most commonly, thermosets are produced by the reaction between a diol, a diisocyanate and a cross-linking agent, which is usually a small molecule that is functionalised with multiple alcohol or isocyanate moieties.[25]

Hard and Soft Block Aggregation

As the chain-extension and cross-linking reactions between polyisocyanate and polyol proceeds, hydrogen-bonding interactions between the produced urethane groups, as well as between urethane and unreacted alcohol, cause aggregation and the formation of hard blocks. As the concentration and size of the hard blocks increase, a physical separation occurs between the long polymer backbone (the soft block) and these aggregates. The driving force of the microphase separation between hard and soft blocks is thermodynamic in nature and governed by the differences in solubility between the two blocks.[26] The rise of this separation is experimentally observed by the occurrence of a reflection at ~100 Å, with small angle X-ray scattering.[27–29]

Reactivity and Catalysis

It is generally accepted that the mechanism by which urethane formation proceeds involves the nucleophilic attack of the alcohol on the carbon of the isocyanate, before proton transfer onto the nitrogen.[26] Auto-catalysis has been proposed whereby the isocyanate groups are activated by hydrogen bonding interactions with urethane species, and as conversion increases so does the rate of urethane formation. The introduction of catalytic species also strongly affects the rate of urethane formation.

Base catalysis of urethane formation is proposed to build upon the hydrogen-bonding interactions that activate the isocyanate bonds in the auto-catalysed method. The electron-donating nature of tertiary amines is suggested to stabilise the partially cationic hydrogen bonding between alcohol and isocyanate (Scheme 2). Tertiary amines with a stronger propensity to donate its electron pair (higher donor number (DN)), increase the relative rate constant of urethane formation. The presence of different concentrations of tertiary amines does not, however, increase the concentration of the hydrogen-bonded alcohol/isocyanate complex, but instead stabilises the complexes that form (Table 1).[26,30] Rate constants have been shown to be dependent on the concentration of the added tertiary amine catalyst, presumably because of increasing the number of alcohol/isocyanate hydrogen-bonding complexes that are stabilised with catalyst.

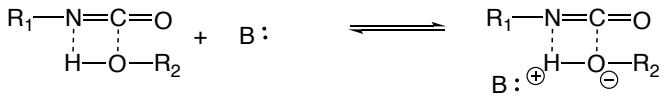

Scheme 2 – Hydrogen-bonded assisted, base-catalysed urethane formation.

Tertiary Amine	DN	Relative Rate Constant
Uncatalysed	-	1
Quinoline	30.4	6
Pyridine	36.7	11
Tributylamine	-	54
Triethylamine	50.7	134
DABCO	-	1206

Table 1 – Tabulated data displaying the correlation between the donor number of different amines and their catalytic effect on urethane formation.[26]

A number of different organometallic complexes have also been shown to display catalytic activity toward the formation of urethanes, with particular industrial focus on dibutyltin complexes (Bu_2SnX_2, where X is an anion).[31] For the organotin species, the mechanism of catalysis is less clearly defined, but are generally assumed to act as Lewis acids. *Bloodworth* and *Davies* propose that catalysis involves the coordination of the isocyanate reagent (through the nitrogen atom) with an alkoxide organotin complex, formed from the alcoholysis of the starting catalytic species.[32] Mixtures of organotin and tertiary amine catalysts have been observed to increase the rate constant further still.[33]

Applications - Elastomers

Due to the diverse range of physical properties that can be obtained from polyurethanes, the scope of their application has been found to be equally broad. The main forms in which polyurethanes are used are spread over a spectrum of high or low density, ranging from tens to thousands of kilograms per cubic metre (Figure 5).[34]

As the focus of this project is to synthesise self-healing solid elastomers, the appropriate place to start, when discussing the applications of polyurethanes, is with polyurethane elastomers. Polyurethanes elastomers are used with either a solid or a cellular composition, and these compositions represent the use for high density polyurethanes, from 1200 kg/m^{-3} to 300 kg/m^{-3} respectively.[34] The elastomeric characteristics of the materials are obtained from the selection of the diol used and the hard block aggregated that are formed. Typically, diol pre-polymers with a molecular weight ranging from 5000–10,000 g/mol, that are composed of flexible polymer backbones (poly(tetrahydrofuran), polyester polyols and polyether polyols), are used.[35] It is essential that the selected polymer is telechelic in nature. The synthetic procedure used to form polyurethane elastomers varies depending on the product. For elastomers that are thermoset in nature (forming a cross-linked polyurethane network), the

product cannot be re-shaped, and so the reaction is conducted in a cast. Introduction of the reagents into the cast is therefore typically achieved in one of two ways: cast moulding or rapid injection moulding (RIM).[25] Cast moulding is typically conducted in two-steps, starting with the synthesis of a pre-polymer, by reaction of the diol with excess diisocyanate, before introduction of the pre-polymer, cross-linking agent and catalyst into the mould. RIM involves a one-step method of mixing the reagents, shortly before transfer into the cast.[26] One significant benefit of using a two-step method over the 'one shot' method is the significant reduction in risk of toxic exposure (by inhalation) to small diisocyanate molecules on the jobsite. Preparation of the less volatile isocyanate-functionalised pre-polymer can be conducted in controlled conditions at chemical plants, before transfer of the less hazardous pre-polymer onto the jobsite, where urethane formation can proceed.[25,34]

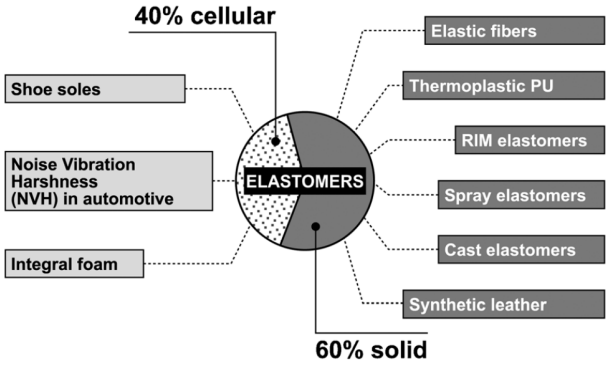

Figure 5 – Chart displaying percent usage of polyurethane elastomers.[34]

Most polyurethane materials are also dispersed in an organic solvent. Cross-linking and solvent evaporation typically occur simultaneously; careful consideration of the volatility of the solvent must be taken.[36] The presence of volatile organic solvents within many polyurethane formulations is an area of specific environmental concern, with significant industrial ambition to avoid their use.[37]

When comparing the physical characteristics of polyurethane-cross-linked elastomers to vulcanised polymeric backbones, the most prominent elastomeric materials used globally, similar performances can be expected. The stress at break of natural, styrene/butadiene or chlorophene rubbers typically reach values in excess of 500%,[16,25,38,39] while polyurethanes based on polybutadienes reach between 200 - 1000%,.[25 40] Strain at break values also (20–70 MPa) reflect this similarity in nature between vulcanised and urethane cross-linked elastomeric materials.[16,25,38,40]

The excellent resistance to dynamic mechanical forces, as well as resistance to fats and oils, paired with the multitude of processing methods that may be used to form the materials, from casting, spraying, injecting, extruding and centrifugal casting, make polyurethanes useful for a wide range of applications. As a result, application ranges from micrometre-thick insulating coatings on electronic goods, to multi-tonne tyres for vehicles.[34]

Applications - Foams

The most prominent application for polyurethanes is in foams, representing two thirds of the usage for polyurethane raw materials.[34] All polyurethane foams are produced using the same chemical principle: the reaction of isocyanate and water forms an unstable carbamic acid, which, after decomposition into amine and carbon dioxide, reacts with excess isocyanate to form the polyurethane (Scheme 3). The presence of gaseous carbon dioxide acts as a 'blowing agent' which gives the material its porous appearance.

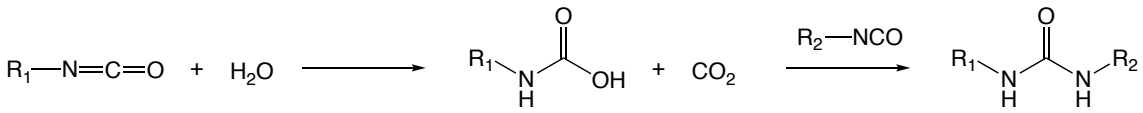

Scheme 3 – Formation of the urea bond via a carbamic acid, from the reaction between an isocyanate and water.

Flexible polyurethane foams are typically produced from the reaction between polyols, of molecular weight between 3000–4000 g/mol and a functionality of 3, and cross-linked with aliphatic diisocyanates. Production of highly resilient flexible foams (HR) uses similar reagents, using a larger molecular weight of the polyol with a higher degree of functionality, and often adding ethylene oxide to enhance the reactivity of the alcohol groups on the polyol. High density polyurethane foams are also produced in a similar fashion, using similar polyols and by differing the diisocyanate and blowing agents used. To obtain the rigid physical nature of these foams, aromatic diisocyanates are used, creating a more rigid and sterically hindered hard block.[34]

Flexible polyurethane foams find abundant use as mattresses and synthetic pillows, due to the ability of manufacturers to closely control the firmness of the products with varying pore sizes. Approximately 30% of global polyurethane consumption, however, goes to use as rigid foams, due to the multitude of combinations possible between physical properties and processing methods. The main application of rigid polyurethane foams is insulation. The excellent thermally insulating characteristics of polyurethane foams (0.024 $Wm^{-1}K^{-1}$) make

them a commonly chosen material for both industrial and domestic insulation (Figure 6).[34] A vital consideration to make when using foams as insulators in domestic applications is their fire resistance. Polyisocyanurate-based polyurethane foams were used as insulation in external cladding on the Grenfell Tower in London, which famously caught fire, releasing hydrogen cyanide when burning, killing at least 80 people in 2017.[41] Flame-retardants may be added to decrease flammability. Noise insulation is also a common application for polyurethane foams, with an average of 14 m^2 of insulating foam used in every car; the light-weight of polyurethane foams make them a favoured choice for car manufacturers.[34]

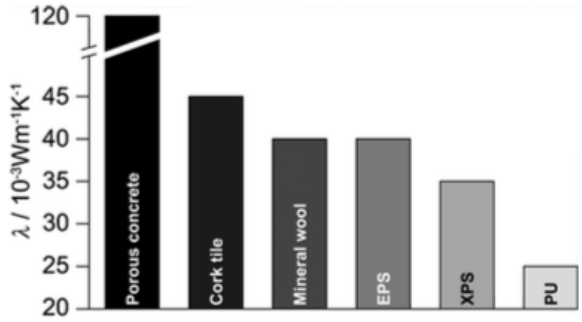

Figure 6 – Graph displating the thermally-insulating performance ($10^{-3}Wm^{-1}K^{-1}$) of commercially-used thermal insulators.[34]

Applications - Polyurethane Adhesives and Coatings

Polyurethanes are also abundantly used as coatings, deposited on the surface of metal, wood, plastics and textiles. Multilayer polymer coating systems on automotives are used to improve aesthetics and resist corrosion. A two-component is system typically comprised of a hydroxyl acrylate polyol and aliphatic polyisocyanates, and applied layer-by-layer starting with electrodeposition followed by spray coating. The use of polyurethanes as coatings for wood act as a water-proofing layer, as well as improving the physical durability and appearance of the surface. In coatings for this application two-component systems, typically using 2,4- or 2,6-toluenediisocyanate (TDI) as the diisocyanate, are formulated in volatile solvents for rapid drying. Again, hydroxypolyacrylate are the most commonly used polyols for this application.[34]

The durability of polyurethanes against physically demanding environments have also been the reason for their use as adhesives. Adhesive applications from footwear to food packaging are possible due to the ability to produce polyurethanes with a high degree of flexibility or rigidity. The adhesives can be dispersed in solvent or aqueous media, and applied in a one component system, cured by water from atmospheric moisture, or in a two-component system, with addition of a cross-linking agent to cure the adhesive. Polyesters are typically

used as the polyol, in combination with aromatic diisocyanates, although the use of toxic diisocyanate in adhesives for food packaging is closely regulated. A curing step, typically by laminating the adhesive-coated material to the other substrate at elevated temperatures (<150 ºC) and pressure (and moisture if a one-step system is used), is normally required for optimal adhesive strength. This heating step is required to be above the melting point of the polymer backbone, if a crystalline thermoplastic polyurethane is used, to obtain a sufficiently tacky surface.[34]

Current Areas of Research

Due to the large number of different methods by which polyurethanes can be produced, and hence their vast number applications, there is a wide scope for development and optimisation of current polyurethane systems in both their chemistry and production.

A continuing theme in research for the past two decades has been the investigation of cross-linked polymeric systems that can be selectively de-cross-linked, avoiding the complications of recyclability mentioned briefly at the start of this chapter. These reversible cross-linked polymeric systems span a large variety of chemical bonds, including materials made from very similar starting materials to those of the polyurethanes mentioned above.[26] Poly(oxime-urethane)-based materials, produced from the reaction between oxime (which itself is produced from the condensation reaction between aldehyde-functionalised reagents and hydroxylamine) and isocyanate, has been recently shown to be a readily recyclable alternative from similar starting materials.[42] Plasticity has also been induced into polyurethane systems that were previously thought to be permanently cross-linked.[43] This was achieved by increasing dibutyltin dilaurate (DBTDL) loadings and promoting transcarbamoylation exchange.

With increasing focus on the impact of industry on both global and local environment, industry is making strong efforts to improve the existing methods of polyurethane production, by removal of toxic catalysis and by avoiding the use of volatile organic compounds. In foam manufacturing, for example, supercritical CO_2 globally replaced CFCs as the blowing agent in the 1990s, as a response to evidence of their damage to the ozone layer.[44] Significant reduction in the use of solvent-borne surface and finishing coats in the polyurethane coating industry, replaced by water-borne alternatives, has already been achieved. Significant focus on curing at decreased temperatures, as well as on increasing curing times, looks to further reduce the energy consumption of the coating process.[34]

1.1.3 Physical Characterisation of Viscoelastic Materials

The focus of this project was to synthesise and characterise (both chemically and physically) elastomeric materials, and to observe the changes induced by the inclusion of dynamic chemical moieties within the polymer backbone. As both classical and thermoplastic elastomers were studied in this project, particular focus was paid to the differences between the behaviours of these two classes of materials when analysed using a variety of physiochemical techniques.

Elasticity is a physical property observed in many macromolecules, both natural [45] and man-made, and is characterised by the ability of a material to instantaneously return to its original shape and size after being temporarily deformed. The 'memory' of the original shape results from the presence of cross-links. In thermoset elastomers, these cross-links are permanent chemical bonds, whereas in thermoplastic elastomers these cross-links are physical bonds, i.e. hydrogen bonding or other van der Waals interactions. Many materials composed of polymer backbones with high degrees of flexibility, that do not crystallise, possess elastic properties at temperatures above their glass transition temperature; metals and glasses rarely have elastic limits higher than 1%, due to the localisation of their atomic structure. The glass transition temperature (T_g) occurs in amorphous polymeric materials as the transition from brittle glass-like properties to a softer rubbery state; this is characterised by a large change in the heat capacity of the material at a certain temperature (Figure 7). T_g depends on the amount of energy required to move polymer chains over one another, and so the following factors, that affect the freedom of rotation about chain links, strongly affect T_g: chain flexibility, molecular structure (steric effects), molar mass, and branching and cross-linking.[46] Typically, the glass transition temperature of solid polymeric materials is determined using differential scanning calorimetry, looking particularly at the change in heat capacity of the material against temperature; at T_g, a marked change in the heat capacity is observed.

As with all physical models, the theory of rubber-like elasticity does not perfectly fit the behaviour of most elastic materials in practice. In fact, most elastic materials display time or frequency-dependent viscosity, with the corresponding behaviour named 'viscoelasticity'. This behaviour consists of a delay in shape recovery after the release of a load. To study the dependence of materials on these variables, a variety of analytical techniques are commonly used, and will be discussed below.[47]

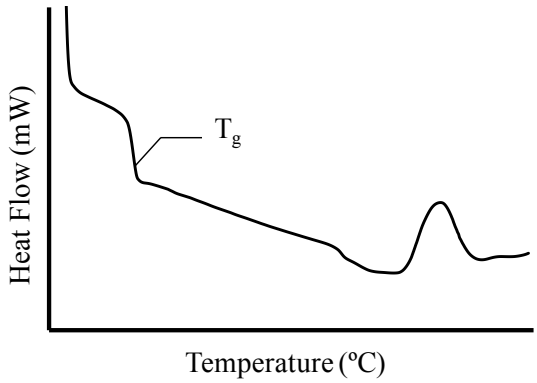

Figure 7 – Graph displaying a common DSC trace of an elastomer (T_g = glass transition temperature).

Dynamic Mechanical (Thermal) Analysis

Analysis of the physical responses of materials to low strains is commonly conducted using dynamic mechanical thermal analysis (DMTA), from which four key physical parameters may be determined: the storage modulus (E'), the loss modulus (E"), the complex modulus (E^*) and the phase angle (δ) (Equation 1).[47]

$$E^* = \frac{Stress}{Strain} \quad (a); \quad E' = \frac{Stress}{Strain} cos\delta \quad (b); \quad E'' = \frac{Stress}{Strain} sin\delta \quad (c); \quad tan\delta = \frac{E''}{E'} \quad (d)$$

Equation 1 – a) Relationship of the complex modulus (E) to stress and strain; b) Relationship of the storage modulus (E') to stress, strain and phase angle (δ); c) Relationship of the loss modulus (E") to stress, strain and phase angle (δ); d) Relationship of the phase angle (δ) to storage and loss moduli.*

An oscillating uniaxial tension or compression, at low strain (<1 %, and hence within the linear, elastic region of the viscoelastic materials), is applied to a sample that is held axially between two clamps. The stress response of the material to the sinusoidal force is observed at varying temperatures and frequencies (Figure 8a, 8b and Figure 9). At temperatures below T_g, thermoset and thermoplastic elastomeric materials behave as glassy, stiff solids, resulting in an increase in the storage modulus, as well as an increase in loss modulus when approaching T_g, observed by the hysteresis between applied strain and the resulting stress. As a consequence, elastomeric materials below T_g behave analogously to a stiff spring, requiring more energy to deform, as well as losing more energy as heat. As temperature is increased E' and E" decrease, as polymer chains begin to move more freely over one another, until a plateau is eventually reached. The behaviour of the materials, particularly in this transition region, is also strongly dependent on the frequency of the applied strain. If the frequency of the applied strain is high enough, there will not be sufficient time for the polymer chains to relax before release and

reapplication of the strain, causing a behaviour more analogous to that observed below T_g. At temperatures ranging within the rubbery plateau, there is sufficient energy for the polymer chains to move over one another, with little hysteresis between applied strain and the stress response of the material, corresponding to a low tan(δ). Increasing the temperature further results in differing responses depending on the thermoset or thermoplastic nature of the elastomers. Thermoset materials, with irreversible covalent bonds between polymer strands, are typically observed to show little deviation from the rubber plateau until temperatures are sufficiently high to degrade covalent bonds. Thermoplastics, by contrast, typically display a decrease in both E' and E" as the physical bonding between polymer strands break, and the material melts.[47,48] Vitrimeric materials with thermally responsive dynamic bonding between polymer strands, as will be discussed later in this section, show intermediate behaviour between the two; as temperature increased, the activation energy for the dynamic exchange at cross-linking nodes is reached, and the materials begin to flow.

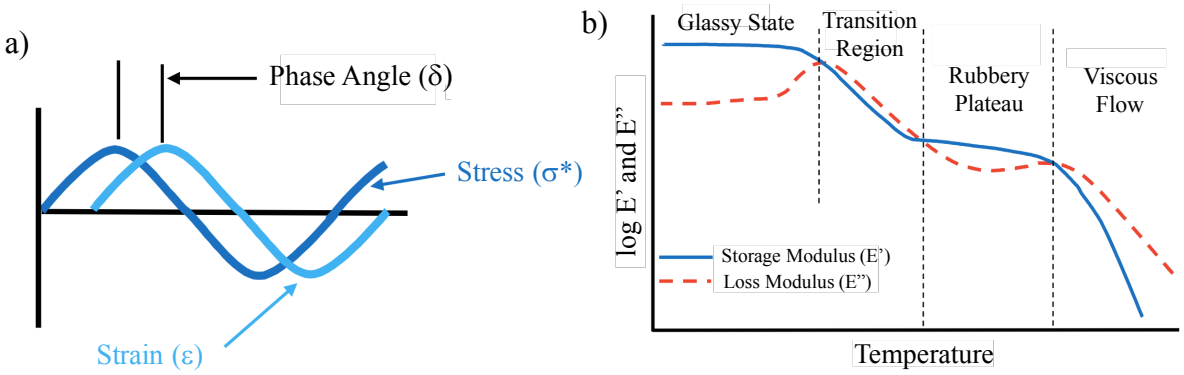

Figure 8 – a) Graph displaying a generic hysteresis between sinusoidally-oscillating stress and the subsequent strain response – adapted from a TA Instruments training document.[49]; b) Graph displaying the rheology of a generic rubbery material, storage and loss moduli (E' and E" respectively) vs temperature – adapted from a TA Instruments training document.[49]

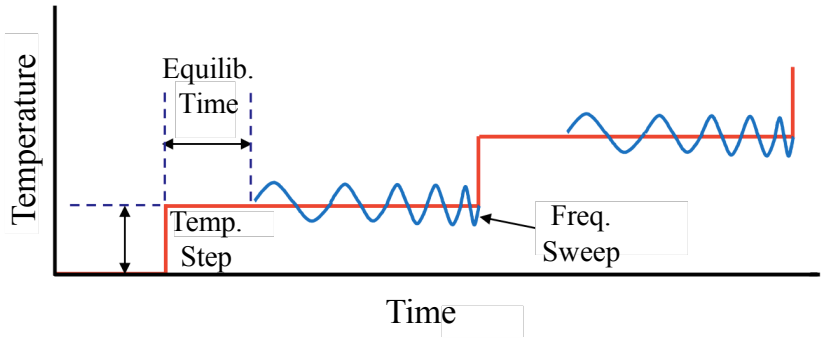

Figure 9 – Graph displaying a Dynamic Mechanical Thermal Analysis testing program – adapted from a TA Instruments training document.[49]

Stress/Strain Cycling

Application of stresses beyond the linear elastic domain of viscoelastic materials, allows for the analysis of their viscous behaviour. In a similar fashion to DMTA, solid samples are held between two clamps, and an axial sinusoidal tension is applied in an oscillating manner.[48]

For materials that display purely (or predominantly) elastic behaviour, the stress produced with this dynamic mechanical testing will be proportional to the strain on both loading and unloading. The stress/strain graph that is produced is subsequently a straight line (Figure 10a). Conversely, materials that show plastic behaviour display significant differences between loading and unloading cycles, qualitatively observed by a permanent deformation of shape and quantitatively by the permanent change in strain (Figure 10b). Viscoelastic materials behave partly viscous and partly elastic, insofar as they do return to their starting strain after the load is removed; stress is not observed to be proportional to strain, which also differs when loading vs unloading (Figure 10c).[50,51] This results in a characteristic hysteresis related to the energy lost during loading/unloading cycles.

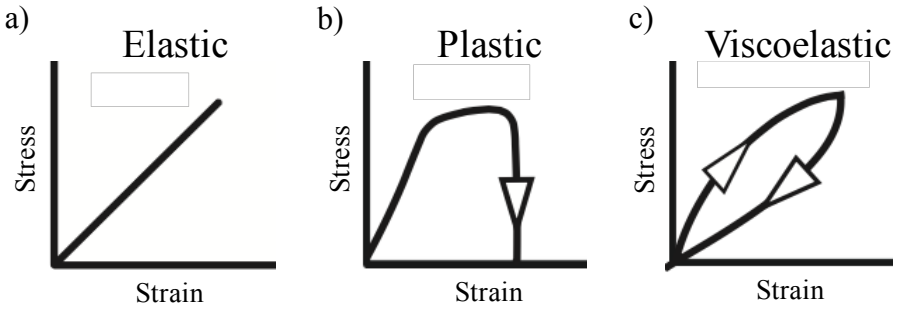

Figure 10 – Graphs representing the physical response of three types of materials (a) elastic, b) plastic and c) viscoelastic) to stress/strain cycling.

The theories to explain these experimental observations are commonly described in three ways: 1) the Boltzmann superposition, whereby the loading history of the material is considered to be additive to the total deformation; 2) the differential model, whereby a spring and dashpot model is used to describe both the viscous and elastic components of the materials' behaviours; 3) and the molecular model which considers the behaviours of the molecules themselves.[50]

Vulcanised rubbers have been observed to behave differently on consecutive loading/un-loading cycles; this phenomenon is named the Mullins effect.[52] The behaviour that was observed, conforms to the following criteria: the mechanical response of a material is

markedly different between first and second loading and unloading cycles; stress softening appears each time the maximum strain is increased,[53] the material 'remembers' the direction and sign of the maximum strain; the material 'forgets' the loading history after some time.[54] the molecular reasoning for these observations is still under debate.[54]

Stress Relaxation

The behaviour of viscoelastic materials may also be followed over long time-periods by stress relaxation experiments. This analytical technique involves the instantaneously applied, and constantly held, deformation of a material (by elongation or shear) and observes the evolution of stress with time.[48]

Purely elastic materials display a constant stress response for the duration of the time that the force is held (Figure 11a); viscous materials, on the other hand, display a decay to zero in stress as soon as the strain is applied (Figure 11b); viscoelastic materials display a combination of the two behaviours with stress relaxation over considerably longer time scales (Figure 11c).[48]

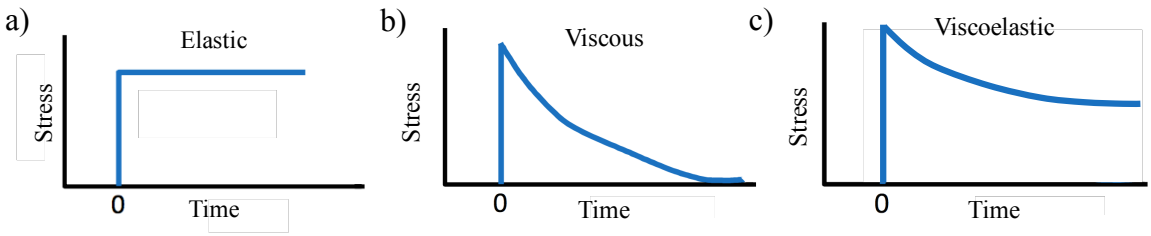

Figure 11– Graphs representing the stress response of three materials (a) elastic, b) viscous and c) viscoelastic) in a generic stress-relaxation test – adapted from a TA Instruments training document.[49]

For materials that are based on dynamic chemical bonds (Vitrimers), relaxation is also strongly dependent on the kinetics of chemical exchange between said dynamic bonds. Variable-temperature stress relaxation also provides a powerful insight into the activation energy of the dynamic exchange. As temperature is increased, relaxation is shifted to shorter time-scales as a result of increased exchange rate.[55,56] If stress relaxation is due to the exchange between dynamic bonds, the characteristic relaxation times vs temperature should show Arrhenius-like dependence.[56–58]

Elongation Until Break

The maximum stress and strain that an elastomeric material can withstand is typically analysed using elongation until break measurements, whereby the material is stretched to high strains until the physical breakage of the sample.[48]

Materials are often observed to rupture in one of two ways: with elastic-brittle breakage, or by plastic deformation (plasticity), with this behaviour strongly affected by temperature and strain rate.[50] For both thermoplastic and thermoset elastomers at temperatures within the rubbery plateau, load rises approximately linearly with increasing elongation, as is typically seen with stress/strain cycles (Figure 12). At elevated temperatures, a yield point (stress at which permanent deformation occurs) is often observed shortly before failure. In contrast, for materials that do not behave as elastomers, necking and cold-drawing behaviours at large extensions often occurs due to alignment of polymer chains, and formation of crystalline domains.[48]

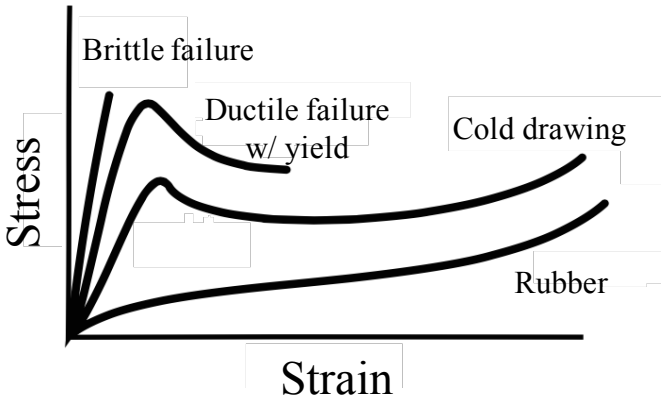

Figure 12 – Graphs representing the stress/strain response of different materials up to strain breakage.

1.2 Dynamic Covalent Networks/Vitrimers

1.2.1 Definition and Common Behaviours of Dynamic Covalent Networks

At the turn of the 21st century, a new class of polymer was introduced, rising between the groups of thermoplastics and thermosets: Dynamic Covalent Networks (DCNs) (also often referred to as Covalent Adaptable Networks (CANs)). These materials display physical characteristics similar to the two well-established types of polymer networks (thermoplastics and thermosets); but with more plasticity than traditional thermoset materials, and better physical integrity at elevated temperatures than thermoplastics. Chemically, this intermediate behaviour is achieved by using dynamic reversible and exchangeable chemical bonds at the cross-linking points between polymer chains, rather than physical or non-dynamic† chemical bonds. DCNs may be further subdivided into two categories, depending on the mechanistic nature of the chemical exchange: those with a *dissociative* chemical exchange, via a reversible addition rearrangement, and those with an *associative* chemical exchange (often referred to as Vitrimers) (Figure 13).[12,55]

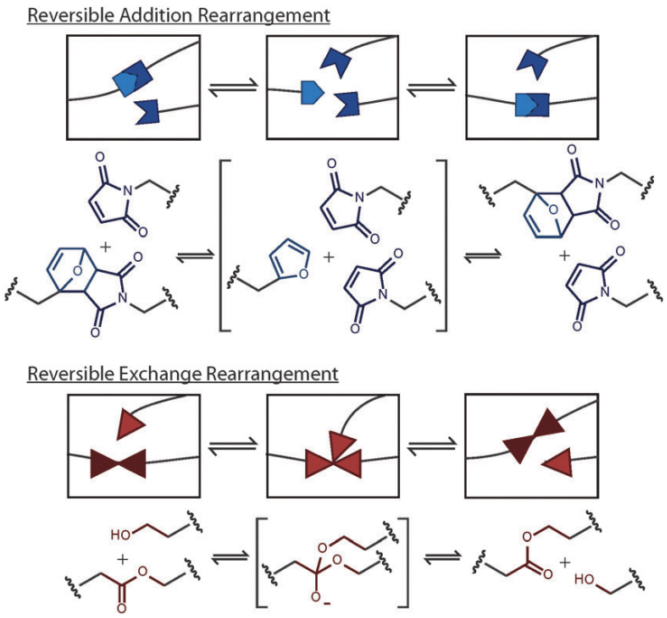

Figure 13 – Schematic representation of dynamic covalent networks of either dissociative (addition rearrangement) or associative (exchange rearrangement) nature.[55]

† The term 'irreversible' is not used here, to describe the chemical bonds that make up the backbones and cross-links of traditional thermoset materials, as all polymers are de-polymerised once a certain temperature is reached.

The archetypical chemical reaction often used to describe dissociative chemical exchange in DCNs is the Diels-Alder reaction between a diene (usually furan) and dienophile (usually maleimide). Dissociative chemical exchange mechanisms require the breaking of the coupled product into its constituent reagents before exchange with alternative coupling reagents. By contrast, associative chemical exchange passes through an intermediate in which the coupled product and alternative coupling reagents are all chemically bonded; transesterification is often used as an example in this case. This important chemical distinction gives rise to clear physical differences between the two sub-classes (Figure 14).[55]

At elevated temperatures with dissociative DCNs, the chemical equilibrium of the Diels-Alder reaction is shifted towards dissociation; the breaking of chemical cross-links and re-arrangements of polymer strands causes the material to undergo stress relaxation. At high enough temperature, a gel-sol phase transition occurs (with a sharp decrease in viscosity), behaving similarly to thermoplastic materials. For associative DCNs, the degree of cross-linking remains much more stable at elevated temperature, due to the associative mechanism of exchange. Increasing the temperature of these networks causes a more gradual decrease in viscosity, analogous to the behaviour of silica.[55]

The physical state of the sample is very important when considering the freedom with which polymer strands can move, and thus the rate at which bond exchange can occur. At temperatures below the glass transition temperature (T_g), polymer strands are more restricted than at temperatures above T_g. The rate of chemical exchange between polymer strands in the bulk also differs greatly from the same exchange in gels or in solutions. However, careful attention must be paid when comparing different samples in different physical states or media and phases.

With these considerations in mind, it is possible to assess the behaviour of dynamic materials when exposed to a change in temperature, for better definition and classification of new systems and distinction from already existing classical materials. The well-established parameter T_g is known to be affected by the chemical composition of the polymer backbone, particularly the backbone flexibility. The temperature at which dynamic materials lose structural integrity and begin to flow, is defined, by *Leibler et al.*,[56] as the topology freezing temperature (T_v), and is entirely dependent on the kinetics of the exchanging cross-links. If the T_g of the material is well below the T_v, the change in viscosity of the material on increasing temperature begins while the material is already a viscoelastic liquid. Consequently, diffusion of the exchanging chemical moieties is already apparent, thus the change in viscosity follows the Arrhenius law (Figure 14a). In contrast, when T_v is well below T_g, diffusion of exchanging

chemical moieties is the limiting factor. As the material is heated above T_g diffusion becomes more apparent, thus viscosity sharply decreases following the Williams-Landel-Ferry (WLF) model (Figure 14b).

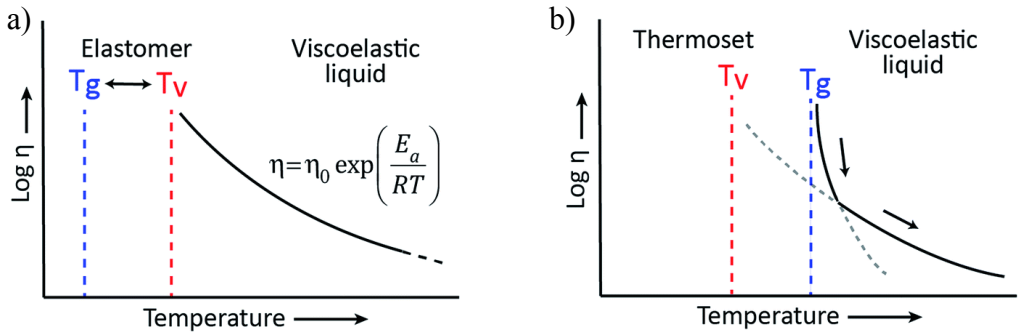

Figure 14 – Graphs depicting the evolution of viscosity of dynamic covalent networks following either the a) Arrhenius or b) WLF model.[12]

The question of whether chemical cross-links are present at all should also be considered when comparing the performance of the dynamic material to a classical material: only direct comparisons of un-cross-linked dynamic covalent materials with thermoplastics, and dynamic covalent networks with thermoplastics should be made.

1.2.2 Dissociative Dynamic Covalent Networks

As mentioned above, the Diels-Alder exchange reaction is the most often used to exemplify dissociative chemistry when reviewing dissociative DCNs, due to the frequency of use in the literature. A strong advantage of its use is the higher tolerance of the Diels-Alder coupling to the presence of other chemical moieties and to the presence of water and oxygen, as well as the ability to tune the coupling over a wide range of temperatures – the Diels-Alder reaction meets many of the criteria for "click" reactions. We will now evaluate some specific examples of its use, as well as some examples of other dissociative exchange chemistries used to make DCNs; this section will group each exchange chemistry by the stimulus required to activate the dissociative exchange reaction.

Thermally Reversible Networks

Furan/maleimide

The application of the Diels-Alder exchange reaction for use as a cross-linking agent in materials dates back as far as 1969,[59] when DuPont published a patent detailing the use of a

saturated polymer backbone, produced by condensation polymerisation, terminated at the chain-ends with, or baring at pendent positions, furan moieties, which was then reacted with the di- or tri-maleimide-functionalised cross-linking agent. In the opposite case, i.e. polymers functionalised with maleimide, *Stevens* and *Jenkins* published work in which a polystyrene backbone, was functionalised with maleimide in mild Friedel-Crafts conditions.[60] This modified polystyrene was then subsequently cross-linked in a Diels-Alder [4+2] cycloaddition, to form cross-linked materials. In both of these examples work, as well as with many examples described in this section, did not explore the reversibility of the Diels-Alder adduct, but instead used this chemistry solely for cross-linking. The first case in which the reversibility of this chemistry was studied by *Chujo et al.*,[61] whereby an pendent-furan- and maleimide-functionalised polyoxazolene was reversibly cross-linked at elevated temperatures. More recently, *Wudl et al.* similarly showed that a tetra-furan-functionalised cross-linking agent reacts with a maleimide chain-extender to reversibly form transparent thermally-mendable polymeric materials (Scheme 4).[62] In all of these cases, as well as in many other studies conducted since the first conception of the idea in 1969,[63–66] this thermally activated cross-linking of polymer strands is well suited for application due to the orthogonal nature of the Diels-Alder reaction with other chemical functionalities present on the polymer backbone. The reversibility of the produced materials is activated by simply holding the ends of two severed pieces together and heating to ~120 ºC, without the need of a chemical catalyst; the healed materials could withstand ~57% of the original load before breaking.[62]

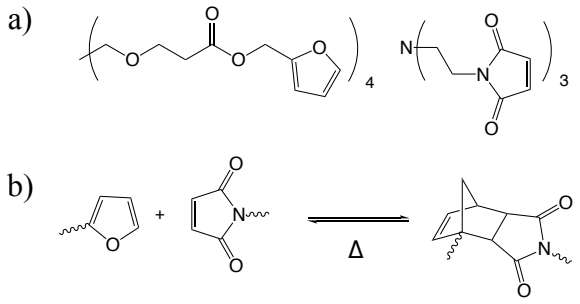

Scheme 4– a) Monomers used by Wudl et al. to produce thermally mendable polymeric materials;62 b) Diels-Alder reaction between furan and maleimide derivatives.

Fulvene/Cyanofumarate

Work published by *Lehn* and co-workers demonstrated the versatility of the Diels-Alder reaction by investigating the coupling of a tetra-fulvene-functionalised polyethylene glycol with a bis(dicyanofumerate) cross-linking agent (Scheme 5a).[67] Chain-extension of linear

fulvene terminated polyethylene glycol with the same bis(dicyanofumerate) agent, to form linear dissociative exchange polymers, were also prepared (Scheme 5b). Despite the mechanical properties of the resulting materials being only qualitatively characterised, self-healing of the material after cutting was clear at room temperature, without the need of an external chemical stimulus.

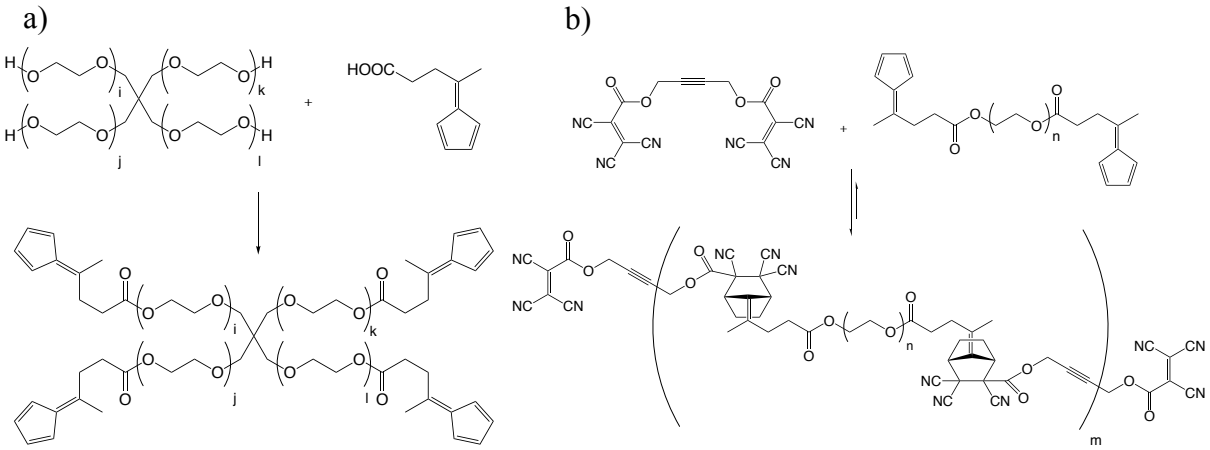

Scheme 5 – a) Synthesis of tetra-fulvene-functionalised polyethylene glycol;[67] b) Linear chain-extension of polyethylene glycol via the fulvene/cyclopentadiene Diels-Alder reaction.

Dicyclopentadiene

Polyisobutylenes containing cyclopentadiene at terminal positions and at pendent positions were synthesised, by *Kennedy* and *Castner*,[68] to investigate the use of the dicyclopentadiene Diels-Alder condensation to form cross-linked networks. In this work, the reaction between dimethylcyclopentadienealuminium and halogenated butyl rubbers yielded polymers with cyclopentadiene moieties randomly distributed along the polymer backbone. Cross-linking of the modified polymers was observed at room temperature (Scheme 6), and self-healing of cut samples achieved by compression moulding at 150 ºC.

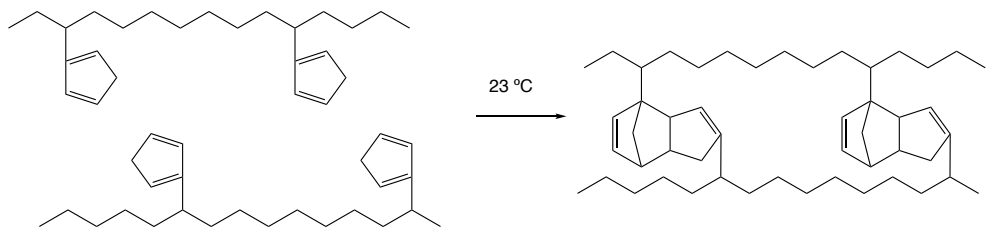

Scheme 6 – Dynamic covalent networks from cyclopentadiene-functionalised polyethene.[68]

The use of the dicyclopentadiene condensation as a chemistry for cross-linking polymers was further investigated almost three decades later, by *Wudl et al.,*[69] with the preparation of cross-linked materials based on a variety of polymer backbones. These materials were synthesised from a dicyclopentadiene-containing macrocycle (B), formed from the ring-closing bis-lactonisation of dicyclopentadiene diacylchloride (A) (Scheme 7), which was subsequently simultaneously polymerised and cross-linked by ring-opening polymerisation in the presence of the Theil's acid trimer (C), at 120 ºC. The resulting materials gave a wide range of properties, depending on the polymer backbone[‡] used: when based on polybutane, tough and ductile materials (E = 2.63 GPa) were obtained; but when based on polyethylene glycol, stronger stiffer and more brittle materials (E = 3.26 GPa) were instead obtained. Up to 60% of the physical performance of the material could be recovered, by stimulating the reversible Diels-Alder reaction at the cross-linking points by heating.

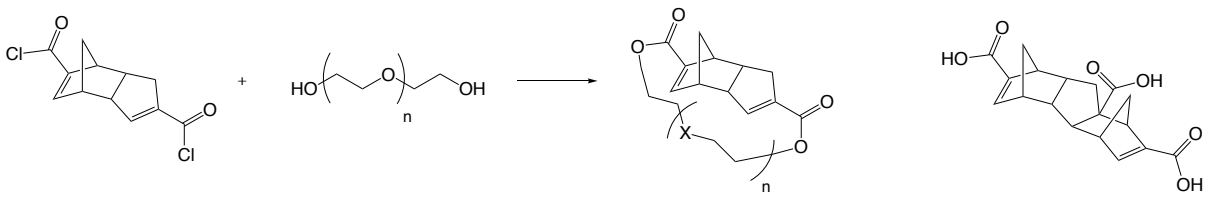

A **B** **C**

Scheme 7 – Ring-closuing bis-lactonisation and Theil's Acid.[69]

Imine/Diene

The imine bond has been found to act as both a diene and a dienophile for Diels-Alder condensation reactions,[70–72] but has, so far, not been realised as a chemistry for reversible cross-linking (Scheme 8). In this hetero-Diels-Alder reaction, and as in classical Diels-Alder reactions, the HOMO-LUMO energy gap is a key parameter to consider; introduction of electron-withdrawing or donating substituents onto either diene or dienophile can strongly influence the regioselectivity of the product. The conditions for the reverse, retro-hetero-Diels-Alder, reaction have rarely been explored, with hydrolysis given as the most common mechanism.

[‡] It is also suggested that the degree of cross-linking between these two materials may also differ, causing varying physical characteristics

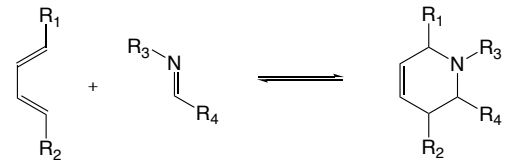

Scheme 8 – Diels-Alder reaction between imine and diene

The key role that the imine bond plays in this project, as will be discussed in detail later in this text, gives this reaction interesting potential for incorporation of dissociative nodes in an imine-functionalised network, or on polymers produced from imine polycondensation.

Alkoxyamine Exchange

In 2006, the thermally induced exchange of alkoxyamines (Scheme 9) was used to create dissociative dynamic covalent polymer networks, by the group led by *Takahara*.[73] Poly(methacrylic ester)s, containing alkoxyamine units on the side chains, were heated, initiating the radical exchange between the alkoxyamine moieties, leading to cross-linked materials when heated at 100 ºC. De-crosslinking the material was achieved by swelling the material in a good solvent for the backbone, and heating to 100ºC, resulting in a solution of polymers with a molecular weight almost identical to the reagents before cross-linking.

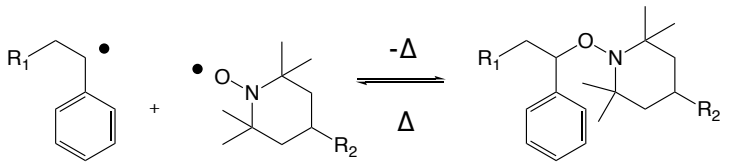

Scheme 9 – Reversible exchange of alkoxyamines.[73]

Photochemically Reversible Networks

[2+2] photocycloaddition reactions – and [4+4] in the case of anthracene - have also been used as cross-linking chemistries to form a variety of polymer networks. In this case photo-excitation of species, using near-ultraviolet wavelengths of light, is necessary to overcome the symmetry "forbidden" process of [2+2] cyclisation, to form dissociative DCNs. These systems are in close analogy to their thermally-activated counterparts, differing only in the need for longer wavelengths of UV-light to trigger cross-linking and shorter wavelengths for scission.

Cinnamic Acid

In 2005,[74] *Jünger* and co-workers demonstrated the formation of cross-linked materials in which the [2+2] photocyclisation of cinnamic acid was used as the cross-linking chemistry (Figure 15a). These materials were composed of a covalently cross-linked polybutylacrylate network, grafted with cinnamic acid moieties. By irradiation with UV light (>260 nm) a series of new temporary cross-links were produced, from the photocyclisation of the pendent cinnamic acid moieties (Figure 15b), resulting in the temporary fixation of a new shape; when irradiated with a different wavelength of UV light (<260 nm), this temporary shape was reversed and the material reverted to its original shape (Figure 15b). When compared to thermally induced shape-memory materials, it is noted, the 'shape-fixity rate' is slower, due to the differing nature of cross-linking chemistry: in photo-induced shape-memory materials temporary cross-links are created and broken, rather than the freezing and thawing of polymer chains as found in thermally-induced shape-memory materials.

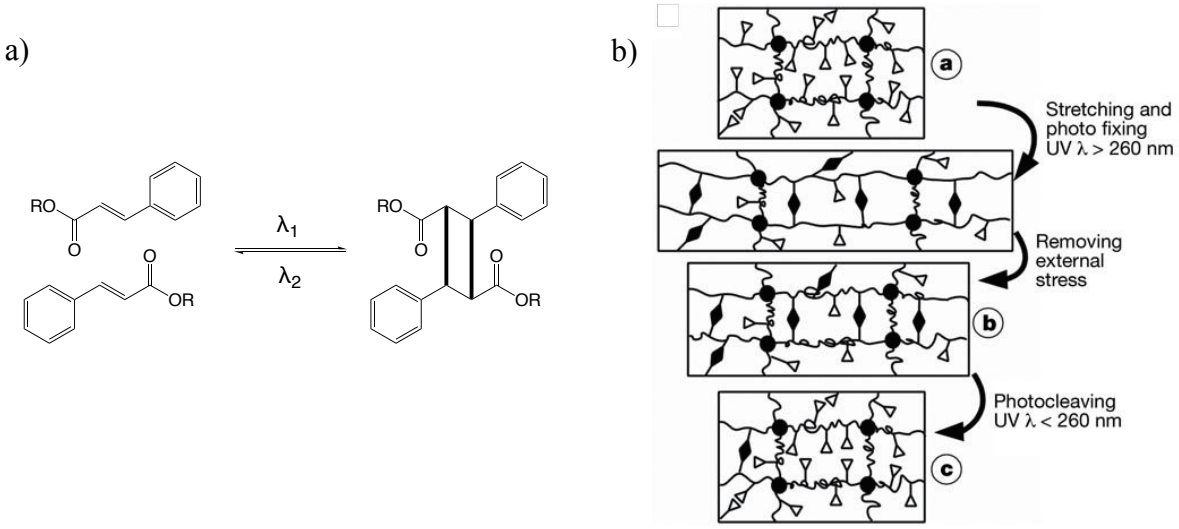

Figure 15 – a) Schematic representation of the reversible photocylisation of cinnematic acid; b) – Cartoon demonstrating the molecular arrangement within shape memory materials (filled circles – permanent cross-links, filled diamonds – photo-reversible cross-links, open triangles – unreacted chromophores).[74]

Anthracene and Coumarin

The dynamic nature of the photodimerisation of anthracene molecules (Scheme 10) has been studied, in the context of reversible polymeric materials in some detail,[75–78] dating back to as early as 1996.[79]

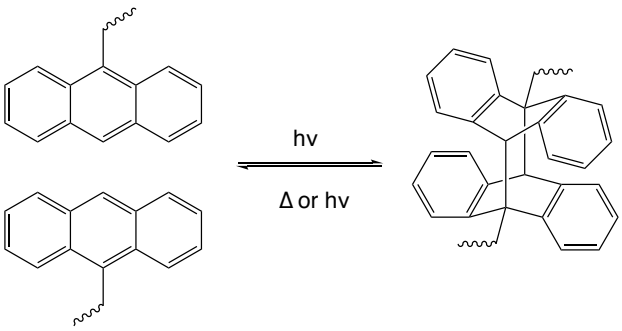

Scheme 10 – Reversible photodimerisation of anthracene.

Introduction of anthracene moieties at pendent position along epoxy-based networks, as in the work of *Schlögl et al.*,[80] and at pendent positions along poly(methacrylate)s, as published by *Tamaki et al.*,[81] lead to the formation of cross-linked polymer networks after by irradiation with light of wavelength >350 nm and which can be reversed by irradiation with light of wavelength <300 nm or heating. In both cases, the reversibility of the cross-linking was proved to be effective after multiple cycles of formation and breaking. In the case of the epoxy-based networks, the physical characterisation of the materials was investigated in detail; it was shown that the materials self-healed (back to pristine materials) after rupture from physical stress and irradiation with UV-light (>300 nm) and heating (60 ºC). Load-displacement studies revealed that healing efficiency can be increased by increasing the concentration of anthracene along the polymer backbone - optimised materials managed to bear 84.4% of the original load after the third cycle of repair.

Similarly to anthracene, the coumarin moiety also undergoes photo-induced dimerisation when irradiated with UV light (>300 nm) (Scheme 11). The use of the coumarin cyclisation as a reversible cross-linking chemistry in polymers was demonstrated by *Zhao* and co-workers, when poly(ferrocenylsilane) was functionalised with coumarin at pendent positions along the backbone and irradiated with light (>300 nm) to form cross-linked networks.[82] Varying the content of coumarin along polymer backbone was investigated, and it was found that backbones with pendent positions saturated with coumarin, and hence a high degree of cross-linking when irradiated, were only partially reversible. This incomplete reversibility is likely due to inefficiency in the photoscission.

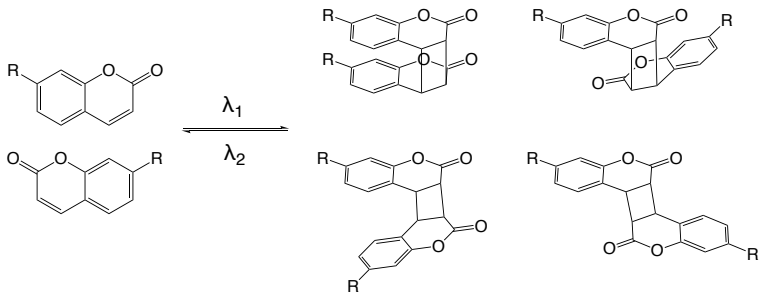

Scheme 11 – Reversible photodimerisation of coumarin.

Chemically Reversible Networks

Disulfide

Reduction of a disulfide bridge to the constituent thiol moieties or oxidation of thiols to form disulfide bonds is also a commonly used chemistry for the formation of dissociative covalent chemical networks. The earliest example of this chemistry's usage for this application came from *Chujo et al*.[83] in which a poly(N-acetyl-ethylenimine) was functionalised with anthracene-disulfide at pendent positions. The disulfide exchange was then chemically activated by reduction with sodium borohydrate and subsequent oxidation, in air, to form polymer networks with disulfide bridges. The nature of this seminal dynamic network, was, in fact, dissociative in nature.

Since this work, many groups have applied this concept into networks based on a variety of polymer backbones.[83–86] Recently, a study from *Odriozola* and co-workers presented the implementation of disulfide bridges within a poly(urea-urethane) network.[87] This work utilised the hydrogen-bonding association of the urea-urethane moieties, and is further discussed later in this chapter.

The abundant presence of the disulfide linkage in traditional polybutadiene rubbers, cross-linked by vulcanisation, makes this linkage an attractive target for the modification of already existing materials. This modification is hoped to be the basis of a possible pathway to reversing materials which have until now been thought to be permanent.[16,17,88]

Acetals and Ketals

A less explored, and equally interesting, chemical moiety used to reversibly cross-link polymer strands is the acetal. Due to the abundance of alcohol functionalised polymers, and the low cost of multiply aldehyde-functionalised small molecules, which could be used as a polymer cross-linker, it is interesting to note that few publications using this chemistry vis-à-

vis cross-linking bulk polymers, could be found.[89–91] In one example,[89] *Lenz* first describes synthesising linear polymers from ester monomers containing acetal rings of different sizes. This polymerisation was described to have require harsh conditions using toxic catalysts (190 ºC, $Pb(OAc)_2 \cdot 3H_2O$), with subsequent cross-linking of the polymer backbone from opening of the acetal rings. This cross-linking could be achieved using a variety of reducing agents, but always required a catalyst and inhibitory amounts of heat.

1.2.3 Associative Dynamic Covalent Networks

Associative covalent networks, also commonly referred to as 'vitrimers', provide a class of materials with a different physical response to the same heat, light and chemical stimuli. As mentioned at the beginning of this section, the archetypical chemical moiety most often used to describe materials with these chemical and physical responses is the ester bond (and transesterification exchange); this chemistry, as well as a selection of other chemical exchange reactions of the same classification, will be explored here.

Thermally Reversible Networks

Carboxylate Transesterification

The use of the exchange between ester groups to form DCNs was first demonstrated by the *Leibler* Group.[56] In this novel work, a polymer network, containing ester bonds within both the backbone and at cross-linking points, was formed from the reaction between diglycidyl ether bisphenol A and fatty di- and tricarboxylic acids in the presence of zinc acetate heptahydrate as a catalyst (Figure 16).

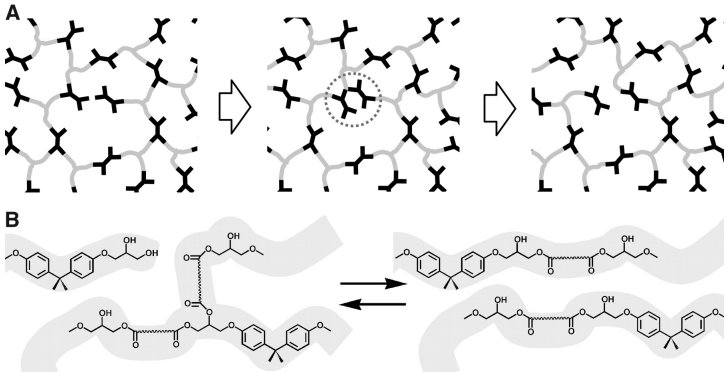

Figure 16 – a) Cartoon representation of a vitrimeric network based on reversible transesterification; schematic representation of the reversible chemical structures involved in the network.[56]

At room temperature, the resulting material behaved as an elastomer (E = ~4 MPa, elongation at break ~180%); the concentration of ester bonds within the materials, measured by FTIR, was found to be isothermal, confirming the associative nature of the dynamic material. Solubility experiments, in trichlorobenzene, demonstrated the insolubility and permanence of the network. The behaviour of the material at elevated temperatures revealed complete relaxation (tendency to zero of the modulus G) and an increase viscosity with increasing temperature that followed the Arrhenius Law. Reprocessing, recycling and reshaping of the fatty acid-based materials was also demonstrated in this paper, as well as in subsequent publications,[92–94] wherein ground and remoulded samples (240 ºC for 3 minutes) regained ~100% of the original mechanical strength – the amount of catalyst used played an important role in the time-scale of self-healing.

Poly(caprolactone) (PCL) and polylactide-based networks have also been a foundation on which vitrimers have been investigated.[95,96] The presence of ester bonds within PCL backbones enabled plasticity to be achieved by activation of the trans-esterification using neutralised 1,5,7-triazabicyclo[4.4.0]dec-5-ene base (TBD), already present from its use a catalyst from the chain-extension polymerisation of the PCL diacrylate, via a thiol-ene Michael addition with a tetrathiol cross-linker. As a result, shape-memory materials were produced, with the ability to be temporarily re-formed, and recovered by simply heating. The presence of ester bonds within polylactide network, built from the chain-extension/cross-linking reaction between 4-arm star poly((+)lactide) and methylenediphenyl diisocyanate using $Sn(oct)_2$ as a catalyst, allowed for the formation of vitrimers. The materials were engineered to fully relax after just 1000 s at 120 ºC.

Due to the nature of the reverse transesterification reaction requiring the presence of a catalyst, catalyst leaching - and subsequent inefficiency of the reverse reaction - is a major problem inherent to vitrimers based on the exchangeable ester bond.

Vinylogous Urethane Exchange

As an alternative to the transesterification exchange, *Du Prez* and co-workers investigated the application of vinylogous urethane moieties instead of amide bond within thermoset cross-links.[97] They noted that the benefit of the thermodynamically more favoured amide bond was also the drawback, as the exchange reaction would require more chemically-demanding conditions. To avoid this problem, the chemically related vinylogous urethane was

explored (Scheme 12c), displaying reversible network formation with only the use of heat as a stimulus.

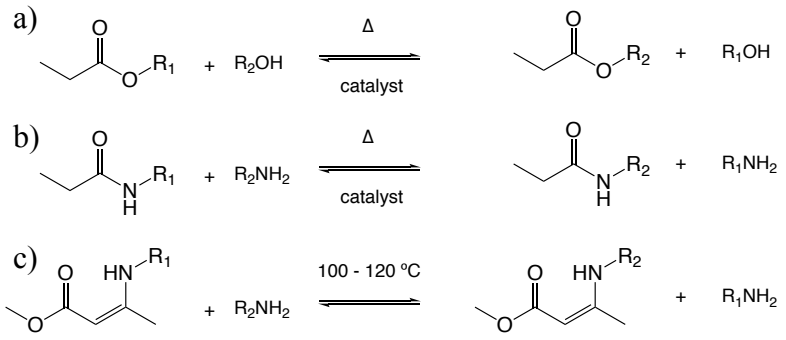

Scheme 12– a) Transesterification exchange; b) transamidation exchange; c) Vinylogous urethane exchange.

Synthesis of the cross-linked materials was achieved by condensation polymerisation of a diacetoacetate and di- and tri-amine functionalised cross-linkers. The resulting material was found to relax following the Arrhenius Law, with full relaxation being achieved after as fast as 85 s. The material could be recycled, after grinding, by compression moulding, with the recycled material displaying no change in either the Young's modulus (~2.4 GPa) nor stress at break value (~90 MPa).

Most recently, the use of a wide range of catalysts was investigated with the aim of gaining better control over the kinetics of vinylogous transamination. It was shown that a fine degree of control over the reaction kinetics, and hence the time/temperature needed for full relaxation of the material, can be obtained by careful selection of the catalyst additive.[98]

Transcarbamoylation

Another analogue of the urethane bond, the oxime-carbamate, was recently implemented in a dynamic polymer network.[42] In these systems, and conversely to classic polyurethane synthesis, no catalyst was needed to produce poly(oximes) from the proposed reaction between hexamethylene-1,6-diisocyanate and oxime-functionalised triethylene glycols (Scheme 13). This work has strong relevance to the current-day synthesis of polyurethanes due to the need for only slight alteration of commercially available starting materials – the oxime functionality is readily obtained from polyols and the diisocyanate needs no modification.

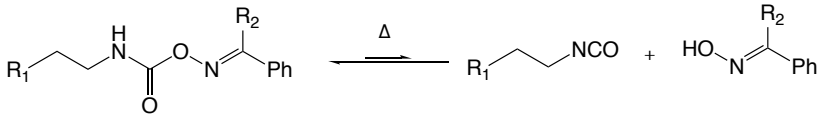

Scheme 13 – Transcarbamoylation exchange.

Using this chemistry, the robust dynamic materials produced were found to display remarkable elasticity and strength (stress 49.1 MPa, strain 677%), which regenerated structural integrity impressively close to the pristine material after being recycled (by hot-press) as many as four times.

Boronic Ester Exchange

Chemists' limited control over exchange kinetics within bulk materials, and hence their inability to control and tune the physical behaviour of these materials, was addressed by *Guan et al.* in 2015.[99] The strategy to gain this control was through the synthesis of a dynamic polymer network containing two distinct boronic esters (Figure 17) as cross-linking moieties: one that undergoes exchange at a faster rate than the other. Ring-opening polymerisation of di-hydroxycyclooctene produced the 1,2-diol-containing polymer backbone, which was subsequently cross-linked by condensation with either boronic ester cross-linker.

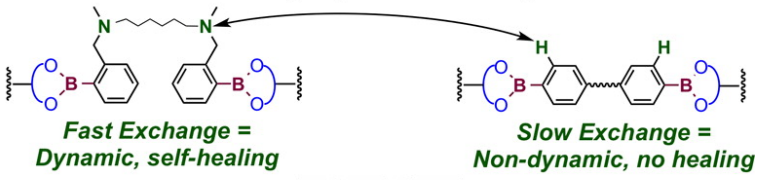

Figure 17 – Schematic representation of two distinct boronic ester cross-linkers displaying differing exchange rates.[99]

More recently, this chemistry was applied to three of the most commercially used polymer backbones: poly(methyl methacrylate), polystyrene, and high-density polyethylene.[100] In this work, the vitrimers were prepared by controlled radical polymerisation (for PMMA and PS) and post-polymerisation condensation of the boronic ester with the 1,2-diol-functionalised polymer. In each publication, both 2015 and 2017, the rheological properties of the materials could be finely tuned by altering the polymer molecular weight, the fraction of fast/slow exchanging boronic ester used, and the cross-link density. Optimised materials had relaxation times of as short as 13 seconds, and could be ground and reprocessed using injection-moulding, extrusion, or compression-moulding.

Transalkylation of Triazonium Salts

Alkylated triazonium salts, and the exchange reaction between them, were used as the chemical basis for the synthesis of dynamic alkane networks. In a recent study,[58] a polymer backbone was produced from the thermal alkyne-azide cycloaddition 'non-click' reaction between α-azide-ω-alkyne functionalised alkanes, and simultaneously cross-linked using bis-halogen-functionalised alkanes. Two exchange mechanisms have been suggested: nucleophilic attack of a counter ion on the triazonium, followed by dissociation and reaction with the alkylhalide cross-linker; or a concerted exchange between alkylated triazonium salts and unalkylated triazoles (Scheme 14).[12] Conducive to the expected behaviour of vitrimers, the materials based on cross-links of triazonium salt showed stress-relaxation behaviours that follow the Arrhenius Law, with full relaxation observed within 30 minutes at 130 ºC and seconds at 200 ºC. By substituting the counter ion with a counter ion of differing electronegativity, tuning of the relaxation times can be controlled.

When compared to vitrimeric materials produced by other chemistries, vitrimers based on alkylated triazonium salts are more expensive, less easy to scale up, and use hazardous reagents that would likely prohibit their production on a large scale.

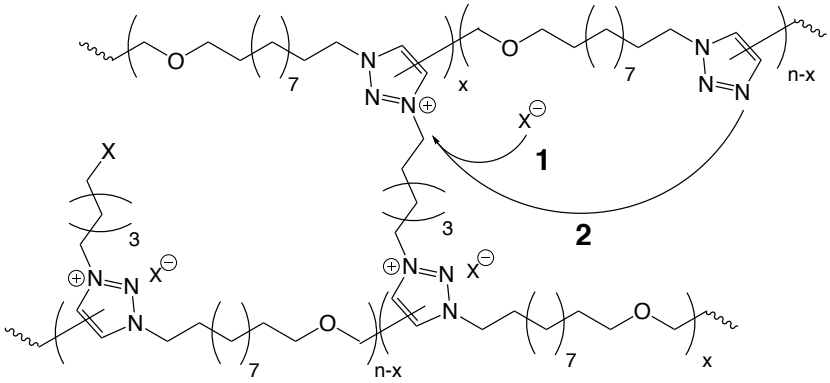

Scheme 14 –Transalkylation of triazomium salts via 1) nucleophilic attack of a halide counterion, or 2) concerted exchange.

Siloxane Silanol Exchange

Research into the addition/elimination reaction of silanols, applied to dynamic covalent networks, was revitalised by *McCarthy et al*, having spent almost six decades relatively unexplored since its inception in 1954.[101] Stress-relaxation experiments of PDMS networks were previously qualitatively investigated, showing increased rate of relaxation in acidic or basic conditions.[102] Thermal degradation of similar materials were also observed due to

hydrolysis and the formation of cycles; to avoid this, silanoate tetramethylammonium salts were devised as initiators of rapid exchange below 130 ºC converting any permanent cross-links into base-catalysed 'living' chain ends.[103]

Olefin Metathesis Exchange

Cross-linked polybutadiene networks, previously thought to be permanently fixed, were successfully rearranged via olefin metathesis using Grubbs' second generation catalyst.[104] [105] The polybutadiene networks were prepared by conventional free radical cross-linking in benzoyl peroxide, before being swollen in DCM and subsequent addition of Grubbs' catalyst.

Physical analysis of the response of the material to exchanging cross-linking points revealed decreasing Young's modulus with increasing catalyst loading, and a strong dependence of stress-relaxation on catalyst loading (following an exponential decrease in modulus), whereas control materials that did not contain Grubbs' catalyst displayed no adaptive properties.

Photochemically Reversible Networks

Thiol/Ene "Click" (Allyl Sulfide)

As well as photocyclisation, as used in the dissociative Diels-Alder chemistry detailed earlier, light-induced radical-mediated addition-fragmentation also yields materials capable of physical adaptation when stimulated by light. Using allyl sulfide bonds as cross-linking points has been a particular focus of the *Bowman* group and has been implemented within networks based on ethylene glycol as well as methacrylate backbones.[106–109] The addition-fragmentation chain-transfer (AFCT), by which the allyl-sulfide are dynamic, was studied in the context of stress relaxation; it was found that the photo-induced AFCT demonstrated a >75% reduction in final stress after polymerisation.[109] Adhesive applications for these materials have been suggested, wherein the substrate, on which the polymer is applied, is sensitive to stresses.

1.2.4 Dynamic Covalent Networks Based on Imine Chemistry

The Imine Bond

The dynamic covalent bond used to build the dynamic materials in this project was the imine bond. The main chemical and physical characteristics of the imine bond, and of materials based on polyimines (or close analogues), will be discussed in the following section.

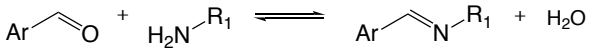

Scheme 15 – Condensation reaction between an aromatic aldehyde and a primary amine to form an imine and water.

Discovered by Hugo Schiff in 1864,[110] the product of the condensation reaction between primary amines and aldehydes, the imine (Scheme 15), is an important reversible tool used by organic chemists for the past 150 years. Azeotropic conditions are usually used, with continuous removal of water (by heating under reflux and using drying agents) driving the reaction toward the formation of the imine. Three types of equilibrium controlled reactions have been observed in imine chemistry:[111]

a) *Hydrolysis* – In the presence of water, the imine bond can be converted back to its starting materials (Scheme 16). This reaction is both acid- and base-catalysed.

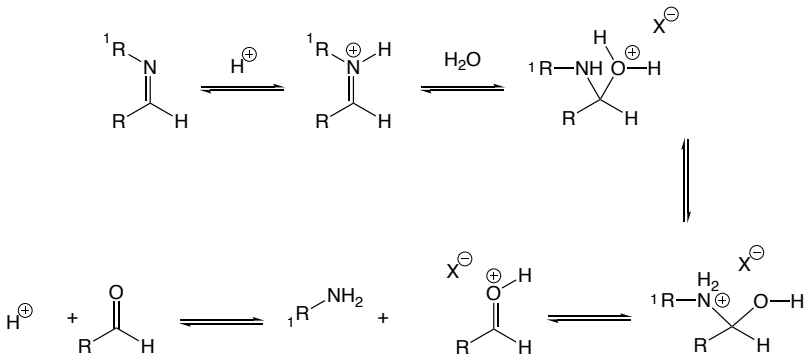

Scheme 16 – Proposed mechanism of imine hydrolysis – in the presence of acidic water

b) *Exchange* – In the presence of primary amines, imine bonds undergo transimination via nucleophilic attack of the amine on the protonated imine. The produced imine contains different R groups (Scheme 17);

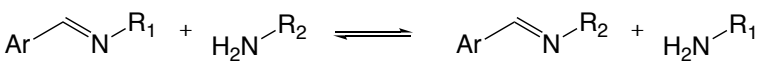

Scheme 17 – Transimination exchange.

c) *Metathesis* – In the presence of imines containing different R groups, exchange of the differing imines can occur, resulting in new imines that contains new combinations of R groups (Scheme 18).

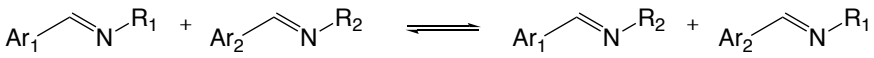

Scheme 18 – Imine metathesis

Kinetics of Imine Formation and Exchange

The kinetic rates of these reversible and exchangeable reactions can be strongly influenced by the nature of the R group. Condensation of aromatic aldehydes and aliphatic amines yield imines that are considerably more stable to hydrolysis than any other combination of R groups; this is due to the stronger nucleophilic nature of aliphatic amines and stronger electrophilic nature of aromatic aldehydes compared to their counterparts.[112,113] Structural effects on the rates and equilibria of imine formation and exchange are still poorly understood. Analysis of the transimination reaction between an imine based on an aromatic amine with an aliphatic amine (in organic solvent), by ^{1}H NMR, proved that the formation of imines from aliphatic amines was favoured by more than an order of magnitude: $k_{aliphatic} = 0.6\ M^{-1}s^{-1}$ vs $k_{aromatic} = 1.7 \times 10^{-2}\ M^{-1}s^{-1}$. The kinetic rate of the reverse and exchange reactions can also be strongly influenced by pH – both acid and base can act as a catalyst for imine formation, with acid enhancing the electrophilicity of the aldehyde by protonation, and base facilitating the dehydration, however mechanistic study of imine formation in organic solvents is still rare.[114] The chemical model for the formation of imines in aqueous conditions, proposed by *Hine* and *Via* and *Lehn et al*., details the formation of an intermediate species (hemiaminal) between reagents and products (Figure 18).[115,116] The rate of imine exchange is widely accepted to be accelerated by some degree in acidic conditions due to the protonation and thus enhanced electrophilicity of the imine.

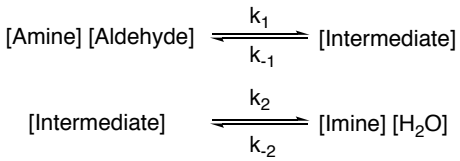

Figure 18 – Formation of an imine from aldehyde and amine via an intermediate

The kinetic rate of the reverse and exchange reactions can also by influenced by other catalysts. Microencapsulated scandium triflate was used by *Giuseppone et al*. to generate dynamic combinatorial libraries of imines, which typically have the strong requirement of fast exchange between library members.[116] Tris(2,2,2-trifluoroethyl)borate [$B(OCH_2CF_3)_3$] was investigated by *Reeves and co-workers* finding its use as a versatile catalyst for the condensation of a variety of primary amines and aldehydes, with up to 100% conversion in 1 hour.[117]

Extension of the imine reaction from small molecules to polymeric materials (using the imine formation and exchange as the covalent bonds with which polymers are formed) should be viewed through the lens of polycondensation. As condensation polymerisations follow a step-growth mechanism, the molecular weight (i.e. the degree of polymerisation) and the polydispersity index (PDI) of polyimines is dependent on the 'functionality conversion (p)'. Driving the reaction toward the formation of imines, using any of the methods described above, will therefore increase the molecular weight (this inverse proportionality is shown below in the Carothers equation), and decrease the polydispersity index of the resultant polymer. Further, precise control over the functionality conversion will give precise control over the molecular weight.

$$DP = \frac{1 + r}{1 + r - 2rp}$$

Equation 2 – Equation mathematically describing the degree of polymerisation of a step-grown polymerisation (DP = degree of polymerisation, r = stoichiometric ratio, p = functionality conversion).

$$PDI = 1 + p$$

Equation 3 – Equation mathematically describing the polydispersity index of a step-growth polymerisation.

$$p = \frac{(N_0 - N)}{N_0}$$

Equation 4 – Equation mathematically describing the functionality conversion (p) (N_0 = amount of starting funtionality, N = amount of functionality after the reaction is finished).

Materials Based on the Imine bond

Imine within the main-chain

A number of studies have been conducted on polymeric materials that contain imine linkages within the polymer backbone, produced through polycondensation of aldehyde and

amino-functionalised monomers. Extra attention should be paid in noting the linear or cross-linked natures of these materials, making only appropriate comparisons.

Recently the *Zhang* group developed polyimine networks based on the condensation of terephthaldehyde and a mixture of diethylenetriamine and tris(2-aminoethyl)amine. The resulting cross-linked materials were found to possess a T_g of 58 ºC and a stress at break value of 40 MPa. When stress relaxation experiment were conducted on the materials, an Arrhenius temperature dependence was found, conducive expectations of vitrimeric behaviour. When ground, the material could be recycled by heat compression moulding. Interestingly malleability of the materials could be induced by soaking in water, reshaping the material and allowing to dry, resulting in a new fixed shape.[118] This work was further investigated by incorporation of the polyimines into woven carbon fibre composites;[119] the resulting material showed an order of magnitude increase in tensile strength (400 MPa), with only a slight decrease in elongation (strain%) at break – from 5% in the unreinforced to 3.3% in the reinforced materials.

Imine-Derivatives on the Side-Chain

The formation of a linear co-polymer (more specifically a dimer of two different polymers), with an acylhydrazone linkage, by the reaction between hydrazide-functionalised poly(ethylene glycol) and aldehyde-functionalised poly-styrene, was conducted by *Zhu and co-workers*. The produced amphiphilic dimer was found to self-assemble into different morphologies (such as micelles, short branched rods, vesicles and LCVs) at room temperature, as a result of the dynamic hydrogen-bonding interactions between the acylhydrazones. Reversibility of the dimer was achieved by hydrolysis of the acylhydrazone in aqueous acidic conditions.[120]

In 2005, *Labo Lehn* reported the synthesis of two linear polyacylhydrazones from the condensation of bis-hydrazine and dialdehyde-functionalised monomers. It was observed that, when dissolved in acidic DMSO and mixed, exchange between the acylhydrazones of the two polymers (up to 32% in three days) occurred in solution at room temperature.[121,122] Subsequent studies from the *Lehn* group, in which the effect of the presence of the hydrogen bonding interaction between carbonyl and secondary amine of acylhydrazones,[123] as well as the introduction of π-stacking moieties and chemical moieties capable of sensing metals among others,[124–127] is discussed later in this chapter.

Imines on the Side-Chain

The functionalisation of polymers with imine linkages (and their derivatives) along the side of the backbone has also been explored by a number of groups. A variety of different polymer morphologies, such as bottlebrushes,[128] core cross-linked stars (CSS)[129] and amphiphilic linear block co-polymers,[130] are accessible with side-chain imine-functionalised polymer backbones. Most relevant to this project, are the examples in which side-chain functionalisation has been used to produce cross-linked polymer networks; most previous work using this approach, however, use these new materials to make pH responsive hydrogels.[131] The swollen state of the polymer networks drastically change the physical behaviours of the material, and so cannot be used to compare the work in this project. Interestingly, many of these examples are based on backbones composed of bio-based polymers, continuing the movement away from backbones produced from non-renewable sources.[132,133]

Recently, *Zhao* and *Xu et al.* introduced amine functionalities on side-chains of polybutadienes, by post-polymerisation modification via the thiol-ene 'click' reaction between 1,2-alkenes, along the polybutadiene backbone, and cystamine. After cross-linking with benzene-1,3,5-tricarbaldehyde, stretchable and robust transparent polymer films were found (E = 1.1–31.4, elongation at break = 41–75%). The materials were found to be re-mouldable and recyclable by hot pressing (with sufficient energy to reach the E_a of imine exchange).[134]

1.2.5 Applications

To consider the possible applications of dynamic covalent materials, it is reasonable to look at applications in which analogous materials – thermosets and thermoplastics – are currently utilised. Applications that have been suggested and targeted by other groups will also be addressed.

A vast quantity of elastomers, using non-dynamic cross-linking chemistries, are used as gaskets or sealants. Damage of these materials usually often occurs in the form of microscopic cracks which eventually lead to complete degradation. Using dynamic materials as direct replacements for these conventional materials would require the new materials to possess similar robustness to temperatures, pressures and weathering conditions.[76] In a similar way, but on a more macroscopic scale, welding of plastics could be used to repair larger scale damage of materials.[135] An example may be the repairing of punctured tyres or inner tubes, which are currently, at best, repaired by glues possessing different (and hence sub-optimal) physical properties.

The use of dynamic materials, in place of thermosets, as electronic insulators is suggested by *Iyer* and *Wong*,[136] whereby, upon damage of the insulator, it may be heated and washed away with solvent as opposed to stripping and reworking the circuit, as is the conventional approach. In the field of non-linear optical materials, the use of thermally-activated dynamic cross-links between dendritic optical chromophores can enhance their stability as well as temporarily curing them, allowing for the introduction of a second chromophore without inducing phase separation.[137]

As mentioned briefly in previous sections, dynamic covalent networks have also been used to create thermally, chemically and photo-reversible hydrogels. Hydrogels are widely seen, and have been increasingly used, in the domain of tissue engineering and drug delivery (in the form of vesicles) due to their physical likeness to biological tissues and proteins. The use of these stimuli responsive networks could give the ability to selectively dissolve chemical cross-links to release chemical payloads or flush tissue scaffolds away.[138]

Curing contraction, i.e. the contraction of a material due to the decrease in volume as monomers are polymerised, can lead to the generation of stress on a surface on to which the polymer may be applied. These physical phenomena cause problems in the domain of dental materials, whereby a gap between a cavity and filling can allow space for bacteria to thrive, or the tooth may be damaged due to stress caused by the filling material itself. The presence of exchangeable bonds within polymer materials has been proved to generate considerably less surface stress and curing contraction.[76,139]

Acylhydrozone-based polymers mentioned briefly above, and which will be elaborated later on, have been shown to selectively complex with alkali metal ions, and generate different optical signals in the presence of specific ions - these materials may be useful as sensors.[124]

1.2.6 Drawbacks

As mentioned when describing the seminal work of *Leibler et al*., with their synthesis of DCNs via the transesterification reaction, the main drawbacks faced by groups in the field is the limited control over the kinetic rate of exchange of the dynamic system. The main method that has been used to increase kinetic control requires the incorporation of high concentrations of solvent within the materials, however, this causes problems with catalyst leaching out from the materials, an increase in the cost of synthesis and potential danger from toxicity of the catalyst. The method that was undertaken to solve this lack of kinetic control in this project

was to introduce a second dynamically exchanging chemical functionality which exchanges at a faster kinetic rate.

A common issue with many of the dynamically cross-linked materials is stress-relaxation from strains held over long time periods, as well as creep. Creep and stress-relaxation are inherent to the dynamic exchange due to the adaptation of the materials to their newly elongated shape. To overcome this, researchers must find a way to kinetically 'freeze' the dynamic exchange (or sufficiently slow the exchange to negligible rates) at operating temperatures.

1.3 Supramolecular Polymers

The development of supramolecular chemistry, i.e. the study of non-covalent interactions between molecular species, has been of keen interest to polymer scientists with the ambition to obtain dynamic materials, for almost thirty years.[140] The idea of non-covalent assemblies was, however, not far from the discussion at the very inception of the reasoning for what constitutes classical, covalently-bonded polymers. Although facing little controversy today, Staudinger's explanation, that macromolecular species are held together by covalent bonds, faced strong criticism. Critics argued that single molecules with a large M_w do not exist, but instead polymers, like silk and rubber, were rather non-covalently bonded aggregates – "*Dear colleague, abandon your idea of large molecules, organic molecules with molecular weights exceeding 5000 do not exist. Purify your products such as rubber, they will crystallize and turn out to be low molecular weight compounds.*" - H. Wieland.[1] It is an ironic twist of fate that polymer chemistry should come full-circle, with this pronounced interest and fast progress using similar chemical theory to that which was disproved almost a century ago.[141]

1.3.1 Defining Supramolecular Polymers

Polymers may be functionalised with supramolecular moieties in a variety of different ways, with the supramolecular bond having differing influence on the physical properties of the resulting material. Supramolecular polymers may be composed of a backbone of small monomers held together by non-covalent, rather than covalent, interactions (Figure 19);[142] main-chain supramolecular polymers extend this concept to the non-covalent linear chain-extension of larger, covalently bonded, telechelic pre-polymers (Figure 20);[143] covalent polymers may be functionalised with supramolecular moieties at pendent positions along the backbone (side-chain), either chemically attached dangling from or intrinsic to the backbone itself, and act as cross-linking nodes (Figure 21).[144,145] If we look at polymer networks held together with cross-linking nodes of supramolecular nature in the same paradigm as we established in the previous section, i.e. associative and dissociative dynamic networks, it is clear to see that these networks can be considered predominantly *dissociative*, as complete dissociation of complementary moieties is (almost always, depending on the non-covalent bond used) necessary for exchange between supramolecular groups.

Figure 19 – Cartoon representing the difference between classical covalent polymers (left) and supramolecular polymers (right).[142]

Figure 20 – Cartoon representing main-chain supramolecular polymers (red object represents a self-complementary supramolecular moiety, black line represents a classical covalent polymeric backbone.

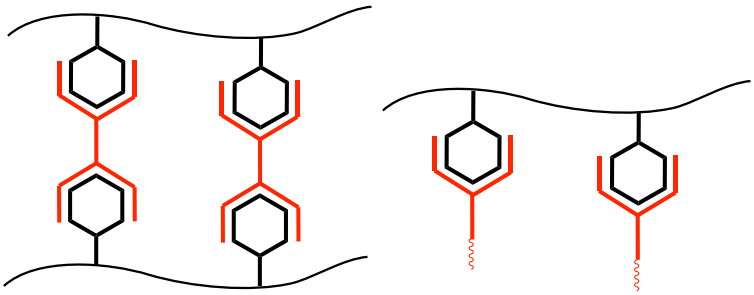

Figure 21 – Cartoon representing side-chain supramolecular polymers (black hexagon represents a side chain hetero-complementary supramolecular moiety, red object represents a complementary cross-linker/functionalising agent.

1.3.2 Physical Characteristics

Supramolecular Polymers

The physical characteristics of polymers composed of small monomers held together by non-covalent interactions strongly depend on both the physicochemical nature of the bonding and the chemical structure of the small molecule itself. To produce linear supramolecular polymers with molecular weights comparable to their covalently bound counterparts, the non-covalent interactions must be both strong (high K_a) and directional. The presence of impurities may also have a drastic effect on molecular weight, therefore a high degree of purity is also required. Many of the non-covalent interactions that are used to form supramolecular species are strongly affected by temperature, resulting in unconventional temperature dependence of the materials.[142] Most often, supramolecular polymers of this definition are studied in either the sol or the gel, with further working into bulk materials almost never conducted;[146] this is due to the important influence of solvents on the formation of supramolecular aggregates.[147] These soft materials have been proposed for a variety of

applications, from use in biomedicine as filaments used to signal cells, to semi-conducting nanofibers and photoconductive nanowires used in molecular electronics.[148]

Main-Chain Supramolecular Polymers

Systems that fall into the category of main-chain supramolecular polymers display physical properties that are strongly dependent on the telechelic polymer backbone on which they are based. One of the main benefits of using supramolecular bonds as the chain-extension chemistry for (macro)monomers, is the ability to easily tune the polymeric composition of the system, and, therefore, easily tune the resulting physical properties of the material.[143] This ease of tuning results from the dynamic and stimulus-responsive nature of the supramolecular interactions that hold the (macro)monomers together. As with the *supramolecular polymers* mentioned above, the molecular weight of main-chain supramolecular polymers is strongly dictated by the strength of the non-dynamic associations between supramolecular moieties (K_a).[149,150] Any decrease (which can be achieved using a multitude of different stimuli) in K_a will push the system towards de-polymerisation. The extent of de-polymerisation of main-chain supramolecular polymers goes beyond any covalently bonded alternative – thermoset materials cannot be melted and linear thermoplastics are very viscous in the melt, whereas the viscosity of main-chain supramolecular (macro)monomers may be considerably lower, due to their lower M_n.[150]

The responsiveness to stimuli also unlocks possibilities of repair to localised damage; self-healing systems based on main-chain supramolecular polymers have been demonstrated using heat, light mechanical stress and pressure.[75,150,151] One physical property that must be considered for this avenue of development, is the freedom with which polymer chains may move over one another; rubbery materials (above their T_g), therefore, make particularly good polymeric targets.[152]

Side-Chain Supramolecular Polymers and Supramolecular Polymer Networks

Similarly to main-chain supramolecular polymers, the physical properties of systems containing supramolecular moieties on the side-chains are largely controlled by the nature of the polymeric backbone. As the polymer backbone, on which the supramolecular moieties are attached, are covalently bonded macromolecules, depolymerisation beyond the size of the backbone itself is not possible. The supramolecular bonds in side-chain-functionalised systems are mainly reserved for one of two functions: pendent functionalisation or cross-linking.

Pendent functionalisation of polymeric backbones has been used to create materials with non-covalent liquid crystalline mesogens, by post-polymerisation modification;[153] functionalisation of polymer backbones with moieties capable of forming complementary pairs with nucleic bases, has also been achieved by a modular 'plug and play' strategy. Both post-polymerisation modification and 'plug and play' are well-described ways by which polymers may be functionalised at pendent positions to achieve materials with new dynamic behaviours.[145154] The non-covalent self-assembly of supramolecular species along the same polymer backbone has also been described. This 'self-functionalisation' strategy encourages supramolecular-driven folding of macromolecules.[155]

Cross-linking side-chain functionalised supramolecular polymers has most commonly been achieved using hetero-complementary motifs. This system has been demonstrated by either the incorporation of hetero-complementary pairs on two distinct polymer backbones followed by mixing, or by introduction of the pairing moiety as a small molecule.[155] Side-chain functionalisation of polystyrene and poly(methyl methacrylate) backbones with diamidopyridine and UPy respectively, yielded blended cross-linked films.[156]

A distinction, that is rarely made when assessing side-chain supramolecular systems, is the different nature of bonding between the polymer backbone and supramolecular moiety. It is regularly the case, in both post-polymerisation and plug and play strategies, that the supramolecular unit is attached with branching chains on the polymer backbone (usually with an alkyl spacer), rather than intrinsically to the polymer backbone itself. These two systems are often conflated, but differing physical properties can arise from the presence of the alkyl spacer. Kevlar®, for example, displays an extremely high tensile strength-to-weight ratio due to the regularity of spacing between amide units, as well as rigidity of the aromatic polymer backbone, which would not be the case if the aromatic amides were present on branching chains.[13] The prevalence of side-chain-functionalised polymers in nature is also often referred to, exemplified using DNA and peptides, but fail to mention the rarity with which one finds the supramolecular moiety attached with pendent spacers, or in a branched manner. The work in this thesis draws much closer analogy to these systems found in nature, as the hydrogen bonding UPy is intrinsic to the polymer backbone, rather than dangling from pendent branching chains.

1.3.3 Mechanisms of Association

Supramolecular Polymer

Unlike the polymerisation of covalently bonded polymer, where the equilibrium of the reaction is shifted firmly toward polymerisation and hence is under kinetic control, thermodynamic parameters, such as concentration, temperature and pressure, have a significant effect on the degree of polymerisation of supramolecular polymers. There are three major mechanisms by which supramolecular polymers grow: isodesmic, ring-chain and cooperative. Isodesmic is analogous to the step-growth polymerisation of condensation or addition polymers, with the degree of polymerisation strongly dependent on the K_a of the monomers; ring-chain is dependent on the equilibrium between cycling and linear species, and so concentration is a dominant parameter; and the cooperative mechanism proceeds in a nucleation and growth fashion.[157,158]

Main-Chain Supramolecular Polymer

Similarly to classical supramolecular polymers, the equilibrium in main-chain supramolecular polymers is strongly affected by thermodynamic parameters. The equilibrium between monomers, oligomers and polymers can be influenced by any external stimulus that influences K_a of the non-covalent interactions between the telechelic species, such as temperature, concentration, pressure, and pH. The equilibrium between cyclic and linear species is also a key factor, affected by (macro)monomer M_w flexibility, concentration, temperature, directionality and strength of binding motif. Unlike in supramolecular polymers, the degree of polymerisation of a main-chain supramolecular polymer may also be influenced by the presence of chain-stoppers (i.e. small molecules with the same non-covalent binding motif, but not attached to a (macro)monomer).[149]

Again, there are three mechanisms by which main-chain supramolecular polymers may grow: isodesmic, nucleation-growth and 'open supramolecular liquid crystal' (SLC).[149] Similarly to the isodesmic mechanism by which supramolecular polymers may grow, the isodesmic mechanism governing main-chain supramolecular polymerisation states that the degree of polymerisation is strongly dependent on the K_a of the binding motif (Equation 5, Figure 22a). A nucleation-growth mechanism may occur when additional binding motifs are activated upon the initial non-covalent bonding or upon reaching a certain degree of polymerisation (C^*). These additional binding motifs may stabilise, or be additive to, the initial

binding constant, thus increasing K_a and the degree of polymerisation. The open supramolecular liquid crystal mechanism for supramolecular chain-extension is reserved for systems in which the specific spatial and orientation ordering of the binding motifs imparts liquid crystalline properties into the material. In this case, polymerisation proceeds in a stable manner until a critical concentration at which nematic ordering is reached (C_i), presumably stabilising and increasing the binding constant and hence sharply increasing the degree of polymerisation.

$$DP = \sqrt{K_a[M]}$$

Equation 5 – Equation mathematically describing the degree of polymerisation of a supramolecular polymerisation for isodesmic growth.

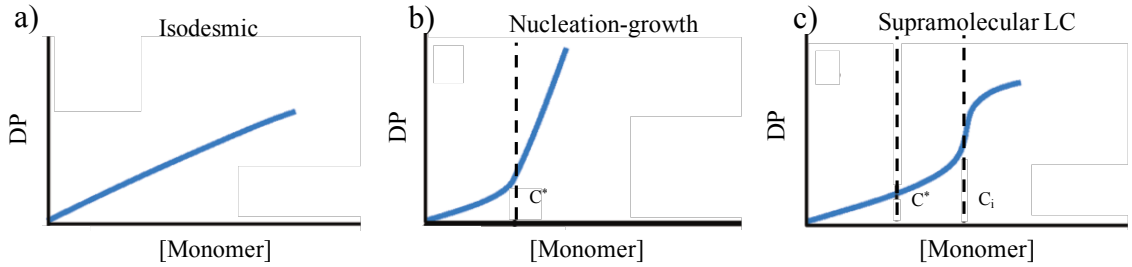

Figure 22 – a) Graph of the evolution of the degree of polymerisation for an example isodesmic supramolecular polymerisation.; b) Evolution of the degree of polymerisation for an example nucleation and growth supramolecular polymerisation; c) Evolution of the degree of polymerisation for a cupramolecular liquid crystal polymerisation.[149]

Side-Chain Supramolecular Polymer and Supramolecular Polymer Networks

The mechanism and kinetics of the formation of networks, with cross-linking driven by supramolecular bonding, from side-chain functionalisation has been studied in less detail than the other two regimes, mentioned above. The relationship between association constant and degree of polymerisation, does indeed hold for both linear and cross-linked supramolecular polymer systems.[146] Analysis by *Rubinstein* and *Semenov* determined expressions that describe the gelation behaviour of systems containing 'stickers' along the polymer backbone. Their work considered the probabilities of the supramolecular moieties associating in an intra-chain or inter-chain fashion, depending on the density of stickers along the backbone, and the concentration of the system (Figure 23). *Rubinstein* and *Semenov* reached a number of conclusions: continuous reversible gelation is not a thermodynamic transition as all thermodynamic parameters are constant at the gel point; phase separation must accompany gelation, unless strong excluded volume monomer-monomer repulsions are present; and that

gelation implies that intra-chain associations are replaced by inter-chain associations, with repulsion between non-associating pairs shifting equilibrium toward association and thus promoting gelation and cross-linking.[159]

Although not exclusive to side-chain supramolecular systems, the consequence of the clustering of supramolecular moieties and hence the formation of domains rich in cross-linking nodes, producing in homogeneous structures, may result in a net increase in the strength of the materials due to cluster-enhanced associations.[146]

The dynamic behaviour of systems cross-linked by supramolecular bonds is influenced by both the timescales with which supramolecular bonds form and break, and the relaxation of chains or chain segments of the polymer backbone; the former is largely governed by the equilibrium of binding constants, and the later by more classical physical descriptions of polymer chain dynamics (namely reptation). It can be summarised that the extent of cross-linking is, in fact, governed by the rate of dissociation, i.e. a slow rate of dissociation produces strong cross-linking.[146]

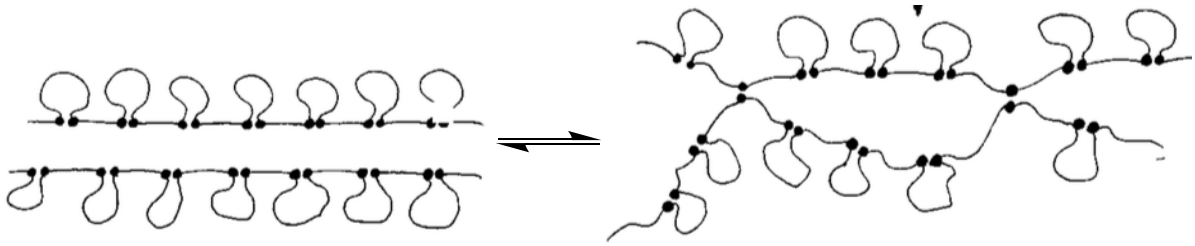

Figure 23- Cartoon representing the physical behaviour of polymer containing 'stickers' along the polymer backbone.[159]

1.3.4 The Chemistry of Supramolecular Polymer Networks

Due to the fact that the field of supramolecular chemistry, and its synthesis with polymer chemistry, is so well established, a multitude of different non-covalently bonding motifs have been explored in deep detail. Extensive reviews of the field, that detail the chemistries used to construct supramolecular polymers within each of the regimes that are detailed above, are available.[4,75,140,142,148,160–163] As the regime of *Supramolecular Polymers* does not describe the systems studied in this thesis, these will not be described in any further detail. Instead, main-chain and side-chain supramolecular polymers will be described, with a particular focus on elastic networks that are cross-linked by supramolecular bonds and studied in the bulk.

Hydrogen Bonding

One of the first discoveries and subsequent industrial-scale uses of man-made polymer fibres that are cross-linked by hydrogen bonding motifs (along the polymer backbone), came with Carothers' discovery of nylon. In fact, if one considers the hydrogen bonding nature of nylon adequate to classify it as a supramolecular polymer, then most thermoplastic materials (including polyurethanes) must also come under that same classification; for this reason, most academics do not, and the first 'true' supramolecular polymer comes some 50 years after the discovery of nylon. Since then, the field has been dominated by hydrogen bonding motifs as the supramolecular bond of choice.

The work of Stadler *et al*., between the '80s and '90s, involved the modification of linear polydienes (particularly polybutadiene) with a urazoylbenzoic acid derivative, by reaction with pendent alkenes, which undergoes self-complementary hydrogen bonding (Figure 24a and b).[164–166] The thermoplastic elastomer that was produced displayed classical rubber behaviour between –53 and 55 ºC, but with an unexpectedly high modulus, which was later attributed (by X-ray scattering) to a second degree of arrangement of the urazoyl (or carboxyl) moieties driven by dipole-dipole interactions.

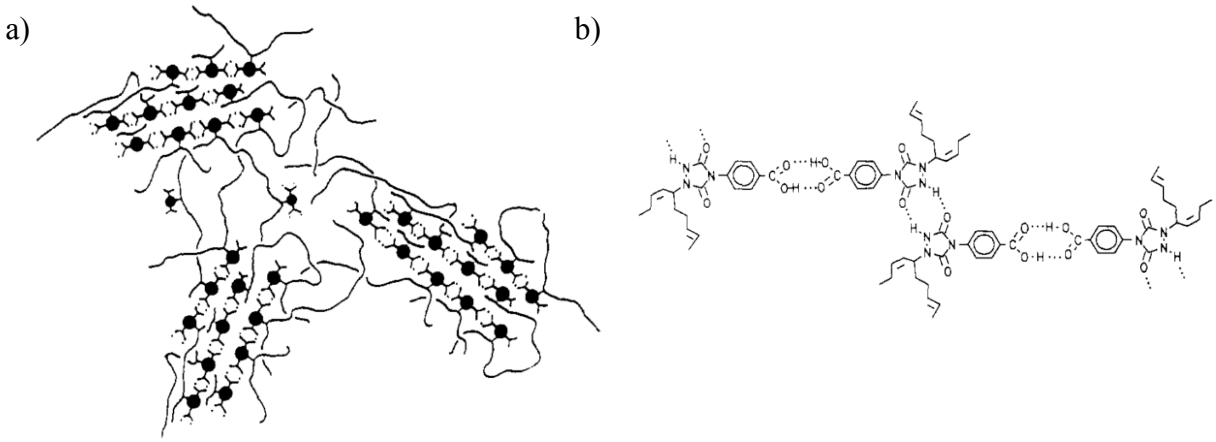

Figure 24 – a) Cartoon representing the functionalisation of polybutadiene with hydrogen-bonding chemical moieties;[164] b) Schematic representation of the hydrogen bonding of urazole-functionalised polybutadiene.[164]

The formation of bulk cross-linked networks, based on poly(propylene oxide) and pol(ethylene oxide) backbones functionalised with UPy (DF = 3), was demonstrated by *Meijer et al*., in 1999.[167] The networks that resulted displayed typical viscoelastic behaviours at room temperature, with a sharp decrease in viscosity when the temperature was increased. This

temperature-dependent viscosity was attributed to the dissociation of UPy dimers, and de-polymerisation of the network.

Since this publication, the UPy hydrogen-bonding motif has been the most popular motif used to form supramolecular polymer networks by many groups,[168–171] largely due to its ease of synthesis, ability to be attached to polymer backbones in a relatively modular fashion, and its high K_a (44-50 kJ/mol).[172] A variety of polymer backbones have been studied: polyurethanes from multihydroxyl-functionalised ε-caprolactone,[168] polysiloxane, polyethylene/butadiene, polyethers, polycarbonates and polyesters,[173] *branch*-polyhexene,[169] poly(butyl acrylate),[170] and *o*-phthalaldehyde-*co*-5-nitroisophthal-aldehyde,[171] among others. For this reason, the UPy unit was used as the supramolecular motif in this project.

There have been some publications reporting the incorporation of UPy within the polymer backbone, rather than attached from pendent chains, such as work from Meijer,[174] Baaijens and Weng.[175,176] In all cases, a bi-functional UPy synthon was produced, featuring isocyanate moieties flanking a central UPy core (Scheme 19). *Meijer et al*. co-polymerised this synthon with dihydroxyl-functionalised poly(ethylene glycol), forming linear polyurethane hydrogels, which were observed to microphase separate into disorganised dispersions, in both the dry and swollen states.[174] *Baaijens et al*. investigated the incorporation of similar UPy motifs into dihydroxyl-functionalised poly(propylene adipate) (2000 g/mol) backbones. The produced polyurethane-based materials from this work, studied in the bulk, were found to possess viscoelastic behaviour, depending on the nature of the flanking isocyanates.[175]

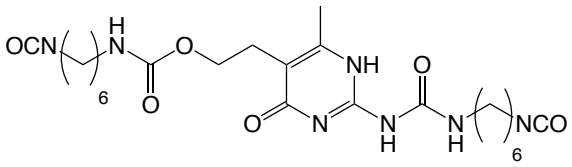

Scheme 19 – Diisocyanate-functionalised ureidopyrimidinone.

When the spacers between the resulting urethane were linear in nature (using hexamethylene-1,6-diisocyanate (HDI)), a rubbery plateau between -40 and 60 ºC was observed, with a modulus of ~10 MPa. When the flanking spacers were cyclic in nature and hence more rigid (using isophorene diisocyanate (IPDI)), a more linear transition from T_g to melt was observed, with no pronounced rubbery plateau. Both materials were observed to flow at ~60 ºC, with the linear synthon resisting temperatures up to 120 ºC. Elongation until break studies of both materials displayed thermoplastic elastomeric behaviour. For the material based on the flexible

synthon a higher Young's modulus, and therefore stiffer material was observed (E = 3.3 MPa) compared to the material based on the cyclic IPDI synthon (E = 1.7 MPa). The ultimate tensile stress was also found to be higher when using the linear synthon, but a lower strain at break was observed (σ_T = 2.4 MPa and ε_{max} = 3.1 compared to σ_T = 0.97 MPa and ε_{max} = 4.4, respectively) (Figure 25).

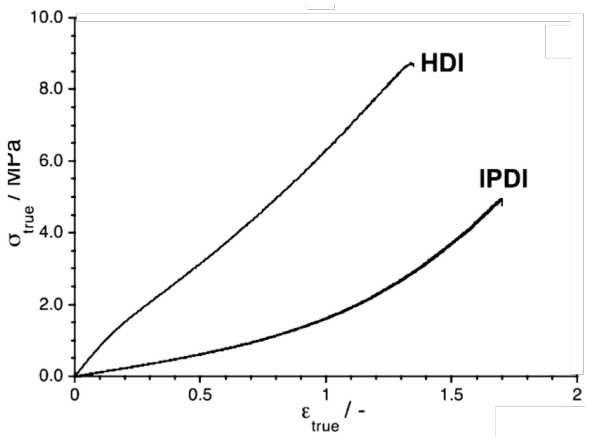

Figure 25 – Stress/strain behaviour of HDI- and IPDI-functionalised ureidopyrimidinone.[175]

The enhancement of physical properties of polyurethanes has also been explored by *Hayes et al*. in a study observing the effect of hard-end group composition on the thermal and mechanical properties of polybutadienes.[177,178] Chain-end modification of hydroxyl-functionalised polybutadienes was achieved by preparation of a diisocyanate pre-polymer before reaction with a varying composition of hydrogen-bonding morpholine moieties, producing a cross-linked elastic material. Mechanical analysis of the materials found that the inclusion of aromatic urea or urethanes in close proximity to the hydrogen-bond accepting morpholine moieties at the chain-ends, produced a more classical rubbery behaviour as well as higher ultimate tensile strengths (σ_T = 5 MPa).

In work by *Weck* and co-workers,[179,180] pendent functionalisation of poly(norborene) with thymine and/or cyanuric acid was achieved by ring-opening metathesis polymerisation of norborene-functionalised thymine and/or cyanuric acid, before crosslinking using bi-functional small molecules featuring two 'Hamilton wedge' motifs. The physical properties of the resulting viscous materials could be tuned, depolymerised, and a gel-sol transition initiated, by varying the degree of functionalisation and introduction of competing chain-stoppers.

Thermoplastic elastomers that were cross-linked by hydrogen-bonding urea moieties were produced, by *Bouteiller et al*.,[181] based on side-chain modified amine-functionalised

poly(dimethyl siloxane). Materials that displayed elasticity at room temperatures were produced, which underwent a melting transition at temperatures above 100 ºC, caused by de-cross-linking from the dissociation of the hydrogen-bonds.

Cross-linked networks have also been achieved using linear chain-end functionalised supramolecular polymers. The ability of barbituric acid to form hydrogen-bonding clusters, between multiple barbituric acid moieties, was used as the chemical impetus for work published by *Thurn-Albrecht and co-workers*.[182] Chain-end modification of azide-functionalised poly(isobutylene) with barbituric acid derivatives, by the copper(I)-catalysed alkyne-azide 'click' reaction, yielded self-healing elastic materials. Cross-linking could be observed, by X-ray scattering as disordered sphere-like aggregates forming a highly-connected supramolecular polymer network.

A final system involving a cross-linked hydrogen-bonding network, which has been well-explored by a number of groups, involves the association of small molecules into an elastic network. First described by *Leibler et al.*,[183,184] the interaction between di-and tri-functional fatty acids modified with amidoethyl imidazolidone, di(amidoethyl) urea, and diamido tetraethyl triurea, each with molecular weights below 300 g/mol, were found to form highly stretchable materials (ε_{max} = ~600 %) that could resist up to 3.5 MPa of stress. This material, consisting of relatively weak and disordered non-covalent interactions based on small cyclic monomers, is unprecedented. Continuation of this work, to decrease the creep behaviour of the material, saw the attachment of the imidazole and urea moieties onto a bisphenol and bis-aniline backbone.[185] The resulting polymer network was found to have a T_g at ~15 ºC, and modulus of between 0.05 and 1 MPa at room temperature, depending on the degree of cross-linking. Creep resistance was also achieved using this modification, while maintaining the self-healing ability of the material.

Metal-Ligand

The ability of metal centres to coordinate to a number of different ligands simultaneously has been the chemical foundation on which the next most popular non-covalent interaction used to create supramolecular networks, is based.[186]

Arguably the most common ligand/metal complexes that have been exploited to date are the terpyridine or bipyridine ligands, complexed with metal centres with and oxidation state of +2. A variety of reports have been published by the *Schubert* group whereby different macromolecular architectures have been synthesised by functionalising polymer backbones

either with the metal complex directly, or with an appropriate ligand before introduction of the metal salts that subsequently form the complex.[187] The use of a bipyridine ligand derivative to form cross-linked networks of polyacrylate, when complexed with Fe(II), Co(II), Mn(II) or Cu(II), was exemplified in 2015.[188] In this work, laurylmethacrylate was copolymerised with a methacrylate monomer that had been modified (by azide-alkyne 'click' chemistry) with the bipyridine analogue triazole-pyridine. After RAFT polymerisation of the monomers, and introduction of the metal salts, self-healing polymer networks were obtained. In a similar fashion, *Schubert et al.* reported the copolymerisation of terpyridine-functionalised acrylate monomers, which were also copolymerised with lauryl methacrylate via RAFT polymerisation.[189,190] Again, self-healing cross-linked films were obtained after addition of either iron(II) sulfate or a variety of Cd(II) salts. Interestingly, when co-polymerised with methyl methacrylate, no self-healing was observed.

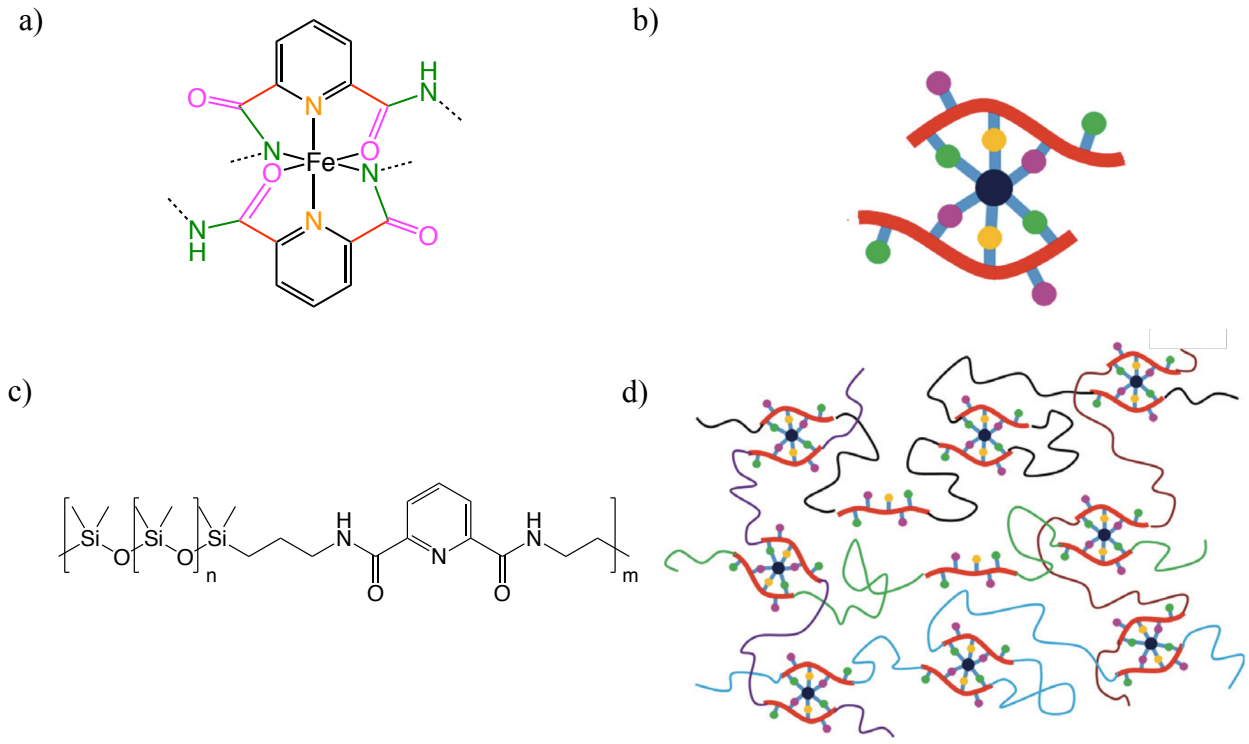

Figure 26 – a) Schematic representation of the meal-ligand complexation between iron(III) and 2,6-pyridinedicarbonyl (pdca); b) Cartoon representation of the Fe-pdca complex;[191] c) Schematic representation of a pyridine1,2-dicarbonyl-co-PDMS co polymer; d) Cartoon representing the network formed on addition of iron(III) salts.[191]

A highly stretchable self-healing cross-linked material, using a similar strategy to the work conducted in this thesis, was recently produced by *Bao et al.*.[191] In their work, α,ω-aminopoly(dimethylsiloxane) (M_n 5000–7000 g/mol) was copolymerised, by condensation polymerisation, with 2,6-pyridinedicarbonyl (pdca) dichloride, yielding a colourless viscous

liquid. Cross-linking was then activated by addition of iron(III) chloride, forming a dark red solid, resulting from the formation of the Fe(III)-pdca complex (Figure 26a–d). The resulting material was found to possess a T_g below –90 ºC (in accordance to PDMS-based materials), and resistance to heats up to 70 ºC. Rheological analysis of the materials revealed a low Young's modulus (0.54 MPa) at room temperatures, and a relatively linear transition from T_g to viscous flow on increasing temperature. On stretching the material, very high elongation values could be obtained (ε_{max}= ~3200 %) however, prominent plasticity deformation was observed at strains as low as 30%. The material was also observed to self-heal at room temperature and temperatures as low as –20 ºC, with a high healing efficiency (90% and 68% respectively).

Guan and co-workers utilised the ability of metal centres to complex with a number of ligands simultaneously, by creating a cross-linked polymer network from imidazole-functionalised polystyrene and Zn(II).[192] In this publication, styrene was first co-polymerised with 4-vinylbenzyl chloride, via free-radical polymerisation, before post-polymerisation modification with imidazole acrylate monomer, via RAFT polymerisation. The resulting imidazole modified polystyrene was then cross-linked with the formation of Zn-imidazole complexes, by addition of zinc di[bis(trifluoromethylsulfonyl)-imide], yielding a robust, non-tacky elastic solid. Thermal characterisation showed a ~40 ºC increase in T_g upon cross-linking, and good thermal stability beyond 200 ºC. The material was also found to be strong and stretchable, with ε_{max}= 77–695 % and σ_T = 1.1–7.0 MPa. Self-healing analysis also demonstrated the ability of the material to recover both Young's modulus and yield strength almost quantitatively, after cutting through the partial thickness of the material and allowing to recover in ambient conditions.

π-π-Stacking

The preparation of materials cross-linked by the π-π-stacking between electron-poor and electron-rich aromatic moieties has been studied in detail by researchers at Reading University.[160,161] Work lead by *Colquhoun* and *Hayes* produced materials composed of naphthalene diimide within the polymer backbone; the electron-poor naphthalene diimide moieties were co-polymerised with poly(propylene oxide) and poly(ethylene oxide), by condensation between chain-end amino-functionalised polyethers and naphthalene tetracarboxylic dianhydride. Cross-linking was achieved by the addition of α,ω-naphthylpolybutadiene, functionalised by urethane formation between α,ω-diisocyanato-

polybutadiene before urethane formation with 1-aminonaphthylene (Figure 27).[193,194] The resulting materials were found to comprise crystalline hard blocks of a size indicative of aromatic π-π stacks, by X-ray scattering. Mechanical analysis of the materials revealed a T_g of ~–20 ºC and a linear transition from T_g to viscous flow between a temperature range of –20 to 110 ºC. The materials were observed to be stretchable (ε_{max} = 170%), mechanically tough (σ_T = 510 MPa) and self-healable, with recoverability of these parameters by 95 % and 91 % respectively.

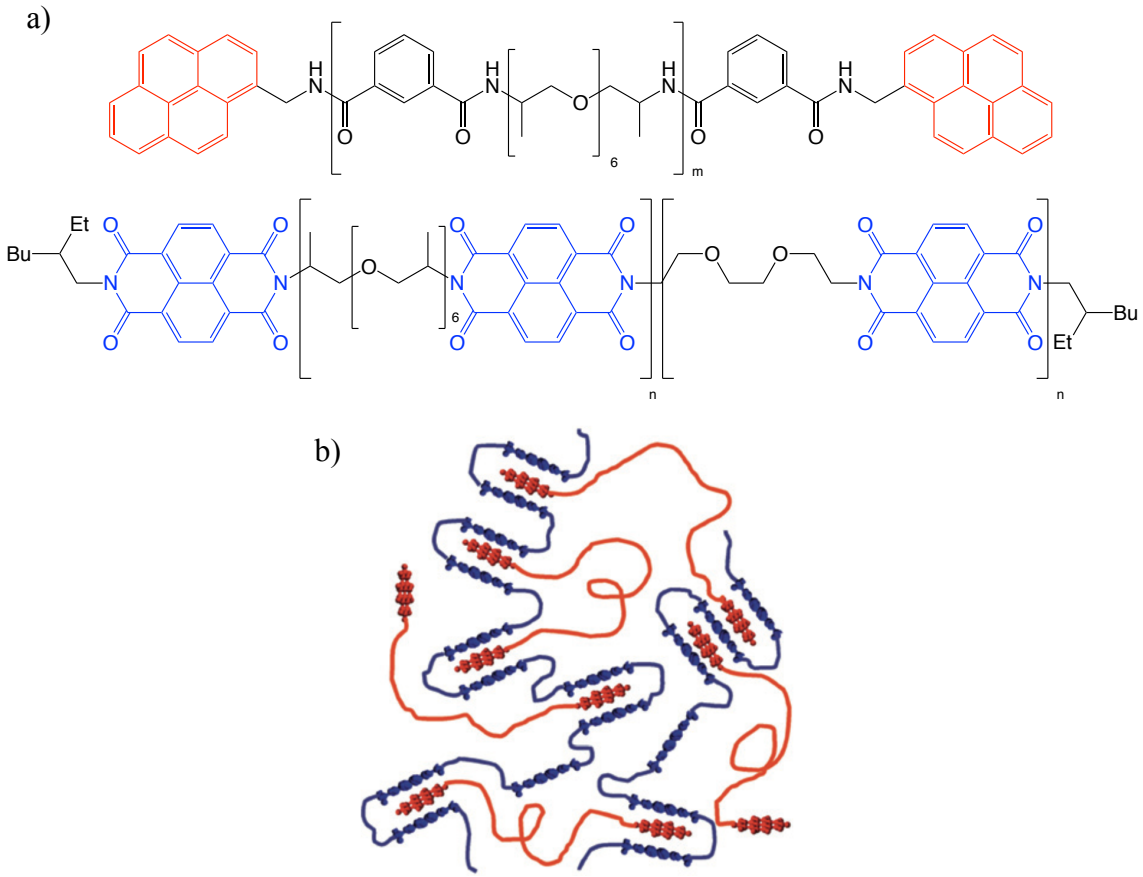

Figure 27 – a) Schematic representation of naphthyl-functionalised aromatic polyamide (based on PPG), and a naphthylenemaleimide-functionalised PPG; b) Cartoon representation of a chain-folded polymer induced by the π-π stacking of naphthylene and naphthylmaleimide.[195]

Similar networks, based on poly(dimethyl siloxane) were also synthesised and characterised. [195] In this report, crystalline cross-linked materials with a T_g of ~97 ºC and a T_m ~200 ºC were found, which were found to self-heal at ~115 ºC (temperatures up to 85 ºC below T_m).

The synthesis of a self-healing polyurethane based on modified poly(ethylene-*co*-butylene), caused by the π-π-stacking of N-(4-Methoxybenzyl)-1-(4- nitrophenyl) end-groups, was also investigated by *Hayes et al.*.[196] In this work, commercially-supplied hydroxyl-functionalised poly(ethylene-*co*-butylene) was first modified with isocyanates at the chain-

ends, before reaction with N-(4-Methoxybenzyl)-1-(4- nitrophenyl)methanamine. The resulting solid films were found to be comprised of stacked urea moieties within the hard block (with reflections at 5.64 Å obtained by WAXS) as well as larger hard domains (55 Å) resulting from microphase separation. A relatively robust and stretchable nature was found on stress-strain studies, with ε_{max} = 69 % and σ_T = 0.89 MPa Most notably, the materials were observed to self-heal after being cut at 45 ºC after just 15 minutes, with a healing efficiency of greater than 99%.

Ionic Interactions

Ionic interactions have been of interest to produce dynamic materials cross-linked by supramolecular interactions. In a recent publication, *Heinrich* and *co-workers* payed attention to the scalability of their methods.[197] This work involved the modification of, already widely used on industrial scale, bromobutyl rubber with butylimidazole. The modification used the N-alkylation reaction between bromide moieties, present in abundance along the polymer backbone, and secondary amine of the imidazole moiety. The resultant cross-linked elastic material was found to be cured (74% bromine conversion) at 100 ºC, but remain soluble in chloroform, indicating the physical nature of the cross-links. Mechanical testing found a stretchability of 1000% and tensile strength of 9 MPa. A pronounced strain-hardening was observed between 700 and 800%, which was attributed to the reorganisation of cross-linking points. Analysis by stress-strain cycling at lower strains (50–200%) showed a pronounced stress-softening with hysteresis and permanent residual strain. Thermal analysis found a T_g of –67 ºC, matching that of traditional vulcanised butyl rubber. Self-healing behaviour of the ionomer was found at room temperature after 24-hour healing time, and up to ~95% of the original strain could be recovered after 8 days of self-healing time (Figure 28).

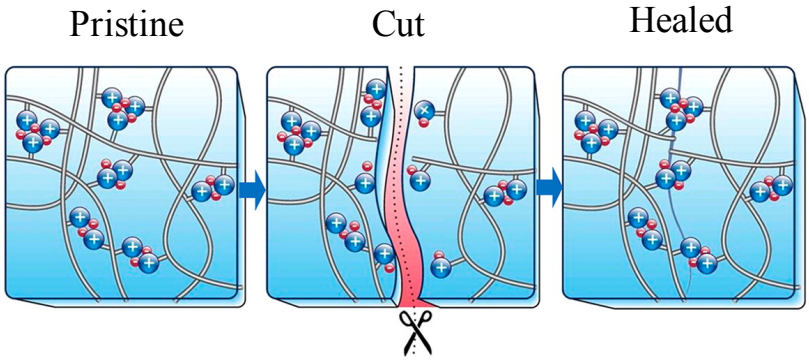

Figure 28 – Cartoon representation of bromobutylrubber containing ionic cross-links.[197]

The use of carboxylated polyacrylonitrile (carboxylated nitrile rubber or XNBR) as the backbone for ionomeric materials was studies by *Ibarra* and *Valentín et al.*[198,199] In their work, XNBR was ionically cross-linked using magnesium oxide, resulting in a robust, elastic, cross-linked material with a T_g at ~0 ºC. DMTA measurements at elevated temperatures displayed an increase in tan δ between the temperatures 50–150 ºC, which was attributes to an 'ionic transition temperature'. At room temperature, tensile strengths of up to 39 MPa and elongations of up to 595% at break were obtained, depending on the amount of metal oxide cross-linking agent was used. Materials containing small amounts of covalent cross-links (produced by introduction of peroxide) as well as ionic cross-links were also produced; these hydride materials were found to have a greater stretchability than their purely ionic counterparts.

Hybrid materials, containing prominently ionic cross-links and a small amount of covalent cross-links have also been studied by *Xu et al.*[200] In this publication, the pendent alkene bonds (from the 1,2 isomer) of polybutadiene were modified with carboxylic acid and primary amine moieties, by thiol-ene 'click'. The ionomers were further cross-linked by a second thiol-ene 'click' reaction between main-chain alkene bonds and a trithiol-functionalised cross-linking agent. The resulting elastomeric solid was found to possess good stretch ability (ε_{max} = 400 %) and tensile strength (σ_T = 6 MPa) depending on covalent cross-linking density. Despite the content of covalent cross-linking, the self-healing character of the materials was found to be unperturbed.

1.3.5 Applications

A variety of applications have been proposed for supramolecular materials; for hydrogels, biomedical applications tend to be the most targeted (most commonly 'scaffolds' onto which new tissue may grow after damage), due to the similarity in physical nature of hydrogels to animal tissue.[148] The ability to de-polymerise the materials with high efficiency offers a strong possibility for good clearance from the body.

Metallosupramolecular polymers have been applied to photovoltaics, as emissive materials, with benefits coming from their light weight and low cost of production.[4] A large amount of research interest has also been geared towards their use as molecular electronics,[201] as well as backbones onto which information may be stored. Another key area of research for metal-containing supramolecular polymers is for their function as sensors for both organic and metallic species.[4]

Main-chain supramolecular polymers have been targeted for use in ink-jet printing inks, as well as investigation for their use in 3-D printing inks.[162,202] Their low viscosity in the melt makes supramolecular polymers attractive alternatives to prevent clogging of ink dispensing nozzles. Supramolecular polymers have also been investigated for their use within the lithographic printing process, due to their increased solubility at elevated temperatures.[162]

It is clear that the dominant application envisaged for materials cross-linked with reversible supramolecular bonds is within self-healing materials.[150,160] The ability for materials to be regenerated after damage, or dissolved into their (macro)monomers and re-polymerised, makes them an attractive source for recyclable alternatives to materials that are currently unrecyclable.

1.3.6 Drawbacks

Despite the promising outlook at both the synthesis and applications of materials based on supramolecular polymer chemistry, some key drawbacks have been identified. Compared to their covalently bonded counterparts, supramolecular polymers comprise considerably weaker chemical bonds, and, consequently, supramolecular materials tend to be less robust to physical stresses. This decrease in physical durability is often exacerbated at elevated temperatures (particularly in the case of H-bonding and π-π stacking systems), due to the increase in rate of dissociation/association.[203,204]

Another drawback, that is often encountered when investigating the chemical composition of supramolecular polymers, is the limited choice of chemical techniques available to characterise chemical composition (and the chemical processes by which materials are obtained) of solid materials. Although this drawback is not limited to supramolecular materials, it is made particularly challenging for researchers to garner accurate data of the chemical exchange that occurs within the dynamic materials, when only a handful of analytical techniques are available.[205]

1.4 Double Dynamic Materials

To overcome the drawbacks of materials based on dynamic covalent and non-covalent bonds, i.e. the limited kinetic control of the former, and weak molecular associations of the latter, the introduction of two dynamic chemical functions within the same material has been investigated by a growing number of groups.

As the name implies, 'double-dynamic' materials contain two dynamic chemical functional groups, and can be categorised into three broad groups: 1) materials that contain two *non-covalently* bonding moieties; 2) those that contain both a *non-covalent* and a reversibly *covalent* bonding moiety; 3) and, materials that contain two dynamic *covalent* moieties.

As the main goal of including two dynamic chemical functionalities is to reduce the effects of the drawbacks of each component, a relative difference between the kinetic rates of bond association/disassociation of the two dynamic moieties is preferable. Orthogonality of the stimulus to which each component may associate/disassociate is also desirable, to allow greater control and ability to finely tune the physical response of the materials in controlled conditions.[206] A recent review, published by *Weck et al.* details double-dynamic systems containing polymers with orthogonal supramolecular functionality;[207] the examples discussed in the following section, however, have been chosen as they focus on taking advantage of the orthogonality for the optimisation of the dynamic properties of the resulting materials.

1.4.1 Non-Covalent/Non-Covalent

At present, the most explored combination of dynamic chemical moieties, within the field of double-dynamic materials, are systems containing two *non-covalent* chemistries. A variety of chemical functionalities have been explored, producing materials that were studied as both gels and in the bulk.

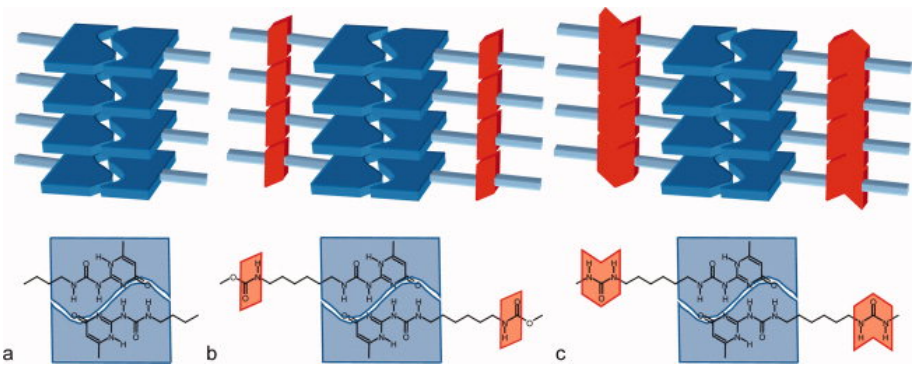

Figure 29 – Cartoon and schematic representations of hydrogen-bond assisted stacking of ureidopyrimidinones.[208]

The UPy chemical functionality has been used in combination with other hydrogen-bonding groups,[208–210] as well as metal-ligand,[211–213] and host-guest associating moieties.[214] Chain-end functionalisation of amino and hydroxyl-functionalised pol(ethylene butylene) and PDMS backbones was achieved by reaction with isocyanate ureidopyrimidinone. π-π-stacking of the UPy dimers was observed to be stabilised by hydrogen-bonding between the urea and urethane linking functionalities (Figure 29), resulting in a deviation of the material's behaviour away from classical viscoelastic behaviour.[208,209]

Materials composed of hetero-functionalised poly(ethylene butylene), featuring ureidopyrimidinone at one chain-end and a benzene triamide (BTA) derivative at the other, were studied in the bulk by *Meijer* and *Palmans et al.* (Figure 30).[210] The functionalised polymer was observed to form similar urea/urethane-assisted ureidopyrimidinone π-π stacks, as well as hydrogen-bonding assisted benzene π-π stacks at the other chain-end. The resulting cross-linked network was analysed by DSC, revealing a transition at 37 ºC and 140 ºC postulated as the result of the melting of the UPy and BTA stacks respectively. The ureidopyrimidinone melting transition was also reflected in the mechanical performance of the material, with a significant loss of elasticity at 40 ºC.

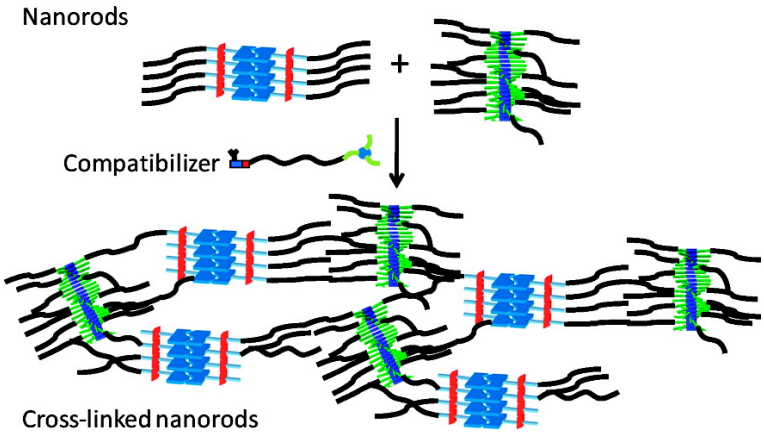

Figure 30 – Cartoon representation of the cross-linked networks formed from the hydrogen-bond assisted stacking of ureidopyrimidinone (blue) and benzene triamide (dark blue) [210]

The synthesis of materials containing both a ureidopyrimidinone and a terpyridine chemical function was achieved by *Schubert et al.* using both a small molecular core and a hetero-functionalised poly(ε-caprolactone) backbone.[211,212] In the latter system, ring-opening polymerisation of ε-caprolactone with hydroxyl-functionalised terpyridine (using tin octanoate as a catalyst), followed by reaction with isocyanate-functionalised ureido-pyrimidinone,

yielded a polymeric film. The formation of hydrogen-bonding ureidopyrimidinone dimers promoted the linear chain-extension and could be reversed simply by heating; this was followed by an indicative temperature-dependent decrease in viscosity, at temperatures above 40 ºC. At higher temperatures (>90 ºC) a more gradual decrease in viscosity was observed, attributed to the weakening of metal-ligand coordinative bonds. Addition of a competing ligand hydroxyethyl ethylenediaminetriacetic acid (HEEDTA) was also found to de-polymerise the material, due the breakage of the terpyridine/Zn or Fe complex along the polymer backbone.

Reflecting its popularity in metal-containing supramolecular polymers, terpyridine has also been a popular choice in double-dynamic systems containing two *non-covalent* chemical functionalities. A main-chain supramolecular polymer, using the orthogonal moieties terpyridine and 'Halmilton's wedge' was synthesised by *Hirsch and co-workers*.[215] In this study, polymerisation was achieved using a variety of M^{2+} ions and a bis-cyanurate derivative, and confirmed by ^{1}H NMR titrations, and UV-Vis spectrophotometry. The gel that resulted was found to be composed of particles with a hydrodynamic radius of ~5 μm, and could be reverted back to the sol by either acidification (breaking the ureidopyrimidinone dimers) or addition of a competing ligand (HEEDTA).

The terpyridine motif was combined with guanidiniocarbonyl pyrrole carboxylate, in a double-dynamic metal-ligand/ionomer small molecule which underwent stimulus responsive cyclisation and linear polymerisation.[216] *Gröhn* and *Schmuck et al.* observed the reversible self-assembly of the hetero-bifunctional small molecule promoted by acidic pH and on addition of iron(II) salts, and reversed by neutralisation or addition of a competing ligand (HEEDTA). The formation of linear polymer strands was confirmed by both cryoTEM and SANS.

Palladium-centred metal complexes were also investigated by *Huang* and *colleagues*.[217,218] In these studies, triazole-palladium complexes were used to complex both cryptand/paraquat and crown-ether/dialkyl ammonium based 'daisy chain' polymeric systems (Figure 31). Reversible dissolution of the polymer networks could be achieved physically (heating) and chemically (addition of competing ligands or basification of the gels).

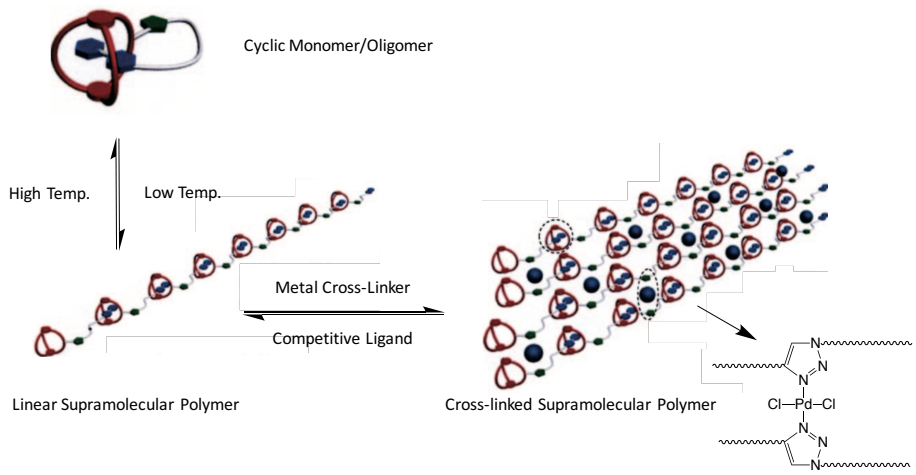

Figure 31 – Cartoon and schematic representations of the double-dynamic supramolecular networks produced by Huang et al.[218]

Ionic interactions have also been used within double-dynamic supramolecular polymer systems, in combination with both hydrogen-bonding and metal-ligand motifs.

Liu and *co-workers* synthesised statistically-distributed polyacrylate co-polymers from acrylamide, acrylonitrile and 2-acrylamido-2-methyl-1-propanesulfonic acid.[219] The resulting hydrogel was cross-linked chemically, by reaction with poly(ethylene glycol)diacrylate, and physically by dipole-dipole interactions of CN-CN. and hydrogen-bonding interactions of amide chemical functions. Mechanical testing proved the material to be highly stretchable and robust (ε_{max} = 716 %, σ_T = 8.31 MPa), with a large degree of recoverable plastic deformation observed on stress-strain analysis, presumably due to the exchanging nature of the dynamic crosslinking bonds.

The carboxylate ion as a dynamic chemical function has been explored by three groups in the context of double-dynamic systems.

Van Duin et al. studied the effect of adding primary alkylamines to maleated poly(ethylene propylene).[218] The resulting reaction caused cross-linking via the ring-opening of the pendent maleic anhydride and formation of an ammonium carboxylate salt and a hydrogen-bonding amide moiety. Films, obtained by compression moulding, were produced and found to display robust and stretchable (σ_T = ~4.5 MPa, ε_{max} = ~550 %) physical properties, as well as being reversibly de-crosslinked at elevated temperatures. Addition of potassium salts further increased the physical properties of the materials, due to the stronger ionic interaction between carboxylate rather than alkylammonium as the counter ion.

Barikani and *Baharvand et al.* demonstrated the use of carboxylate ions as cross-linking agents in alginate-based linear polyurethanes.[220] Robust and stretchable physically cross-linked

networks were produced from the ionic interaction between carboxylate-alkylammonium pairs, and hydrogen-bonding associations between urethane moieties. Physical analysis of the materials proved a maximum stress of 48 MPa and maximum strain at 859 %. The presence of the ionic interactions was observed to significantly improve creep-deformation; no studies in which the self-healing of the double-dynamic material could be compared to control samples were conducted, and so any significance in difference in association kinetics between ionic and hydrogen-bonding recovery is, so far, unexplored.

The cross-linking of carboxylated nitrile rubbers, via the formation of carboxylate/sulfate ion pairs and copper/nitrile coordination, was investigated by *Ibarra* and colleagues.[221] Both cross-linking bonds were shown to be formed on addition of anhydrous copper sulfate, with the coordination complex predominating. Cross-link densities could be increased with increasing $CuSO_4$ concentration, causing a respective increase in T_g. Physical analysis of the materials displayed rubbery behaviour, and no decrease in modulus at temperatures as high as 200 ºC. Unfortunately, no mention of depolymerising the materials was reported for this promising material.

1.4.2 Covalent Reversible/Non-Covalent

Double-dynamic systems composed of one dynamic *covalent* and one *non-covalent* chemical functionality have also been explored by a number of groups.

The use of the acylhydrazone as a reversible covalent group, as well as a ligand and a non-covalent group, has been explored by *Lehn and coworkers*. In 2013,[123] a telechelic PDMS backbone was functionalised with aromatic aldehyde at the chain-end, before linear polymerisation, by reaction with carbohydrazide, to form bis-iminocarbohydrazide moieties along the backbone. The ambition in this publication was to observe the effects of the reversibility of both the imine component of the acyl hydrazone and the hydrogen bonding capacity of this iminourea-type motif. Mechanical analysis of the materials proved the material to be stretchable with a maximum strain at break of 100%. Self-healing of the materials was also investigated, finding no obvious difference between samples containing acid, which catalyses acyl hydrazone exchange; it was therefore concluded that self-healing is mainly driven by hydrogen-bonding. Strain recovery of up to 90% was observed in self-healed samples. *Lehn et al.* also investigated the linear polymerisation of homo-functionalised telechelic small molecules containing ‘Hamilton’s wedge’ at the chain-ends and the acyl hydrazone function in the core.[222] Polymerisation was triggered by either non-covalent or

covalent assembly: by the addition of a bi-functional molecule containing cyanuric acid derivatives, or by association of aldehyde- and acyl hydrazine-functionalised 'Hamilton Wedge' derivatives. De-polymerisation was observed on addition of a competing aldehyde component, or by addition of a competing cyanurate derivative.

'Metallodynamers' were synthesised by *Lehn and colleagues* with the study of acyhydrazone as a ligand to Zn^{2+} and Ni^{2+}.[125] Aldehyde-functionalised quinoline was first reacted with acylhydrazine-functionalised PDMS, to form the tridentate ligand. Following this, complexation with both zinc(II) and nickel(II) ions was observed to cause linear polymerisation of the systems, depending on the concentration of the polymer in solution, even when exchanging the quinoline derivative for a pyridine analogue. In this publication, the imine bond allowed for the fast reshuffling between monomers and oligomers, while the metal salts enabled folding of the polymer chain. These dynamic behaviours were observed in the bulk.

A constitutional dynamer library was constructed by *Lehn et al.*, with the aim to generate a linear poly(siloxane) chain-extended with imine moieties.[124] In this investigation, four components were mixed in a DCM/acetonitrile solvent mixture: 1) a di-amino naphthyl derivative; 2) diamino-tri-dimethyl siloxane; 3) a dialdehyde naphthyldimaleimide derivative; 4) and, a dialdehyde-tri-dimethylsiloxane. Upon mixture of the components and addition of alkali metal salts, a folded polymer was observed, composed of the π-π stacking of the aromatic electron-poor and rich pairs, and complexation of the metal ions by the imine-pyridine moiety (Figure 32).

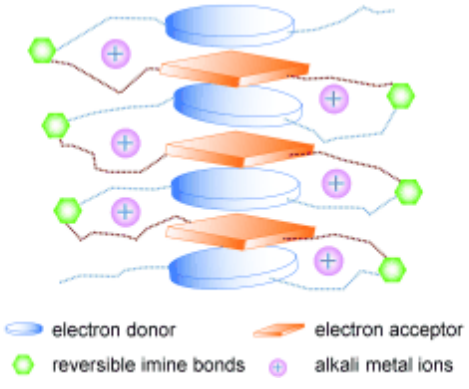

Figure 32 – Cartoon representation of the folding of PDMSs containing naphthyl and naphthyldimaleimide moieties along the backbone, with the complexation of alkyl metal ions by imine bonds.[124]

With regards to hydrogen-bonding motifs, that have been used in the context of double-dynamic systems, a similar range, as seen in *non-covalent*/*non-covalent* systems, have been exploited in reversible *covalent*/*non-covalent* systems.

A combination of carboxylic acid-imidazolinone/amide interactions and transesterification was used by *Tournilhac* and *Michaud* and *co-workers*,[185] as an amalgamation of two seminal projects published by *Leibler et al.*, discussed earlier in this chapter.[183] [56] In this work, carboxylic acid-functionalised fatty acids were partially functionalised with imidazolinone derivatives before polymerisation with the di- and tetra-epoxides bisphenol A (DGEBA) and 4,4′-methylenebis(N,N- diglycidylaniline) (TGMDA). The resulting imidazolinone/polyester hybrid system was found to be insoluble in organic solvents, due to the presence of the covalent polyester network, with a T_g at ~13 ºC. At elevated temperatures (>100 ºC), the presence of the polyester network stabilised the mechanical integrity of the materials. At room temperature, creep deformation, previously observed in the linear polyester networks, was greatly reduced. Self-healing analysis of the materials showed the ability to recover up to 100% of the mechanical performance of the pristine samples.

The differences in timescales of kinetic exchange between *non-covalent* and reversible *covalent* bond exchange was recently demonstrated by *Konkolewicz et al*.[223] In this work, a polyacrylate containing pendent ureidopyrimidinone and furan/maleimide moieties was synthesised (Figure 33); the resulting materials were found to be stretchable (ε_{max} = ~320%) and self-healable. Importantly, only partial self-healing (~50% of mechanical resistance) was observed at room temperature, attributed to the relatively weak nature of the initial supramolecular bonding, however, when the temperature was increased (90 ºC), a much higher degree of self-healing was observed (~95% of mechanical resistance), attributed to the activation of the Diels-Alder adduct with a much higher bond dissociation energy. Improvement of this system, in terms of mechanical and self-healing properties, was achieved, by incorporation of each of the double-dynamic components onto separate networks before mixture and subsequent formation of an interpenetrating double network.[224]

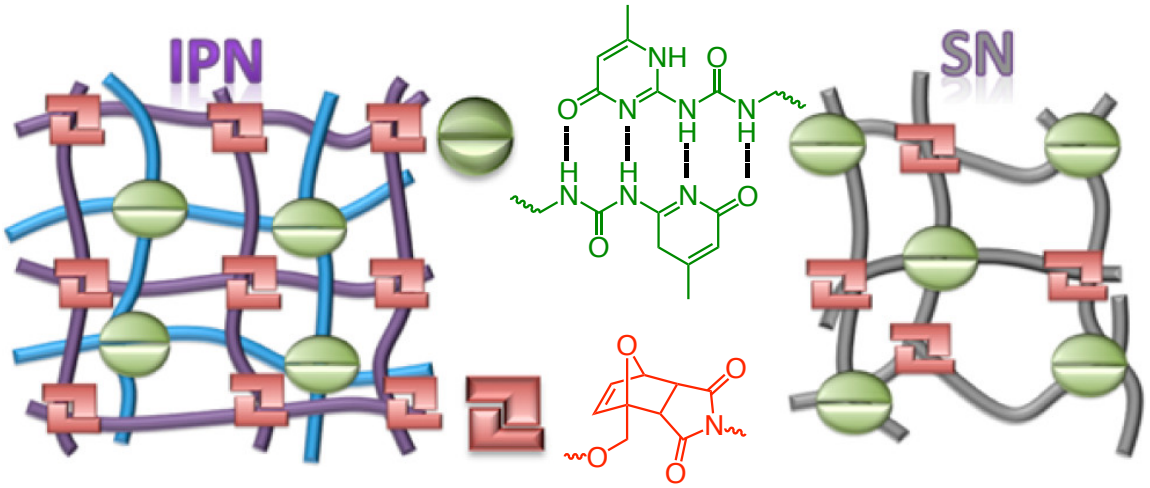

Figure 33 – Cartoon and schematic representations of double-dynamic networks cross-linked by both self-complementary ureidopyrimidinone dimers (green), and the furan/maleimide Diels-Alder adduct (red).[224]

An early example of a double-dynamic network comprised of the ureidopyrimidinone and the disulfide bonds (used as the non-covalent and reversible covalent moieties, respectively) was published in 2005 by *Meijer* and *co-workers*.[225] In this work, two monomers were generated from a homo-functionalised small molecule containing a disulfide bond in its core – to observe dynamic exchange within the polymer and diasteriomeric chiral centres. At low concentrations, homochiral cycles were observed to form readily (driven by H-bond exchange), due to the occurrence of a large difference in stability between those and heterochiral cycles at higher concentrations, the formation of homo- and heterochiral linear polymers as observed with a considerable decrease in chiral self-selection. Chemical formation of diastereoisomers was also observed to occur by disulfide exchange, promoted by reduction of the disulfide bridge.

Linear poly(urea-urethane)s based on poly(propylene oxide) containing aromatic disulfides, were found to chemically exchange at both room temperature and elevated temperatures (>90 ºC) (Figure 34).[87,226] The two temperatures of exchange were observed by both stress-relaxation and self-healing experiments: significant relaxation was observed at elevated temperatures (at 150 ºC full relaxation was observed after 4 minutes) which was attributed to the breakage of quadruple H-bonding aggregates in the polymer hard-block; significant self-healing was observed at room temperature (97% of mechanical strength was restored), attributed to disulfide exchange.

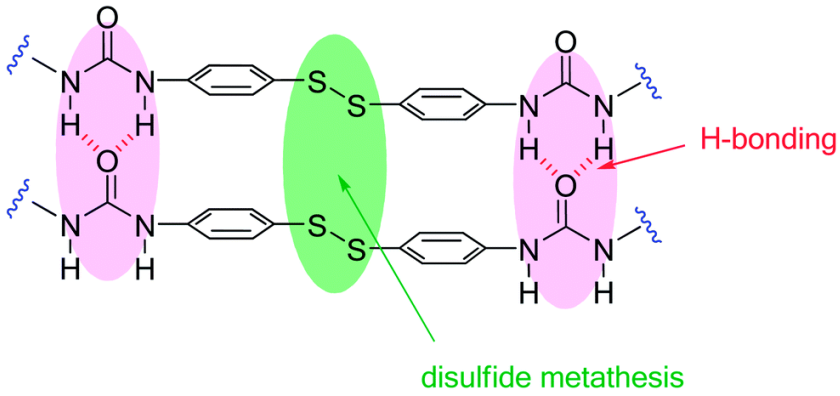

Figure 34 – Double-dynamic cross-linking node containing urea hydrogen bonding pairs (pink) and disulfide bonds (green).[226]

The hydrogen-bonding association of a polyacrylate, functionalised with pendent amide groups located on a polymer backbone, produced from the ROP of cyclooctadiene, was used in combination with olefin metathesis, catalysed by the addition of Grubb's Second Generation Catalyst.[227] The incorporation of the sacrificial hydrogen-bonding moieties dramatically increased the maximum strain-at-break and toughness of the materials (σ_T = 1.66 MPa and ε_{max} = 938%). The materials were observed to self-heal at 50 ºC after cutting the material, reaching 90% mechanical recovery; this was attributed to the olefin metathesis, which was not hindered by the presence of hydrogen-bonding amide moieties.

The use of the host-guest supramolecular association of pillar[5]ene and imidazole has been explored in the context of double-dynamic systems by two groups. In both cases, due to the weak mechanical strength of the host-guest association, the produced materials were weak gels. *Q-Z Yang et al.* formed linear polymers from the [4+4] cycloaddition of anthracene and pillar[5]ene-imidazole.[228] The resultant gels were observed to undergo a gel-sol transition from heating for 1 minute, and heating for 1 day with light irradiation, attributed to the dissociation of the host-guest assembly and the retro-cyclisation of anthracene dimers, respectively. *Y-W Wang et al.* produced similar linear polymers based on the pillar[5]ene-imidazole host-guest assembly, and a diselenium reversible covalent bond within the backbone.[229] The resulting gel was found to be de-polymerised on introduction of both a reducing agent, due to the reduction of the diselenium bridge, and a competing guest, such as adiponirtile, due to its better affinity for pillar[5]ene compared to imidazole.

1.4.3 Covalent Reversible/Covalent Reversible

The incorporation of two dynamic *covalent* chemical moieties, to create a double-dynamic network, has been considerably less explored than any of the other double-dynamic systems.

Sumerlin et al. explored the linear polymerisation of a hetero-functionalised small molecule that contained a furan linked via an oxime bond to a furfuryl-maleimide moiety at each end.[230] Simultaneous de-protection of the furfuyl-maleimide moiety (to yield maleimide), and polymerisation, from Diels-Alder reaction with the furan present at the other chain-end, was achieved by simply heating the system in solution. De-polymerisation of the produced polymer was tested with regards to both the oxime and the oxanabornene chemical functions. First, acid-catalysed exchange of the oxime bonds was successfully conducted by addition of mono-functionalised alkoxyamine at 60 ºC; a considerable decrease in molecular weight was observed, by SEC after 4 and 6 days, in the resulting material. De-polymerisation of the material, by inducing the retro-Diels-Alder, was achieved by simply heating the material (160 ºC) in DMSO; after cooling, the Diels-Alder reaction was re-initiated and a healed polymer material was re-formed.

Self-healing hydrogels, containing both acylhydrazone and disulfide moieties, at cross-linking points, were synthesised by *Liu* and *Chen* and co-workers.[231] In this study, tri-aldehyde functionalised poly(ethylene glycol) (M_n = 3000 Da) was prepared, before cross-linking with dithiodipropionic acid dihydrazide in water; gelation was observed to occur within only 5 minutes at pH 6 and room temperature. Rheological analysis of the samples at different pHs and containing differing amounts of catalyst (aniline) revealed that both the acylhydrazone and disulfide moieties are kinetically locked in neutral conditions, by estimating the dissociation rate of the bonds from the crossover frequency of G' and G"; the rate of dissociation does, however, increase with decreasing pH, due to the acid-catalysed dynamic exchange of the acylhydrazone moieties. Dynamic exchange within the materials was also accessible in basic conditions, in which the disulfide bond exchange is catalysed. The usefulness of this exchange was exemplified by conducting self-healing tests at pHs 6, 7 and 9; at pHs 6 and 9, self-healing was observed, after 48 and 24 hours, due to the dynamic exchange of both acylhydrazone and disulfide, respectively; at neutral pH, no self-healing was observed. Tensile strength recovery of up to 50% were observed from an initial stress maximum of 80 kPa and strain maximum at ~650%.

In a similar approach, *Chen* and *Li* synthesised a double-dynamic material, which contained acylhydrazone and disulfide cross-linking moieites, based on poly(triazole),from the alkyne-azide 'click' reaction of methyl 3,5-dipropargyloxylbenzoate and methyl 3,5-bis(4-azidobutoxy)benzoate.[231] Post-polymerisation modification of the poly(triazole), by reaction of the pendent amines with a dialdehyde-functionalised cross-linking agent (also containing a disulfide moiety within its core) yielded gels that underwent gel-sol transitions in either reducing or acidic conditions. Stress and strain maxima of the gels were observed to reach 160 kPa and ~55%, respectively; as well as possessing the ability to recover up to 85% of their structural performance after dissolution and remoulding.

1.5 Aims, Objectives and Applications

1.5.1 Aims and Applications

With our industrial partner Soprema, the work in this project is aimed at the synthesis and characterisation of materials that are suitable for use in outdoor conditions. As Soprema specialise in both interior and exterior building materials (such as waterproofing and sealing, insulation and ground and roof surfacing), applications could be envisaged as sealants, gaskets or coatings as pure materials, or be combined into composites for surfacing larger areas. The physical and chemical stability at temperatures ranging from –30 ºC to +80 ºC, are therefore paramount; resistance to weathering by chemical or mechanical degradation is also key, with the materials, therefore, requiring good resistance to hydrolysis and physical erosion. By including the dynamic chemical functionalities into the materials, dissolution, and the ability to reprocess the materials in relatively short timeframes are also targeted.

The specific chemical focus of this work is to combine dynamic covalent and non-covalent chemical moieties within one material, in an effort to precisely control the process of self-healing. The presence of the fast exchange between dynamic *non-covalent* bonds is anticipated to rapidly respond damaged areas of the material with weak (low dissociation constant) chemical interactions; after this initial weak self-healing, stronger and kinetically slower, dynamic *covalent* bonds will reinforce the healed area, producing an improved healing efficiency.

The imine bond will be the dynamic *covalent* chemistry that will be used in this work. In the established paradigm of Dynamic Covalent Networks, detailed above, imine networks may behave as both dissociative and associative networks, vis-à-vis the hydrolysis and

exchange of imine moieties, respectively. This may be activated by alterations in the pH, temperature or presence of catalyst. The ureidopyrimidinone will be the dynamic *non-covalent* chemistry used in this work. The strong association constant and ease of synthesis are the main reasons for its selection. The spontaneous formation of ureidopyrimidinone dimers is observed at room temperature in a range of solvents, and can be selectively broken (to form the monomeric species) by changing both pH and temperature.

1.5.2 Establishing a Physical Standard

The establishment of a benchmark, to which the physical performance of new materials should meet, is strongly related to the application in which the materials will be used. As the exact application for new dynamic materials is often vague, as with any new domain of science, control materials, which contain non-dynamic chemical analogues as cross-linking functions, are often used as the current standard. In our case, three control materials were synthesised in parallel to the double-dynamic materials of focus.

As mentioned earlier in this chapter, polyurethane elastomers are viewed as exceptionally durable elastomeric materials, reflected in their huge market share. The current standard for polyurethane thermoset elastomers is described in Table 2; importantly, these values are the generally expected values to which thermoset polyurethanes may perform, and are strongly dependent on which diisocyanate, polyol and chain-extender/cross-linker is selected. It would be promising, therefore, for the double-dynamic elastomeric materials, produced in this project, to match or exceed any of the values observed with polyurethanes. A general expected performance of thermoset polyurethanes is also given in Table 2.

As with classical thermosets, the physical behaviours of materials cross-linked with dynamic chemical bonds are strongly influenced by both the nature of the polymer backbone and the chain-extending/cross-linking bonds. For dynamic covalent networks, it is often the case that high tensile strengths require the sacrifice of elongation performance, and vice versa. Tensile strengths as high as 93% (with only 7.5% elongation at break),[97] and elongations as high as 650% (with stresses as high as 50 MPa) have been previously reported from materials using dynamic covalent networks.[42] Polymeric networks formed from supramolecular interactions largely display the lowest tensile strengths out of all of the materials discussed, but are often highly stretchable; tensile strengths of 15 MPa and elongation at break of 616% have been reported.[232]

	Tensile Strength (MPa)	Elongation at Break (%
Thermoset PU (ref. 25)	70	500 – 1000
Thermplastic PU (ref. 25)	33	600
Dynamic Covalent Network (ref. 42)	50	650
Supramolecular Network (ref. 232)	15	616

Table 2 – Expected optimal tensile strength and elongation until break of polymeric materials

1.6 References

1. Mülhaupt, R. Hermann staudinger and the origin of macromolecular chemistry. *Angew. Chemie - Int. Ed.* **43,** 1054–1063 (2004).
2. Europe, P. PlasticsEurope Market Research Group (PEMRG) / Consultic Marketing & Industrieberatung GmbH. (2016).
3. Freinkel, S. *Plastic: A Toxic Love Story*. (Houghton Mifflin HArcourt, 2011).
4. Whittell, G. R., Hager, M. D., Schubert, U. S. & Manners, I. Functional soft materials from metallopolymers and metallosupramolecular polymers. *Nat. Mater.* **10,** 176–188 (2011).
5. Matyjaszewski, K., Gnanou, Y. & Leibler, L. *Macromolecular Engineering*. *Macromolecular Engineering* (Wiley-VCH Verlag GmbH & Co. KGaA, 2011). doi:10.1002/9783527631421.ch1
6. Rahimi, A. & García, J. M. Chemical recycling of waste plastics for new materials production. *Nat. Rev. Chem.* **1,** 46 (2017).
7. Geyer, R., Jambeck, J. R. & Law, K. L. Production, use, and fate of all plastics ever made. *Sci. Adv.* **3,** (2017).
8. Freinkel, S. A Brief History of Plastic's Conquest of the World. *Scientific American* (2011). at <https://www.scientificamerican.com/article/a-brief-history-of-plastic-world-conquest/>
9. Peplow, M. The plastics revolution: how chemists are pushing polymers to new limits. *Nature* **536,** 266–268 (2016).
10. Schneiderman, D. K. & Hillmyer, M. A. 50th Anniversary Perspective: There Is a Great Future in Sustainable Polymers. *Macromolecules* **50,** 3733–3749 (2017).
11. Ravve, A. *Principles of Polymer Chemistry*. (Springer New York, 2012). doi:10.1007/978-1-4614-2212-9
12. Denissen, W., Winne, J. M. & Du Prez, F. E. Vitrimers: permanent organic networks with glass-like fluidity. *Chem. Sci.* **7,** 30 (2016).
13. Chatzi, E. G. & Koenig, J. L. Morphology and Structure of Kevlar Fibers: A Review. *Polym. Plast. Technol. Eng.* **26,** 229–270 (1987).
14. Blackwell, J. & Ross, M. X-ray studies of the structure of polyurethane hard segments. *J. Polym. Sci. Polym. Lett. Ed.* **17,** 447–451 (1979).
15. Directive 2008/98/EC of the European Parliament and of the Council - On Waste and Repealing Certain Directives. *Off. J. Eur. Union* (2008).
16. Imbernon, L. & Norvez, S. From landfilling to vitrimer chemistry in rubber life cycle. *Eur. Polym. J.* **82,** 347–376 (2015).
17. Adhikari, B., De, D. & Maiti, S. Reclamation and recycling of waste rubber. *Prog. Polym. Sci.* **25,** 909–948 (2000).
18. Karger-Kocsis, J., Mészáros, L. & Bárány, T. Ground tyre rubber (GTR) in thermoplastics, thermosets, and rubbers. *J. Mater. Sci.* **48,** 1–38 (2013).
19. EC. Novel Devulcanization Machine for Industrial and Tyre Rubber Recycling. *Horizon 2020* (2017). at <http://cordis.europa.eu/project/rcn/196391_en.html>
20. Pérez, G., Vila, A., Rincón, L., Solé, C. & Cabeza, L. F. Use of rubber crumbs as drainage layer in green roofs as potential energy improvement material. *Appl. Energy* **97,** 347–354 (2012).
21. Alsdorf, P., Krieg, R. & WENSKE, G. Devulcanisation product consisting of scrap rubber, a devulcanisation compound, a method for producing same, the reuse thereof in fresh mixtures and the use thereof for producing injection moulded parts. (2002). at <https://www.google.com.au/patents/EP1232205A1?cl=en>

22. Yang, Y. *et al.* Recycling of composite materials. *Chem. Eng. Process. Process Intensif.* **51,** 53–68 (2012).
23. Zia, K. M., Bhatti, H. N. & Ahmad Bhatti, I. Methods for polyurethane and polyurethane composites, recycling and recovery: A review. *React. Funct. Polym.* **67,** 675–692 (2007).
24. Pickering, S. J. Recycling technologies for thermoset composite materials—current status. *Compos. Part A Appl. Sci. Manuf.* **37,** 1206–1215 (2006).
25. Hepburn, C. *Polyurethane Elastomers*. (Elsevier Sceince Publisher LTD, 1992).
26. Delebecq, E., Pascault, J., Boutevin, B. & Ganachaud, F. On the Versatility of Urethane / Urea Bonds : Reversibility , Blocked. *Chem. Rev* **113,** 80–118 (2013).
27. Elwell, M. J., Ryan, A. J., Grünbauer, H. J. M. & Van Lieshout, H. C. In-Situ Studies of Structure Development during the Reactive Processing of Model Flexible Polyurethane Foam Systems Using FT-IR Spectroscopy, Synchrotron SAXS, and Rheology. *Macromolecules* **29,** 2960–2968 (1996).
28. Ryan, A. J. *et al.* Dynamics of (micro)phase separation during fast, bulk copolymerization: some synchrotron SAXS experiments. *Macromolecules* **24,** 2883–2889 (1991).
29. Ryan, A. J., Macosko, C. W. & Bras, W. Order-disorder transition in a block copolyurethane. *Macromolecules* **25,** 6277–6283 (1992).
30. Sardon, H. *et al.* Synthesis of polyurethanes using organocatalysis: A perspective. *Macromolecules* **48,** 3153–3165 (2015).
31. Silva, A. L. & Bordado, J. C. Recent Developments in Polyurethane Catalysis: Catalytic Mechanisms Review. *Catal. Rev.* **46,** 31–51 (2004).
32. Bloodworth, A. J. & Davies, A. G. 975. Organometallic reactions. Part I. The addition of tin alkoxides to isocyanates. *J. Chem. Soc.* 5238 (1965). doi:10.1039/jr9650005238
33. Subrayan, R. P., Zhang, S., Jones, F. N., Swarup, V. & Yezrielev, A. I. Reactions of phenolic ester alcohol with aliphatic isocyanates?transcarbamoylation of phenolic to aliphatic urethane: A13C-NMR study. *J. Appl. Polym. Sci.* **77,** 2212–2228 (2000).
34. Engels, H. *et al.* Polyurethanes: Versatile Materials and Sustainable Problem Solvers for Today's Challenges. *Angew. Chemie Int. Ed.* **52,** 9422–9441 (2013).
35. Sharmin, E. & Zafar, F. in *Polyurethane* (InTech, 2012). doi:10.5772/51663
36. Dušek, K. & Dušková-Smrčková, M. Network structure formation during crosslinking of organic coating systems. *Prog. Polym. Sci.* **25,** 1215–1260 (2000).
37. Potter, T. A., Schmelzer, H. G. & Baker, R. D. High-solids coatings based on polyurethane chemistry. *Prog. Org. Coatings* **12,** 321–338 (1984).
38. Shanks, R. A. & Kong, I. in 11–45 (2013). doi:10.1007/978-3-642-20925-3_2
39. Lal, J. & Scott, K. W. Properties and structure of elastomers. *J. Polym. Sci. Part C Polym. Symp.* **9,** 113–134 (2007).
40. Araújo, R. C. S. & Pasa, V. M. D. Mechanical and thermal properties of polyurethane elastomers based on hydroxyl-terminated polybutadienes and biopitch. *J. Appl. Polym. Sci.* **88,** 759–766 (2003).
41. Grenfell Tower Fire. (2017). at <https://en.wikipedia.org/wiki/Grenfell_Tower_fire>
42. Liu, W. *et al.* Oxime-Based and Catalyst-Free Dynamic Covalent Polyurethanes. *J. Am. Chem. Soc.* **139,** 8678–8684 (2017).
43. Zheng, N., Fang, Z., Zou, W., Zhao, Q. & Xie, T. Thermoset Shape-Memory Polyurethane with Intrinsic Plasticity Enabled by Transcarbamoylation. *Angew. Chemie Int. Ed.* **55,** 11421–11425 (2016).
44. Althausen, F., Raffel, R., Ebeling, W. & Eiben, R. A process and device for producing foam using carbon dioxide dissolved under pressure. (1996). at <https://encrypted.google.com/patents/WO1996016782A1?cl=pt>

45. Attenburrow, G., Barnes, D. J., Davies, A. P. & Ingman, S. J. Rheological properties of wheat gluten. *J. Cereal Sci.* **12,** 1–14 (1990).
46. Cowie, J. M. G. & V., A. Polymers: Chemistry and Physics of Modern Materials. (CRC Press, 2007).
47. Menard, K. P. Dynamic Mechanical Analysis: A Practical Introduction. (CRC Press, 2008).
48. Ward, I. M. & Sweeney, J. *Mechanical Properties of Solid Polymers*. (John Wiley & Sons, Ltd, 2012). doi:10.1002/9781119967125
49. TA Instruments. Dynamic Mechanical Analysis - Basic Theory and Applications Training. at <www.tainstruments.com/wp-content/uploads/CA-2016-DMA.pdf>
50. Vincent, J. in *Structural Biomaterials* (Princeton University Press, 2012).
51. Bauman, J. T. *Fatigue, Stress, and Strain of Rubber Components*. (Carl Hanser Verlag GmbH & Co. KG, 2008). doi:10.3139/9783446433403
52. Diani, J., Fayolle, B. & Gilormini, P. A review on the Mullins effect. *Eur. Polym. J.* **45,** 601–612 (2009).
53. DeSimone, A., Marigo, J.-J. & Teresi, L. A damage mechanics approach to stress softening and its application to rubber. *Eur. J. Mech. - A/Solids* **20,** 873–892 (2001).
54. Nguyen, Q. T., Tinard, V. & Fond, C. The modelling of nonlinear rheological behaviour and Mullins effect in High Damping Rubber. *Int. J. Solids Struct.* **75–76,** 235–246 (2015).
55. Kloxin, C. J. & Bowman, C. N. Covalent adaptable networks: smart, reconfigurable and responsive network systems. *Chem. Soc. Rev.* **42,** 7161–73 (2013).
56. Montarnal, D., Capelot, M., Tournilhac, F. & Leibler, L. Silica-Like Malleable Materials from Permanent Organic Networks. *Science (80-.).* **334,** 965–968 (2011).
57. Zhang, L. & Rowan, S. J. Effect of Sterics and Degree of Cross-Linking on the Mechanical Properties of Dynamic Poly(alkylurea−urethane) Networks. (2017). doi:10.1021/acs.macromol.7b01016
58. Obadia, M. M., Mudraboyina, B. P., Serghei, A., Montarnal, D. & Drockenmuller, E. Reprocessing and Recycling of Highly Cross-Linked Ion-Conducting Networks through Transalkylation Exchanges of C-N Bonds. *J. Am. Chem. Soc.* **137,** 6078–6083 (2015).
59. Craven, J. M. Cross-linked thermally reversible polymers produced from condensation polymers with pendant furan groups cross-linked with maleimides. (1969). at <https://www.google.com/patents/US3435003>
60. Stevens, M. P. & Jenkins, A. D. Crosslinking of Polystyrene via Pendant Maleimide Groups. *J. Polym. Sci.* **17,** 3675–3685 (1979).
61. Chujo, Y., Sada, K. & Saegusa, T. Reversible Gelation of Polyoxazoline by Means of Diels-Alder Reaction. *Macromolecules* **23,** 2636–2641 (1990).
62. Chen, X. *et al.* A thermally re-mendable cross-linked polymeric material. *Science (80-.).* **295,** 1698–702 (2002).
63. Rana Gheneim and Alessandro Gandin, C. P.-B. Diels-Alder Reactions with Novel Polymeric Dienes and Dienophiles: Synthesis of Reversibly Cross-Linked Elastomers. *Macromolecules* **35,** 7246–7253 (2002).
64. Laita, H., Boufi, S. & Gandini, a. The application of the Diels-Alder reaction to polymers bearing furan moieties. 1. Reactions with maleimides. *Eur. Polym. J.* **33,** 1203–1211 (1997).
65. Dello Iacono, S. *et al.* Thermally activated multiple self-healing diels-alder epoxy system. *Polym. Eng. Sci.* **47,** 21–25 (2017).
66. Cheng, X. *et al.* A facile method for the preparation of thermally remendable cross-linked polyphosphazenes. *J. Polym. Sci. Part A Polym. Chem.* **51,** 1205–1214 (2013).

67. Reutenauer, P., Buhler, E., Boul, P. J., Candau, S. J. & Lehn, J. M. Room temperature dynamic polymers based on Diels-Alder chemistry. *Chem. - A Eur. J.* **15,** 1893–1900 (2009).
68. Kennedy, J. P. & Castner, K. F. Thermally reversible polymer systems by cyclopentadienylation. II. The synthesis of cyclopentadiene-containing polymers. *J. Polym. Sci. Polym. Chem. Ed.* **17,** 2055–2070 (1979).
69. Murphy, E. B. *et al.* Synthesis and Characterization of a Single-Component Thermally Remendable Polymer Network: Staudinger and Stille Revisited. *Macromolecules* **41,** 5203–5209 (2008).
70. Alder, K. Neuere Methoden der Praparativen Organischen Chemie. *Verlag Chemie* 251–412 (1943).
71. Nicolaou, K. C., Snyder, S. A., Montagnon, T. & Vassilikogiannakis, G. The Diels-Alder reaction in total synthesis. *Angew. Chemie - Int. Ed.* **41,** 1668–1698 (2002).
72. Yuan, Y., Li, X. & Ding, K. Acid-free aza Diels-Alder reaction of Danishefsky's diene with imines. *Org. Lett.* **4,** 3309–3311 (2002).
73. Higaki, Y., Otsuka, H. & Takahara, A. A thermodynamic polymer cross-linking system based on radically exchangeable covalent bonds. *Macromolecules* **39,** 2121–2125 (2006).
74. Lendlein, A., Jiang, H., Junger, O. & Langer, R. Light-induced shape-memory polymers. *Nature* **434,** 879–882 (2005).
75. Bergman, S. D. & Wudl, F. Mendable polymers. *J. Mater. Chem.* **18,** 41–62 (2008).
76. Kloxin, C. J., Scott, T. F., Adzima, B. J. & Bowman, C. N. Covalent adaptable networks (CANs): A unique paradigm in cross-linked polymers. *Macromolecules* **43,** 2643–2653 (2010).
77. Reutenauer, P., Boul, P. J. & Lehn, J. M. Dynamic Diels-Alder reactions of 9,10-dimethylanthracene: Reversible adduct formation, dynamic exchange processes and thermal fluorescence modulation. *European J. Org. Chem.* 1691–1697 (2009). doi:10.1002/ejoc.200801269
78. Roy, N. & Lehn, J. M. Dynamic Covalent chemistry: A facile room-temperature, reversible, diels-alder reaction between anthracene derivatives and n-phenyltriazolinedione. *Chem. - An Asian J.* **6,** 2419–2425 (2011).
79. Coursan, M., Desvergne, J. P. & Deffieux, A. Reversible photodimerisation of ω-anthrylpolystyrenes. *Macromol. Chem. Phys.* **197,** 1599–1608 (1996).
80. Radl, S. *et al.* New strategies towards reversible and mendable epoxy based materials employing [4πs + 4πs] photocycloaddition and thermal cycloreversion of pendant anthracene groups. *Polym. (United Kingdom)* **80,** 76–87 (2015).
81. Matsui, J., Ochi, Y. & Tamaki, K. Photodimerization of Anthryl Moieties in a Poly(methacrylic acid) Derivative as Reversible Cross-linking Step in Molecular Imprinting. *Chem. Lett.* **35,** 80–81 (2006).
82. Zhao, D., Ren, B., Liu, S., Liu, X. & Tong, Z. A novel photoreversible poly(ferrocenylsilane) with coumarin side group: synthesis, characterization, and electrochemical activities. *Chem. Commun. (Camb).* 779–81 (2006). doi:10.1039/b515413h
83. Chujo, Y., Sada, K., Naka, a, Nomura, R. & Saegusa, T. Synthesis and redox gelation of disulfide-modifed polyoxazoline. *Macromolecules* **26,** 883–887 (1993).
84. Yang, Y., Lu, X. & Wang, W. A tough polyurethane elastomer with self-healing ability. *Mater. Des.* (2017). doi:10.1016/j.matdes.2017.04.015
85. Michal, B. T., Jaye, C. A., Spencer, E. J. & Rowan, S. J. Inherently photohealable and thermal shape-memory polydisulfide networks. *ACS Macro Lett.* **2,** 694–699 (2013).

86. Pepels, M., Filot, I., Klumperman, B. & Goossens, H. Self-healing systems based on disulfide–thiol exchange reactions. *Polym. Chem.* **4,** 4955 (2013).
87. Martin, R. *et al.* The processability of a poly(urea-urethane) elastomer reversibly crosslinked with aromatic disulfide bridges. *J. Mater. Chem. A* **2,** 5710 (2014).
88. Rajan, V. V., Dierkes, W. K., Joseph, R. & Noordermeer, J. W. M. Science and technology of rubber reclamation with special attention to NR-based waste latex products. *Prog. Polym. Sci.* **31,** 811–834 (2006).
89. Lenz, R. W. Structure, Properties, and Cross-linking Reactions of Poly(ester acetals). *Macromolecules* **2,** 129–136 (1969).
90. Philipp, W. H. & Hsu, L. C. Three methods for in situ cross-linking of polyvinyl alcohol films for application as ion-conducting membranes in potassium hydroxide electrolyte. *NASA Tech. Pap.* (1979). at <http://hdl.handle.net/2060/19790012957>
91. Sheibley, D. W. & Manzo, M. Polyvinyl alcohol membranes as alkaline battery separators. in 8 (1982).
92. Yu, K., Taynton, P., Zhang, W., Dunn, M. L. & Qi, H. J. Reprocessing and recycling of thermosetting polymers based on bond exchange reactions. *RSC Adv.* **4,** 10108 (2014).
93. Capelot, M., Montarnal, D., Tournilhac, F. & Leibler, L. Metal-catalyzed transesterification for healing and assembling of thermosets. *J. Am. Chem. Soc.* **134,** 7664–7667 (2012).
94. Altuna, F. I., Pettarin, V. & Williams, R. J. J. Self-healable polymer networks based on the cross-linking of epoxidised soybean oil by an aqueous citric acid solution. *Green Chem.* **15,** 3360 (2013).
95. Zhao, Q., Zou, W., Luo, Y. & Xie, T. Shape memory polymer network with thermally distinct elasticity and plasticity. *Sci. Adv.* **2,** e1501297–e1501297 (2016).
96. Brutman, J. P., Delgado, P. A. & Hillmyer, M. A. Polylactide vitrimers. *ACS Macro Lett.* **3,** 607–610 (2014).
97. Denissen, W. *et al.* Vinylogous urethane vitrimers. *Adv. Funct. Mater.* **25,** 2451–2457 (2015).
98. Denissen, W. *et al.* Chemical control of the viscoelastic properties of vinylogous urethane vitrimers. *Nat. Commun.* **8,** 14857 (2017).
99. Cromwell, O. R., Chung, J. & Guan, Z. Malleable and Self-Healing Covalent Polymer Networks through Tunable Dynamic Boronic Ester Bonds. *J. Am. Chem. Soc.* **137,** 6492–6495 (2015).
100. Röttger, M. *et al.* High-performance vitrimers from commodity thermoplastics through dioxaborolane metathesis. *Science (80-.).* **356,** 62–65 (2017).
101. Zheng, P. & McCarthy, T. J. A surprise from 1954: Siloxane equilibration is a simple, robust, and obvious polymer self-healing mechanism. *J. Am. Chem. Soc.* **134,** 2024–2027 (2012).
102. Lee, T. C. P., Sperling, L. H. & Tobolsky, A. V. Thermal stability of elastomeric networks at high temperatures. *J. Appl. Polym. Sci.* **10,** 1831–1836 (1966).
103. Gilbert, A. R. & Kantor, S. W. Transient catalysts for the polymerization of organosiloxanes. *J. Polym. Sci.* **40,** 35–58 (1959).
104. Lu, Y. X. & Guan, Z. Olefin metathesis for effective polymer healing via dynamic exchange of strong carbon-carbon double bonds. *J. Am. Chem. Soc.* **134,** 14226–14231 (2012).
105. Lu, Y. X., Tournilhac, F., Leibler, L. & Guan, Z. Making insoluble polymer networks malleable via olefin metathesis. *J. Am. Chem. Soc.* **134,** 8424–8427 (2012).
106. Kloxin, C. J., Scott, T. F., Park, H. Y. & Bowman, C. N. Mechanophotopatterning on a photoresponsive elastomer. *Adv. Mater.* **23,** 1977–1981 (2011).

107. Scott, T. F., Schneider, A. D., Cook, W. D. & Bowman, C. N. Photoinduced Plasticity in Cross-Linked Polymers. *Science (80-.).* **308,** 1615–1617 (2005).
108. Scott, T. F., Draughon, R. B. & Bowman, C. N. Actuation in crosslinked polymers via photoinduced stress relaxation. *Adv. Mater.* **18,** 2128–2132 (2006).
109. Kloxin, C. J., Scott, T. F. & Bowman, C. N. Stress Relaxation via Addition−Fragmentation Chain Transfer in a Thiol-ene Photopolymerization. *Macromolecules* **42,** 2551–2556 (2009).
110. Schiff, H. No Title. *Ann. Chem.* **131,** 118 (1864).
111. Belowich, M. E. & Stoddart, J. F. Dynamic imine chemistry. *Chem. Soc. Rev.* **41,** 2003 (2012).
112. Ciaccia, M., Pilati, S., Cacciapaglia, R., Mandolini, L. & Di Stefano, S. Effective catalysis of imine metathesis by means of fast transiminations between aromatic–aromatic or aromatic–aliphatic amines. *Org. Biomol. Chem.* **12,** 3282 (2014).
113. Ciaccia, M., Cacciapaglia, R., Mencarelli, P., Mandolini, L. & Stefano, S. Di. Fast transimination in organic solvents in the absence of proton and metal catalysts. A key to imine metathesis catalyzed by primary amines under mild conditions. *Chem. Sci.* **4,** 2253–2261 (2013).
114. Ciaccia, M. & Di Stefano, S. Mechanisms of imine exchange reactions in organic solvents. *Org. Biomol. Chem.* **13,** 646–654 (2015).
115. Hine, J. & Via, F. A. Kinetics of the formation of imines from isobutyraldehyde and primary aliphatic amines with polar substituents. *J. Am. Chem. Soc.* **94,** 190–194 (1972).
116. Giuseppone, N., Schmitt, J. L., Schwartz, E. & Lehn, J. M. Scandium(III) catalysis of transimination reactions. Independent and constitutionally coupled reversible processes. *J. Am. Chem. Soc.* **127,** 5528–5539 (2005).
117. Reeves, J. T. *et al.* A General Method for Imine Formation Using $B(OCH_2CF_3)_3$. *Org. Lett.* **17,** 2442–2445 (2015).
118. Taynton, P. *et al.* Heat- or water-driven malleability in a highly recyclable covalent network polymer. *Adv. Mater.* **26,** 3938–3942 (2014).
119. Taynton, P. *et al.* Repairable Woven Carbon Fiber Composites with Full Recyclability Enabled by Malleable Polyimine Networks. *Adv. Mater.* n/a-n/a (2016). doi:10.1002/adma.201505245
120. He, L. *et al.* Self-assembled encapsulation systems with pH tunable release property based on reversible covalent bond. *Chem. Commun.* **46,** 7569 (2010).
121. Ono, T., Nobori, T. & Lehn, J. M. Dynamic polymer blends--component recombination between neat dynamic covalent polymers at room temperature. *Chem Commun* 1522–1524 (2005). doi:10.1039/b418967a
122. Skene, W. G. & Lehn, J.-M. P. Dynamers: Polyacylhydrazone reversible covalent polymers, component exchange, and constitutional diversity. *Proc. Natl. Acad. Sci.* **101,** 8270–8275 (2004).
123. Roy, N., Buhler, E. & Lehn, J. M. Double dynamic self-healing polymers: Supramolecular and covalent dynamic polymers based on the bis-iminocarbohydrazide motif. *Polym. Int.* **63,** 1400–1405 (2014).
124. Fujii, S. & Lehn, J. M. Structural and functional evolution of a library of constitutional dynamic polymers driven by alkali metal ion recognition. *Angew. Chemie - Int. Ed.* **48,** 7635–7638 (2009).
125. Chow, C. F., Fujii, S. & Lehn, J. M. Metallodynamers: Neutral dynamic metallosupramolecular polymers displaying transformation of mechanical and optical properties on constitutional exchange. *Angew. Chemie - Int. Ed.* **46,** 5007–5010 (2007).

126. Folmer-Andersen, J. F. *et al.* Cooperative, bottom-up generation of rigid-rod nanostructures through dynamic polymer chemistry. *Polym. Int.* **59,** 1477–1491 (2010).
127. Tolmer-Andersen, J. F. & Lehn, J. M. Constitutional adaptation of dynamic polymers: Hydrophobically driven sequence selection in dynamic covalent polyacylhydrazones. *Angew. Chemie - Int. Ed.* **48,** 7664–7667 (2009).
128. Wang, C., Wang, G., Wang, Z. & Zhang, X. A pH-responsive superamphiphile based on dynamic covalent bonds. *Chem. - A Eur. J.* **17,** 3322–3325 (2011).
129. Jackson, A. W., Stakes, C. & Fulton, D. A. The formation of core cross-linked star polymer and nanogel assemblies facilitated by the formation of dynamic covalent imine bonds. *Polym. Chem.* **2,** 2500 (2011).
130. Bae, Y., Fukushima, S., Harada, A. & Kataoka, K. Design of environment-sensitive supramolecular assemblies for intracellular drug delivery: Polymeric micelles that are responsive to intracellular pH change. *Angew. Chemie - Int. Ed.* **42,** 4640–4643 (2003).
131. Deng, G., Tang, C., Li, F., Jiang, H. & Chen, Y. Covalent cross-linked polymer gels with reversible sol-gel transition and self-healing properties. *Macromolecules* **43,** 1191–1194 (2010).
132. Zhang, Y., Tao, L., Li, S. & Wei, Y. Synthesis of multiresponsive and dynamic chitosan-based hydrogels for controlled release of bioactive molecules. *Biomacromolecules* **12,** 2894–2901 (2011).
133. Ding, C. *et al.* Dually responsive injectable hydrogel prepared by in situ cross-linking of glycol chitosan and benzaldehyde-capped PEO-PPO-PEO. *Biomacromolecules* **11,** 1043–1051 (2010).
134. Zhang, H. *et al.* Recyclable polybutadiene elastomer based on dynamic imine bond. *J. Polym. Sci. Part A Polym. Chem.* 1–7 (2017). doi:10.1002/pola.28577
135. Zou, W., Dong, J., Luo, Y., Zhao, Q. & Xie, T. Dynamic Covalent Polymer Networks: from Old Chemistry to Modern Day Innovations. *Adv. Mater.* 1606100 (2017). doi:10.1002/adma.201606100
136. Iyer, S. R. & Wong, P. K. Die attach adhesive compositions - US5912282 A. (1999). at <https://www.google.com/patents/US5912282>
137. Kim, T.-D. *et al.* Ultralarge and Thermally Stable Electro-optic Activities from Diels–Alder Crosslinkable Polymers Containing Binary Chromophore Systems. *Adv. Mater.* **18,** 3038–3042 (2006).
138. Wang, H. & Heilshorn, S. C. Adaptable Hydrogel Networks with Reversible Linkages for Tissue Engineering. *Adv. Mater.* **27,** 3717–3736 (2015).
139. Davidson, C. L. & Feilzer, A. J. Polymerization shrinkage and polymerization shrinkage stress in polymer-based restoratives. *J. Dent.* **25,** 435–440 (1997).
140. Lehn, J.-M. Supramolecular polymer chemistry – scope and perspectives. *Polym. Int.* **51,** 825–839 (2002).
141. Serpe, M. J. & Craig, S. L. Physical organic chemistry of supramolecular polymers. *Langmuir* **23,** 1626–1634 (2007).
142. Brunsveld, L., Folmer, B. J. B., Meijer, E. W. & Sijbesma, R. P. Supramolecular Polymers. *Chem. Rev.* **101,** 4071–4098 (2001).
143. Yang, S. K., Ambade, A. V & Weck, M. Main-chain supramolecular block copolymers. *Chem. Soc. Rev.* **40,** 129–137 (2011).
144. Binder, W. H. & Zirbs, R. in *Hydrogen Bonded Polymers SE - 109* **207,** 1–78 (2006).
145. Weck, M. Side-chain functionalized supramolecular polymers. *Polym. Int.* **56,** 453–460 (2007).
146. Seiffert, S. & Sprakel, J. Physical chemistry of supramolecular polymer networks. *Chem. Soc. Rev.* **41,** 909–930 (2012).

147. Steed, J. W. & Atwood, J. L. in *Supramolecular Chemistry, 2nd Edition* (Wiley, 2009). doi:10.1002/9780470740880
148. Aida, T., Meijer, E. W. & Stupp, S. I. Functional Supramolecular Polymers. *Science (80-.).* **335,** 813–817 (2012).
149. Fox, J. D. & Rowan, S. J. Supramolecular polymerizations and main-chain supramolecular polymers. *Macromolecules* **42,** 6823–6835 (2009).
150. Vaiyapuri, R., Greenland, B. W., Colquhoun, H. M., Elliott, J. M. & Hayes, W. Evolution of supramolecular healable composites: a minireview. *Polym. Int.* **63,** 933–942 (2014).
151. Yang, Y. & Urban, M. W. Self-healing polymeric materials. *Chem. Soc. Rev.* **42,** 7446–67 (2013).
152. Herbst, F., Döhler, D., Michael, P. & Binder, W. H. Self-healing polymers via supramolecular forces. *Macromolecular Rapid Communications* **34,** 203–220 (2013).
153. Kato, T. & Frechet, J. M. J. Stabilization of a liquid-crystalline phase through noncovalent interaction with a polymer side chain. *Macromolecules* **22,** 3818–3819 (1989).
154. Ilhan, F., Gray, M. & Rotello, V. M. Reversible Side Chain Modification through Noncovalent Interactions. 'Plug and Play' Polymers. *Macromolecules* **34,** 2597–2601 (2001).
155. Pollino, J. M. & Weck, M. Non-covalent side-chain polymers: design principles, functionalization strategies, and perspectives. *Chem. Soc. Rev.* **34,** 193 (2005).
156. Gooch, A., Murphy, N. S., Thomson, N. H. & Wilson, A. J. Side-chain supramolecular polymers employing conformer independent triple hydrogen bonding arrays. *Macromolecules* **46,** 9634–9641 (2013).
157. De Greef, T. F. A. *et al.* Supramolecular Polymerization. *Chem. Rev.* **109,** 5687–5754 (2009).
158. Smulders, M. M. J. *et al.* How to distinguish isodesmic from cooperative supramolecular polymerisation. *Chem. - A Eur. J.* **16,** 362–367 (2010).
159. Semenov, A. N. & Rubinstein, M. Thermoreversible Gelation in Solutions of Associative Polymers. 1. Statics. *Macromolecules* **31,** 1373–1385 (1998).
160. Hart, L. R., Harries, J. L., Greenland, B. W., Colquhoun, H. M. & Hayes, W. Healable supramolecular polymers. *Polym. Chem.* **4,** 4860 (2013).
161. Burattini, S., Greenland, B. W., Chappell, D., Colquhoun, H. M. & Hayes, W. Healable polymeric materials: a tutorial review. *Chem. Soc. Rev.* **39,** 1973–1985 (2010).
162. Bosman, A. W., Sijbesma, R. P. & Meijer, E. . Supramolecular polymers at work. *Mater. Today* **7,** 34–39 (2004).
163. Armstrong, G. & Buggy, M. Hydrogen-bonded supramolecular polymers: A literature review. *J. Mater. Sci.* **40,** 547–559 (2005).
164. Stadler, R. & de Lucca Freitas, L. Thermoplastic elastomers by hydrogen bonding 1. Rheological properties of modified polybutadiene. *Colloid Polym. Sci.* **264,** 773–778 (1986).
165. De Lucca Freitas, L. L. & Stadler, R. Thermoplastic elastomers by hydrogen bonding. 3. Interrelations between molecular parameters and rheological properties. *Macromolecules* **20,** 2478–2485 (1987).
166. Hilger, C., Dräger, M. & Stadler, R. Molecular Origin of Supramolecular Self-Assembling in Statistical Copolymers. *Macromolecules* **25,** 2498–2501 (1992).
167. Lange, R. F. M., Van Gurp, M. & Meijer, E. W. Hydrogen-bonded supramolecular polymer networks. *J. Polym. Sci. Part A Polym. Chem.* **37,** 3657–3670 (1999).
168. Wietor, J. L., Van Beek, D. J. M., Peters, G. W., Mendes, E. & Sijbesma, R. P. Effects of branching and crystallization on rheology of polycaprolactone supramolecular

polymers with ureidopyrimidinone end groups. *Macromolecules* **44,** 1211–1219 (2011).
169. Rieth, L. R., Eaton, R. F. & Coates, G. W. Polymerization of Ureidopyrimidinone-Functionalized Olefins by Using Late-Transition Metal Ziegler-Natta Catalysts: Synthesis of Thermoplastic Elastomeric Polyolefins. *Angew. Chemie* **113,** 2211–2214 (2001).
170. Lewis, C. L., Stewart, K. & Anthamatten, M. The influence of hydrogen bonding side-groups on viscoelastic behavior of linear and network polymers. *Macromolecules* **47,** 729–740 (2014).
171. Kaitz, J. A. *et al.* Depolymerizable, adaptive supramolecular polymer nanoparticles and networks. *Polym. Chem.* **5,** 3788 (2014).
172. Söntjens, S. H. M., Sijbesma, R. P., Van Genderen, M. H. P. & Meijer, E. W. Stability and lifetime of quadruply hydrogen bonded 2-Ureido-4[1H]-pyrimidinone dimers. *J. Am. Chem. Soc.* **122,** 7487–7493 (2000).
173. Folmer, B. J. B., Sijbesma, R. P., Versteegen, R. M., van der Rijt, J. A. J. & Meijer, E. W. Supramolecular Polymer Materials: Chain Extension of Telechelic Polymers Using a Reactive Hydrogen-Bonding Synthon. *Adv. Mater.* **12,** 874–878 (2000).
174. Guo, M. *et al.* Tough stimuli-responsive supramolecular hydrogels with hydrogen-bonding network junctions. *J. Am. Chem. Soc.* **136,** 6969–6977 (2014).
175. Söntjens, S. H. M. *et al.* Thermoplastic elastomers based on strong and well-defined hydrogen-bonding interactions. *Macromolecules* **41,** 5703–5708 (2008).
176. Fang, X. *et al.* Biomimetic Modular Polymer with Tough and Stress Sensing Properties. *Macromolecules* **46,** 6566–6574 (2013).
177. Merino, D. H. *et al.* A systematic study of the effect of the hard end-group composition on the microphase separation, thermal and mechanical properties of supramolecular polyurethanes. *Polym. (United Kingdom)* **107,** 368–378 (2016).
178. Woodward, P. J. *et al.* Hydrogen bonded supramolecular elastomers: Correlating hydrogen bonding strength with morphology and rheology. *Macromolecules* **43,** 2512–2517 (2010).
179. Nair, K. P., Breedveld, V. & Weck, M. Complementary hydrogen-bonded thermoreversible polymer networks with tunable properties. *Macromolecules* **41,** 3429–3438 (2008).
180. Nair, K. P., Breedveld, V. & Weck, M. Modulating mechanical properties of self-assembled polymer networks by multi-functional complementary hydrogen bonding. *Soft Matter* **7,** 553 (2011).
181. Colombani, O. *et al.* Attempt toward 1D cross-linked thermoplastic elastomers: Structure and mechanical properties of a new system. *Macromolecules* **38,** 1752–1759 (2005).
182. Yan, T., Schröter, K., Herbst, F., Binder, W. H. & Thurn-Albrecht, T. Unveiling the molecular mechanism of self-healing in a telechelic, supramolecular polymer network. *Sci. Rep.* **6,** 32356 (2016).
183. Cordier, P., Tournilhac, F., Soulié-Ziakovic, C. & Leibler, L. Self-healing and thermoreversible rubber from supramolecular assembly. *Nature* **451,** 977–980 (2008).
184. Montarnal, D., Tournilhac, F., Hidalgo, M., Couturier, J. L. & Leibler, L. Versatile one-pot synthesis of supramolecular plastics and self-healing rubbers. *J. Am. Chem. Soc.* **131,** 7966–7967 (2009).
185. Sordo, F., Mougnier, S. J., Loureiro, N., Tournilhac, F. & Michaud, V. Design of Self-Healing Supramolecular Rubbers with a Tunable Number of Chemical Cross-Links. *Macromolecules* **48,** 4394–4402 (2015).

186. Winter, A. & Schubert, U. S. Synthesis and characterization of metallo-supramolecular polymers. *Chem. Soc. Rev.* **45,** 5311–5357 (2016).
187. Schubert, U. S. & Eschbaumer, C. Macromolecules containing bipyridine and terpyridine metal complexes: Towards metallosupramolecular polymers. *Angew. Chemie - Int. Ed.* **41,** 2892–2926 (2002).
188. Sandmann, B. *et al.* The self-healing potential of triazole-pyridine-based metallopolymers. *Macromol. Rapid Commun.* **36,** 604–609 (2015).
189. Bode, S. *et al.* Self-healing polymer coatings based on crosslinked metallosupramolecular copolymers. *Adv. Mater.* **25,** 1634–1638 (2013).
190. Bode, S. *et al.* Self-healing metallopolymers based on cadmium bis(terpyridine) complex containing polymer networks. *Polym. Chem.* **4,** 4966 (2013).
191. Li, C.-H. *et al.* A highly stretchable autonomous self-healing elastomer. *Nat Chem* **8,** 618–624 (2016).
192. Mozhdehi, D., Ayala, S., Cromwell, O. R. & Guan, Z. Self-Healing Multiphase Polymers via Dynamic Metal–Ligand Interactions. *J. Am. Chem. Soc.* **136,** 16128–16131 (2014).
193. Burattini, S. *et al.* A Healable Supramolecular Polymer Blend Based on Aromatic π - π Stacking and Hydrogen-Bonding Interactions. 12051–12058 (2010).
194. Burattini, S. *et al.* A self-repairing, supramolecular polymer system: healability as a consequence of donor–acceptor π–π stacking interactions. *Chem. Commun.* 6717 (2009). doi:10.1039/b910648k
195. Burattini, S., Colquhoun, H. M., Greenland, B. W. & Hayes, W. A novel self-healing supramolecular polymer system. *Faraday Discuss.* **143,** 251 (2009).
196. Feula, A. *et al.* A Thermoreversible Supramolecular Polyurethane with Excellent Healing Ability at 45 °c. *Macromolecules* **48,** 6132–6141 (2015).
197. Das, A. *et al.* Ionic Modification Turns Commercial Rubber into a Self-Healing Material. *ACS Appl. Mater. Interfaces* **7,** 20623–20630 (2015).
198. Malmierca, M. A. *et al.* Characterization of Network Structure and Chain Dynamics of Elastomeric Ionomers by Means of 1 H Low-Field NMR. *Macromolecules* **47,** 5655–5667 (2014).
199. Mora-Barrantes, I., Malmierca, M. A., Valentin, J. L., Rodriguez, A. & Ibarra, L. Effect of covalent cross-links on the network structure of thermo-reversible ionic elastomers. *Soft Matter* **8,** 5201 (2012).
200. Wang, D. *et al.* Intelligent rubber with tailored properties for self- healing and shape memory. *J. Mater. Chem. A Mater. energy Sustain.* **3,** 12864–12872 (2015).
201. Frampton, M. J. & Anderson, H. L. Insulated Molecular Wires. *Angew. Chemie Int. Ed.* **46,** 1028–1064 (2007).
202. Hart, L. R. *et al.* 3D Printing of Biocompatible Supramolecular Polymers and their Composites. *ACS Appl. Mater. Interfaces* **8,** 3115–3122 (2016).
203. Krieg, E., Bastings, M. M. C., Besenius, P. & Rybtchinski, B. Supramolecular Polymers in Aqueous Media. *Chem. Rev.* **16,** 2414–2477 (2016).
204. Rybtchinski, B. Adaptive supramolecular nanomaterials based on strong noncovalent interactions. *ACS Nano* **5,** 6791–6818 (2011).
205. Yang, L., Tan, X., Wang, Z. & Zhang, X. Supramolecular Polymers: Historical Development, Preparation, Characterization, and Functions. *Chem. Rev.* **115,** 7196–7239 (2015).
206. Li, S.-L., Xiao, T., Lin, C. & Wang, L. Advanced supramolecular polymers constructed by orthogonal self-assembly. *Chemical Society Reviews* **41,** 5950 (2012).

207. Elacqua, E., Lye, D. S. & Weck, M. Engineering Orthogonality in Supramolecular Polymers: From Simple Scaffolds to Complex Materials. *Acc. Chem. Res.* **47,** 2405–2416 (2014).
208. Botterhuis, N. E., van Beek, D. J. M., van Gemert, G. M. L., Bosman, A. W. & Sijbesma, R. P. Self-assembly and morphology of polydimethylsiloxane supramolecular thermoplastic elastomers. *J. Polym. Sci. Part A Polym. Chem.* **46,** 3877–3885 (2008).
209. Kautz, H., van Beek, D. J. M., Sijbesma, R. P. & Meijer, E. W. Cooperative End-to-End and Lateral Hydrogen-Bonding Motifs in Supramolecular Thermoplastic Elastomers. *Macromolecules* **39,** 4265–4267 (2006).
210. Mes, T. *et al.* Network formation in an orthogonally self-assembling system. *ACS Macro Lett.* **1,** 105–109 (2012).
211. Hofmeier, H., El-ghayoury, A., Schenning, A. P. H. J. & Schubert, U. S. New supramolecular polymers containing both terpyridine metal complexes and quadruple hydrogen bonding units. *Chem. Commun. (Camb).* **1,** 318–319 (2004).
212. Hofmeier, H., Hoogenboom, R., Wouters, M. E. L. & Schubert, U. S. High molecular weight supramolecular polymers containing both terpyridine metal complexes and ureidopyrimidinone quadruple hydrogen-bonding units in the main chain. *J. Am. Chem. Soc.* **127,** 2913–2921 (2005).
213. Shi, L. *et al.* Engineering a polymeric chiral catalyst by using hydrogen bonding and coordination interactions. *Angew. Chemie - Int. Ed.* **45,** 4108–4112 (2006).
214. Li, S.-L. *et al.* Formation of polypseudorotaxane networks by cross-linking the quadruple hydrogen bonded linear supramolecular polymers via bisparaquat molecules. *Chem. Commun.* **47,** 10755 (2011).
215. Grimm, F., Ulm, N., Gröhn, F., Düring, J. & Hirsch, A. Self-assembly of supramolecular architectures and polymers by orthogonal metal complexation and hydrogen-bonding motifs. *Chem. - A Eur. J.* **17,** 9478–9488 (2011).
216. Gröger, G. *et al.* Switchable supramolecular polymers from the self-assembly of a small monomer with two orthogonal binding interactions. *J. Am. Chem. Soc.* **133,** 8961–8971 (2011).
217. Yan, X. *et al.* A multiresponsive, shape-persistent, and elastic supramolecular polymer network gel constructed by orthogonal self-assembly. *Adv. Mater.* **24,** 362–369 (2012).
218. Wang, F. *et al.* Metal coordination mediated reversible conversion between linear and cross-linked supramolecular polymers. *Angew. Chemie - Int. Ed.* **49,** 1090–1094 (2010).
219. Zhang, Y., Li, Y. & Liu, W. Dipole-dipole and h-bonding interactions significantly enhance the multifaceted mechanical properties of thermoresponsive shape memory hydrogels. *Adv. Funct. Mater.* **25,** 471–480 (2015).
220. Daemi, H. *et al.* A robust super-tough biodegradable elastomer engineered by supramolecular ionic interactions. *Biomaterials* **84,** 54–63 (2016).
221. Ibarra, L., Rodríguez, A. & Mora-Barrantes, I. Crosslinking of carboxylated nitrile rubber (XNBR) induced by coordination with anhydrous copper sulfate. *Polym. Int.* **58,** 218–226 (2009).
222. Kolomiets, E. & Lehn, J. Double dynamers: molecular and supramolecular double dynamic polymers. *Chem. Commun.* 1519 (2005). doi:10.1039/b418899c
223. Zhang, B. *et al.* Self-healing, malleable and creep limiting materials using both supramolecular and reversible covalent linkages. *Polym. Chem.* **6,** 7368–7372 (2015).
224. Foster, E. M. *et al.* Effect of Polymer Network Architecture, Enhancing Soft Materials Using Orthogonal Dynamic Bonds in an Interpenetrating Network. *ACS Macro Lett.* 495–499 (2017). doi:10.1021/acsmacrolett.7b00172

225. ten Cate, A. T., Dankers, P. Y. W., Sijbesma, R. P. & Meijer, E. W. Disulfide Exchange in Hydrogen-Bonded Cyclic Assemblies: Stereochemical Self-Selection by Double Dynamic Chemistry. *J. Org. Chem.* **70,** 5799–5803 (2005).
226. Rekondo, A. *et al.* Catalyst-free room-temperature self-healing elastomers based on aromatic disulfide metathesis. *Mater. Horizons* **1,** 237–240 (2014).
227. Neal, J. A., Mozhdehi, D. & Guan, Z. Enhancing Mechanical Performance of a Covalent Self-Healing Material by Sacrificial Noncovalent Bonds. *J. Am. Chem. Soc.* **137,** 4846–4850 (2015).
228. Xu, J. F., Chen, Y. Z., Wu, L. Z., Tung, C. H. & Yang, Q. Z. Dynamic covalent bond based on reversible photo [4 + 4] cycloaddition of anthracene for construction of double-dynamic polymers. *Org. Lett.* **15,** 6148–6151 (2013).
229. Wang, Y. *et al.* Dual-Stimuli-Responsive Fluorescent Supramolecular Polymer Based on a Diselenium-Bridged Pillar[5]arene Dimer and an AIE-Active Tetraphenylethylene Guest. *Macromolecules* **50,** 5759–5766 (2017).
230. Mukherjee, S., Brooks, W. L. A., Dai, Y. & Sumerlin, B. S. Doubly-dynamic-covalent polymers composed of oxime and oxanorbornene links. *Polym. Chem.* **7,** 1971–1978 (2016).
231. Deng, G. *et al.* Dynamic hydrogels with an environmental adaptive self-healing ability and dual responsive Sol-Gel transitions. *ACS Macro Lett.* **1,** 275–279 (2012).
232. Chino, K. & Ashiura, M. Themoreversible Cross-Linking Rubber Using Supramolecular Hydrogen-Bonding Networks. *Macromolecules* **34,** 9201–9204 (2001).

Chapter 2: Synthesis and Characterisation of Main-Chain Supramolecular Polymers from Polyisoprene

2.1 Introduction

The first strategy taken to achieve the aim of this project was to synthesise polymeric materials based on a polyisoprene (PI) backbone functionalised with ureidopyrimidinone (UPy) quadruple hydrogen-bonding moieties at the chain ends, and functionalised with amine/aldehyde moieties along the backbone (Figure 35). The materials aimed to be a blend of main-chain and side-chain functionalised polymers. The strategy to achieve these materials comprised first the synthesis of a PI backbone functionalised with alkyne units (or a protected analogue) at both chain-ends, followed by reaction of these bonds with separately prepared azide-functionalised UPy synthons. The 1,2 and 3,4-alkene bonds along the PI backbone would then subsequently be used to attach amine and aldehyde moieties, which undergo dynamic imine formation and exchange, by reaction with silane.

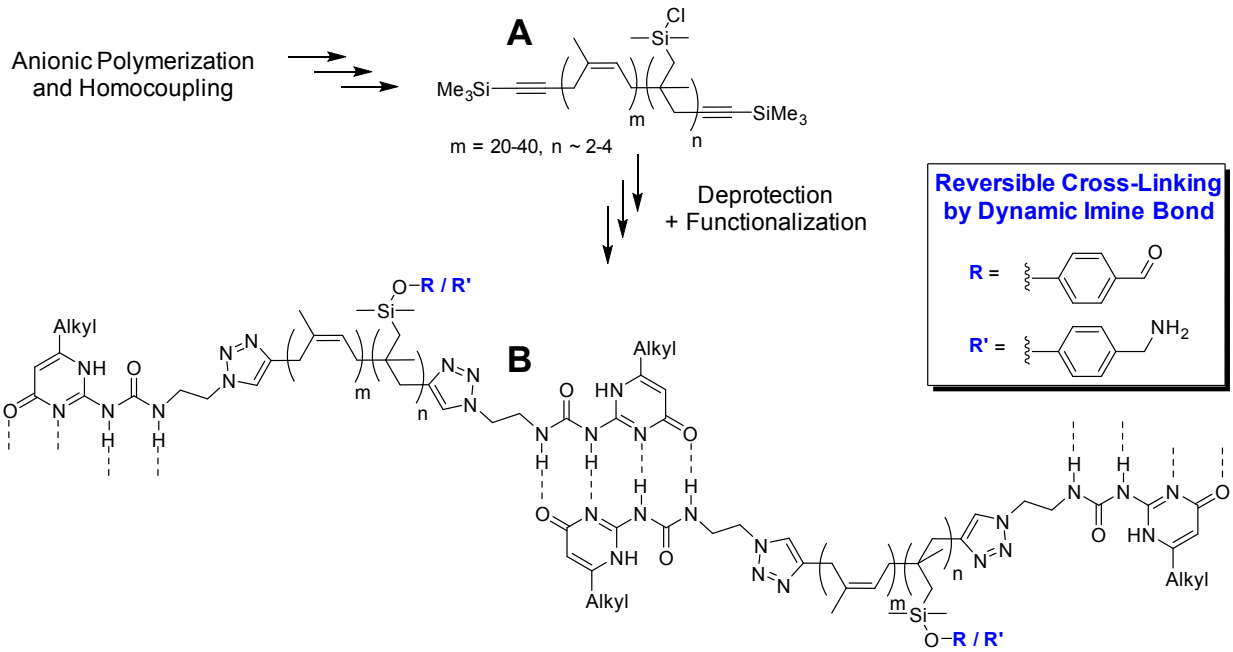

Figure 35 – Synthetic strategy proposed for the synthesis of modular double-dynamic polymeric materials

One of the main problems faced by industry in the production of new functional polydienes is the ability to produce well-defined α,ω-bi-functional polymers with control over their microstructure, molecular weight and with control over the degree of functionality. The

microstructure of the PI backbone, i.e. the relative quantity of different isomeric structures in the polymer backbone, has an instrumental influence on the physical properties of the resultant material.[1,2] Four microstructures are present in PIs: *cis*- and *trans*-1,4, 3,4 and 1,2 (Scheme 20). The elastomeric property of PI (which is the main reason of interest in PI) results from the presence of the *cis* and *trans*-1,4 isomers; PIs with high *cis/trans*-1.4 content are highly elastomeric.[3,4]

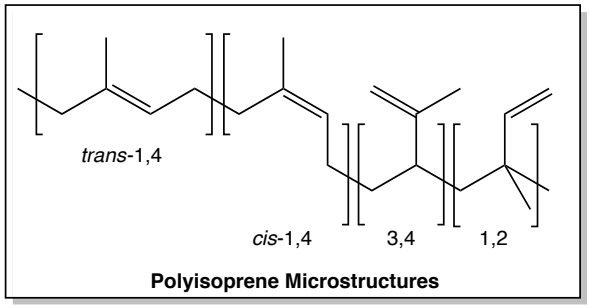

Scheme 20 – microstructures of polyisoprene

Classically, the synthesis of highly elastomeric PIs without chemical functionalisation at the chain-ends, or with functionalisation at one chain-end, is easily achieved (and achieved at industrial scales) by a 'living' anionic methodology in non-polar solvents, typically using organolithium initiating agents. However, most of the common initiating agents react in a way that allows only one end to propagate in the polymerisation; the other end is left chemically inert and difficult to further modify. Bifunctional initiators, in which two chain-ends remain 'living', are available (naphthalene potassium is the most common choice); however the vast majority are poorly soluble in non-polar solvents and the use of polar solvents, or non-polar solvents with polar additives (particularly THF), has a drastic effect on the microstructural content of the polymer produced.[1–5] An alternative path to bifunctional polydienes has also been investigated by use of a protected functionalised initiator.[6]

With these constraints in mind, it was chosen to synthesise bi-functional PIs using an initiator prepared *in situ* from 1,3-diisopropenyl benzene and *sec*-butyl lithium. This initiator has been previously shown to produce bifunctional PIs with a high content of the *cis*/*trans*-1,4 isomer.[2,7,8] The functionalisation of the chain-ends with the alkyne moiety would be attempted both directly, on termination of the 'living' chains, and indirectly, in a post-polymerisation modification. Incorporation of the UPy hydrogen-bonding moiety would be achieved first by preparation of an azide-functionalised UPy synthon, following an adapted procedure from the literature,[9] followed by the copper-catalysed azide-alkyne cycloaddition (CuAAc) 'click'

reaction. Modification of the pendent alkene moieties present on the PI backbone would be reacted by hydrosilylation catalysed using Karstedt's catalyst.

2.2 Synthesis and Characterisation of Functionalised Polyisoprenes

2.2.1 Synthesis

*Unfunctionalised Polyisoprene (**PI1 CTL**)*

The control PI containing only secondary butane at the chain-ends or along the backbone was synthesised using a classic 'living' anionic procedure in non-polar solvents (Scheme 21).

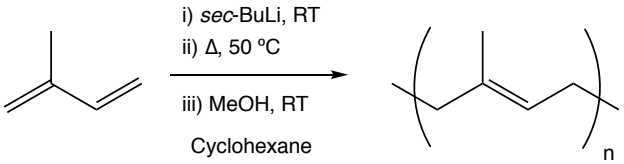

*Scheme 21 – Polymerisation of isoprene, forming unfunctionalised polyisoprene (**PI1 CTL**)*

These conditions required air-free conditions and solvent (cyclohexane) and monomer (isoprene) to be distilled over sodium before use. *Sec*-butyl lithium was synthesised, titrated and used as the initiator for the polymerisation. The polymerisation was achieved in a one-pot fashion, by introduction of solvent, followed by initiator (to quench impurities present in the solvent and on the glassware), before introduction of isoprene under argon overpressure. A molecular weight of 10,000 g/mol was targeted, due to the ease of purification by precipitation of PIs with this molecular weight. Termination of the polymerisation was achieved by introduction of acidified methanol. Purification of the polymer required only precipitation of the polymer in methanol.

*Mono-Alkyne-Functionalised Polyisoprene (**PI1 ALK**)*

Introduction of a chemical moiety, with which the UPy synthon could be reacted, was first attempted by direct termination with propargyl bromide, with the aim of alkyne-functionalisation. This approach however yielded a partially dimerised product, deduced from the observation of a prominent double mass peak on Size Exclusion Chromatography (SEC) (Scheme 22).

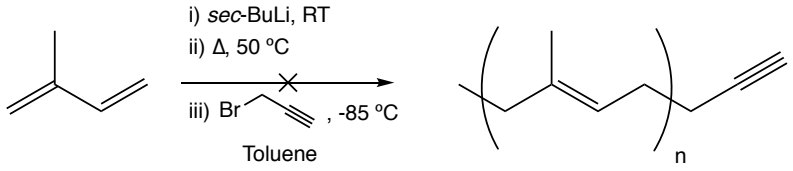

Scheme 22 – Synthesis of mono-alkyne-functionalised polyisoprene, by direct termination with propargyl bromide. This methodology produced a large coupling peak due to dimerisation.

A modified approach was therefore envisaged, in which post-polymerisation of an alcohol-functionalised PI would be required to reach the target (Scheme 23). The alcohol functionality at one chain-end was achieved by initiation and propagation as described above, and termination with ethylene oxide at –85 ºC, yielding **PI1 OH**. Post-polymerisation modification of the purified product was then achieved by reaction with propargyl bromide in basic conditions. The presence of alkyne functionality on the PI was confirmed by ^{1}H NMR spectroscopy, yielding **PI1 ALK**.

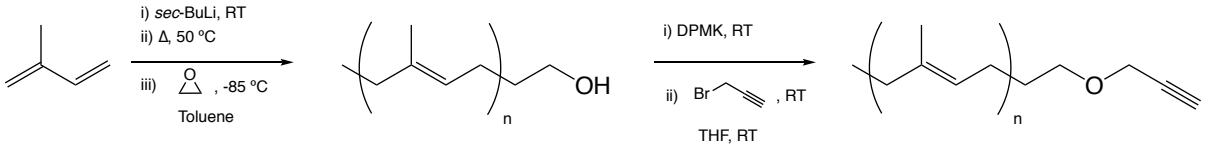

*Scheme 23 – Mono-alkyne functionalised polyisoprene (**PI1 ALK**). Step one produces mono-alcohol functionalised polyisoprene before a second reaction to functionalise with an alkyne moiety*

*α,ω-Alkyne Polyisoprene **PI2 ALK***

To produce bifunctional PIs, a bifunctional initiator was synthesised *in situ* following an adapted procedure previously published by *Lutz et al.*[10] The introduction of 1,3-diisopropenyl benzene and 2 equivalents of *sec*-BuLi was first used to produce an un-functionalised control (**PI2 CTL**) with which we could compare the functionalised analogues after termination with acidified methanol (Scheme 24).

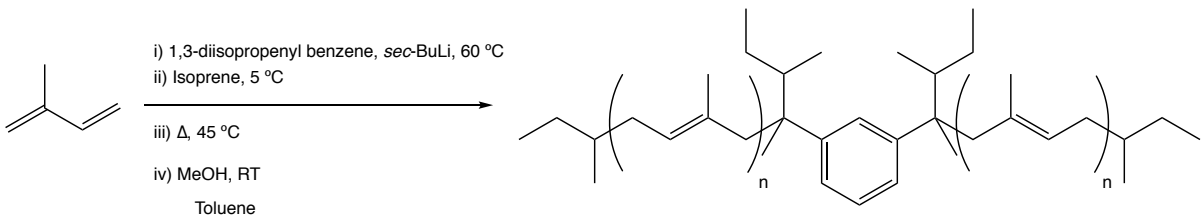

Scheme 24 – Polymerisation of isoprene using 1,3-diisopropenyl benzene as a bifunctional initiator

The alcohol-functionalised analogue was synthesised according to the same conditions using ethylene oxide at –85 ºC (Scheme 25), yielding **PI2 OH**. Interestingly, upon addition of ethylene oxide, the colourless polymer solution was observed to form a gel. This is explained by possible association, by ionic interaction, between alcoholates formed at the chain-ends. Upon addition of acidified methanol, to protonate the alcoholate, a gel-sol transition was observed. Post-polymerisation modification, to introduce the alkyne at the chain-ends, was achieved by reaction with propargyl bromide in basic conditions. Gelation was again observed upon addition of base (diphenylmethyl potassium), and subsequent deprotonation to form the alcholate, before returning to the sol after reaction with propargyl bromide (Scheme 25). The presence of the alkyne functionality was confirmed by ^{1}H NMR spectropscopy, yielding **PI2 ALK**.

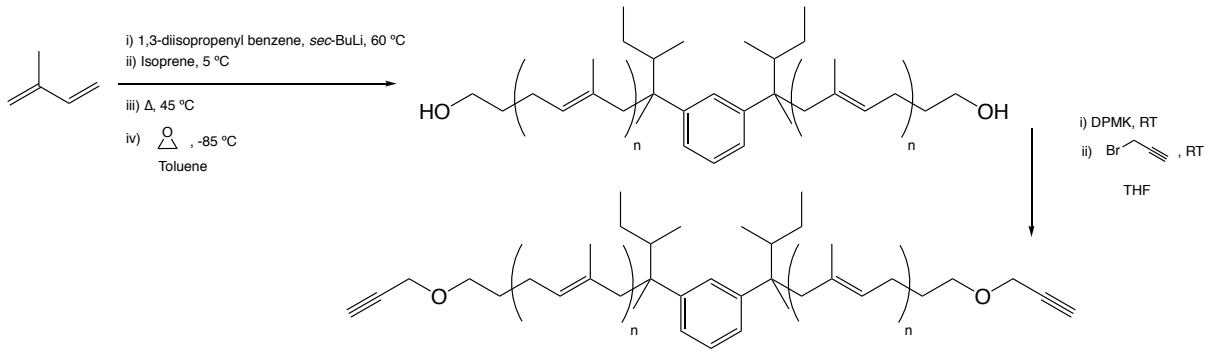

Scheme 25 – Synthesis of bi-alkyne functionalised polyisoprene via dihydroxyl polyisoprene

2.2.2 Characterisation

Microstructural Composition

The microstructural content of each of the produced polymers was quantified by ^{1}H NMR spectroscopy (Table 3). For each of the products, the largest resonance at δ ~5.00 corresponds to sections of the PI backbone with the 1,4 conformation; this resonance was integrated and used as the reference against which all other resonances (resulting from the presence of the other microstructural conformations) were measured (Figure 36). The found integrals were then calculated as a relative percentage using Equation 6.

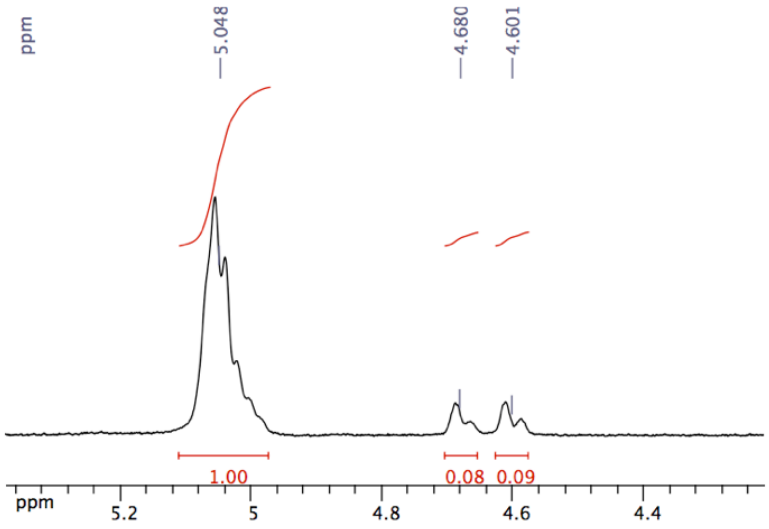

Figure 36 – ^{1}H NMR spectrum of the cis/trans-1,4, 3,4 and 1,2 proton resonances at δ = 5.048, 4.680 and 4.601 respectively.

$$Proportion\ of\ microstructure = \frac{I\ (microstructure\ of\ interest)}{I(5.19-4.19) + I(4.64–4.7 + 4.58–4.62)/2} \times 100$$

Equation 6 – Equation for the calculation of the proportion of microstructural content.[11]

From this analysis, it was found that all of the polymers produced contained a *cis/trans*-1,4 content greater than 90%; the proportion of 1,2 and 3,4 present almost always the same. It could also be concluded that there was no influence on the microstructure when changing the nature of the initiator, as both unfunctionalised PIs (**PI1 CTL** and **PI2 CTL**) possessed almost identical microstructural content; this is conducive to previous publication.[10] With a theoretical molecular weight of 10,000 g/mol for each of these polymers, the number of pendent double bonds can be estimated between 9–13 units per molecule.

	Microstructure		
	cis/trans-1,4	1,2	1,3
PI1 CTL	93%	4%	4%
PI1 OH	92%	4%	4%
PI2 CTL	94%	3%	3%
PI2 OH	91%	5%	4%

Table 3 – Table of the microstructural content for each polymer calculated from the ^{1}H NMR spectra and equation 1

Chemical Functionalisation

Confirming and quantifying the presence of chemical functionality at the chain-ends was also achieved by ^{1}H NMR spectroscopy (Figure 37). Broad resonances at δ ~3.6 were found in the spectra of both hydroxyl-functionalised polymers, which is attributed to the presence of the alcohol functionality at the chain-ends (more precisely the two protons on the adjacent carbon). The degree of functionalisation was calculated using Equation 7 and Equation 8 with the number average molecular weights discussed in the next part of this section.

$$F(OH) = \frac{I(3.65)/2}{\{I(5.15) + I(4.70) + I(4.65)\}/\{[1,4] + 2[1,2] + 2[3,4]\}} \times DP$$

Equation 7 – Equation for the caluclation of the degree of hydroxyl-functionality

$$DP_n = \frac{M_n}{68.12}$$

Equation 8 – Equation for the calculation of the degree of polymerisation

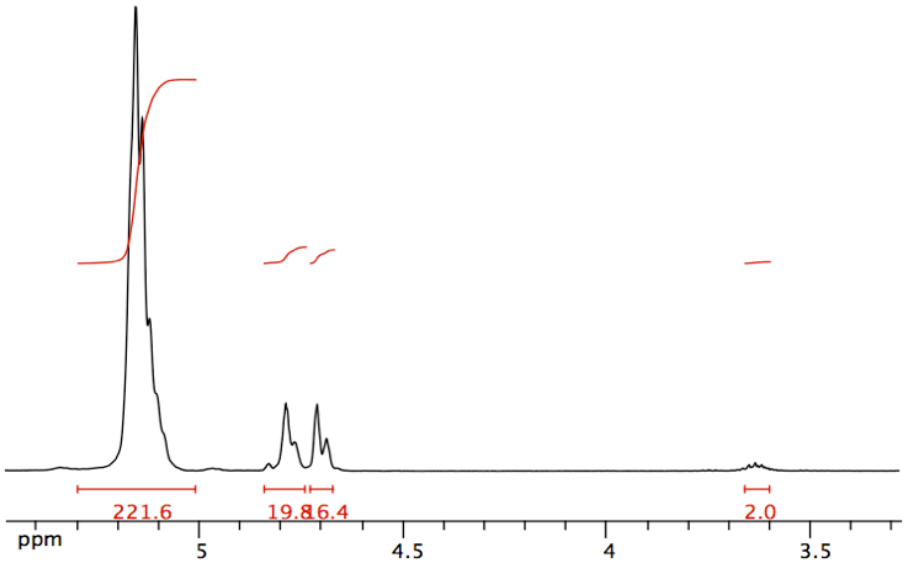

*Figure 37 – ^{1}H NMR spectrum of **PI1 CTL** with cis/trans-1,4, 1,3, 1,2 and –C**H**$_2$OH proton resonances at δ 5.15, δ 4.28, δ 4.19, and δ 3.63 respectively*

The degree of functionalisation for **PI1 OH** was found to be 0.6, considerably below the expected value of 1. It is possible that this discrepancy is observed due to perturbation by the high molecular weight of the PI, and hence low intensity of the protons associated with the

hydroxyl group. Equally this value could be explained as a result of incomplete functionalisation from inefficient termination by ethylene oxide or addition of too little ethylene oxide. The degree of functionalisation for **PI2 OH** was found to be much closer to expectation, with a value of 1.97. It is therefore likely that the low degree of functionalisation calculated for **PI1 OH** is due to poor control over the amount of ethylene oxide added to terminate the living polymer chains. In fact, on multiple executions of the same synthetic protocol, reproducibility of alcohol functionalisation was found to be poor.[§] Nevertheless, the conversion of the alcohol moiety to alkyne, after reaction with propargyl bromide was followed by the downfield shift, to δ 3.58, of the resonance, corresponding to the adjacent CH_2 to the oxygen atom and the formation of a new resonance at δ 4.00, attributed to the alkyne proton.

Polydispersity Index

The dispersity of molecular weights of each of the polymers was analysed by SEC using THF as the mobile phase at concentrations ~3 mg/mL (Figure 38). **PI1 CTL** yielded, as expected, monodisperse polymers with a dispersity of 1.05 (Figure 38a). **PI1 OH** showed minimal increase in dispersity index (1.09). When compared to the use of propargyl bromide as the termination agent, as mentioned above, the absence of any higher molecular weight peaks or shoulders suggested that the decreased nucleophilicity of the alcoholate, compared to the carbanion of the living chain, prevents any dimerization. This result proves a well controlled initiation and termination of the polymer system. A clear difference between systems using *sec*-BuLi and 1,3-diisopropenyl benzene as initiators was observed; a less monodisperse product is formed from using the latter initiator with a polydispersity index of 1.31. The asymmetric nature of the chromatogram, with tailing of the peak (Figure 38b) from the content of lower molecular weight species suggests that this decrease in monodispersity is caused by inefficient initiation. As in the other polymer samples, there are no higher molecular weight species. A final, noteworthy, difference between the two chromatograms is the shifted position of the SEC peak of **PI2 CTL**, towards higher molecular weights. This observation is in agreement with the increase molecular weight observed by light scattering (discussed below).

[§] This is likely to be due to the challenging constraints that were imposed due to safety concerns over the presence of ethylene oxide in the laboratory. The procedure that was used to obtain ethylene oxide involved its distillation from THF solution, with only very small quantities permitted to be used.

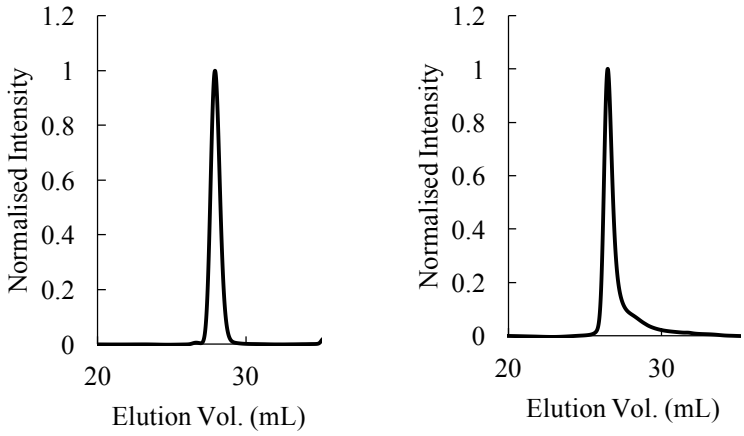

*Figure 38 – Size exclusion chromatograms of **PI1 CTL** (left) and **PI2 CTL** (right)*

Molecular Weight

Quantification of the molecular weight of the polymer materials was measured by light scattering (Table 4). PIs produced from the use of *sec*-BuLi as the initiator produced polymers with molecular weights in good agreement to theoretical M_w of 10,000 g/mol. The use of 1,3-diisopropenyl benzene and sec-BuLi as the initiator, however, had considerable impact on the experimental molecular weight, with M_w of the produced PIs more than two times higher.

	Mn (LS) g/mol	Mw (LS) g/mol
PI1 CTL	8963	13340
PI1 OH	8297	10120
PI2 CTL	24430	31071
PI2 OH	18440	24050

Table 4 – Molecular weights of polyisoprene and modified polyisoprenes as characterised by light scattering

This poor control over the molecular weight using the diisopropenyl benzene initiator is probably caused by some deactivation of the initiator, due to the molecular weight always being higher than expected. This deactivation could be caused by the formation of oligomers driven by ionic interaction between the organolithium species. Neither altering the time allowed for propagation nor the temperature of the reaction had any effect on the molecular weight of the sample.

Viscosity

The viscosity of the PIs produced using both monofunctional *sec*-BuLi and bifunctional diisopropenyl benzene initiators was measured using an Ostwald's viscometer (Figure 39). A

range of solutions were prepared between 5 and 25 g/L in THF. The results from these measurements fall in line with expectation, when considering that the PIs produced using the bifunctional initiator are over two times larger in molecular weight than when using mono-functional initiators. This increased molecular weight causes the increased viscosity compared to the PIs of lower molecular weight.

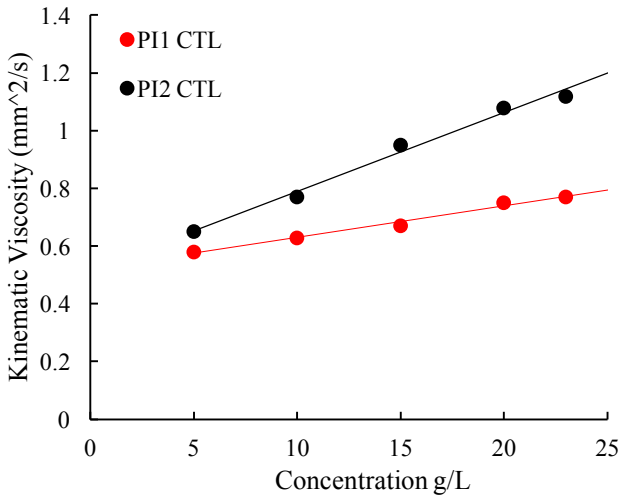

*Figure 39 – Graph of kinematic viscosity vs concentration of isoprene polymerised using a mono-functional initator (**PI1 CTL**) (black) and a bi-functional initiator (**PI2 CTL**) (red)*

2.3 Synthesis and Characterisation of Azide-Functionalised Ureidopyrimidinone

2.3.1 Synthesis and Characterisation

*2-Ethylpentyl Isocytosine (**1**)*

Due to the insolubility of methyl-functionalised isocytosines in many solvents (i.e. polar and non-polar organic solvents: THF, chloroform, methanol, and toluene, etc.), used as the starting materials for the preparation of UPys, a branched 1-ethylpentyl alkyl chain was chosen with the aim of obtaining UPys that are soluble in a variety of solvents. To achieve this, the β-keto ester ethyl 4-ethyl-3-oxooctanoate was synthesised by reacting ethyl potassium malonate with 2-ethylhexanoyl chloride obtained by the reaction of 2-ethylhexanoic acid with oxalyl chloride in DMF. Formation of the heretocyclic isocytosine (**Molecule 1**) was achieved

by ring closure with guanidinium carbonate under reflux in ethanol. As expected, the orange powder was found to be soluble in a variety of polar organic solvents (Scheme 26).

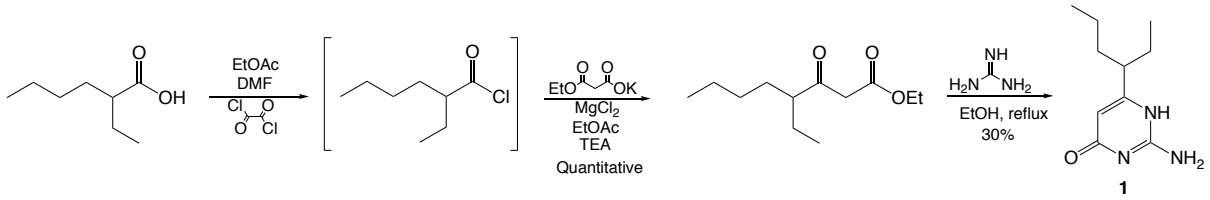

Scheme 26 – Synthesis of the 2-ethylpentyl derivative isocytosine, via a 2-ethylpentyl beta keto ester

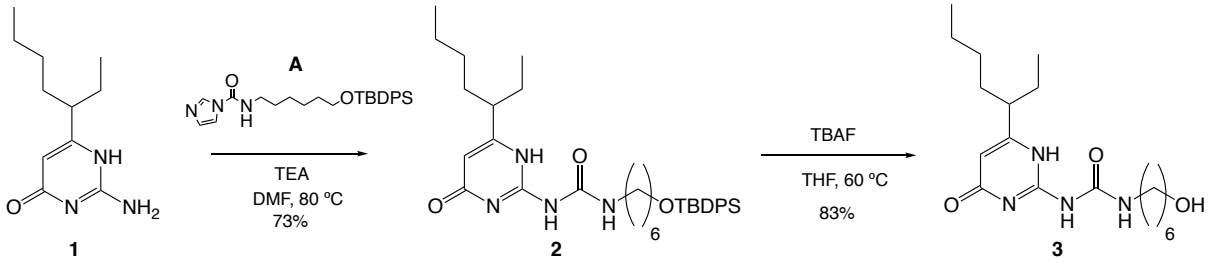

*Scheme 27 – Synthesis of alcohol-functionalised ureidopyrimidione **3***

Formation of the functionalised UPy was then achieved by the substitution reaction between the primary amine of the isocytosine and a carbonyl imidazole functionalised protected alcohol **A**, which was kindly prepared by Dr Antoine Goujon in two steps: reaction of 6-aminohexanol with *tert*-butyldiphenylsilyl chloride followed by reaction of the resulting free primary amine with carbonyldiimdazole. Removal of the *tert*-butyldiphenyl silane protecting group from **Molecule 2** using tetrabutylammonium fluoride yielded the alcohol-functionalised UPy (Scheme 27) (**3**). The presence of self-complementary hydrogen bonding interactions leading to UPy dimers was confirmed, using ^{1}H NMR spectroscopy, by the three downfield resonances assigned to the hydrogen bonding secondary amines – two bonded to a second ureidopyrimidinone molecule, and the third intramolecularly bonded with the carbonyl of the urea.

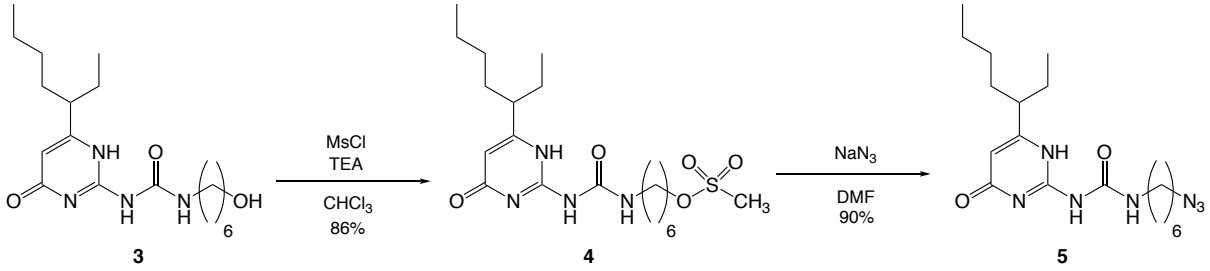

*Scheme 28 – Synthesis of the azide-functionalised ureidopyrimidinone **5***

Obtaining the desired azide functionality was achieved by first activating the alcohol moiety with a chemical functionality that acts as a better leaving group. Previous work within the group, conducted by colleagues working with similar molecules, had found that the desired chemical lability can be achieved by using the 'mesyl' group before substitution with azide. A further two steps were then completed, with reaction of compound **3** with mesylchloride followed by nucleophilic substitution with sodium azide, to yield the desired azide-functionalised UPy product **5** (Scheme 28). The successful synthesis of the product was confirmed by ^{1}H and ^{13}C NMR as well as by MALDI-TOF.

2.4 'Click' Coupling of Azide-Ureidopyrimidinone and Alkyne-Polyisoprene

2.4.1 Synthesis

*Coupling with Mono-Functionalised Polyisoprene (**PI1 UPy**)*

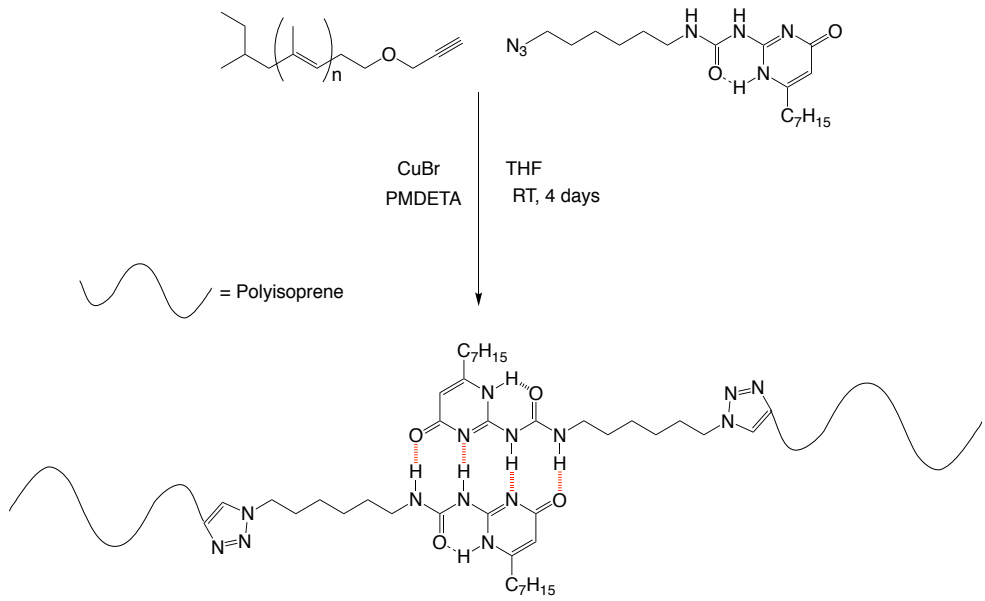

*Scheme 29 – Synthesis of **PI1 UPy** from alkyne-functionalised polysioprene (**PI1 ALK**) and azide-functionalised ureidopyrimidinone (**molecule 5**)*

The functionalisation of mono-alkyne PI (**PI1 ALK**) with the UPy moiety (**5**) was achieved, on a 100 mg scale, in air-free conditions in tetrahydrofuran, catalysed by three molar equivalents of Cu(I)Br (Scheme 29). The reaction was run at room temperature over the course

of four days, yielding pure **PI1 UPy** after removal of the copper(I) salts by complexation with EDTA.

*Coupling with Bi-Functional Polyisoprene (**PI2 UPy**)*

The functionalisation of bi-alkyne-functionalised PI (**PI2 ALK**) with the ureido-pyrimidinone moiety **5** was achieved, on a 500 mg scale, using the same conditions as detailed above (and in the experimental section for this chapter), yielding **PI2 UPy** (Scheme 30).

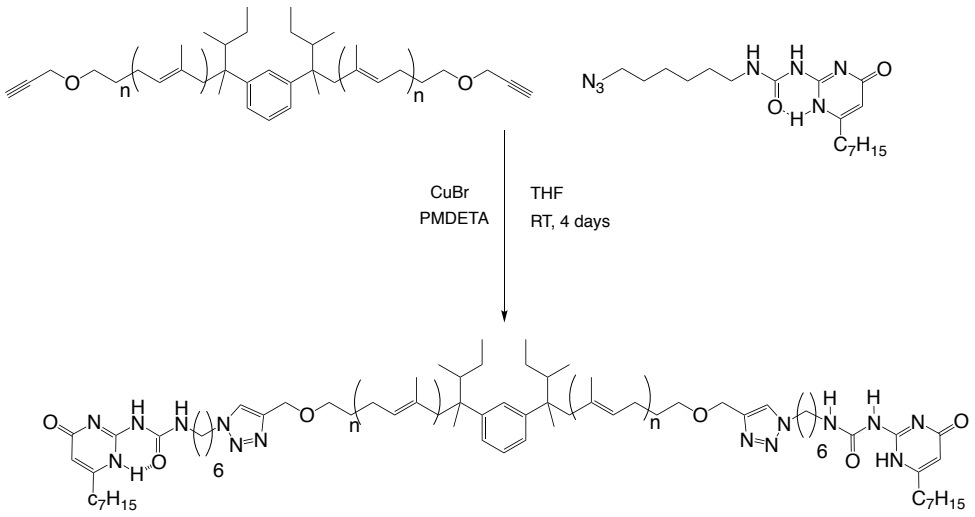

*Scheme 30 – Synthesis of **PI2 UPy** from dialkyne-functionalised polyisoprene (**PI2 ALK**) and azide-functionalised ureidopyrimidinone (**molecule 5**)*

Surprisingly, the products were found to display no clear qualitative physical differences to the starting materials both in the bulk and in a solution; the samples remained as colourless viscous liquids with a similar viscosity. All samples were stored under argon at 3 ºC, due to all coupled samples becoming yellow when stored at room temperature for longer than 3 days.

2.4.2 Physicochemical Characterisation

^{1}H NMR Spectroscopy

To confirm that the 'click' coupling had proceeded to completion, the products **PI1 UPy** and **PI2 UPy** were analysed by ^{1}H NMR spectroscopy; more specifically, we followed the evolution of resonances that could be assigned to the formation of a triazole moiety, and

the disappearance of the chemical shifts attributed to the alkyne unit and CH_2 on the carbon adjacent to the azide moiety from both PI and UPy reagents, respectively. In both cases, after allowing the reactions to proceed at room temperature over 4 days, with complete disappearance of the resonance attributed to the alkyne moieties (δ 4.11), as well as appearance of resonances of the triazole and of the CH_2 adjacent to this newly formed moiety (δ 7.40 and 4.20 respectively) was observed.

Diffusion-Ordered Spectroscopy (DOSY)

In addition to the new proton resonances observed by ^{1}H NMR, the co-existence of both the PI and UPy resonances within **PI1 UPy** was analysed by diffusion-ordered spectroscopy (DOSY) with the aim of proving that both chemical moieties were present on the same molecule, by comparing their diffusion coefficients (Figure 40). As this analysis was intended to only be used to determine whether chemical moieties were present on the same molecule, as opposed to present as a chemically unbound mixture, the concentration of the sample was not considered and, hence, the quantitative values of the diffusion coefficients should be disregarded. Nonetheless, the diffusion coefficients of both the UPy and PI moieties were found to be identical, strongly suggesting that both units are present on the same molecule. Importantly, this is strong evidence that **PI1 UPy** is present as a hydrogen bonded dimer, due to the presence of the resonances at very downfield chemical shifts.

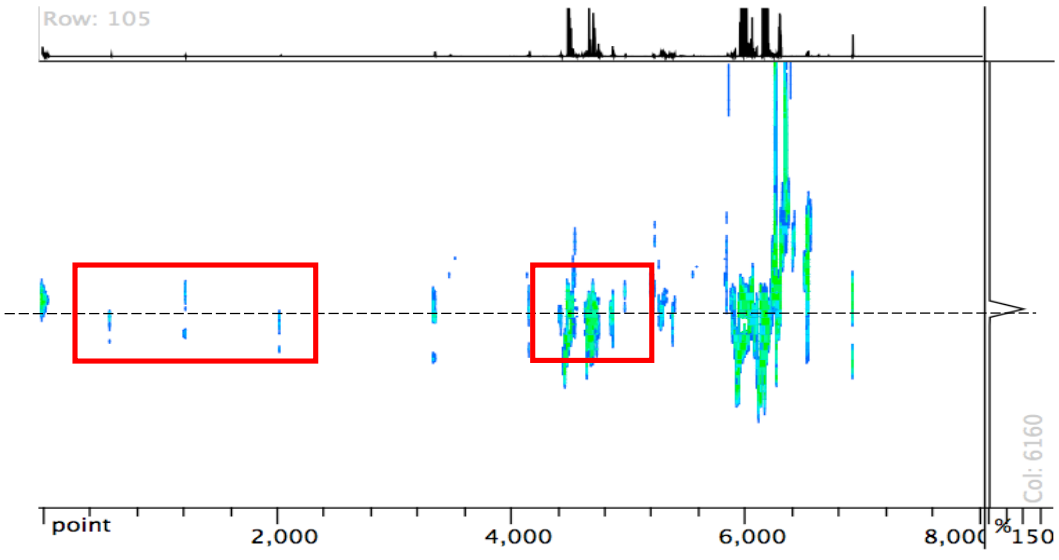

*Figure 40 – DOSY spectrum of mono-UPy functionalised polyisoprene (**PI1 UPy**) - black dashed line added to guide the eye, red boxes to highlight the presence of UPy (left) and PI (right) at the same diffusion coefficient.*

With both proton (^{1}H) and DOSY NMR spectroscopies in hand, it is clear that the azide-alkyne coupling of ureidopyrimidinoe on to functionalised PI chains has been successful. The physical effects of the presence of the UPy, in comparison to unfunctionalised PI controls, will now be discussed.

Size Exclusion Chromatography (SEC)

To analyse how the presence of UPy affects the molecular weight distribution of the sample, **PI1 UPy** and **PI2 UPy** were analysed by SEC (Figure 41). Three concentrations were analysed (5.0, 12.4, 24.7 g/L), and compared to **PI1 CTL** and **PI2 CTL**, to observe any concentration dependence of the supramolecular association. It should also be noted that, as supramolecular association is strongly dependent on solvent interactions, the SEC measurements were taken in THF, which has been described to have a small weakening effect on the hydrogen-bonding interaction between UPys.[12]

PI1 UPy displayed a small shoulder on the higher molecular weight side of the main peak. Due to the main peak remaining largely unchanged, persisting at the same elution volume as **PI1 CTL**, it is quite clear that any higher molecular weight aggregates, caused by the UPy-UPy interactions, are only present in a small quantity. Due to the strong specificity of the UPy, compounded with the fact that the functionality of this sample is only present on one chain-end, only dimeric species are expected; with this in mind, these dimeric species are likely to only be apparent in minor quantities.

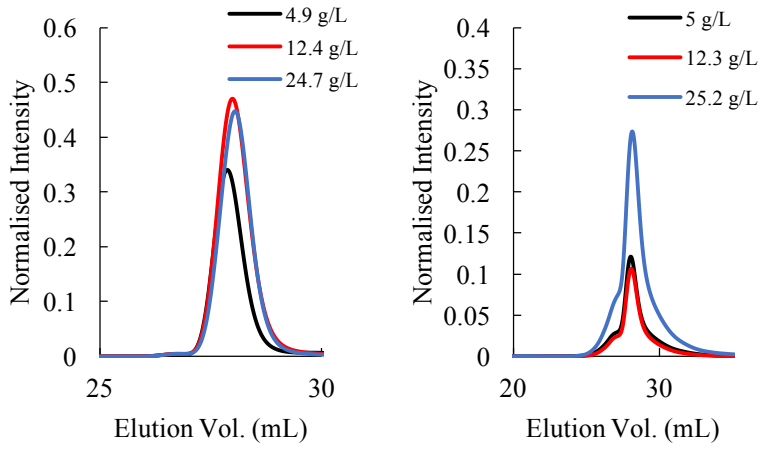

*Figure 41 – SEC chromatographs of **PI1 CTL** (left) and **PI1 UPy** (right) at three concentrations*

PI2 UPy was anticipated to display markedly increased molecular weight, and hence a significant decrease in elution volume, due to the linear chain extension driven by the hydrogen bonds. In fact, on SEC analysis no significant change in the chromatogram was observed, when compared to the **PI2 CTL** (Figure 42). The surprising lack of change in molecular weight distribution strongly implies a lack of strong association by complementary hydrogen bonding between UPy moieties at the PI chain-ends. It may be the case that the shear force implied on the sample, from being passed through the SEC stationary phase, would be enough physical strain to break the UPy association. However, due to previous work in the literature describing the use of GPC (in THF) to successfully analyse main-chain supramolecular polymers held by hydrogen bonded UPys, such behaviour is unlikely.[9,13]

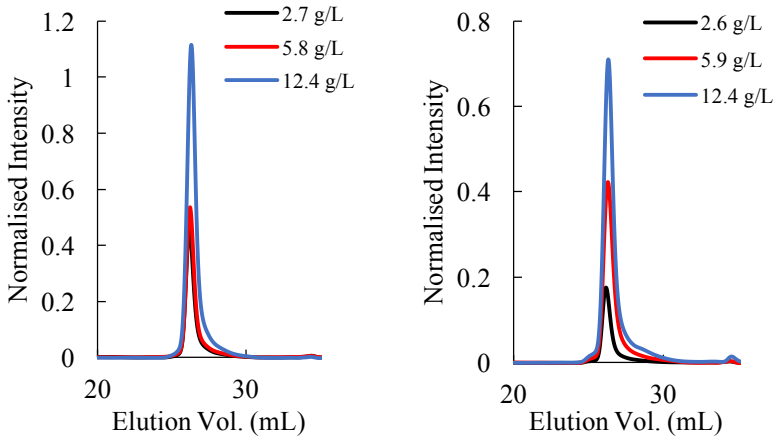

*Figure 42 – SEC chromatographs of **PI2 CTL** (left) and **PI2 UPy** (right) at three different concentrations*

Viscosity

To evaluate whether the coupled products had undergone a change in viscosity, which was expected to arise with increasing molecular weight, the kinematic viscosity of the products in THF was analysed using an Ostwald's viscometer. A range of concentrations were prepared in order to evaluate any concentration dependent aggregation (Figure 43). However, in line with all other physical analyses of the samples detailed above, no change in viscosity was observed when comparing UPy-functionalised PIs to their unfunctionalised counterparts. Neither mono- nor bi-functionalisation of PIs chains with UPy produced polymeric products of physical properties matching products described in the literature.

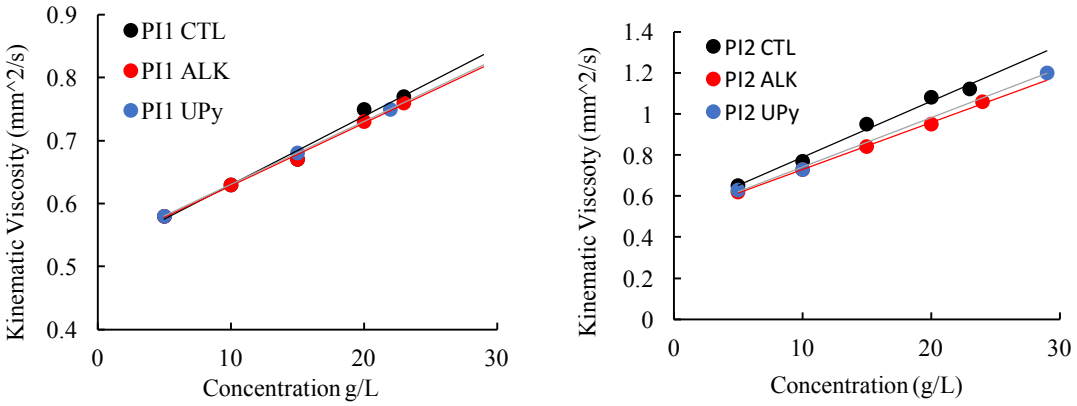

Figure 43 – Kinematic viscosity measurements in THF of mono-functional polyisoprenes (left) and bi-functional polyisoprenes (right) at concentrations between 5 and 30 g/L

In order to evaluate whether this lack of change in viscosity was the product of solvent interaction (THF) disrupting the UPy hydrogen bonding motif, a range of solutions were prepared in chloroform – UPys are most commonly studied in chloroform due to its minimal solvent interaction with the bonding motif.[12] The concentration range was also extended to higher concentrations to observed any dependence of the viscosity on concentration (Figure 44). Again, as observed in THF, no increase in viscosity for **PI2 UPy** was observed in chloroform in any of the concentrations measured, compared to **PI2 CTL**.

These finding strongly suggests that, despite the presence of UPy on the polymer chains, no aggregation of the polymer chains is observed.

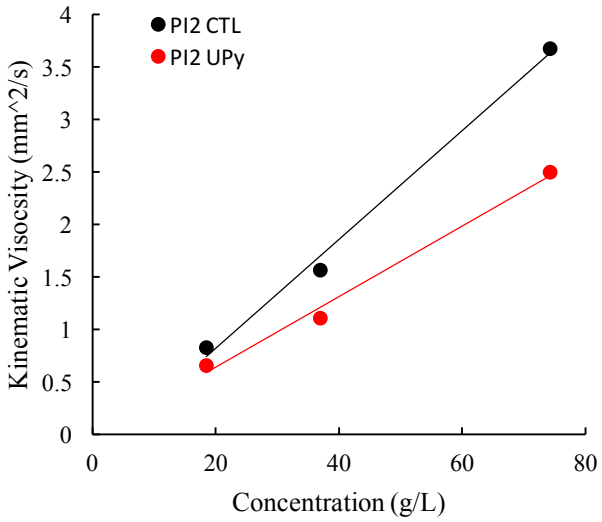

Figure 44 – Kinematic viscosity measurements in chloroform, of bi-functional polyisoprenes at concentrations between 20 and 80 g/L

2.5 Conclusions and Perspectives

The gram-scale preparation of alkyne-functionalised PIs on one chain-end, was successfully achieved by 'living' anionic polymerisation of isoprene, terminated by ethylene oxide, followed by post-polymerisation modification by reaction with propargyl bromide. The product was found to be monodisperse, with a good degree of control over the molecular weight, but the degree of functionality was lower than expected due to inefficient termination of the living chain ends by ethylene oxide. The preparation of PIs functionalised with alkynes on both chain ends was also achieved on the gram scale by the 'living' anionic polymerisation of isoprene, but instead using the bifunctional initiator diisopropenyl benzene; again, post-polymerisation modification, using propargyl bromide, yielded the product. Poor control over the molecular weight of product, due to possible partial inactivity of the initiator, from van der Waals interactions, caused the product to be over double the theoretical molecular weight. This deactivation of the initiator by oligomerisation is also likely to have been the cause of increased polydispersity index, and asymmetry of the peak on GPC analysis.

The synthesis of the azide-functionalised UPy was achieved in eight steps, on the milligram scale. The synthetic procedure, as it was executed, is unlikely to be scalable beyond the gram scale, due to the inconvenience and inhibitory expense of column chromatography at large scale; neither re-crystallisation nor precipitation of many of the products was possible due to the fact that the product was an oil.

The coupling reaction, by the copper(I) catalysed azide-alkyne 'click' reaction, successfully produced PIs functionalised with UPys at either a single or at both chain ends. The coupling was confirmed by the disappearance of proton resonances attributed to the presence of the alkyne moiety and the appearance of resonances attributed to the presence of the triazole, when analysed by ^{1}H NMR; as well as by identical diffusion coefficients of proton resonances attributed to the UPy and the PI backbone. The products showed no qualitative change in physical appearance.

Neither of the UPy-functionalised PIs gave noticeable physical change, when analysed by GPC, and kinematic viscometry – a large increase in molecular weight was anticipated, from the hydrogen-bond driven linear chain-extension of the PI. The following explanations are postulated for this lack of observed supramolecular polymerisation:

- The molecular weight of the PI backbone is close to, or above, the critical entanglement weight, and hence the UPy at the chain-ends are entangled within the polymer backbone inhibiting the self complementary association.[14] At low concentrations, hydrogen

bonding is observed by ^{1}H NMR, however at increased concentrations, broadening of the resonances makes observing any change in UPy caused by concentration impossible to follow;

- The UPy is not present in high enough concentrations to have a significant effect on the physical properties of the material. This is also strongly related to the high molecular weight of the PI backbone – a decrease in molecular weight of the backbone would increase the relative concentration of UPy present in the material;

In the next chapter, a change of strategy was undertaken, keeping these conclusions closely in mind, in order to produce double-dynamic materials.

2.6 References

1. Young, R. N., Quirk, R. P. & Fetters, L. J. in 1–90 (Springer Berlin Heidelberg, 1984). doi:10.1007/BFb0024120
2. Yu, Y. S., Jerome, R., Fayt, R. & Teyssie, P. Efficiency of the sec-Butyllithium/m-Diisopropenylbenzene Diadduct as an Anionic Polymerization Initiator in Apolar Solvents. *Macromolecules* **27,** 5957–5963 (1994).
3. Hseih, H. L. & Quirk, R. P. *Anionic Polymerization - Principles and Practical Applications*. (Marcel Dekker Inc., 1996).
4. Coates, G. W. Precise control of polyolefin stereochemistry using single-site metal catalysts. *Chem. Rev.* **100,** 1223–1252 (2000).
5. Fetters, L. J., Kamienski, C. W., Morrison, R. C. & Young, R. N. Remarks on Organodilithium Initiators. *Macromolecules* **12,** 344–346 (1979).
6. Touris, A., Mays, J. W. & Hadjichristidis, N. Acetylene-Functionalized Lithium Initiators for Anionic Polymerization. Powerful Precursors for 'Click' Chemistry. *Macromolecules* **44,** 1886–1893 (2011).
7. Matmour, R. & Gnanou, Y. Synthesis of complex polymeric architectures using multilithiated carbanionic initiators—Comparison with other approaches. *Prog. Polym. Sci.* **38,** 30–62 (2013).
8. Lutz, P., Beinert, G., Franta, E. & Rempp, P. Kinetics of addition of butyllithium onto diisopropenylbenzene. *Eur. Polym. J.* **15,** 1111–1117 (1979).
9. Bobade, S., Wang, Y., Mays, J. & Baskaran, D. Synthesis and Characterization of Ureidopyrimidone Telechelics by CuAAC 'Click' Reaction: Effect of T g and Polarity. *Macromolecules* **47,** 5040–5050 (2014).
10. Lutz, P., Beinert, G. & Rempp, P. Anionic polymerization and copolymerization of 1,3- and 1,4-diisopropenylbenzene. *Die Makromol. Chemie* **183,** 2787–2797 (1982).
11. Chen, D., Shao, H., Yao, W. & Huang, B. Fourier Transform Infrared Spectral Analysis of Polyisoprene of a Different Microstructure. *Int. J. Polym. Sci.* **2013,** 1–5 (2013).
12. Lange, R. F. M., Van Gurp, M. & Meijer, E. W. Hydrogen-bonded supramolecular polymer networks. *J. Polym. Sci. Part A Polym. Chem.* **37,** 3657–3670 (1999).
13. Bobade, S. L., Malmgren, T. & Baskaran, D. Micellar-cluster association of ureidopyrimidone functionalized monochelic polybutadiene. *Polym. Chem.* **5,** 910–920 (2014).
14. Abdel-Goad, M. *et al.* Rheological properties of 1,4-polyisoprene over a large molecular weight range. *Macromolecules* **37,** 8135–8144 (2004).

Chapter 3: Synthesis of Double-Dynamic Thermoset Elastomers

3.1 Introduction

With the aim of reducing the influence of molecular weight of the polymer backbone on the dynamic interactions, we looked for possible sources of commercially-available elastomeric pre-polymers, as an alternative backbone to the laboratory made polyisoprenes used thus far. Despite being of a slightly different composition, Polyvest® EP HT, based on linear polybutadiene (Scheme 31), was identified as a good alternative due to its hydroxyl-functionalisation at both chain-ends, as well as its lower molecular weight (4000 g/mol). Evonik Industries AG kindly provided the polybutadiene (Polyvest® EP HT) used in this chapter; full characterisation of the supplied material is discussed in the first section of this chapter.

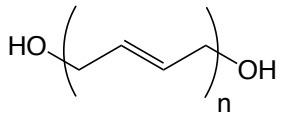

Scheme 31 – Hydroxyl-functionalised polybutadiene

To overcome the challenge of increasing the content of (non-covalent) dynamic groups in the material, and hence the low proportion relative to the molecular weight of the backbone, co-polymerisation of the ureidopyrimidinone moiety with the polybutadiene as a pre-polymer was targeted. As discussed in Chapter 1, incorporation of non-covalently bonding species as cross-linking groups is usually achieved by modification of polymer backbones, with an already high molecular weight, at pendent positions along a polymer chain. The approach taken in this chapter differs from these discussed approaches insofar as the non-covalently bonding group is bifunctional and acts as both a chain-extension and cross-linking agent, becoming intrinsically bonded within the polymer backbone. Very few examples in the literature consider this approach; a notable example of this approach can be seen from the work of *Baaijens* and co-workers in their publication demonstrating the synthesis of diisocyanate-functionalised ureido-pyrimidinone monomers that were co-polymerised with dihydroxyl-functionalised poly(propylene adipate) to form thermoplastic polyurethanes (Scheme 32).[1] Importantly, however, incorporation of a second dynamic functionality was not studied, but instead the

focus was to observed changes in the physical properties of the resultant material when using different diisocyanates within the ureidopyrimidinone synthon (hexamethylene-1,6-diisocyanate or isophorone diisocyanate). The synthesis of the ureidopyrimidinone synthons in this chapter was achieved by closely following the synthetic procedure reported in this publication.

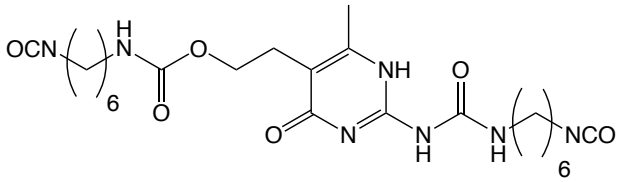

Scheme 32 – Diisocyanate-functionalised ureidopyrimidinone

Our approach to incorporate a second (covalent) dynamic functionality into the material involved the direct modification of chemical functionalities present both on the polymer and on the ureidopyrimidinone, making them suitable for coupling. As proposed in chapters 1 and 2, the imine bond would still be the targeted moiety and so the polybutadiene and ureidopyrimidinone were to be modified with amine and aldehyde moieties respectively. This simultaneous incorporation of both non-covalent and reversible covalent bonding dynamic moieties solves the potential issue of the need to further modify the material after incorporation of the first dynamic moiety.

Accurate comparison of these new materials with appropriate materials that already exist in the literature, or to control materials synthesised in the laboratory, required close chemical analogues to be found. For this, the main chemical components that will affect the physical properties of the double dynamic material are summarised (Figure 45):

- *The soft block*: Polybutadiene with a relatively high content of cis/trans-1,4 microstructure, and therefore elastic in nature. Molecular weight of ~4000 g/mol;
- *The hard block*: Hydrogen-bonding ureidopyrimidinone - structurally rigid with restricted flexibility;
- *Chain-extender/cross/linker*: Covalent imine bond - dynamic with chemical reversibility and exchangeability.

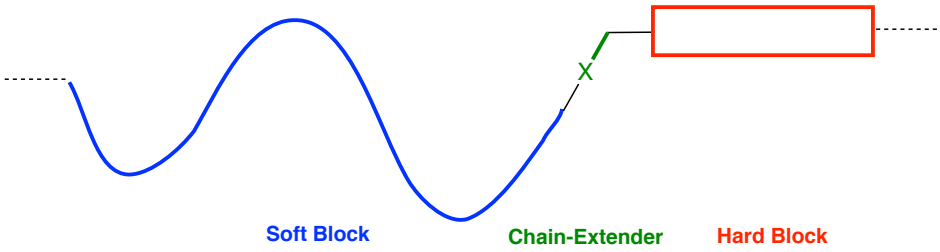

Figure 45 – Illustration of the general composition of double-dynamic materials, containing a long polybutadiene soft block (blue) linked to a hard block based on a supramolecular hydrogen-bonding moiety (red), via a covalent reverisble chain-extender/cross-linker (green)

Removal of either the hard block or the chain-extender, with alternative chemical moieties, was carried out so that the influence of each dynamic moiety could be determined. A series of three control materials were produced changing the following variable:

- *No Dynamic Control* (**CTL0**): The hydroxyl-functionalised polybutadiene was used without modification; hexamethylene-1,6-diisocyanate was copolymerised forming both the hard block and as the chain-extender, in this case hexane was present as the hard block, and urethane bonds used as the chain-extending moiety. This material was used to compare the double-dynamic materials with a control containing a polybutadiene soft block but no dynamic groups;
- *One Dynamic Control (Ureidopyrimidinone)* (**CTL1 UPy**): The hydroxyl-functionalised polybutadiene was co-polymerised with diisocyanate ureido-pyrimidinone. This material was used to compare the double-dynamic materials with a control composed of the same hard block but without reversible chain-extending linkages – giving the ability to observed the influence of the polyimine on the physical behaviour of the material;
- *One Dynamic Control (Imine)* (**CTL1 IMI**): a bis-amine-functionalised polybutadiene was co-polymerised with dialdehyde-functionalised hexane (bis(4-formylphenyl) hexane-1,6-diyldicarbamate) (Scheme 33). This material was used to compare the double-dynamic materials with a control containing only dynamic covalent bonds – giving the ability to observe the influence of the ureidopyrimidinone on the physical behaviour of the material.

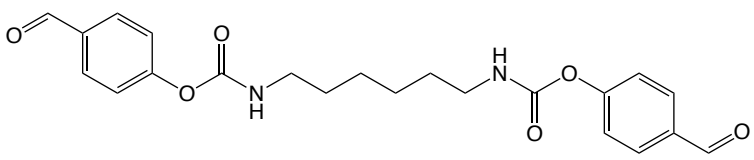

Scheme 33 – Dialdehyde-functionalised hexane derivative

3.2 Results and Discussion

3.2.1 Characterisation of Polybutadiene Pre-Polymer

Microstructural Composition

Similarly to polyisoprene, polybutadiene may exist in different aliphatic isomers, of which varying proportions can be obtained (this is usually achieved by using different polymerisation techniques). Due to the absence of the methyl group, characteristic of the isoprene unit, polybutadiene exists in three microstructures: *cis* and *trans*-1,4 and 1,2. Microstructural composition of the polybutadiene pre-polymer, i.e. the relative proportion of these isomers, was determined by integrating the resonances attributed to each of these microstructures using ^{1}H NMR spectroscopy. The largest multiplet resonance (δ 5.44) is attributed to the internal alkene protons of each of the microstructures, with interference between each of the proton resonances making distinction of the microstructures difficult, the resonance at δ 4.99 is attributed to the terminal alkene protons of only the 1,2 isomer (Figure 46). Due to the overlap of proton resonances from the distinct proton environments, a modification to the equation published by *Tanaka* and *Takeuchi* was determined U Equation 9; the microstructural content for Polyvest® was then calculated and found to be in close agreement to the published data sheet, confirming the high *cis*/*trans*-1,4 isomeric content (Table 5).[2,3] The resulting material is therefore expected to be elastomeric after chain-extension/cross-linking.

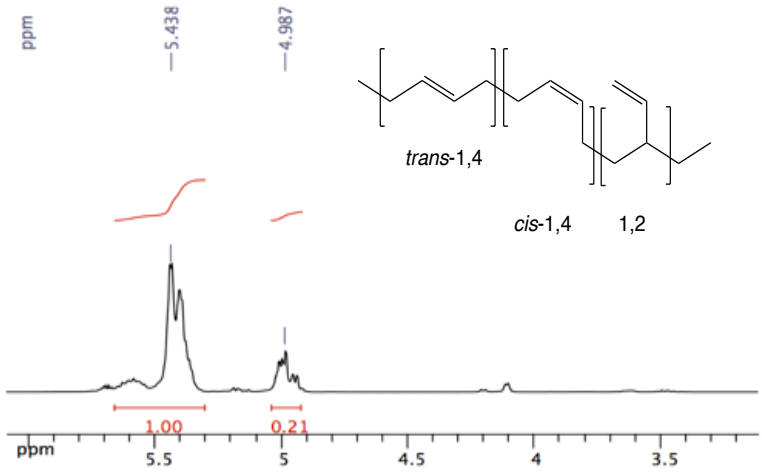

Figure 46 – Partial ^{1}H NMR spectrum of Polyvest® EPHT, displaying proton resonances from the cis/trans 1,4 (δ = 5.438) and 1,2 (δ = 4.987).

$$\frac{I(4.99)}{I(5.44)} = \frac{I(4.99)\times 2}{I(4.99) + 2\{1 - I(4.99)\}}$$

Determined from assuming

$$[1{,}2\ isomer] + [1{,}4\ isomer] = 1$$

Equation 9 – Formulae used to caluclate the relative concentration of microstructures within Polyvest®

Polyvest® Polybutadiene		
Microstructure	Data Sheet Values (%)	Experimental Values (%)
cis-1,4	22	81
trans-1,4	58	
1,2	22	19

Table 5 – Tabulated data of the microstructure of Polyvest® as published by Evonik and as calculated using ^{1}H NMR spectroscopy

Polydispersity Index

Both Size Exclusion Chromatography (SEC) and light scattering (LS) were used to determine the polydispersity index of the Polyvest® samples in THF solution (Figure 47).

By GPC the sample was found to be polydisperse with a PDI (M_n/M_w) of 2.02. The same sample, when analysed by LS, found a similarly polydisperse sample with a PDI of 1.6. It is clear, therefore, that a broad range of molecular weights are present in the sample, making any molecular weight value used a crude average (Table 6). As no values for the polydispersity index of the polymer sample were given by Evonik, it was not possible to compare this observed value with publication.

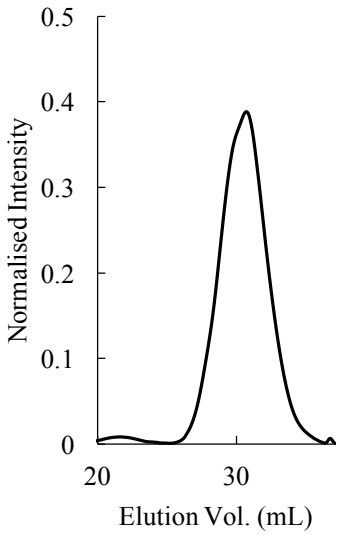

Figure 47 – Size Exclusion Chromatograph of Polyvest® Polybutadiene

Molecular Weight

Light scattering was used to determine the molecular weight of the Polyvest® sample in THF. Little consistency was found after repeated attempts to determine a value for both weight average (M_w) and number average (M_n) molecular weights, with the averages from all measurements tabulated below (Table 6). This inconsistency in producing a precise value for either molecular weight is likely due to the broad polydispersity as discussed above.

Polyvest® EP HT		
	LS	Data Sheet
Mn (Da)	4346 ± 1474	4000
Mw (Da)	6499 ± 1779	-
PDI	1.55	-

Table 6 – Tabulated data of weight average and number average molecular weights as determined by SEC and light scattering compared to the published values given by Evonik

Chemical Functionalisation

The degree of hydroxyl functionalisation was investigated in two ways: first by ^{1}H NMR spectroscopic analysis of the stock polymer, by integration of the proton resonance attributed to the alcohol moiety and calculation of the relative proportion present to the polybutadiene backbone (Figure 48); second, by modification of the chain ends with a UV active moiety, and subsequently analysing the UV intensity versus concentration by UV spectro-photometry.

The weak broad resonance at δ 3.63 was attributed to the presence of C-H protons present the methylene protons on the carbon adjacent to the alcohol group. By integration of this resonance, as well as integration of *cis*/*trans*-1,4 (δ 5.44) and 1,2 (δ 5.44 and 4.99) resonances described above, the degree of hydroxyl functionality could be calculated using Equation 10. The degree of functionalisation was found to be 0.36, considerably lower than the published value in the data sheet (between 3.14 and 3.64), likely due to the very weak presence of the alcohol resonance perturbing the calculated degree of functionality.

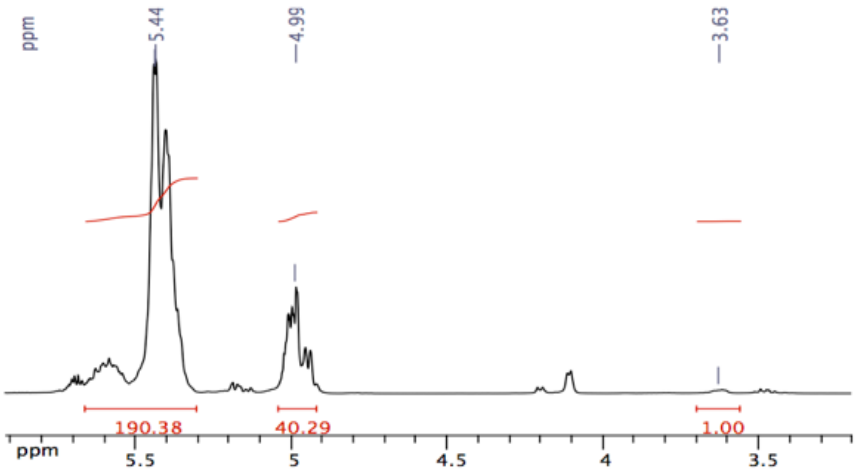

*Figure 48 – Patrial ^{1}H NMR spectrum of Polyvest® EPHT displaying proton resonances from cis/trans-1,4 (δ5.44) and 1,2 (δ5.44 and 4.99) microstructures integrated to the –C**H**$_2$OH resonance (δ3.63)*

$$F(OH) = \frac{I(3.63)/2}{\{I(5.44) + I(4.94\}/\{3[1,2] + 2[1,4]\}} \times DP$$

$$DP = \frac{M_n}{54}$$

Equation 10 – Formulae used to calculate the degree of hydroxyl functionalisation from the integrated proton resonances found by 1H NMR spectroscopy

To double-check this value, the hydroxyl functionalities were functionalised with a UV active naphthalene moiety to enable the determination of the degree of functionalisation by UV spectrophotometry. Modification of the polybutadiene with the naphthyl function was achieved by base-catalysed reaction with naphthyl-1-isocyanate (Scheme 34). A range of solutions at varying concentrations in cyclohexane were prepared, before analysis by UV-Vis spectrophotometry. Plotting the absorbance at 291 nm versus concentration gave a linear plot in close agreement to the Beer-Lambert law (Figure 49).

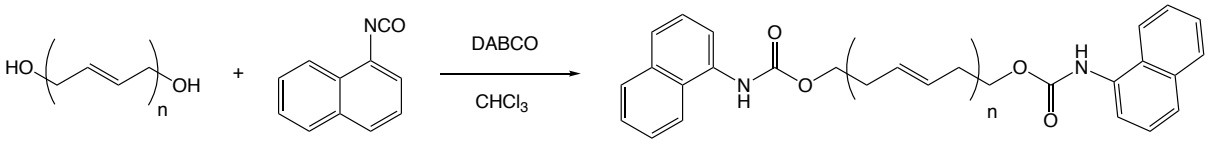

Scheme 34 – Synthesis of naphthyl-functionalised polybutadiene

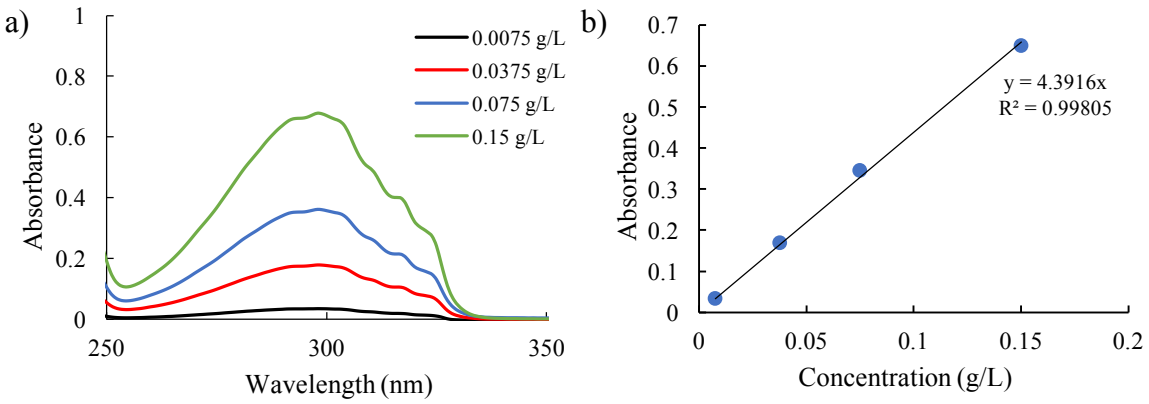

Figure 49 – a) UV spectrum of naphthyl-functionalised polybutadiene at four different concentrations between 250 – 350 nm; b) Beer-Lambert plot of absorbance at 291 nm vs concentration

By using Equation 11 the degree of functionalisation of the polybutadiene was calculated to be between 2.05 and 3.67, depending on the value used for the molecular weight.

$$F(OH) = \frac{M_n \times A/b}{m_p - M_{naph} \times A/b}$$

Equation 11 – Formula used to caluclate the degree of functionalisation of Polyvest® EPHT from the UV data

With this 'over-functionalisation' in mind, the spectrum obtained by ^{1}H NMR displayed resonances that could not be attributed to purely chain-end hydroxyl-functionalised polybutadiene. In addition to the proton resonance at δ 3.65, described above as being attributed to C-H protons on alcohol functionalised carbon, broad weak resonances at δ 2.7 and δ 2.9 were observed, likely due to the presence of epoxide moieties along the polybutadiene backbone. In fact, striking similarity can be seen when comparing Polyvest® and polybutadienes modified with epoxide, in the literature.[4] It is therefore likely that the synthetic procedure used to produce these highly elastomeric hydroxyl-functionalised polybutadienes involved post-polymerisation modification of polybutadiene, synthesised by 'living' anionic polymerisation in non-polar solvents, with an epoxidising agent followed by opening the end-chain epoxide ring to yield alcohol moieties.

It is important to note that, due to the degree of functionality being above two, thermoset elastomers were produced on chain-extension/cross-linking, rather than thermoplastics. Thus, the case that all monomers with which the polybutadiene was co-polymerised act as both chain-extenders and cross-linkers.

Summary of Characterisation and Establishment of Polymer Parameters

In order to use Polyvest® as a pre-polymer for the preparation of co-polymeric dynamic materials, a summary of the characterisation of the polymer, obtained from experimental measurements compared to published data is laid-out in Table 7. The parameters that were then considered for our studies, i.e. an average molecular weight of 5000 Da and a degree of functionality of 4, using the uppermost limits of both parameters; these values were also strongly influenced by initial trial and error studies on the synthesis of control materials. It is clear that any disproportion in the stoichiometry of the starting materials used will strongly effect the molecular weight of the produced material: using either too much or not enough chain-extender/cross-linker will result in materials of lower molecular weight than if stoichiometric amounts are used, however as demonstrated above, the molecular weight and degree of functionalisation of industrial polymers is an average.

	Data Sheet	Experimental	Value Used
Mn (g/mol)	4000	3150 - 6000	5000
Mw (g/mol)	-	5500 - 8500	5000
PDI	-	2.04	2.04
Degree of Functionality	3.14 - 3.64	0.36 - 3.67	4
cis/*trans*-1,4 Content (%)	78%	78%	78%

Table 7 – Tabulated data of all physcial parameters of Polyvest® EPHT obtained from experiments detailed above and as published by Evonik

3.2.2 Synthesis of Ureidopyrimidinone Synthons

*Synthesis of Diisocyanate-Functionalised Ureidopyrimidinone (**5**)*

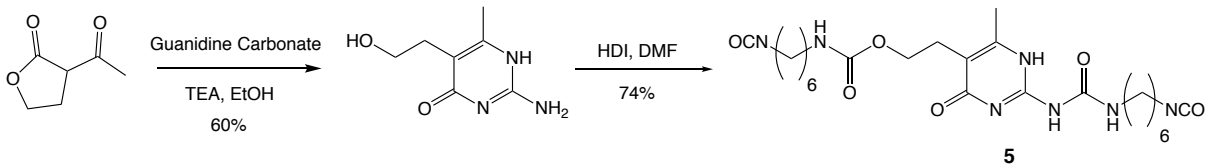

*Scheme 35 – Synthesis of diisocyanate-functionalised ureidopyrimidinone (**5**)*

Similarly to the approach towards the synthesis of the monofunctional ureido-pyrimidinone detailed in Chapter 2, the synthesis of bi-functional ureidopyrimidinones first required the synthesis of an isocytosine. To achieve this, instead of the ring closure of a β-keto

ester, a simultaneous ring-opening and ring closure protocol between 2-acetyl butyrolactone and guanidinium carbonate was utilised. Formation of the diisocyanate functionalised ureidopyrimidinone was then completed by reaction of the hydroxyl and primary amine functions with excess hexamethylene-1,6-diisocyanate to form urethane and urea links respectively (Scheme 35). The urea moiety and the adjacent tertiary amide are responsible for the strong self-complementarity and downfield shift of their protons by ^{1}H NMR spectroscopy.

Due to the sensitivity of isocyanates to nucleophiles, and their particular predisposition to polymerise when difunctional, great care was taken to ensure the reaction and subsequent storage of the difunctionalised ureidopyrimidinone in an air-free and moisture-free environment. The presence of ethanol as a stabilising agent in chloroform caused a notable synthetic stumbling-block. Another notable difficulty of this reaction, and as mentioned in chapter 2, was the very low solubility of methyl-functionalised isocytosines (well known in the literature), with **Molecule 5** being no exception. Experimentally it was necessary to first suspend the isocytosine in dimethyl formamide (DMF) before introduction into HDI. When the isocytosine was, instead, introduced as a dry solid, a mixture of products (including a suspected dimer from the reaction of mono-isocyanate functionalised ureidopyrimidinone with an unfunctionalised counterpart) was observed.

The scalability of this synthetic protocol is particularly promising, due to the relative ease of purification by simple precipitation in non-polar solvents (ether).

*Synthesis of Dialdehyde-Functionalised Ureidopyrimidinone (**6**)*

Reaction of the isocyanate functionalies (**5**) with excess 4-hydroxy benzaldehyde to form dialdehyde-functionalised ureidopyrimidinones was optimised by catalysis with dibutyltin dilaurate (Scheme 36). Again, due to the sensitivity of the diisocyanate functionality to nucleophiles, air and moisture-free reaction conditions were required as well as the use of solvent free from nucleophilic additives. Scalability of the procedure beyond the gram scale can also be easily envisaged due to the ease of purification by simple precipitation.

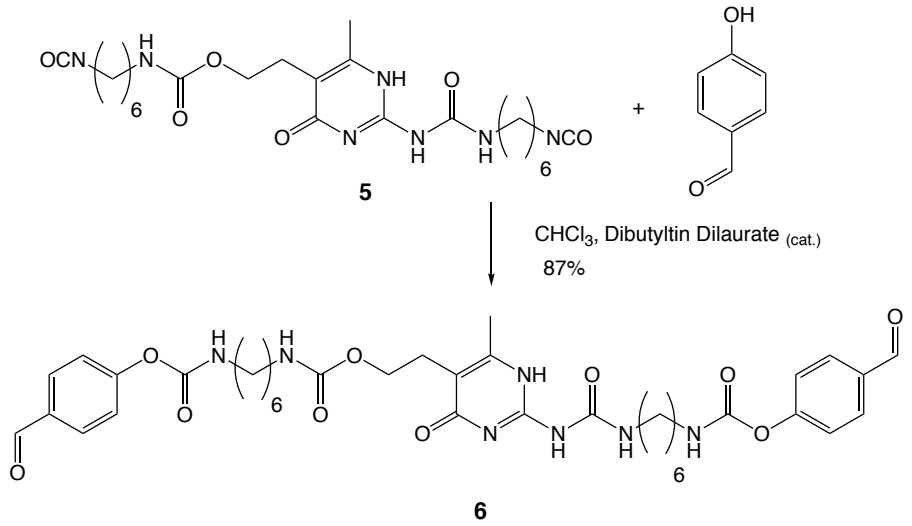

*Scheme 36 – Synthesis of dialdehyde-functionalised ureidopyrimidinone (**6**) from (**5**) and 4-hydroxyl benzaldehyde*

Due to the toxicity of organotin compounds, attempts were made to find alternative conditions, however no alternative reaction conditions (including base catalysis as well as using no catalyst at all) yielded products with as high yield and purity as dibutyltin dilaurate. Any vision for scalability of this reaction should include a full exploration of alternative solvents and catalysts.

*Synthesis of Hexane-Based Dialdehyde (**7**)*

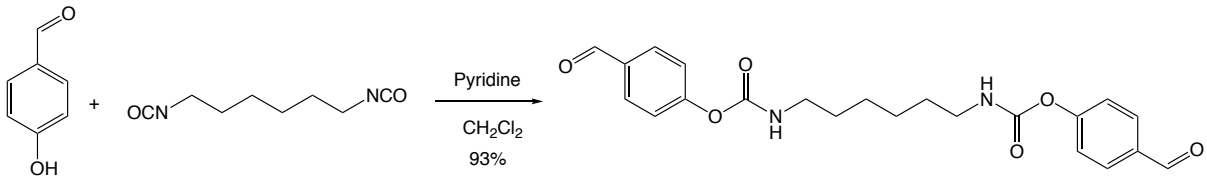

Scheme 37 – Synthesis of hexane-based dialdehyde (7) from 4-hydroxy benzaldehyde and hexamethylene-1,6-diisocyanate

The synthesis of the dialdehyde functionalised monomer **7**, for co-polymerisation with amine-functionalised polybutadiene to form the control material containing no ureido-pyrimidinone moiety was achieved in one-step from commercially available reagents on a multi-gram scale (Scheme 37). A slight excess of 4-hydroxy benzaldehyde was reacted with hexamethylene-1,6-diisocyanate catalysed by pyridine. The solid sample was simply precipitated, in ether, to yield the pure sample.

Unlike the other monomers described above, this reaction could easily be envisaged to be achieved at a larger scale immediately.

3.2.3 Post-Polymerisation Modification of the Polybutadiene – Introduction of Amine Functionality

*Synthesis of Amine-Functionalised Polybutadiene (**PBD NH_2**)*

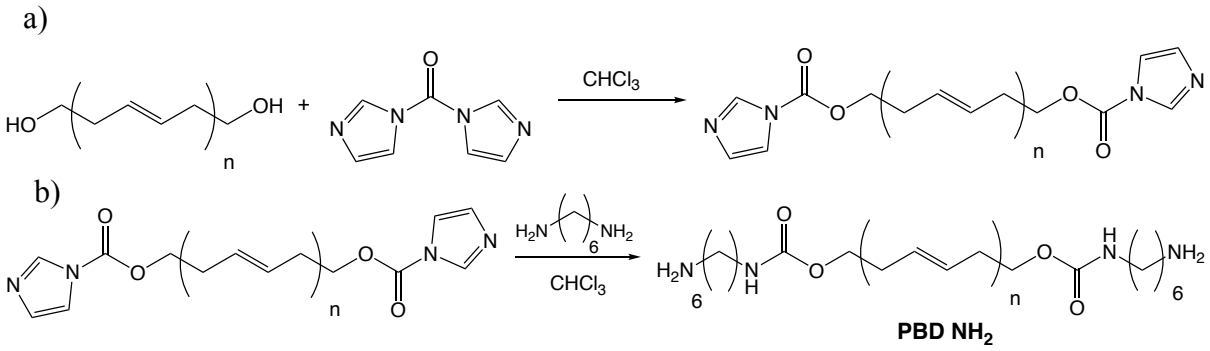

*Scheme 38 – Post-polymerisation modification of Polyvest® EP HT to yeild amine-functionalised polybutadiene **PBD NH_2***

The preparation of a polybutadiene pre-polymer suitable for the reaction with the previously described dialdehyde-functionalised monomers was achieved in two-steps from commercially available reagents, on a multi-gram scale.

The hydroxyl-functionalised polybutadiene was first reacted with carbonyl diimidazole (CDI), in air-free and moisture-free conditions (Scheme 38a). This nucleophilic substitution modified the polybutadiene with carbonyl imidazole functionalities, reacting all chain-end and pendent hydroxyl functional groups. These sites can be used for nucleophilic substitutions to yield a variety of functionality. Due to the imprecise degree of hydroxyl functionalisation of the polybutadiene, this reaction was carried out using a large excess of CDI. The labile nature of the carbonyl imidazole moieties, particularly their susceptibility to nucleophilic substitution with ambient moisture, meant that only crude purification (by precipitation in cyclohexane), without characterisation, was implemented before re-engagement in the next step.

The second step of the synthesis required the reaction of the carbonyl imidazole-functionalised polybutadiene with 1,6-diaminohexane in chloroform (Scheme 38b). Again, air and moisture-free conditions were used to ensure the absence of any other nucleophiles. Due to the presence of the nucleophilic groups at both chain-ends on the 1,6-diaminohexane molecule, the functionalised polybutadiene was introduced dropwise into a solution of a large excess of 1,6-diaminohexane, to avoid the formation of oligomers. Precipitation into methanol yielded pure amino-functionalised polybutadiene (**PBD NH_2**).

3.2.4 Kinetics Experiments for the Formation of Imine

Model Reaction with octylamine

In order to gain an understanding of the reactivity of **Molecule 6** and the subsequent formation of the diimine on reaction with amine-containing compounds, a model reaction was conducted, to monitor the evolution of the different chemical moieties within the reacting system by ^{1}H NMR spectroscopy.

For this study, the reaction between **6** and octylamine, in a 1/2 molar stoichiometry was conducted in DMSO at room temperature in the NMR tube (Figure 50a) with ^{1}H NMR spectra recorded at regular intervals (Figure 50b).

The kinetic model that was used, assumed the formation of a hemiaminal intermediate, according to *Hine* and *Via* and *Giuseppone, Lehn* and *co-workers* (Figure 51a).[5,6] Most previous literature follows the kinetic formation of imines in aqueous conditions, unlike this experiment which is conducted in an organic (hygroscopic) solvent. Assuming that the concentrations of amine and aldehyde are equal, and that the concentrations of produced imine and water are also equal, the differential molar balance in Figure 51b, was determined.

The plot of the relative concentration of each species versus times was constructed (Figure 52) and the data fitted to model curves (dotted lines) determined by integration using first order Euler's method. The model described the behaviour of the system well, with a high initial rate of decrease of the aldehyde (complete disappearance of the proton signal after 7000 s), in combination with a high rate of formation of intermediate; the intermediate is then observed to decrease in combination with the formation of the imine. Over longer time scales the data diverge from the model, which is likely to be due to atmospheric water affecting the equilibrium of the reaction.

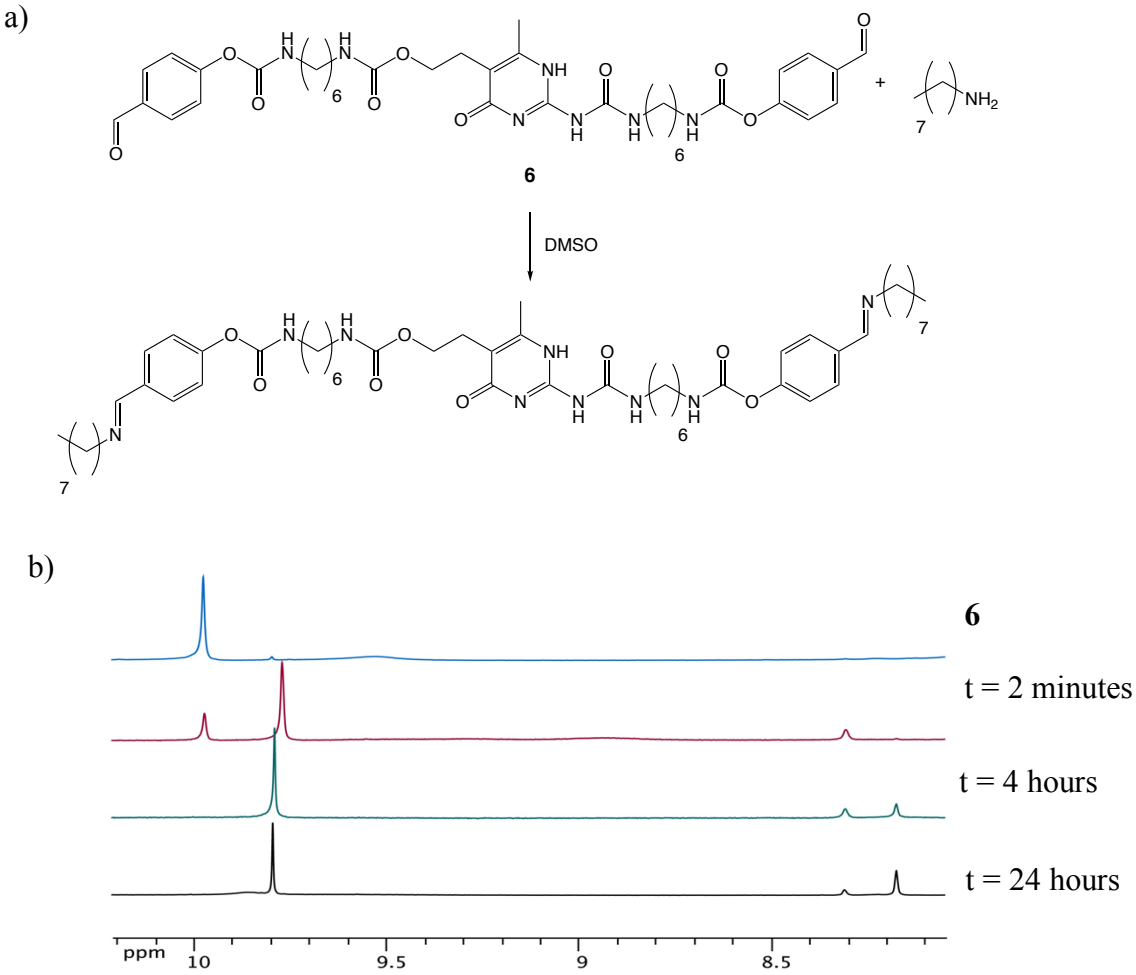

*Figure 50 – a) Schematic representation of the reaction of dialdehyde-functionalised ureidopyrimidinone **6** with octylamine; b) – Partial ^{1}H NMR spectrum of the model reaction between **6** and octylamine*

a)

$$[\text{Amine}]\,[\text{Aldehyde}] \underset{k_{-1}}{\overset{k_1}{\rightleftharpoons}} [\text{Intermediate}]$$

$$[\text{Intermediate}] \underset{k_{-2}}{\overset{k_2}{\rightleftharpoons}} [\text{Imine}]\,[H_2O]$$

b)

$$\frac{d\,[\text{Aldehyde}]}{d\,t} = -k_1\,[\text{Aldehyde}]^2 + k_{-1}\,[\text{Intermediate}]$$

$$\frac{d\,[\text{Amine}]}{d\,t} = k_2\,[\text{Intermediate}] - k_{-2}\,[\text{Imine}]^2$$

$$\frac{d\,[\text{Intermediate}]}{d\,t} = -(k_{-1} + k_2)\,[\text{Intermediate}] + k_1\,[\text{Aldehyde}]^2 + k_{-2}\,[\text{Imine}]^2$$

Figure 51 – a) Kinetic model of imine formation, from amine and aldehyde as proposed by Hine and Via;[5] b) Differential molar balance for each reagent.

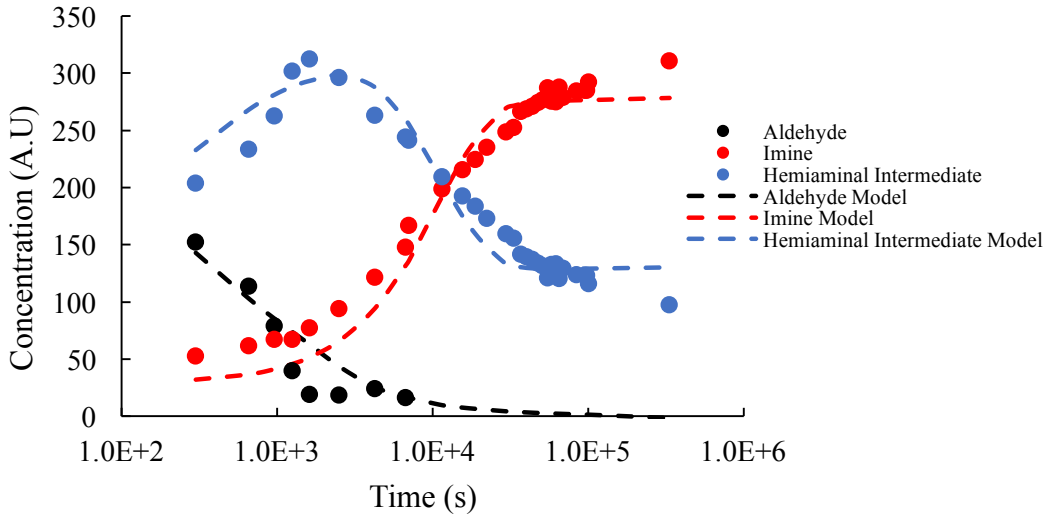

Figure 52 – Plot of concentration of aldehyde (black), imine (red) and intermediate (blue) vs time; dashed line displays the model curves obtained by integration using first order Euler's method

3.2.5 Co-Polymerisations of Control Materials Using Different Catalysts

*Synthesis of No Dynamic Control (**PBD CTL0**)*

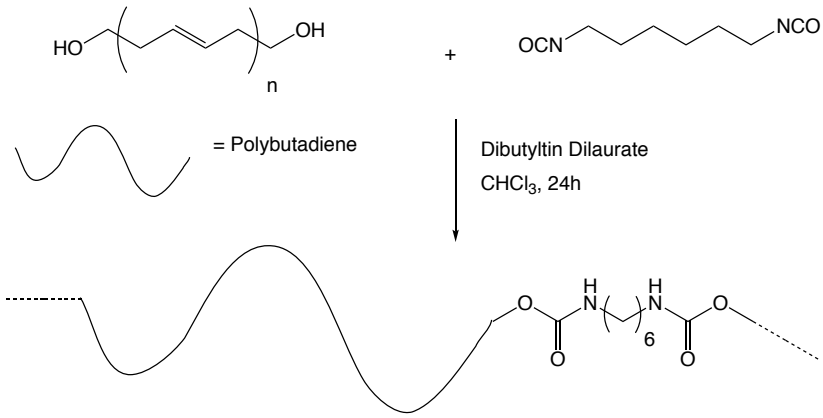

*Scheme 39 – Chain-extension/cross-linking reaction of polybutadiene with hexane-1,6-diisocyanate, yeilding **PBD CTL0***

The formation of the control material, containing no dynamic chemical groups, was achieved from the reaction between hydroxyl-functionalised polybutadiene and hexamethylene-1,6-diisocyanate in chloroform catalysed by dibutyltin dilaurate – using an NCO/OH molar ratio of 2/1 (Scheme 39). The reaction was first conducted in solution in a round-bottom flask, to which a solution of HDI was introduced, before addition of the catalyst, and allowing the chain-extension to occur. A swollen mass of polymer was observed to form

after 4 hours. Evaporation of the solvent yielded a stretchy colourless polymer film (Figure 53).

a) b)

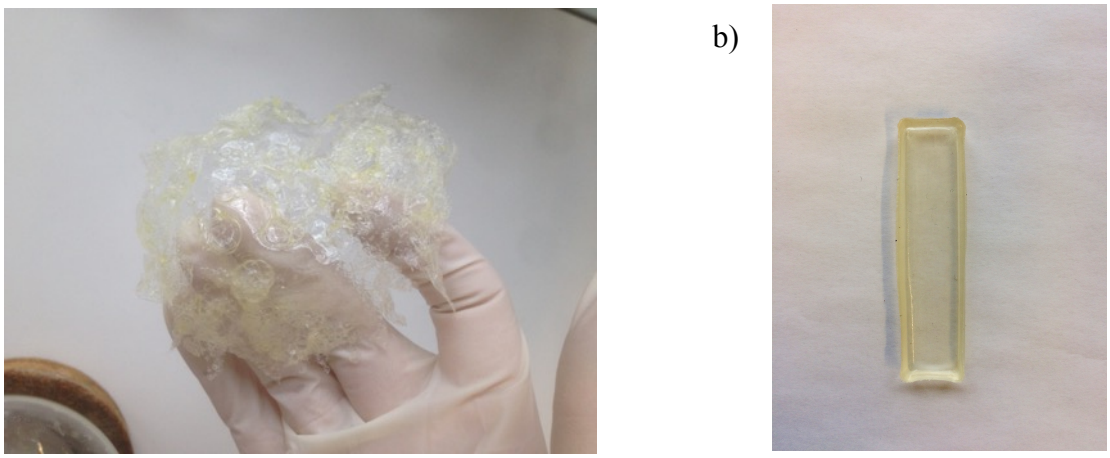

Figure 53 – a) Image of the product from the organotin-catalysed chain-extension/ cross-linking of polybutadiene with hexamethylene-1,6-diisocyanate (HDI); b) image of the same material after moulding.

The physical analysis of these materials required the samples to possess a high degree of homogeneity, ensuring that no bubbles or solids were present in the bulk of the material. As a consequence, the reaction (and all subsequent syntheses of materials physically characterised) was conducted in a Teflon® mould of dimensions 60 mm x 15 mm x 5 mm using the following methodology:

- Solutions of monomer and pre-polymer are prepared in separate vessels free from air and moisture;
- The monomer solution is quickly added to the polymer before addition of catalyst;
- The reaction solution is then pipetted into Telfon® moulds that are partially submerged in a bath of solvent, and the reaction mixture allowed to slowly evaporate at room temperature for 16 hours;
- The solid material is then post-cured under vacuum at 50 ºC for 16 hours.

The speed of evaporation was found to be an important parameter to control; if evaporation was too fast, air bubbles became trapped within the bulk of the material.

*Synthesis of Control UPy (**PBD CTL1 UPy**)*

Extension of these reaction conditions toward the formation of a material containing one dynamic group, i.e. the ureidopyrimidinone, was achieved using the same protocol; again, a 2/1 NCO/OH ratio was used to yield the chain-extended/cross-linked polyurethane network

(**PBD CTL1 UPy**) (Scheme 40). After drying at ambient temperature in an atmosphere of chloroform, a transparent slightly yellow elastomeric polymer was obtained.

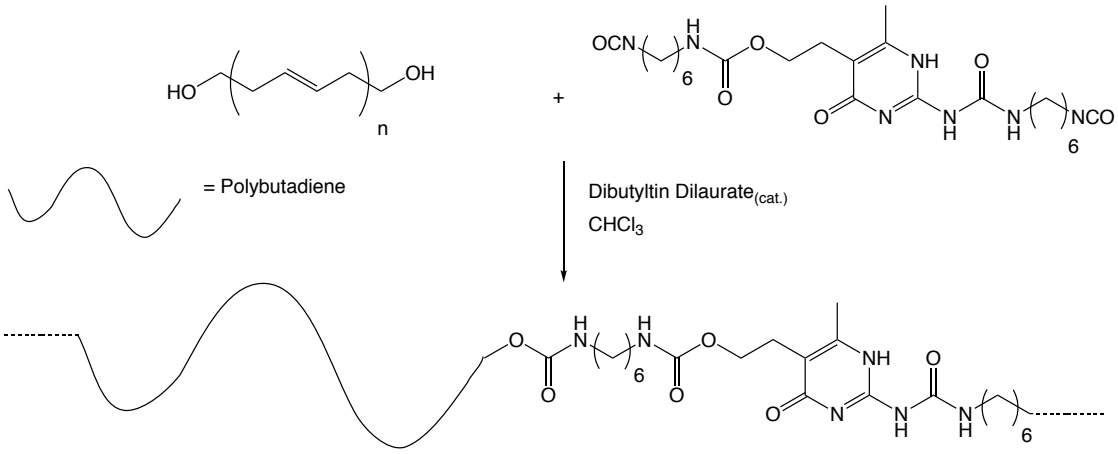

*Scheme 40 – DABCO-catalysed chain-extension/cross-linking of polybutadiene with diisocyanate-functionalised ureidopyrimidinone (**PBD CTL1 UPy**)*

As described in Chapter 1, a significant drawback of using dibutyltin laurate as a catalyst for the synthesis of polyurethanes is its acute toxicity to humans and the significant harm that could occur to aquatic animals if released into the waterways. With this in mind, a series of polymerisations were conducted catalysed by the commercially available, and industrially-used, 1,4-diazabicyclo[2.2.2]octane (DABCO) with a range of catalyst loadings – 1, 10 and 100 mole per cent – and their general physical aspect was compared to samples prepared by dibutyltin dilaurate-catalysed polyaddition (Scheme 41).

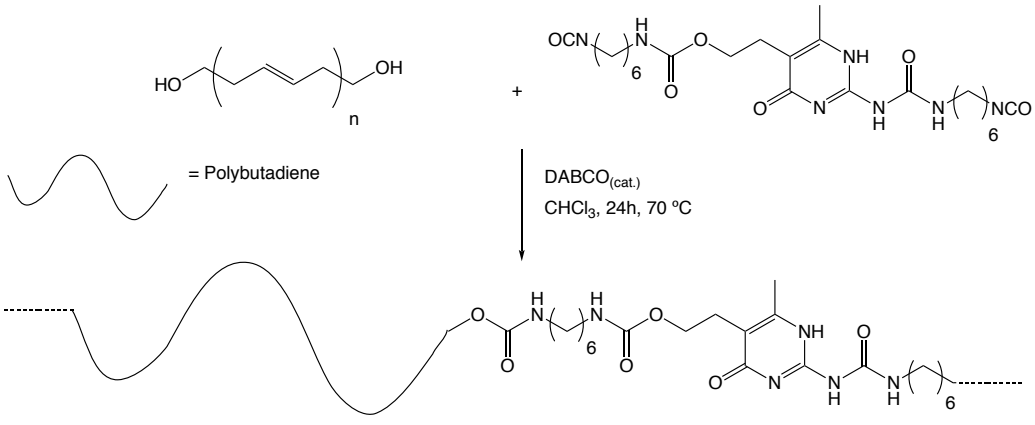

*Scheme 41 – DABCO-catalysed chain-extension/cross-linking reaction of polybutadiene with diisocyanate-functionalised ureidopyrimidinone (**5**)*

In all cases, samples catalysed by DABCO appeared soft and sticky, with poor shape fixation compared to the solid elastomeric samples obtained when catalysed by dibutyltin dilaurate. Qualitatively, slightly more cohesive strength was observed for samples reacted using 10 mole per cent DABCO, while with increased catalyst loadings beyond this amount producing softer more malleable samples (Figure 54).

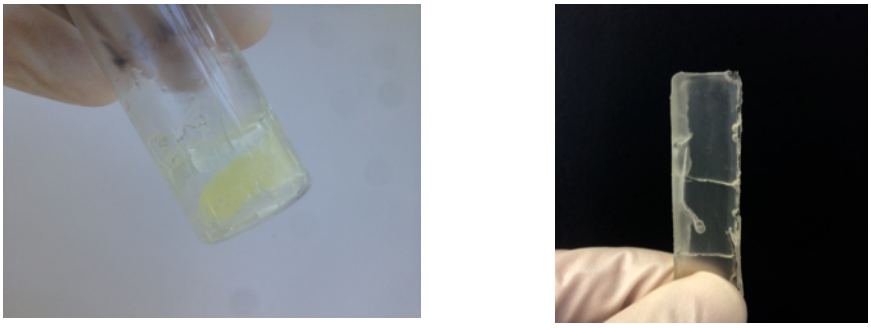

Figure 54 – Images of the product formed from DABCO-catalysed chain-extension/cross-linking

3.2.6 Synthesis of Imine-Based Materials

*Synthesis of Control Imine (**PBD CTL1 IMI**)*

The co-polymerisation of **Molecule 7** with amine-functionalised polybutadiene by polycondensation, forming a material made of polyimine, was conducted without the use of a catalyst (Scheme 42). Upon mixing of solutions of the two reagents, before transfer into the mould, the mixture was observed to gradually take-on a deep yellow/orange colour indicative of the presence of aromatic imines. Unlike any of the other materials, a matte and less transparent appearance of **PBD CTL1 UPy** was observed; after three weeks, a white surface appeared to coat the material.

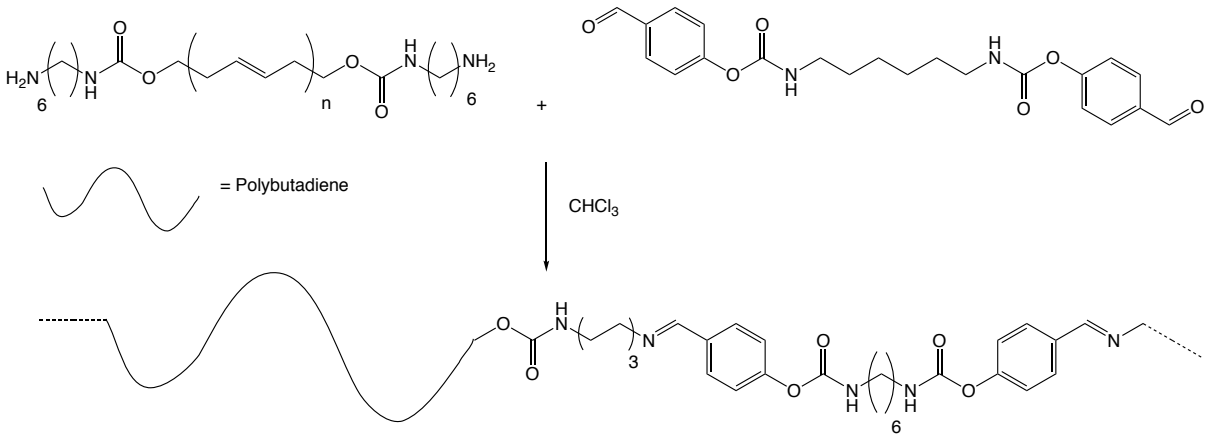

*Scheme 42 – Chain-extension/cross-linking of amine-functionalised polybutadiene with the dialdehyde-functionalised hexane derivative (7) (**PBD CTL1 IMI**)*

*Synthesis of Double Dynamic (**DOUBLE DYNAMIC**)*

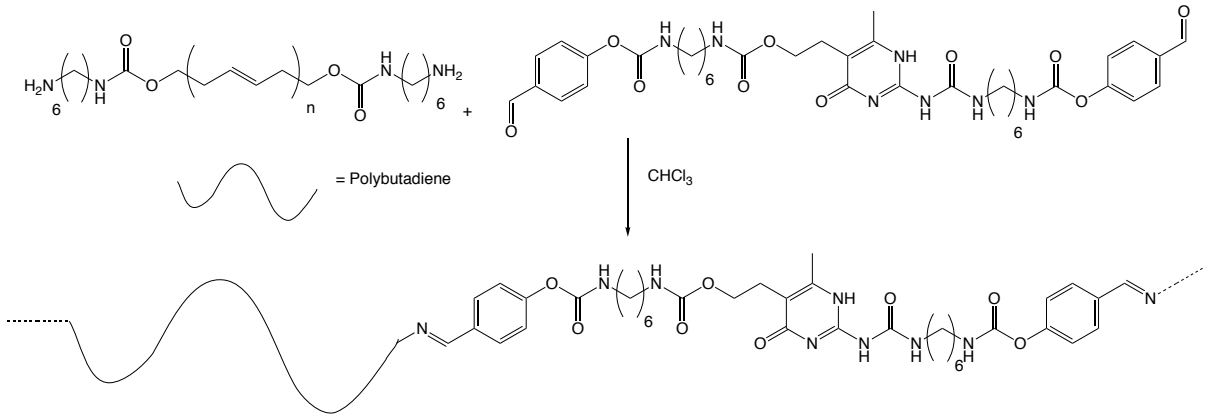

*Scheme 43 – Chain-extension/cross-linking reaction of amine-functionalised polybutadiene with dialdehyde-functionalised ureidopyrimidinone (**DOUBLE DYNAMIC**)*

To synthesise materials containing both dynamic chemical moieties, the co-polymerisation of **Molecule 6** and amine-functionalised polybutadiene was achieved without the use of a catalyst, in chloroform (Scheme 43). In line with the methodology detailed above, the synthesis of these materials involved the mixture of solutions of both reagents before transfer into a mould. As with the synthesis of all other materials, the electrophile/nucleophile ratio, in this case CHO/NH_2, was 2/1. Similarly to **PBD CTL1 IMI**, qualitative confirmation of the presence of aromatic imines was observed by the deep yellow/orange colour taken-on by the material. Another noteworthy observation was the rapid formation of a film at the air/solvent interface, causing a 'rippled' effect on the surface of the material that permanently persisted on the material; this may be due to the enhancement of evaporation, of both water and solvent, at the air/solvent interface driving imine formation to completion.

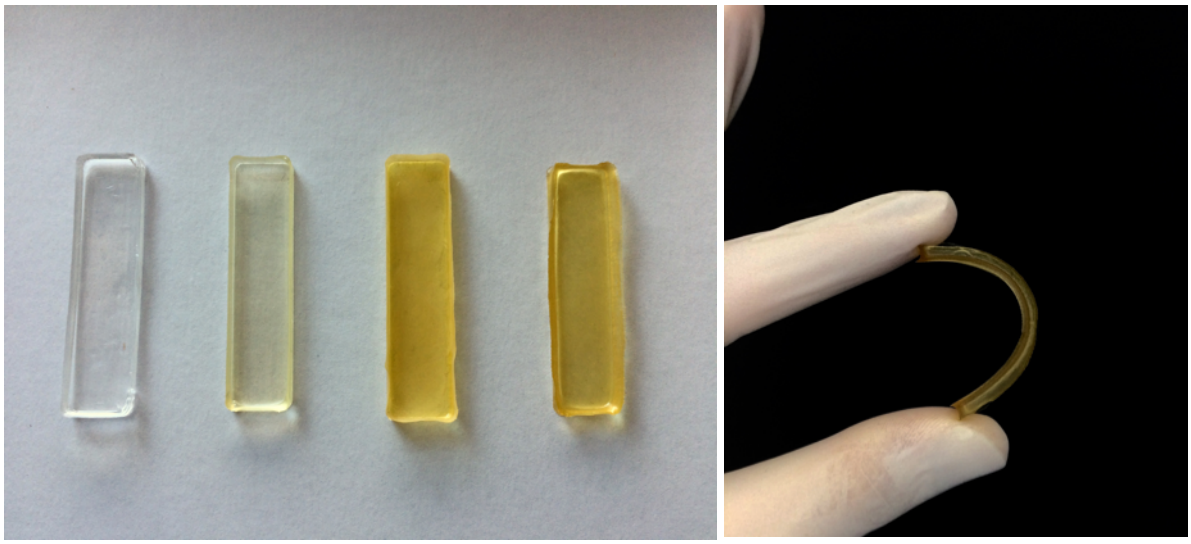

*Figure 55 – Images of all materials produced, as described above (left image: left-to-right: **PBD CTL0**, **PBD CTL1 UPy**, **PBD CTL IMI**, **DOUBLE DYNAMIC**); image of the elastomeric nature of **DOUBLE DYNAMIC** (right image).*

3.3 Conclusions

The synthesis of materials from a commercially-available and supplied polybutadiene pre-polymer backbone was successfully achieved by post-polymerisation modification before co-polymerisation with specifically designed monomers.

The polybutadiene backbones used to synthesise two of the control materials contained hydroxyl-functionality (F(OH) = 2-4) which were subsequently reacted with diisocyanate monomers, to form thermoset materials based on polyurethanes. The monomers which were reacted by polyaddition, were 1) commercially-available HDI, and 2) diisocyanate-functionalised ureidopyrimidinone. Two other materials were synthesised with a polybutadiene backbone that was modified with amino-functionality before polycondensation with 3) dialdehyde-functionalised hexane, and 4) aldehyde-functionalised ureidopyrimidinone. All materials that were produced appeared elastomeric, due to the polybutadiene soft-block.

The synthetic procedures for all materials, as described in this chapter, could easily be envisioned beyond the gram scale, with the average batch size in this project producing 5 g of material. Moreover, the fact that the imine-based polymer networks avoid the use of toxic reagents, i.e. diisocyanates, makes industrial scalability increasingly more promising.

Due to the large polydispersity index, and high degree of chemical functionality of the polybutadiene backbone, stoichiometric ratios with the described monomers are imprecise; the broad average can only be used as a guide. As a consequence, results from all further chemical characterisation should bear this point in mind. The use of a better define polymer backbone, with a more monodisperse range of molecular weights, and more precise degree of functionality, is explored in the final chapter of this thesis.

3.4 References

1. Söntjens, S. H. M. *et al.* Thermoplastic elastomers based on strong and well-defined hydrogen-bonding interactions. *Macromolecules* **41,** 5703–5708 (2008).
2. Tanaka, Y., Takeuchi, Y., Kobayashi, M. & Tadokoro, H. Characterization of diene polymers. I. Infrared and NMR studies: Nonadditive behavior of characteristic infrared bands. *J. Polym. Sci. Part A-2 Polym. Phys.* **9,** 43–57 (1971).
3. Evonik. Evonik - Polyvest® Downloads - Technical Data Sheet Downloads. at <http://adhesive-resins.evonik.com/product/adhesive-resins/en/products/polyvest/Pages/Downloads.aspx>
4. Ren, Y. *et al.* Facile synthesis of well-defined linear-comb highly branched poly(ε-caprolactone) using hydroxylated polybutadiene and organocatalyst. *Eur. Polym. J.* **5,** 27421–27430 (2014).
5. Hine, J. & Via, F. A. Kinetics of the formation of imines from isobutyraldehyde and primary aliphatic amines with polar substituents. *J. Am. Chem. Soc.* **94,** 190–194 (1972).
6. Giuseppone, N., Schmitt, J. L., Schwartz, E. & Lehn, J. M. Scandium(III) catalysis of transimination reactions. Independent and constitutionally coupled reversible processes. *J. Am. Chem. Soc.* **127,** 5528–5539 (2005).

Chapter 4: Characterisation of Double-Dynamic Thermoset Elastomers

4.1 Introduction

From the successful preparation of a double-dynamic elastomeric material, this chapter details that range of techniques used to characterise both the chemical and physical properties of the material. The aim of this characterisation was to understand the chemical differences between **DOUBLE DYNAMIC** and the control materials, and to use this chemical understanding to build an explanation for the differences observed between the materials. As the aim of this project is to incorporate two different dynamic chemical functionalities, that act as kinetic and physical aids to one another, an important area of focus was to try to characterise any kinetic difference between the two chemical functionalities.

As each of the materials are based on the cross-linking of an elastomeric backbone, all of the characterisation techniques investigated the materials in the bulk.

This chapter is organised into three main sections. The first details the limited chemical characterisation that was performed on the materials, in order to decipher the composition of the materials, and how they differ from their monomers. The second section describes the physical characterisation of the materials, attempting to find the key physical elastomeric parameters for accurate comparison to the controls, and currently produced materials. The final section looks at the 'smart' properties of **DOUBLE DYNAMIC**, investigating the new properties that are obtained from the introduction of both dynamic chemistries into the material.

4.2 Results and Discussion

4.2.1 Chemical Characterisation of the Materials

Infrared Analysis

Due to the solid nature of polymer samples, only a very limited number of techniques are available for the chemical characterisation of polymeric materials. The materials detailed above were analysed by Fourier-Transform Infrared (FTIR) spectrophotometry using the attenuated total reflection (ATR) accessory.

FTIR analysis of each material and their constituent monomers was conducted (Figure 56 and Figure 57). In order to follow the progression of imine formation, evolution of absorbance peaks attributed to amine and aldehydes were first followed. Surprisingly, when attempting to identify amine absorbance by comparing the evolution of peaks between polybutadiene pre-polymers (**PBD OH** and **PBD NH_2**), absorbance from neither alcohol nor amine could be identified (with distinct peaks between 3700–3200 cm^{-1} missing) (Figure 56). A notable difference between these two pre-polymers, however, is the presence of the peak at 1730 cm^{-1}, attributed to the C=O urethane stretch. Importantly, all materials derived from this pre-polymer displayed absorbance at this wavenumber, as expected. The presence of many chemical functions absorbing within this range of wavenumbers results in overlapping peaks, with varying widths and numbers of shoulders, that are difficult to distinguish.

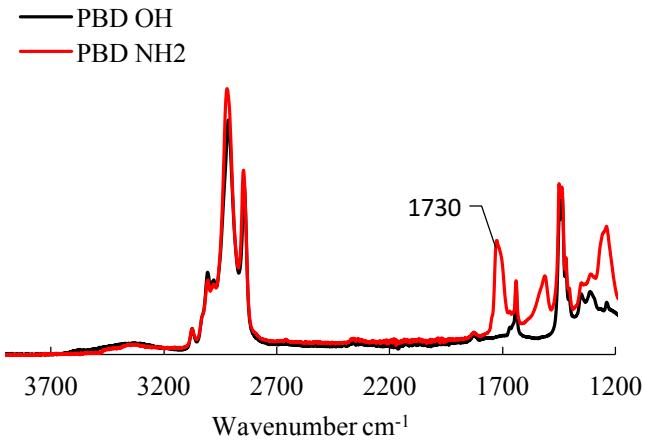

Figure 56 – FTIR spectra of Polyvest® EPHT and amine-modified Polyvest®

Absorbance peaks attributed to the aldehyde C=O stretch (1700 cm^{-1}), appeared, as expected, in both monomers **7** and **6** (Figure 57); these appeared to persist within their respective materials **PBD CTL IMI** and **DOUBLE DYNAMIC**, likely due to the excess amount of aldehyde used in the reaction. A slight shift towards higher wavenumbers was observed in both cases; this may be attributed to the absorbance from the imine moiety overlapping with remaining aldehyde.

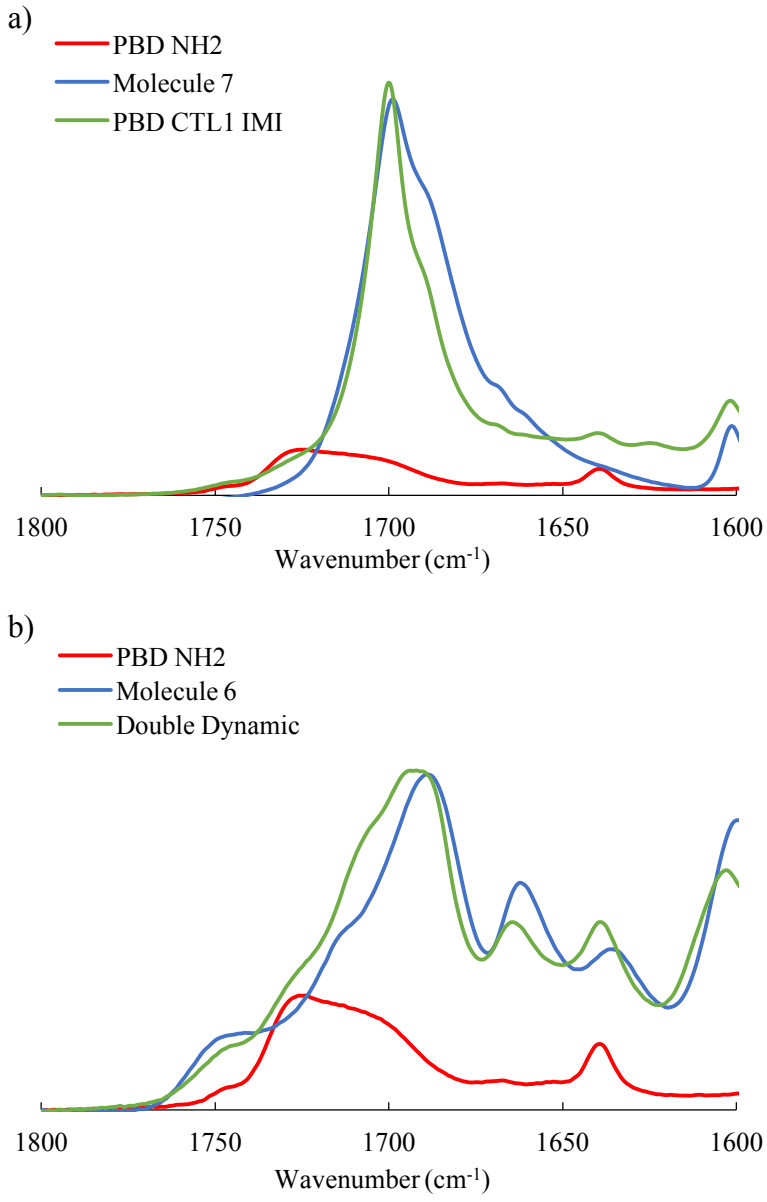

*Figure 57 – a) Partial FTIR spectra of amine-functionalised Polyvest® (red), the dialdehyde-functionalised hexane derivative (**7**) (blue) and **PBD CTl1 IMI**, between 1800 and 1600 cm^{-1}; b) Partial FTIR spectra of amine-functionalised Polyvest® (red), dialdehyde-functionalised ureidopyrimidinone (**6**) and **DOUBLE DYNAMIC**, between 1800 and 1600 cm^{-1}.*

Ninhydrin Amine Test

A qualitative test, to probe the presence of amines within the materials, was conducted by submerging the solid materials in a solution of ninhydrin. Ninhydrin is often used for biochemical application, usually in peptide chemistry, to detect the presence of free primary amines; the mechanism by which this reaction proceeds results in the formation of a strongly purple coloured chromophore (Figure 58).

a) b)

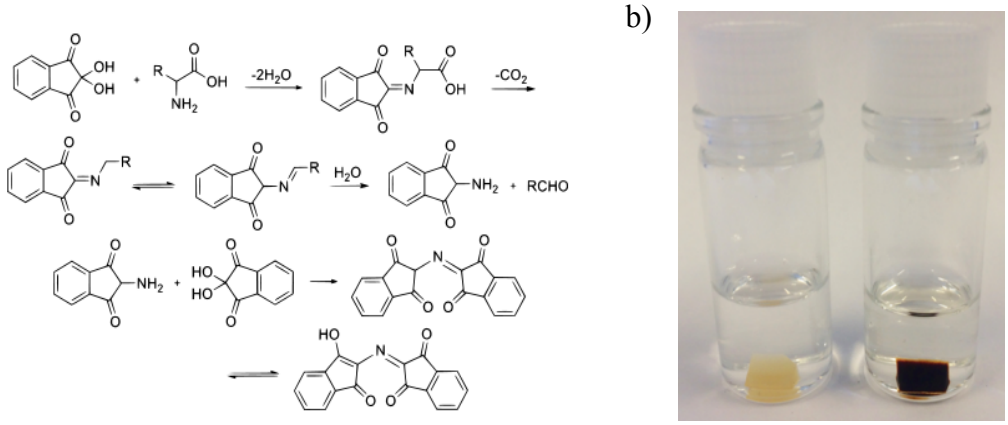

*Figure 58 – a) Schematic representation of the reaction between ninhydrin and a primary amine; b – Image of **PBD CTL1 UPy** (left) and **DOUBLE DYNAMIC** (right) in a ninhydrin solution after 1 day*

After being submerged in a ninhydrin solution overnight, a clear difference was observed between materials based on hydroxyl-functionalised PBD (**PBD CTL1 UPy**) and materials based on amine-functionalised PBD (**DOUBLE DYNAMIC**): a dark purple colour was observed for the latter. The occurrence of this purple colouration could either result from the presence of amines that have remained unreacted during the polymerisation, or could result from to the dynamic exchange or hydrolysis of the imines, with ninhydrin acting as an alternative electrophile with which imines exchange.

The outcome of this experiment proves that, despite aldehyde being present in **DOUBLE DYNAMIC** in a relative excess, the dynamic nature of the imine bond is still activated in the presence of electrophiles, without the need of a catalyst.

4.2.2 Physical Characterisation

Differential Scanning Calorimetry

The effect of temperature on the heat capacitance of each material was analysed by DSC, for a temperature range between –100 and 250 ºC in a nitrogen atmosphere (Figure 59).

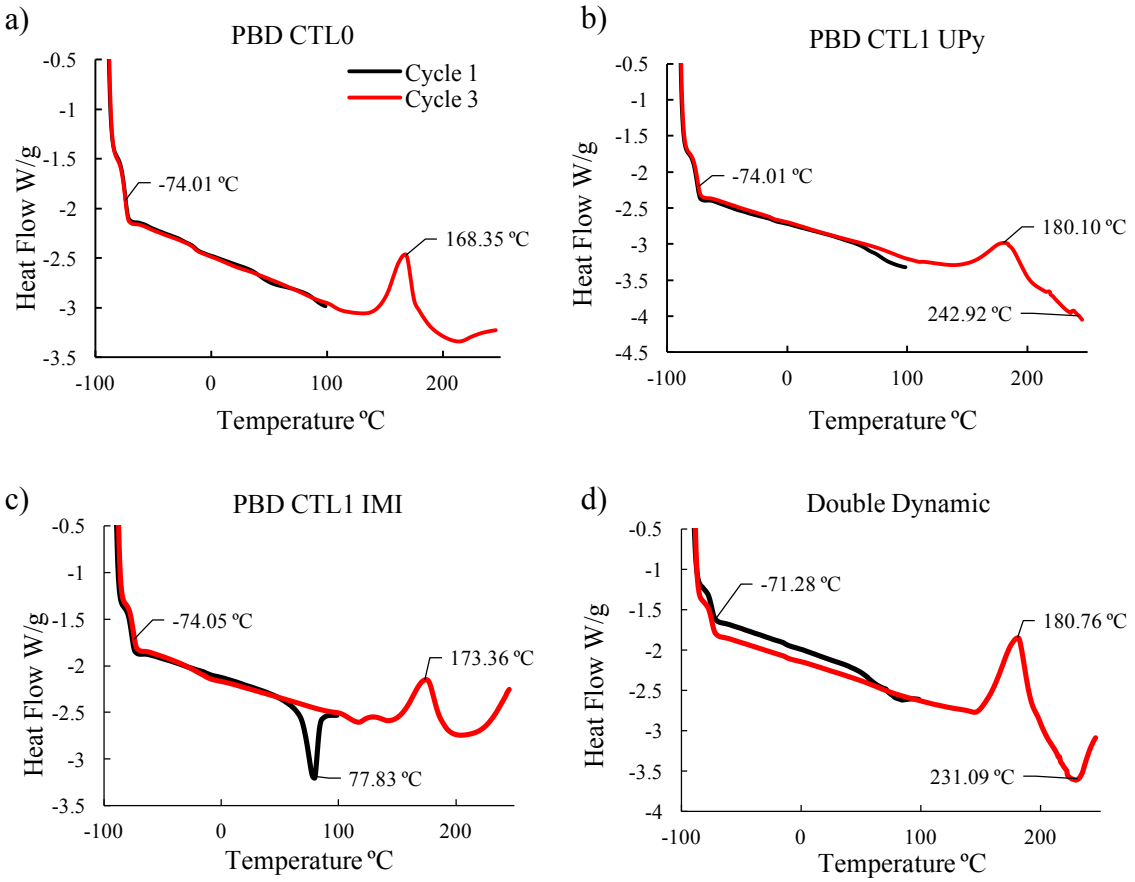

*Figure 59 – Differential Scanning Calorimetry spectra of each thermoset material for temperatures between -100 and 250 ºC. Three cycles, cycle two not depicted: a) **PBD CTL0**; b) **PBD CTL1 UPy**; c) **PBD CTL1 IMI**; d) **DOUBLE DYNAMIC***

For each of the materials, a large exothermic event occurs at ~–74 ºC, likely caused by the materials reaching their glass transition temperature (T_g). This lies in close agreement to the published T_g for Polyvest® at –80 ºC. As the T_g is the same for each of the materials, it is clear that the main chemical influence on T_g comes from the polybutadiene soft block.

The DSC curve for **PBD CTL1 IMI** is the only sample to show any behaviour of interest between –70 and 150 ºC. The endothermic event at 78 ºC could be due to the evaporation of water as a result of incomplete curing of the sample, however no change in the DSC curve is observed around the melting point of water. Alternatively, this endotherm has been observed in other block polyurethanes, being attributed to the dissociation of urethane

soft segment hydrogen bonding.[1] Due to the fact that the thermal history is erased upon the second heating cycle, further examination of the endotherm, observing the effect of annealing, would be needed.

The DSC curves at temperatures above 150 ºC displayed varying behaviour. An exothermic peak at 160–180ºC occurred in each of the samples, which may be attributed to either thermally induced cross-polymerisation or degradation of chemical moieties within the hard block.[2]

Immediately after the exothermic event (230–240 ºC), an endothermic peak is observed exclusively in materials containing ureidopyrimidinone within the hard block. Endothermic events in polyurethanes at these temperatures are usually attributed to the break-up of inter-urethane hydrogen bonding;[1] the break-up of the more strongly hydrogen bonded ureidopyrimidinone assemblies could also be responsible for this endothermic event.

Thermogravimetric Analysis (TGA)

The effect of temperature on the mass of each material was analysed by TGA between a temperature range between 100 and 600 ºC in a nitrogen atmosphere, and is displayed as the derivative of the weight in Figure 60.

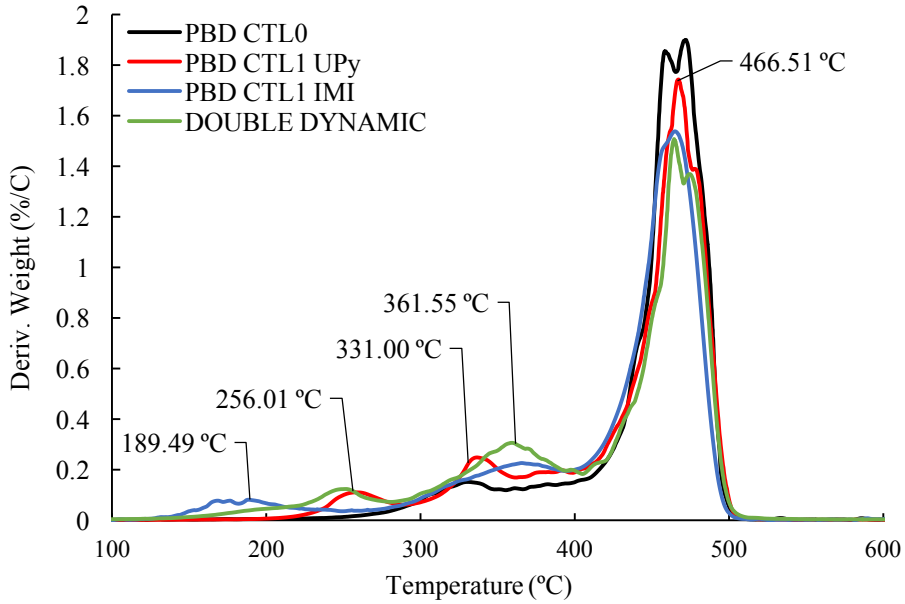

Figure 60 – Thermogravimetric spectra of each thermoset material for a temperature range between 100 and 600 ºC

The thermal behaviour of **PBD CTL0** was observed to match well with previous publication.[3,4] Mass loss occurs in three distinct phases: the first phase of mass loss (at 331 ºC) is observed as a result of the degradation of urea and urethane bonds, with a mass loss of 14%; the second and third stages (starting at 351 ºC with a maximum at 466 ºC) are observed as a result of the degradation of the butadiene backbone itself, with evolution of volatile compounds such as 1,3-butadiene, cyclopentene and 1,3-cyclohexadiene among other, accounting for 86% mass loss.

The behaviour of **PBD CTL1 UPy** extends to a fourth phase, with a mass loss event at a lower temperature below that of the first phase of **PBD CTL0** (256 ºC). The first phase in this case accounts for 5% mass loss, corresponding well to the corresponding weight percentage of ureidopyrimidinone at ~4%; the second phase accounts for 11% of the mass loss; and third and fourth phases accounting for 84% of the loss of mass.

Introduction of the imine chemical functionality as the chain-extending and cross-linking moiety results in materials with a lower first mass loss event. The first mass loss phase, equating to 6% of the total mass, occurs in a broad event over ~133 ºC and peaking at 190 ºC. It is likely that degradation of the imine bond has some role to play in the evolution of this peak. Interestingly, the second mass loss event overlaps with the third at 362 ºC equating to a 20% mass loss. Finally the fourth mass loss event, and degradation of the butadiene backbone occurs at 467 ºC and accounts for a 74% loss of the total mass.

The thermal behaviour of the **DOUBLE DYNAMIC** material includes all of the mass loss events mentioned above. A broad first mass loss event occurring over ~140 ºC peaking at 255 ºC is likely caused by overlapping mass loss events caused by the presence of both imine and ureidopyrimidinone moieties. Similarly to **PBD CTL1 IMI** the second and third mass loss events are also overlapped, equating to 25% of the total loss of mass. The third and final mass loss event occurs, as with the other materials, at 467 ºC and equates for 67% of total mass loss.

	Hard Block Weight %	1st Phase Mass Loss %	Soft Block Weight %	2nd/3rd/4th Phase Mass Loss %
No Dynamic	6	14	94	86
One Dynamic UPy	17	5	83	11 / 84
One Dynamic Imine	14	6	86	20 / 74
Double Dynamic	23	8	77	25 / 67

Table 8 – Tabulated data of hard/soft block mass fraction vs mass loss observed by TGA

X-Ray Scattering

To decipher the way in which the hard and soft blocks are organised within the materials, both wide (WAXS) and small angle X-ray scattering (SAXS) was used to analyse the composition of the solid samples at room temperature (Figure 61a and b); these results are tabulated in Table 9.

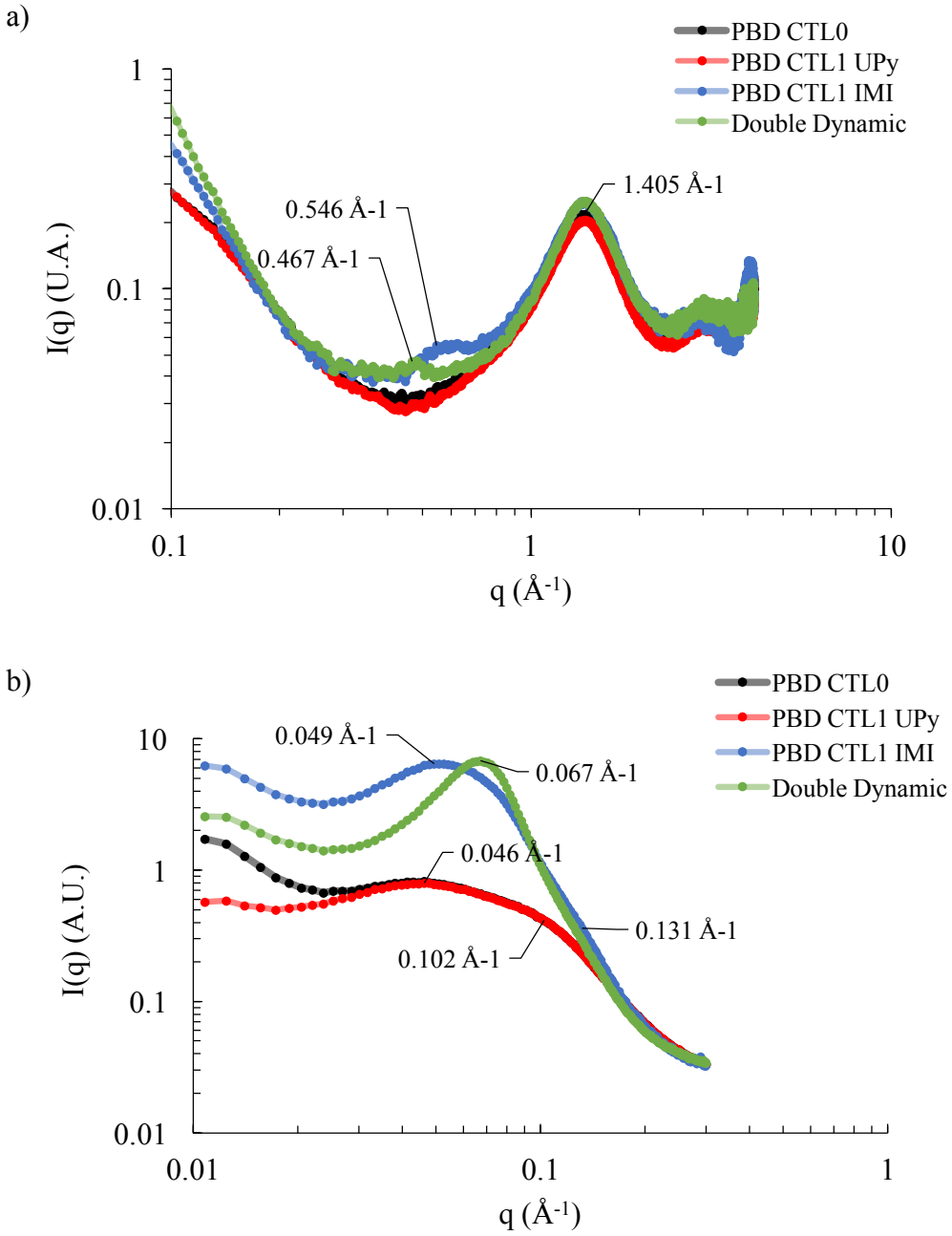

Figure 61 – a) Wide Angle X-Ray Scattering spectra (WAXS) of each thermoset material for a q-range between 0.1 and 4 Å^{-1}; b) Small Angle X-Ray Scattering (SAXS) spectra of each material for a q-range between 0.01 and 0.20 Å^{-1}.

X-Ray scattering analysis revealed the presence of different sized aggregates within the materials. Materials **PBD CTL0** and **PBD CTL1 UPy** displayed very similar scattering behaviour. Using WAXS, a strong reflection at 1.405 $Å^{-1}$ (4.47 Å) was detected in both materials; objects scattering at this length in polyurethane-based materials are typically attributed to hydrogen bonding interactions within the hard block, proving that there is a degree of order driven by hydrogen bonding within the hard blocks of these two materials.[5] Using SAXS, larger objects gave rise to a broad and shouldered reflection, with a maximum at 0.046 $Å^{-1}$(136.59 Å) and shoulder at 0.102 $Å^{-1}$ (61.60 Å); objects scattering at these lengths in polyurethanes are attributed to micro-phase separation between hard and soft blocks.[6]

Similarly to **PBD CTL0** and **PBD CTL1 UPy**, wide angle X-ray scattering of **PBD CTL1 IMI** showed the presence of objects at the size of hydrogen bonds (4.47 Å). A second weaker reflection of a slightly larger object at 0.546 $Å^{-1}$ (11.51 Å) appears, possibly resulting from the presence of aromatic imine or higher order ureidopyrimidinone stacks. Surprisingly, these larger aggregates are not observed in **PBD CTL1 UPy** despite previous publication strongly suggesting their existence in a similar type of system.[7,8] SAXS analysis of **PBD CTL1 IMI** showed a broad reflectance with a peak at 0.049 $Å^{-1}$ (128.23 Å) and shoulder at 0.122 $Å^{-1}$ (51.50 Å), which may be attributed to aggregation of the hard block into nanofibers.

Wide angle X-ray scattering of **DOUBLE DYNAMIC** similarly showed reflectance at 4.5 Å from hydrogen bonding objects, and, similarly to **PBD CTL1 IMI** a weak reflectance at 0.467 $Å^{-1}$ (13.45 Å) matching well with the literature describing higher order ureidopyrimidinone stacking. A strong reflectance was observed by SAXS, with objects of 0.067 $Å^{-1}$ (93.78 Å) suggesting the presence of nanofibers, similarly to **PBD CTL1 IMI**.[7,8] Further characterisation of the materials by variable temperature X-ray scattering is planned, to follow the evolution of these hard-block aggregates at different temperatures.

	WAXS				SAXS			
	q Value (Å-1)	*D-Spacing (Å)*	*q Value (Å-1)*	*D-Spacing (Å)*	*q Value (Å-1)*	*D-Spacing (Å)*	*q Value (Å-1)*	*D-Spacing (Å)*
No Dynamic	1.405	4.47	-	-	0.102	61.6	0.046	136.59
One Dynamic UPy	1.405	4.47	-	-	0.102	61.6	0.046	136.59
One Dynamic Imine	1.405	4.47	0.546	11.51	0.122	51.5	0.049	128.33
Double Dynamic	1.405	4.47	0.467	13.45	-	-	0.067	93.78

Table 9 – Tabulated data of the X-Ray reflections observed by both WAXS and SAXS with the corresponding d-spacings

*Crystallisation of **Molecules 5** and **6***

To further elucidate the physical arrangement of the hard and soft segments within the materials, growth of single crystals of the monomers **5**, **6** and **7**, suitable for single crystal X-

ray crystallography, were attempted. Unfortunately, no single crystals were obtained from the various of techniques and solvent/non-solvent conditions that were tested (i.e. recrystallization from chloroform, THF and DMF, diffusion crystallisation from chloroform and THF), however, remarkably gels were observed to form after ~16 hours, from solutions of **5** and **6** in dimethylformamide (Figure 62). The gel of **6** was analysed by Transition Electron Microscopy (TEM) to observe its microscopic nature (Figure 63).

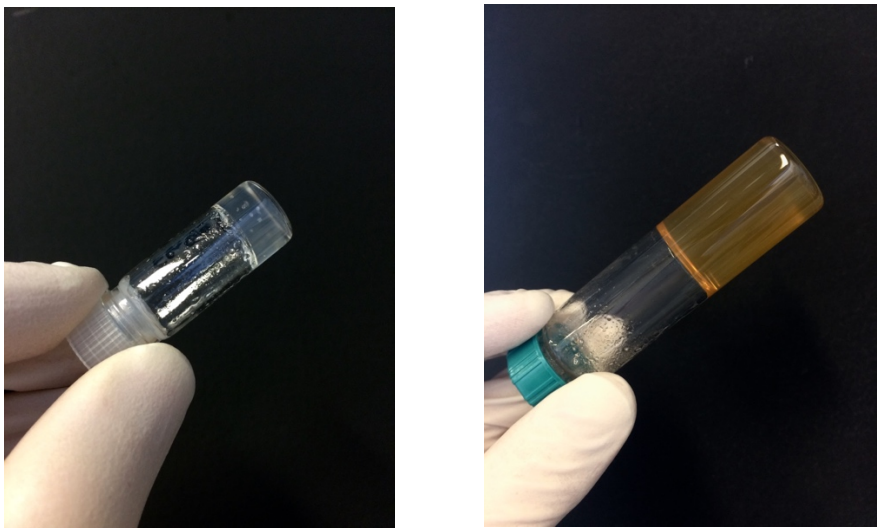

*Figure 62 – Images of the supramolecular gel obtained by dissolution of **6** (left) and **5** (right) in DMF*

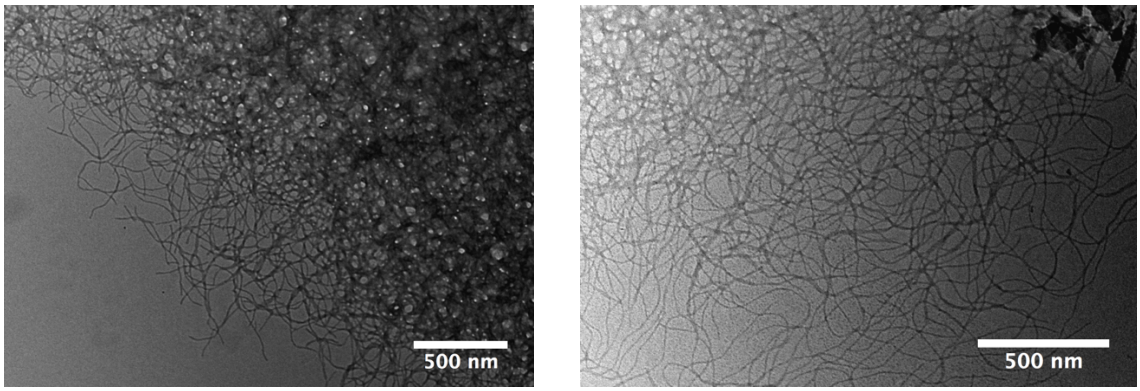

*Figure 63 – Tranisitin Electron Microscope images of the supramolecular gel obtained from **6***

From this microscopy, the gel was observed to be composed of long amorphous fibres; the smallest width, at the edge of the sample, was found at ~6 nm. Thicker fibres of ~17 nm were also found, but are probably due to the fibre aggregation or entanglement. It is proposed that these fibres are the result of supramolecular polymerisation and, due to the fact that gels were only formed from monomers containing the ureidopyrimidinone moiety, this polymerisation is driven by lateral inter ureidopyrimidinone stacking.[8]

Dynamic Mechanical Analysis (DMTA)

Analysis of the behaviour of the materials when stretched at very low strains was conducted using Dynamic Mechanical (Thermal) Analysis (DMTA); the materials were cut to roughly the following dimensions: 40 mm x 10 mm x 1 mm. For each of the DMTA analyses, a sinusoidal force with strains starting at 0.6%, and a peak and trough at 0.8% and 0.4% respectively, was used. The behaviour of the material was followed by observing the change in storage and loss moduli, as well as tangent delta, for a temperature range from –75 ºC to 150 ºC and using a frequency range between 0.1 Hz and 15 Hz (Figure 64a and b).

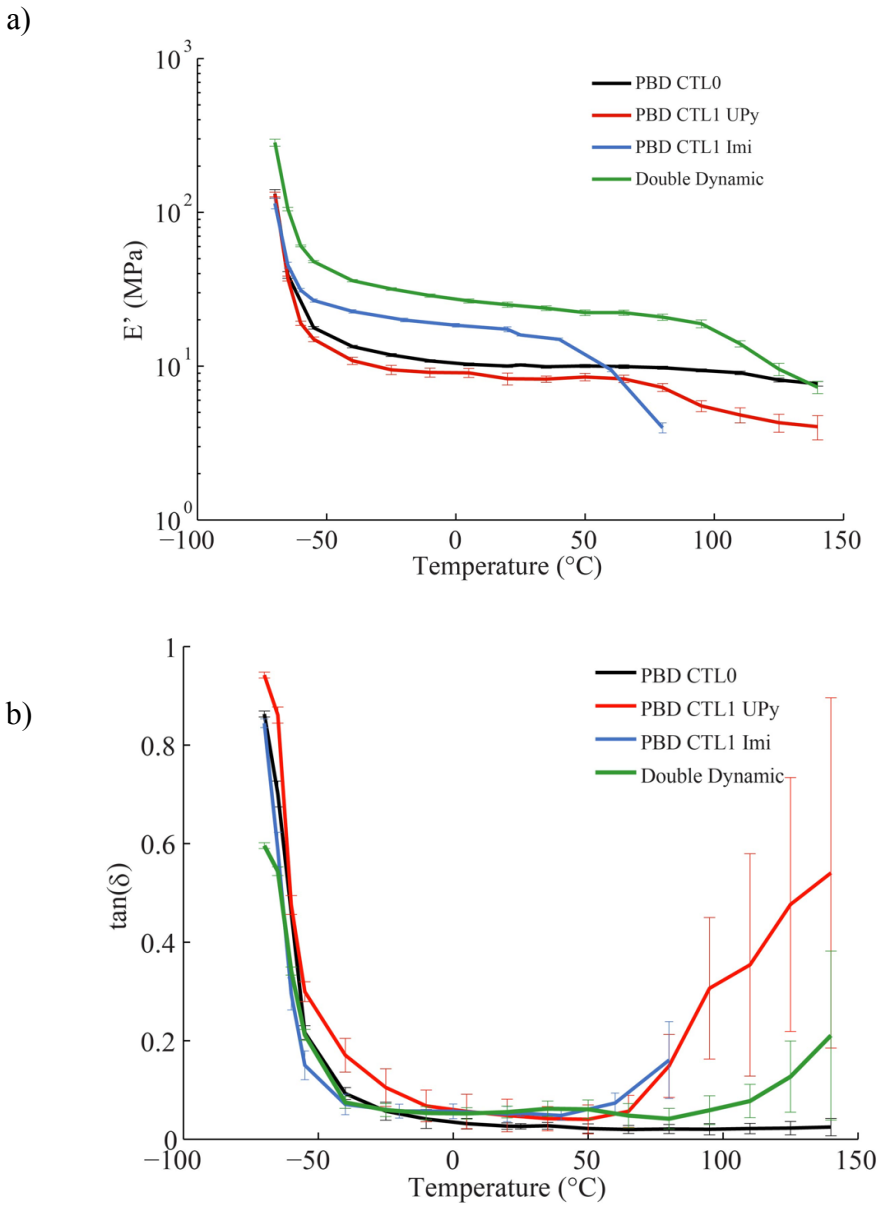

Figure 64 – a) Storage modulus vs temperature, obtained by dynamic mechanical analysis, of each thermoset material at a frequency of 1Hz for a temperature range between –70 and 150 ºC; b) Tan(δ) vs temperature, obtained by DMTA, of each thermoset material at a frequency of 1 Hz for a temperature range between –70 and 150 ºC

The plot of the storage modulus versus temperature, with a frequency of 1 Hz (Figure 64a), reveals three key pieces of information: the storage moduli at temperatures around the rubbery plateau are different for each sample; the glass transition temperature is constant for all samples; and a decrease in storage modulus, with tendency toward a more viscous behaviour, is observed at higher temperatures.

Firstly, an increased storage modulus (E') at temperatures within the rubbery plateau is observed in both materials formed from imine chain-extension/cross-linking chemistries **PBD CTL1 IMI** and **DOUBLE DYNAMIC**. Interestingly, **PBD CTL1 UPy** does not show such an increase, with E' similar to that of **PBD CTL0**. This global increase in E' for both polyimine networks, could be due to the same higher degree of ordering within the hard block, as suggested by SAXS.

Similar behaviour is observed in each of the materials when approaching the glass transition temperature, with a steep increase in E' compounded by a steep increase in tangent delta (Figure 64b) below –50 ºC. This experimental value of T_g lies in close agreement with the result from DSC and literature values for polybutadiene.

At elevated temperatures, all samples containing one or two dynamic chemical moieties display clear divergence from their respective behaviours at room temperature. **PBD CTL1 UPy**, **PBD CTL1 IMI** and **DOUBLE DYNAMIC** all displayed a decreasing E' and increasing Tan delta at temperatures above 50 ºC. However, due to the relaxation of the material at such temperatures absolute values above 50 ºC should not be considered, but only the trend toward viscosity observed. The relaxation of the materials results in samples buckling, in turn causing the measurements produced to be unreliable, as reflected by the large increase in standard deviation. For this reason, absolute values of E' or tan delta should not be considered, but only the trend of increasing viscosity.

The relaxing behaviour observed in exclusively the samples containing dynamic chemical moieties is a good indication that temperature-dependent chemical exchange is occurring within the samples.

Importantly, the observance of rubbery behaviour of **DOUBLE DYNAMIC** between –30 ºC and +80 ºC falls in line with the targeted operating temperature range, as mentioned in the Chapter 1.

The master curves show good cohesion between all data collected at all frequencies and temperatures, as exemplified in Figure 65.

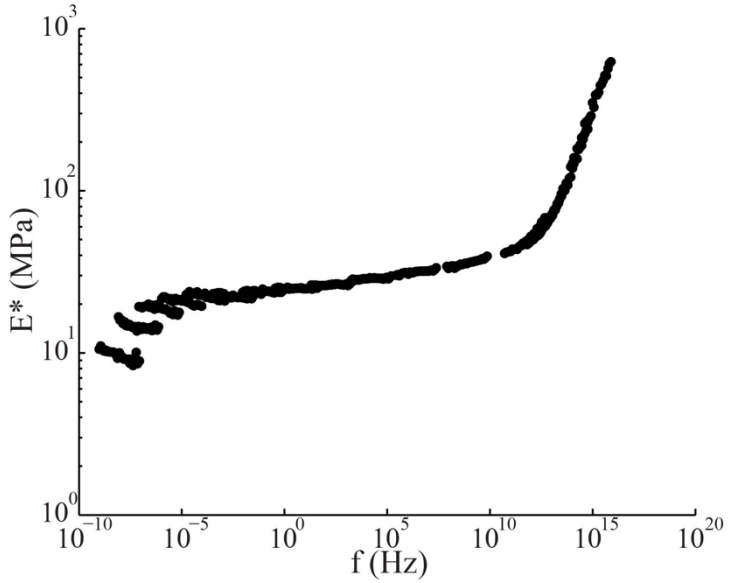

*Figure 65 – DMTA master curve of complex modulus vs frequency for **DOUBLE DYNAMIC***

DMTA studies of different batches of **DOUBLE DYNAMIC**, using the same monomers and stoichiometric ratios, revealed slightly different behaviours between batches. Initially, a remarkably linear transition of E', from the glass transition temperature to 110 ºC was observed (Figure 66a); analysis of a different batch displayed a clearer rubber plateau, before divergence to lower E' values (Figure 66b). This differing behaviour between batches of the same materials shows a clear need to refine the synthetic process, but may also be due the broad average of molecular weights within the Polyvest® batch reflecting the difficulty for stoichiometric control.

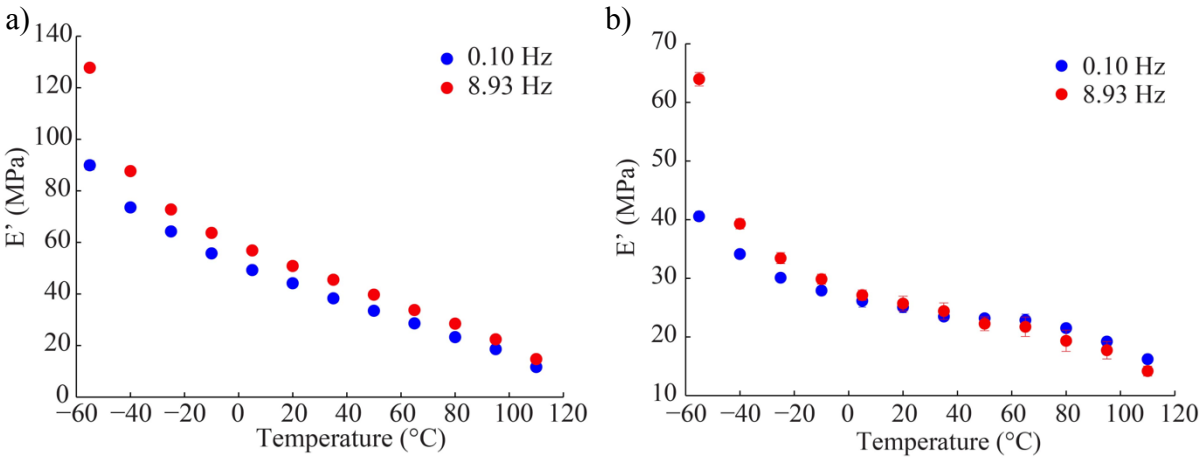

*Figure 66 – a) and b) Plots of storage modulus vs temperature of **DOUBLE DYMAMIC** of the same chemical composition but from different batches*

Stress Strain Cycles

The effect of stresses on the materials beyond Hookean behaviour were analysed by cycling the materials between 0 and 20% stress, for ten cycles, at three distinct frequencies: 10 mHz, 100 mHz, and 1 Hz. All analyses were conducted at room temperature (Figure 67).

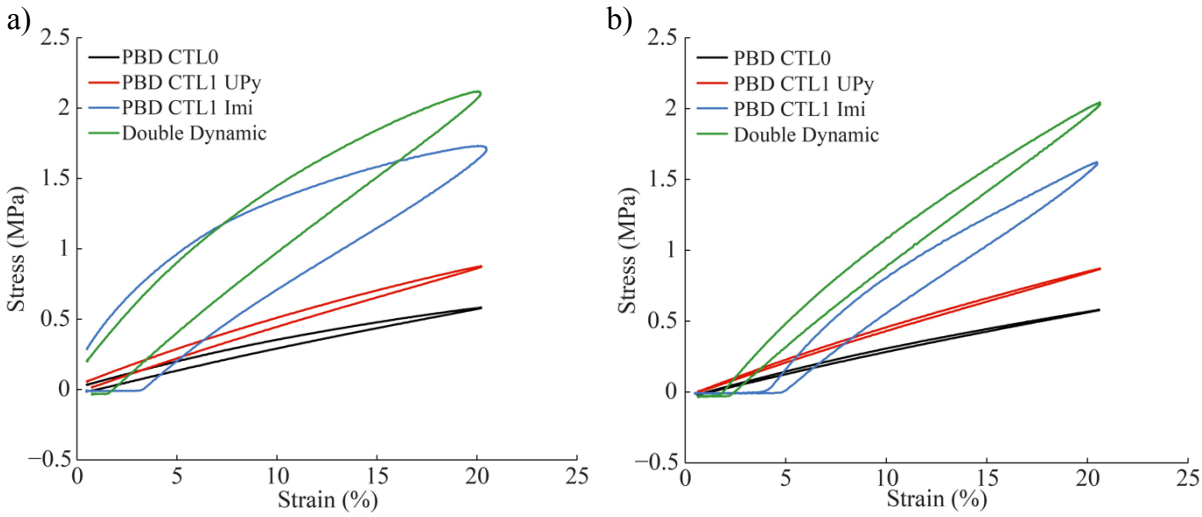

Figure 67 – Stress/strain curves of each thermoset material at a frequency of 100 mHz, first and tenth cycles are correspond to a) and b), respectively

The results from the stress/strain analysis came to three general conclusions: the maximum stress produced at the same maximum strain (20%) greatly differs between materials; the first and last cycles are different to differing extents between materials; and, as observed with DMTA, different batches of materials of identical chemical composition behave differently.

When directly comparing the stress/strain curves produced from each material across all tested frequencies (100 mHz shown in Figure 67), **DOUBLE DYNAMIC** was found to reach a significantly higher strain than all other materials tested. Moreover, the slope of the linear portion of the curve (the Young's modulus) for **DOUBLE DYNAMIC** (E= ~17) is six times greater than **PBD CTL0** (E= ~2.5) confirming that **DOUBLE DYNAMIC** is a considerably stiffer material.

A clear difference between the first and last loading/unloading cycles could be seen when cycling both **DOUBLE DYNAMIC** and **PBD CTL1 IMI** and, to a lesser extent in **PBD CTL1 UPy** and **PBD CTL0** (Figure 67).[9] The evolution of this behaviour in **DOUBLE DYNAMIC** at a frequency of 10 mHz across cycles 1, 2, 5 and 10 is exemplified in Figure 68. The first cycles of **DOUBLE DYNAMIC** and **PBD CTL1 IMI** shows a distinctly different

behaviour to **PBD CTL0** and **PBD CTL1 UPy** from the loading to the unloading of strain, due to a more viscoelastic behaviour; this difference was seen to be considerably smaller on all subsequent loading/unloading cycles. The role of the imine bond as the cross-linking chemistry could play some role in this tendency away from elasticity toward viscoelasticity, with dynamic exchange between imines causing the hysteresis. It may also be the case that the hard block aggregates, observed by X-ray scattering, are broken or disrupted on the first cycle, causing the exaggerated hysteresis on the first cycle. A second distinct behaviour of the imine-containing materials is the lag strain observed in all cycles after the first, whereby the initial input of strain is not immediately followed by a stress response. The precise causes of both of these physical phenomena are still largely unknown, meaning any chemical reasoning posed for the occurrence of this viscoelasticity and relaxation should be given with caution.[9]

The reversibility of these observations was probed in a timed-recovery experiment. **DOUBLE DYNAMIC** and **PBD CTL1 IMI** were cycled 10 times as before, and then left at room temperature over 3 days before being cycled again (Figure 69). Very similar behaviour was observed after waiting, with a large difference between the first and subsequent loading/unloading cycles, proving that this behaviour is in fact recoverable over just 3 days.

As observed with DMTA, the reproducibility of the mechanical performance between batches was found to be low when analysing stress/strain behaviour. When probing the effect of frequency on the behaviour of the material, no consistent global trend was observed (Figure 70). This is likely due to inter-batch differences of the materials that should be the focus for future development of consistent materials.

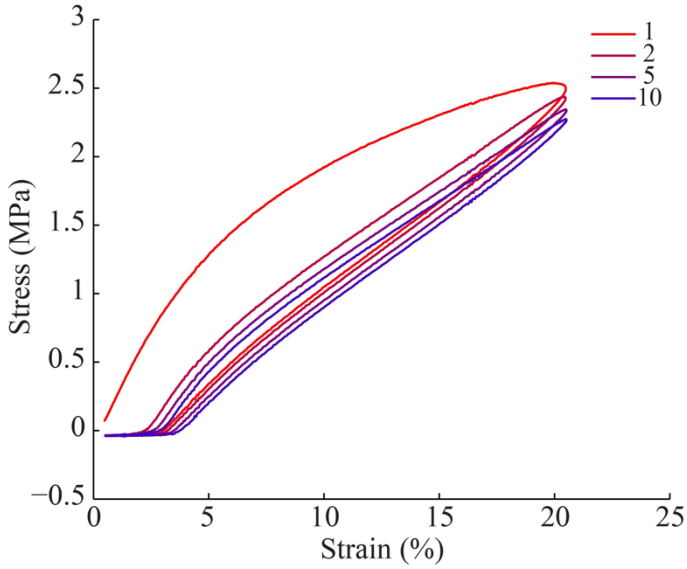

*Figure 68 – Stress/strain curves (10 consequtive cycles) obtained at cycled 1, 2, 5 and 10 for **DOUBLE DYNAMIC** at a frequency of 10 mHz*

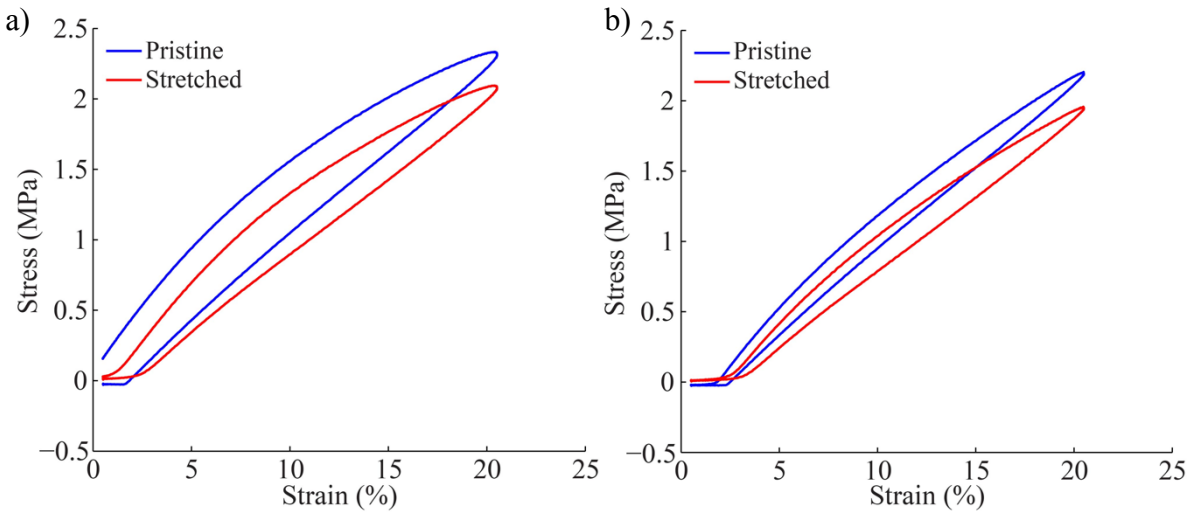

*Figure 69 – a) First and b) tenth stress/strain curves of **DOUBLE DYMAMIC** pristine (unstretched) (blue) and stretched (and allowed to rest for 3 days at RT). Frequency 100 mHz.*

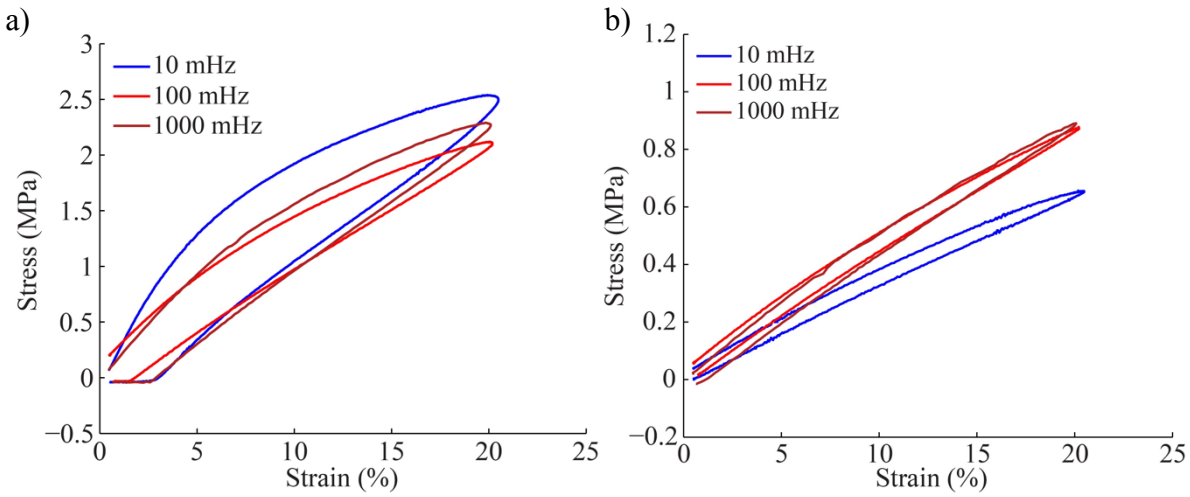

*Figure 70 – a)Stress/strain cycles (first cycle) of **DOUBLE DYNAMIC** at three frequencies; b) Stress/strain cycles (first cycle) of **PBD CTL1 UPy** at three frequencies*

Elongation Until Break

The limit to which the materials could be stretched until their failure, was then analysed by elongation until break studies. All materials were tested at room temperature with a strain rate of 0.4% s^{-1}.

The results from this experiment may be summarised into three main conclusions: all materials displayed classical viscoelastic behaviour; **DOUBLE DYNAMIC** was found to be a stiffer but stronger material than all other samples; and, due to the poorer reproducibility of the results a large range of some of the physical parameters was found.

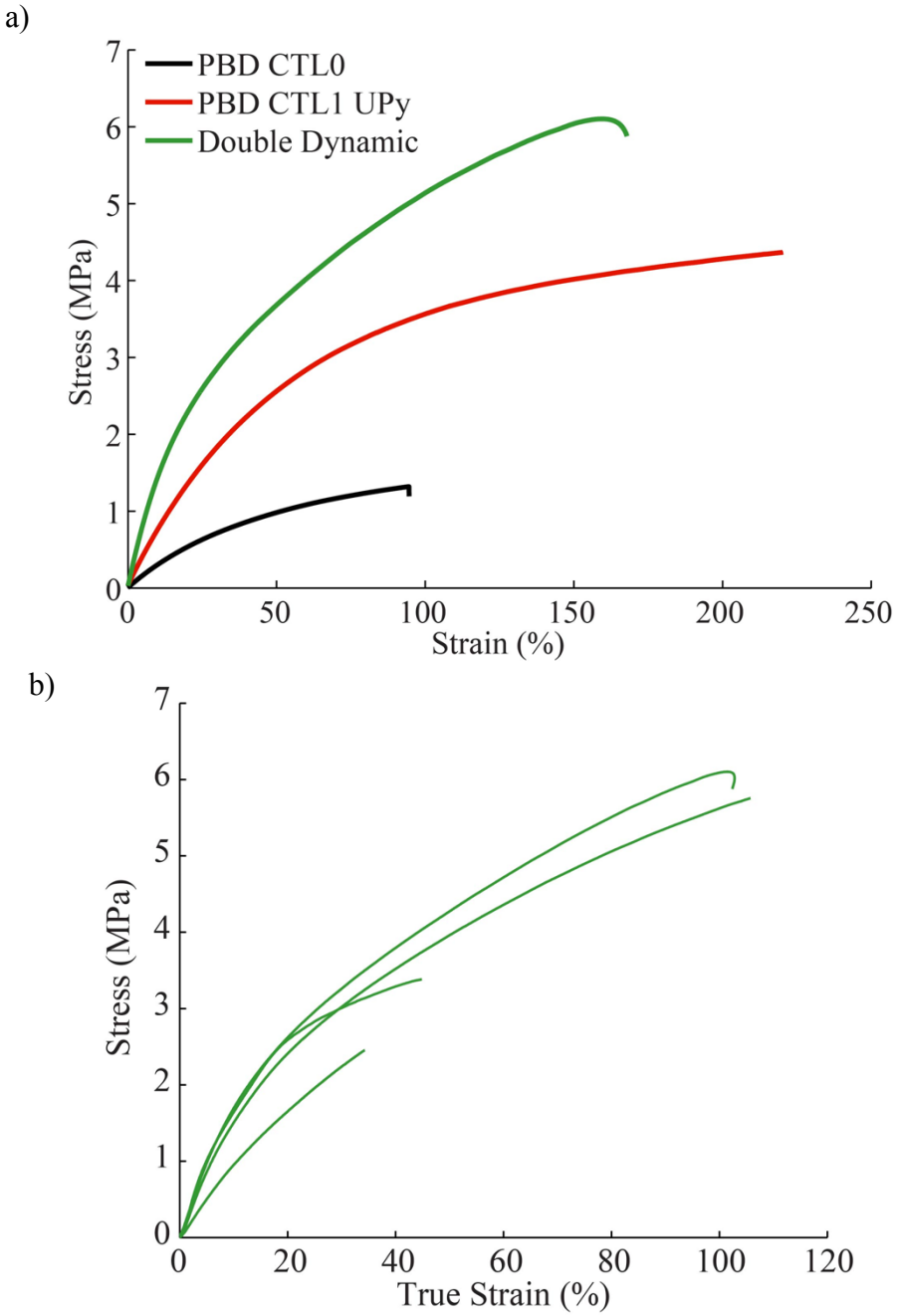

*Figure 71 – a) Elongation until break analysis of three materials (**PBD CTL0**, **PBD CTL1 UPy**, **DOUBLE DYNAMIC**). This plot displays the stress vs engineering strain at a strain rate of 0.4% s^{-1}; b) Evolution of the stress vs true strain displaying the multiple elongation until break tests of **DOUBLE DYNAMIC**, strain rate 0.4% s^{-1}*

All three materials that were tested (**PBD CTL0**, **PBD CTL1 UPy** and **DOUBLE DYNAMIC**) were observed to pass through two distinct regions upon elongation: a Hookean portion at low strain and a Newtonian portion at higher strains. This behaviour conforms to a classical viscoelastic behaviour.

By comparing the highest performing elongation runs (Figure 71) **DOUBLE DYNAMIC** was found to possess a Young's modulus, and therefore a stiffness, almost six times greater than **PBD CTL0** (Table 10). This six fold difference in Young's Modulus

matches well with data obtained from the stress/strain analysis. **DOUBLE DYNAMIC** was also found to be significantly more ductile, with the maximum strain of the material (70% true strain) reaching beyond the limit of the machine. **DOUBLE DYNAMIC** was found to be a considerable stiffer and stronger material than both of the control materials that were tested.

Differences between samples of the same chemical composition were also a key issue with these results. A high degree of reproducibility was found in the linear regions of extension, with minimal differences in the calculated Young's moduli, however, significantly different tensile strengths, and therefore strains at rupture, were found when testing samples of the same composition (Figure 71). This inconsistency results from premature breakage of the material at imperfections along the edges of the sample, due to poor sample preparation. The maximum strains achieved, however, show the prospect of a promising material, as long as imperfection-free samples can be prepared.

	No Dynamic Control	One Dynamic Upy	Double Dynamic
Young's Modulus (MPa)	2.69 (±0.34)	4.90 (±1.35)	14.46 (±3.32)
Tensile Strength (MPa)	0.94 (±0.24)	>3.10 (±0.86)	>4.70 (±1.66)
Strain at Rupture (mm/mm)	0.57 (±0.20)	>2.25 (±0.53)	>1.12 (±0.58)

Table 10 – Tabulated data of the average physical parameters of the materials tested by elongation until break, over 6 experiments.

Stress Relaxation

To explore the relaxation behaviour seen by DMTA, whereby the storage modulus decreased and tangent delta increased to different extents at different temperatures in each material, stress relaxation experiments were conducted. In this analysis, a fixed strain is applied to the material, and the evolution of stress is observed as a function of time. Typically, materials that contain cross-links that reversibly exchange, exhibit temperature-dependent stress relaxation that follows the Arrhenius Law (this law applies when stress relaxation is the result of molecular exchange).

At elevated temperatures, **PBD CTL1 UPy**, **PBD CTL1 IMI** and **DOUBLE DYNAMIC** all displayed changes in DMTA, and so were analysed by stress-relaxation. A fixed strain of 5% was applied to materials of the same dimensions as tested by DMTA, and the evolution of tension stress was followed for all materials containing dynamic chemical moieties (Figure 72 and Appendix).

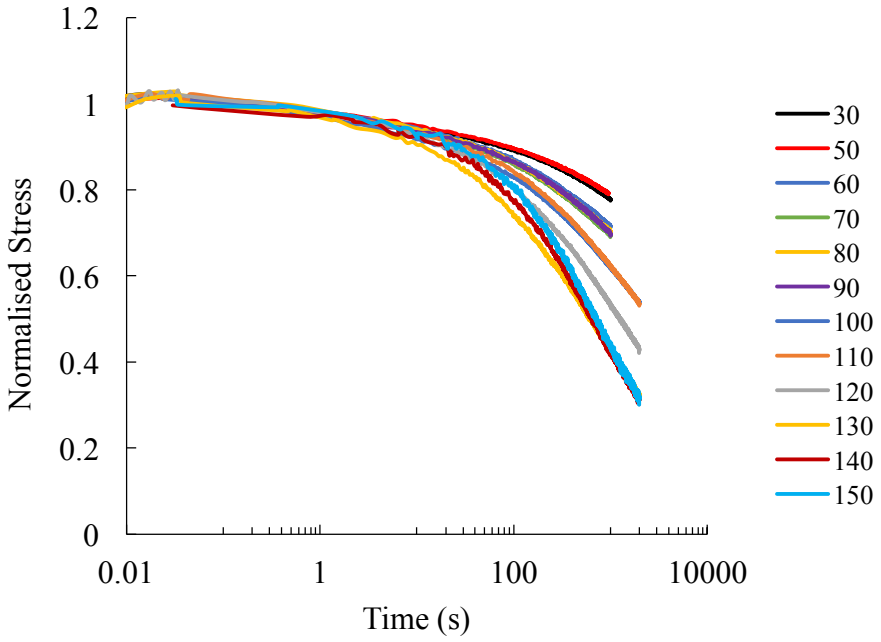

*Figure 72 – Normalised stress relaxation curves (stress vs time) of **DOUBLE DYNAMIC** at different temperatures*

All materials displayed temperature dependent stress-relaxation, confirming the qualitative observation by DMTA analysis. To confirm whether this relaxation behaviour satisfied the Arrhenius Law, an Arrhenius plot was constructed by calculating the characteristic relaxation times (τ^*) by fitting the normalised stress relaxation data to the model in Equation 12.[10] The natural logarithm of the relaxation times ($\ln \tau^*$) were then plotted against 1/T (K); and the activation energy (E_a) obtained from the slope of the line (Equation 13) (Figure 73).

$$Stress(t) = Stress_0 . e^{(-t/\tau*)}$$

Equation 12 – Exponential decay function used as a model to describe dynamic stress relaxation

$$\ln \tau^* = \ln A + \frac{E_a}{RT}$$

Equation 13 – Linearised Arrhenius equation

The activation energies from each material, obtained from Arrhenius analysis, provides insight into their behaviour at elevated temperatures. A lower activation energy (3.56 kJ/mol) was observed for **DOUBLE DYNAMIC**, compared to 5.09 kJ/mol and 13.81 kJ/mol for **PBD CTL1 IMI** and **PBD CTL1 UPy**, respectively. The occurrence of the lower activation energy

in **DOUBLE DYNAMIC** could be due to an additive effect caused by the activation of the dynamic exchange of both dynamic groups at similar temperatures.

The practical utility of the lower activation energy observed in **DOUBLE DYNAMIC** is particularly interesting for the potential of this material's ability to self-heal. As a lower energy is required to trigger relaxation, caused by the dynamic exchange of its constituent chemistry, lower temperatures can be expected to be necessary for activation of dynamic chain movement and self-healing.

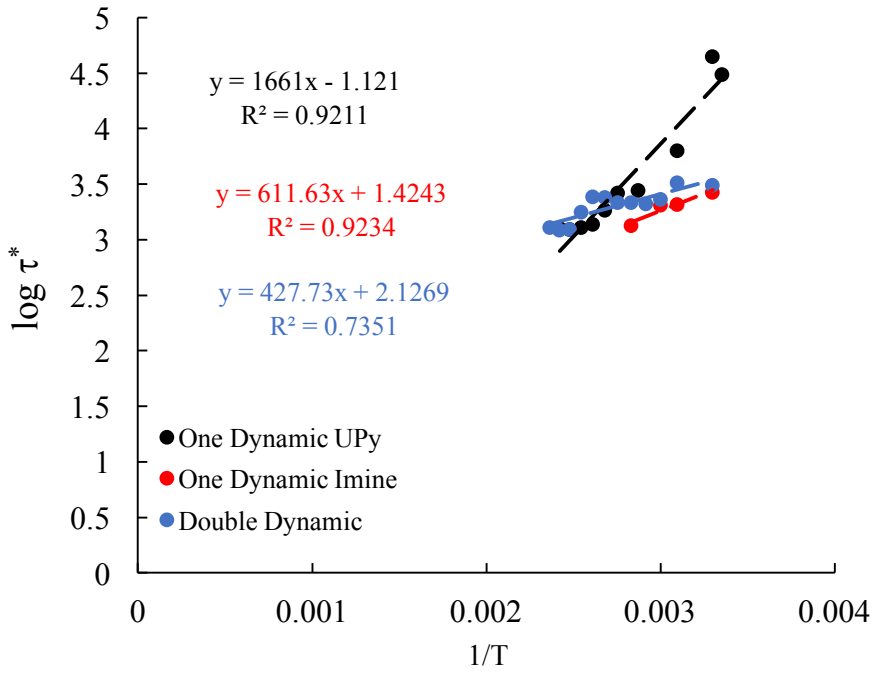

*Figure 73 – Arrhenius plot (log relaxation time (τ^*) vs 1/T) of **PBD CTL1 UPy** (black), **PBD CTL1 IMI** (red), and **DOUBLE DYNAMIC** (blue)*

4.2.3 Recyclability

Solubility and Re-Moulding

To probe the effects of solvent on the materials, and to investigate their response to pH, a series of qualitative tests were devised. Knowing that imines are susceptible to hydrolysis, any real-world application of polyimine-based materials would require some degree of stability after exposure to water. To examine the effect of water on **DOUBLE DYNAMIC**, the material was submerged in neutral water for 3 hours - no swelling response was observed, due to the poor solubility of polybutadiene in water, as well as no observed effect on its structural integrity after drying. The material was then submerged again and the water acidified with 10 weight percent trifluoroacetic acid (TFA) - again, the material was observed to be unaffected by these conditions. In fact, no effect on its structural integrity was observed after submersion in acidified water for as long as three weeks, with the first signs of degradation, at the edges of sample, observed after one month.

The pH responsiveness of **DOUBLE DYNAMIC** was then further investigated by submersion of the material in THF, a good solvent for polybutadiene. A swelling degree of 537% was found after being submerged in neutral THF for 20 minutes; no residual polymer was observed after drying the THF, and, after drying the material, no negative effects on the structural integrity of the sample were observed. These observations suggest that, while swollen in neutral THF, **DOUBLE DYNAMIC** does not dissolve. The material was then swollen again in THF before introduction of 10 weight percent TFA. A marked difference in behaviour was observed, with immediate formation of bubbles on the surface and in the bulk of the material; after 20 minutes, with vigorous shaking, the material was observed to have broken-down completely, with the majority of the bulk material in solution and a small amount of solid in a clear suspension (Figure 74a–c). ^{1}H NMR analysis after addition of TFA to the model reaction, described in Chapter 3, was conducted, revealing a slow but steady regeneration of **Molecule 6** after 5 hours. The slow speed with which the hydrolysis appears to proceed, could explain the persistence of the small amount of solids observed regardless of the quantity of TFA used.

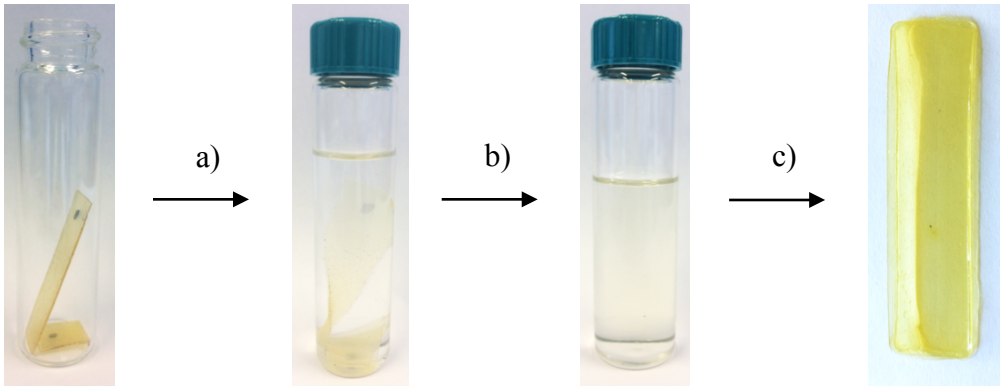

*Figure 74 – Images detailing the solubility of **DOUBLE DYNAMIC** in acidified organic solvent, and the ability to reform bulk elastomers after evaporation: a) add THF, b) add 10 wt% $TFA_{(aq)}$, c) evaporate in air*

Regeneration of the dissolved material was first attempted by neutralising the solution with triethylamine. Turbidity was immediately observed upon addition of the base, yielding a sticky, shapeless solid after evaporation. Regeneration was then attempted without neutralisation of the solution, by concentrating the dissolved material followed by pipetting into a mould, drying in air before post-curing under vacuum at 50 ºC. This method produced a solid material with a markedly decreased elastomeric nature. Physical characterisation of the sample by DMTA revealed a considerable decrease in elastomeric character of **DOUBLE DYNAMIC** after recycling, with a much more linear transition from T_g to viscous flow (Figure 75). A clear decrease in resistance to elevated temperature was also observed, with deterioration of the sample at temperatures above 40 ºC, as well as a marked increase in the storage modulus (100 MPa at 20 ºC) compared to the pristine sample (20 MPa). The cause for the degraded physical performance of **DOUBLE DYNAMIC** after recycling is proposed to be caused by residual trifluoroacetate ions trapping the iminium species, and thus hindering the reformation of imine bonds.

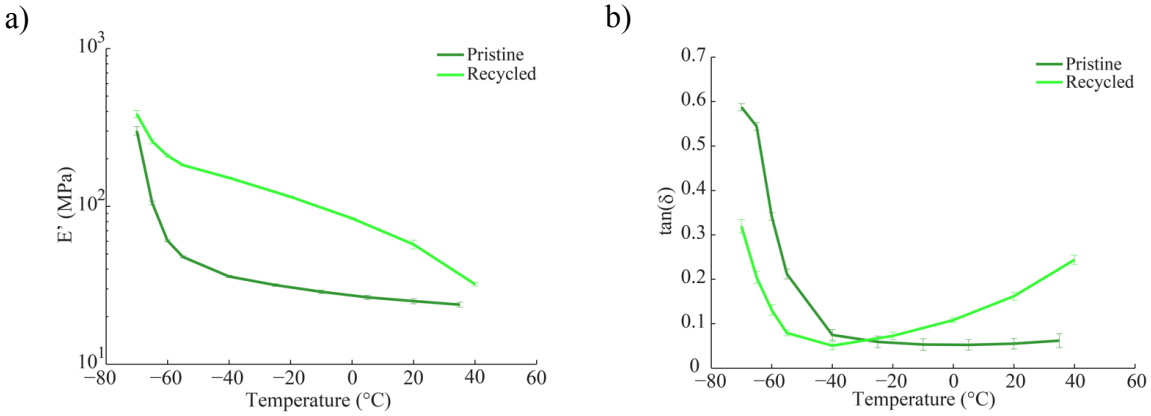

*Figure 75 – a) DMTA plot of storage modulus vs temperature (between -70 and 40 ºC) of pristine and recycled **DOUBLE DYNAMIC**; b) DMTA plot of tan(δ) vs temperature of pristine and recycled **DOUBLE DYNAMIC**, for the same temperature range.*

To overcome this problem, the most recent attempts to optimise the recycling conditions involved the slow neutralisation of the solution by forming a biphasic THF/water mixture containing brine. The aqueous layer was then slowly neutralised with sodium hydrogen carbonate, causing the gradual formation of solids in the organic layer. At neutral pH, the organic phase was observed to have completely gelled, as a result of the re-formation of a cross-linked polyimine network. As the gelation had not occurred within a mould, the material was observed to be very inhomogeneous and therefore physical characterisation could not be performed (Figure 76). Qualitative inspection of the material did however suggest that this material posed physical characteristics more closely matching the pristine material.

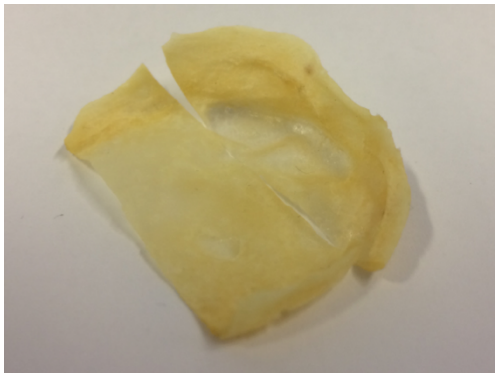

*Figure 76 – Image of **DOUBLE DYAMIC** recycled after neutralisation and evaporation of **DOUBLE DYNAMIC** from a THF solution*

Self-Healing

As with many other materials based on dynamic chemistries, the materials produced from this work were anticipated to display a stimulus responsive self-healing behaviour. Upon cutting, and directly introducing the newly severed ends to each other, with a small amount of pressure, none of the materials displayed any self-healing characteristics at room temperature. At elevated temperatures (110 ºC) with negligible pressure at the contact points, again no self-healing characteristics were observed. In a slightly altered methodology, a small piece of steel (20 g) was heated (110 ºC) and pressed onto a partially severed piece of **DOUBLE DYNAMIC** with a small amount of force (~500 g), analogous to ironing. The steel was then allowed to cool to room temperature (<10 minutes) before being removed, re-heated and re-applied, for 5 cycles. A clear self-repairing of the cut was observed by optical microscopy, in a ‘zip-like’ effect, whereby self-healing proceeded at the edges of the cut toward the middle (Figure 77).

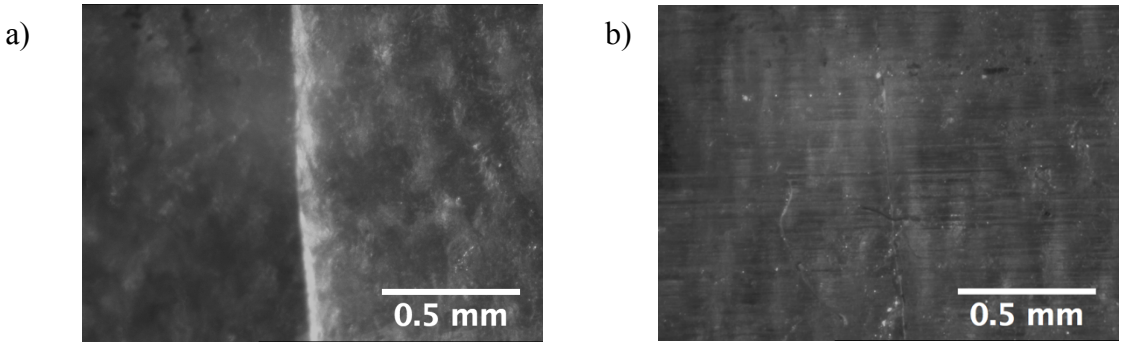

*Figure 77 – Microsope image of **DOUBLE DYNAMIC** a) immediately after being cut through the full thickness, and b) after heat-induced 'self-healing'.*

The self-healing response of the material when exposed to a good solvent (THF) was also investigated by optical microscopy. Due to the typical swelling response of polybutadiene-based materials on exposure to THF, exposure of the partially-cut material was limited to small volumes (one drop) to avoid the deformation of the material's shape. After 5 applications of 1 drop of THF, the material was observed to have partially healed. A 'scar' remained despite a good degree of structural integrity was regained.

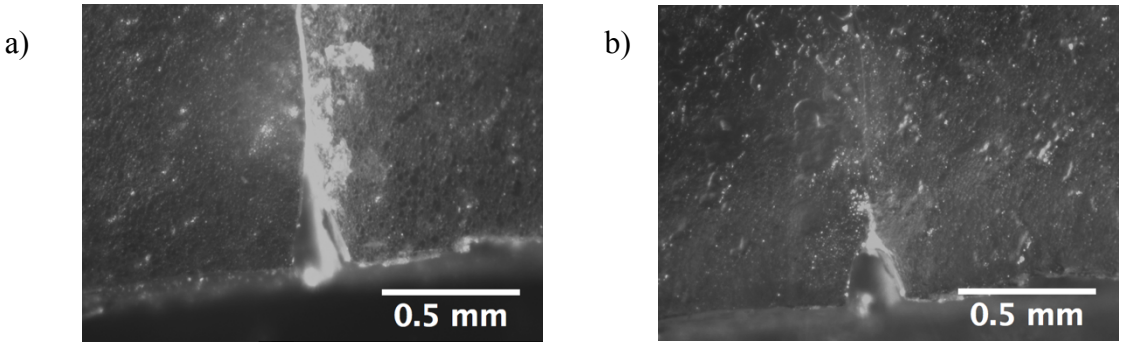

*Figure 78a - Microsope image of **DOUBLE DYNAMIC** a) immediately after being cut through the full thickness and b) after solvent-induced 'self-healing'*

On comparison with both **PBD CTL1 UPy** and **PBD CTL1 IMI**, it was difficult to qualitatively distinguish any difference in their self-healing speed, as all were observed to be recovered (with scarring) after the same 5 cycles of heating. As all materials containing dynamic functionalities did self-heal, compared to **PBD CTL0** which did not, it is clear that both dynamic functionalities are able to, and have an active involvement in, the self-repair of the materials after damage. The ability of the covalently cross-linked **PBD CTL1 UPy** to self-heal is particularly interesting, as the presence of ureidopyrimidinone alone is enough to heal a damaged irreversibly cross-linked network. Quantitative analysis, by elongation until break experiments of repaired samples would be useful to quantify the extent of self-healing.

Thermal stability

Throughout the course of characterising each of the samples, a distinct yellowing of the sample was observed at elevated temperatures. For **DOUBLE DYNAMIC**, this yellowing occurred when exposed to temperatures above 80 ºC for longer than 45 minutes.

*Figure 79 – Two pieces of **DOUBLE DYNAMIC**: above is a pristine sample; below after heating at 130 ºC for 1 hour*

The physical effect that exposure to these conditions had on **DOUBLE DYNAMIC** was drastic. Re-testing of the material, by DMTA, that had been previously tested, and subsequently exposed to temperatures as high as 140 ºC for 1 hour, showed that the physical properties of the material had clearly changed. **DOUBLE DYNAMIC** which had previously been shown to display a more linear transition from T_g to viscous flow, showed a much more distinct rubber plateau at room temperature. In fact, the E' at ambient temperatures was found to decrease (from 40 MPa to 20 MPa) after heating. Complete loss of physical integrity was found when re-heating the pre-heated sample to temperatures above 100 ºC.

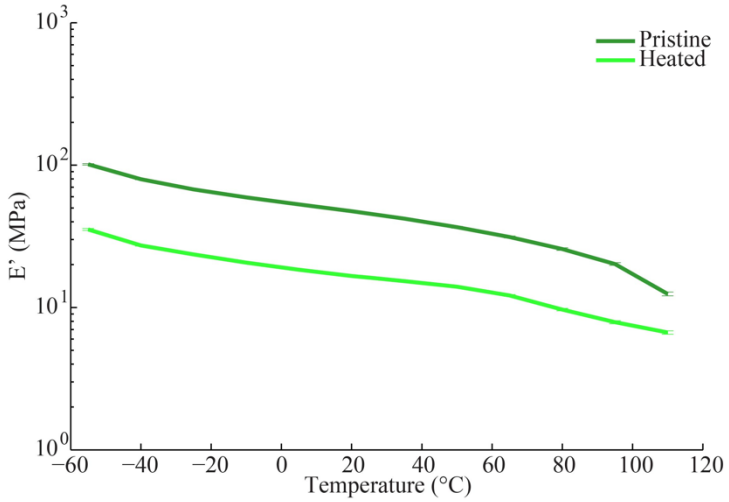

*Figure 80 – DMTA analysis of **DOUBLE DYNAMIC** after heating to 140 ºC. A plot of storage modulus (MPa) vs temperature (ºC) of a pristine samples (light green) and a previously heated sample (dark green)*

DOUBLE DYNAMIC that had previously been exposed to high temperatures was also found to be completely insoluble in conditions that normally solubilise un-heated samples. It was suspected that heating in air could have promoted some degree of oxidation followed by the formation of irreversible cross-links from oxidised species, so a sample was heated in an atmosphere of argon, and its solubility subsequently tested. It was found that heating the sample in an inert atmosphere had no effect, and the material still lost its solubility characteristic.

Adhesion

Adhesion of the sample to PDMS was tested using the JKR model of elastic contact. In this investigation, a PDMS semi-sphere was placed in contact to the surface of the material, with a known force, in a sinusoidal oscillating manner. The adhesive strength of the material was then measured by the force required to remove the PDMS from contact with the material. JKR measurements were taken at three temperatures (25 ºC, 35 ºC and 80 ºC), to investigate the temperature-dependence of adhesion.

No significant adhesion, between PDMS and **DOUBLE DYNAMIC**, was observed across all of the temperatures measured, with a maximum adhesive force of 0.025 N observed at 25 ºC.

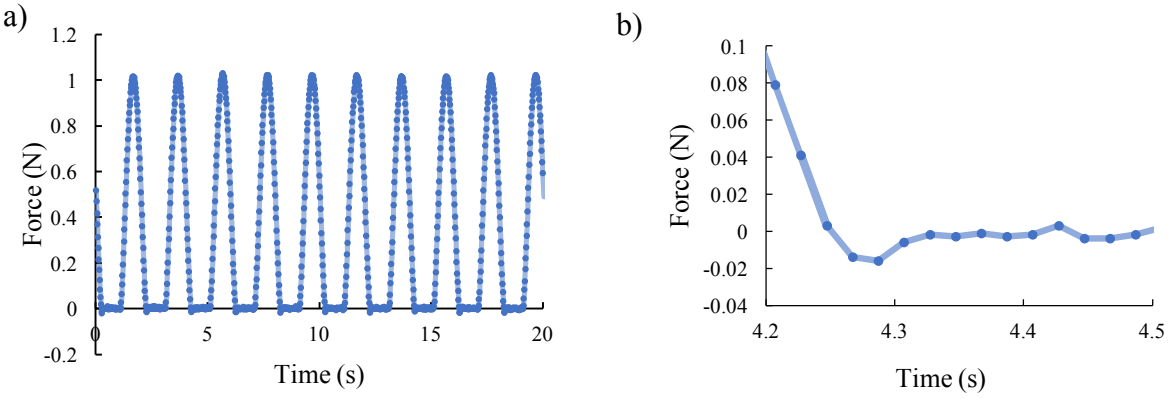

*Figure 81 – a) Plot of force (N) vs time (s) from **DOUBLE DYNAMIC** adhesion testing; b) zoomed to the time of disattachement*

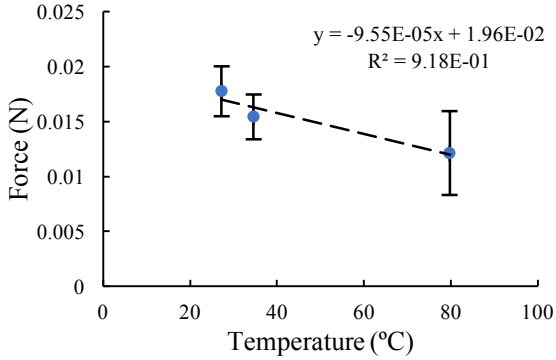

*Figure 82 – Plot of the average adhesive force (N) vs temperature (ºC) of **DOUBLE DYNAMIC***

Following on from the promising self-healing results described above, adhesion between two pieces of **DOUBLE DYNAMIC** was examined next. The extent of self-adhesion when exposed to either of the two stimuli, heat or solvent, was investigated by mounting two pieces of **DOUBLE DYNAMIC** (9.3 mm x 8.5 mm) onto two flat plates with 60 N of compressive force. Upon compressing the samples at 50 ºC for 17 hours an adhesive force of 7 x 10^5 N/m^2 was observed (Figure 83a). With introduction of 2 drops of THF at the interface between the two samples, and compressing them for 5 hours at room temperature, an adhesive force of 2 x 10^5 N/m^2 was observed. Optimisation of the methodology by using a combination of both heat and solvent would likely improve on these already interesting results.

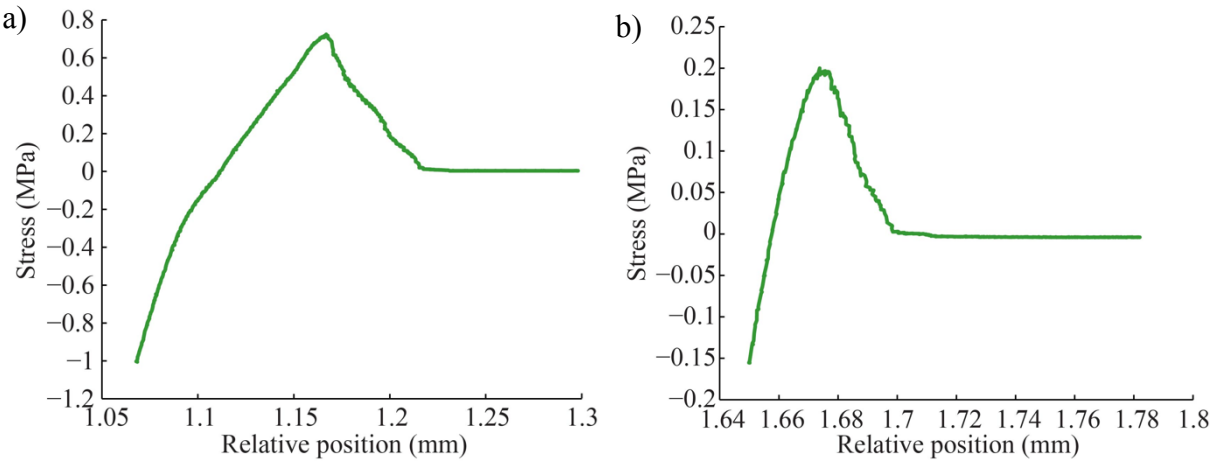

*Figure 83 – a) Plot of stress (MPa) vs relative position (mm) of **DOUBLE DYNAMIC** after 17 hours at 50 ºC; b) Plot of stress (MPa) vs relative position (mm) of **DOUBLE DYNAMIC** after5 hours and introduction of THF*

4.3 Conclusions and Perspectives

The introduction of dynamic chemical functionalities, by co-polymerisation with chain-end functionalised polybutadienes, yielded cross-linked elastomeric materials that behaved differently depending on their chemical composition. Two control samples, that were irreversibly cross-linked by urethane bonds, were investigated and compared to two other materials that were reversibly cross-linked by imine bonds. As well as the chemical difference in the cross-linking chemistry, two materials containing one of the two dynamic chemical functionalities (hydrogen-bonding ureidopyrimidinone and the covalent reversible imine bond) were compared to a material containing both dynamic functionalities.

FTIR analysis of the materials yielded spectra of overlapping peaks, which made distinguishing precise chemical change within the materials, from their starting materials, difficult. Some slight movement in absorbance peaks was observed, which indicate the formation of imine bonds after cross-linking. A qualitative test using ninhydrin gave confirmation of either the presence of excess amine, or the occurrence of chemical exchange between the material and electrophiles.

Physical characterisation of the sample by X-ray scattering revealed clear differences, on the 100 Å scale, between imine cross-linked materials compared to their urethane cross-linked counterparts, likely due to differences in hard-block aggregation. This difference correlated well with differences in global storage modulus of the materials, where both imine cross-linked materials had a notably increased value. At low temperatures, all materials displayed the same T_g. Stress/strain cycling of each of the dynamic materials revealed a significantly more prominent viscoelastic behaviour, compared to urethane cross-linked materials which were more elastic. Elongation until break studies revealed that the material containing two dynamic functionalities were stiffer and stronger materials than both urethane-based materials. The influence of the imine bond at high temperatures was found to be significant, with considerably faster relaxation behaviour in imine cross-linked materials.

Crystallisation experiments of ureidopyrimidinone monomers gels were likely composed of supramolecular stacks of ureidopyrimidinone nanofibres. These nanofibers may also stack among the amorphous polymer backbone, causing the observed physical differences.

The double-dynamic material was found to be soluble in acidified THF, and able to be regenerated, however further optimisation of the conditions is needed. Temperature and solvent responsive self-healing and self-adhesion of the samples was observed by optical microscopy, quantification of the strength of this repair is ongoing.

4.4 References

1. Seymour, R. W. & Cooper, S. L. Thermal Analysis of Polyurethane Block Polymers. *Macromolecules* **6,** 48–53 (1973).
2. Rubner, M. F. Synthesis and characterization of polyurethane-diacetylene segmented copolymers. *Macromolecules* **19,** 2114–2128 (1986).
3. Tingfa, D. & Junfeng, L. Estimation of major volatile products from the first stage of the thermal decomposition of hydroxy-terminated polybutadiene binder. *Thermochim. Acta* **184,** 81–90 (1991).
4. Cao, Z., Zhou, Q., Jie, S. & Li, B. G. High cis-1,4 Hydroxyl-Terminated Polybutadiene-Based Polyurethanes with Extremely Low Glass Transition Temperature and Excellent Mechanical Properties. *Ind. Eng. Chem. Res.* **55,** 1582–1589 (2016).
5. Prisacariu, C. *Polyurethane Elastomers*. (Springer Vienna, 2011). doi:10.1007/978-3-7091-0514-6
6. Blackwell, J. & Ross, M. X-ray studies of the structure of polyurethane hard segments. *J. Polym. Sci. Polym. Lett. Ed.* **17,** 447–451 (1979).
7. Wietor, J. L., Van Beek, D. J. M., Peters, G. W., Mendes, E. & Sijbesma, R. P. Effects of branching and crystallization on rheology of polycaprolactone supramolecular polymers with ureidopyrimidinone end groups. *Macromolecules* **44,** 1211–1219 (2011).
8. Appel, W. P. J., Portale, G., Wisse, E., Dankers, P. Y. W. & Meijer, E. W. Aggregation of ureido-pyrimidinone supramolecular thermoplastic elastomers into nanofibers: A kinetic analysis. *Macromolecules* **44,** 6776–6784 (2011).
9. Nguyen, Q. T., Tinard, V. & Fond, C. The modelling of nonlinear rheological behaviour and Mullins effect in High Damping Rubber. *Int. J. Solids Struct.* **75–76,** 235–246 (2015).
10. Obadia, M. M., Mudraboyina, B. P., Serghei, A., Montarnal, D. & Drockenmuller, E. Reprocessing and Recycling of Highly Cross-Linked Ion-Conducting Networks through Transalkylation Exchanges of C-N Bonds. *J. Am. Chem. Soc.* **137,** 6078–6083 (2015).

Chapter 5: Synthesis and Characterisation of Double-Dynamic Thermoplastic Elastomers

This work was carried out in collaboration with Georges Formon

5.1 Introduction

In order to gain better control over the chemical composition of the materials, it was necessary to use a better-defined polybutadiene backbone. The large polydispersity index, and broad range obtained when quantifying the degree of functionality, of Polyvest® (Chapter 4), resulted in a material with physical parameters that were difficult to define; the large degree of uncertainty, with regards to the stoichiometric ratio needed, was of particular hindrance. This stoichiometric uncertainty results in uncertainty in determining the presence of labile chemical functionalities, with a possible unknown effect on the dynamic chemistry occurring within the materials.

The pre-polymer Krasol® LBH-P 3000, an α,ω-hydroxyl-functionalised polybutadiene, was kindly provided by Cray Valley USA, LLC, and was the backbone from which the better-defined polybutadiene-based elastomeric materials were synthesised in this chapter.

The precise bi-functionality, at the chain-ends, of this pre-polymer meant that the resulting materials differed greatly from the materials discussed in the previous two chapters. The role of the monomer, with which the polybutadiene was co-polymerised, is exclusively reacted in a chain-extension fashion. All materials in this chapter were therefore investigated through the lens of thermoplastic elastomers, with particularly close analogy to thermoplastic polyurethanes (TPUs).

This chapter follows the structure set in the previous two chapters. Characterisation of the polymer backbone was first completed, before synthesis of the materials containing both dynamic chemical moieties. The physical and chemical properties of the materials were then tested through a range of temperatures and applied stresses, followed by analysis of the recyclable and dynamic properties that set these materials apart from classical materials currently on the market.

5.2 Results and Discussion

5.2.1 Characterisation of Polybutadiene Pre-Polymer

Microstructural Composition

Using the same analytical methods as detailed in Chapter 3, the microstructural composition of Krasol® was determined by using ^{1}H NMR spectroscopy, with the respective ratios of each of the isomers calculated using the proton resonances at ~5 ppm. One key difference between the ^{1}H NMR spectrum of Krasol® compared to Polyvest® was the overlap between resonances attributed to 1,2 and *cis*/*trans*-1,4 isomers (δ 5.54 and δ 5.35 in Figure 84). This did not pose a problem, however, as the number of protons that cause these resonances has been well attributed in the literature.[1]

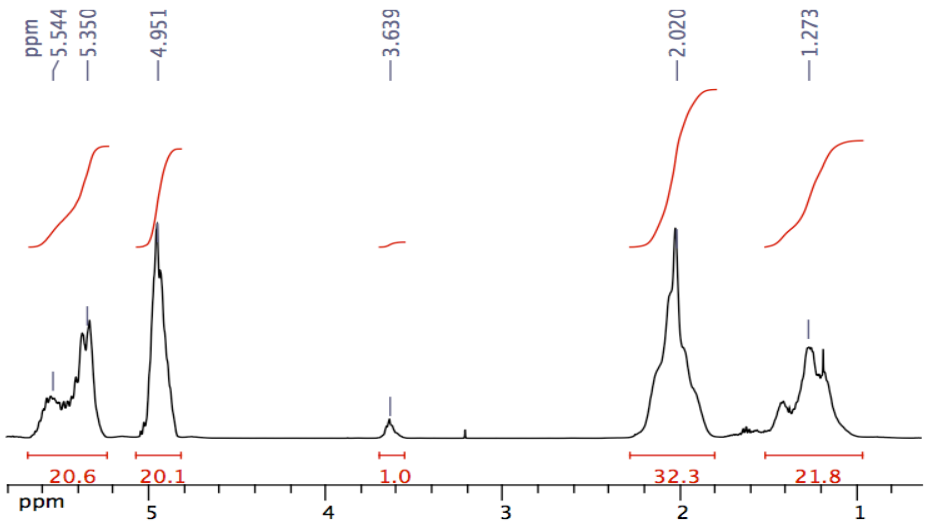

Figure 84 – Partial ^{1}H NMR spectrum of Krasol®

From the ^{1}H NMR analysis, Krasol® was found to possess a markedly different microstructure to Polyvest®, which was in close agreement with the published data sheet for the sample. The content of the *cis*/*trans*-1,4 isomer along the polybutadiene backbone was found to be considerably lower, and, as this isomer is responsible for the elastomeric properties of polybutadiene, the materials produced from using this backbone were anticipated to be somewhat less elastomeric. The tabulated findings from this analysis with comparisons to the data sheet and Polyvest® are presented in Table 11.

Krasol® Polybutadiene			Polyvest® Polybutadiene
Microstructure	Data Sheet Values (%)	Experimental Values (%)	Experimental Values (%)
cis-1,4	12.5	33 - 36	81
trans-1,4	22.5		
1,2	65	64 - 67	19

Table 11 – Table of data of the microstructural composition of Krasol® as published by Cray Valley, and determined by ^{1}H NMR spectroscopy

Polydispersity Index

The polydispersity index of Krasol® was determined by SEC and LS with samples prepared in THF solution.

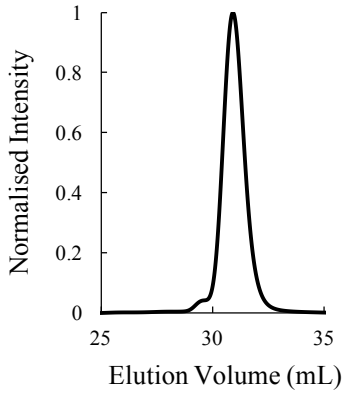

Figure 85 – SEC chromatogram of Krasol® using a THF mobile phase

The polydispersity obtained by SEC, using a reference of polystyrene, was found to be 1.11, notably lower than the value given by the manufacturer of 1.35. When analysing the sample by LS, an even more monodisperse value of 1.05 was found. Comparing these values to the polydispersity index of 2.03 found from Polyvest®, Krasol® was found to be a better defined polymer with regards to the range of molecular weights present within the sample.

Molecular Weight

Light scattering was again used to determine the molecular weight of Krasol®, with online detection after SEC of the sample, in a solution of THF.

The molecular weights obtained from two different samples were found to be consistent; the detected value is tabulated in Table 12 below, and compared to the data published by the manufacturer. The low polydispersity index of the Krasol® is likely the cause for these consistent molecular weight values, unlike Polyvest®.

	Krasol® Polybutadiene		Polyvest®
	Data Sheet	Experimental Values	Experimental
Mn (Da)	3200	2487 - 2912	3150 - 6000
Mw (Da)	-	2653 - 3024	5500 - 8500
PDI	1.35	1.04 - 1.11	2.04

Table 12 – Tabulated data of the molecular weight of Krasol® as published by Cray Valley and as deterined by SEC and light scattering

As the molecular weight is over 1000 Da lower than Polyvest® a relatively greater concentration of dynamic chemical moieties will be present in all resultant materials, as well as a greater hard-block to soft-block ratio.

Chemical Functionalisation

The degree of functionality of Krasol® was determined using three methods. First, the sample was analysed by ^{1}H NMR, and the appropriate resonances were compared, in order to calculate the degree of functionality. The polybutadiene was then functionalised with the UV-active naphthylene chemical function to enable analysis by UV spectrophotometry. Finally, this naphthylene-functionalised polybutadiene was analysed by ^{1}H NMR.

Analysis by ^{1}H NMR of the stock polymer was conducted by integration of the broad resonance at δ 3.65, attributed to the two protons on the carbon adjacent to the alcohol-functionalised carbon. This integral was set to 1, and the ratio of the integrals of the resonances attributed to the protons in the 1,2 and *cis*/*trans*-1,4 environments were obtained. Using the formula detailed in Chapter 3, a degree of functionality from 1.55–1.98 was obtained, depending on the M_n value used.[2]

Functionalisation of Krasol® was achieved by reaction of the α,ω-hydroxyl-functionalised polybutadiene with 1-naphthyl isocyanate, using the same procedure as detailed in Chapter 3. The polymer, of a similar physical nature to the starting material, was then analysed by UV-Vis in a cyclohexane solution with the following concentrations: 0.032 g/L, 0.064 g/L and 0.16 g/L. The spectra that resulted showed a similar broad peak at 291 nm, due to the presence of the naphthyl functionality, and the relationship between concentration and intensity of absorption was followed (Figure 86a); this dependency was found to satisfy the Beer-Lambert Law (Figure 86b). Using the formula detailed in Chapter 3, the degree of functionality was calculated to be between 1.42–1.82.

Finally, the ^{1}H NMR spectrum was recorded on the naphthyl-functionalised polybutadienes, using the resonances attributed to the naphthylene functionality as a reference. The degree of functionality was found, in this case between 1.34 and 1.73.

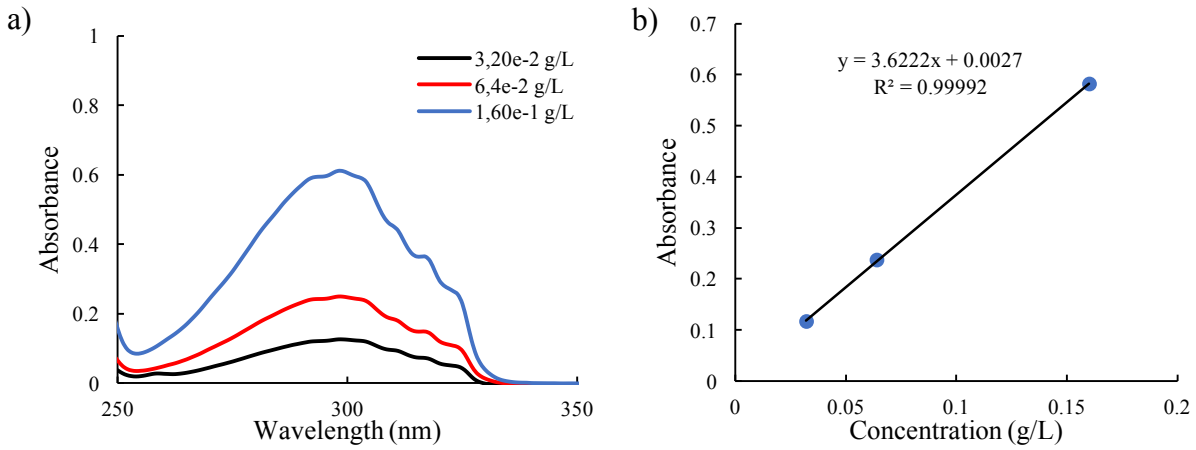

Figure 86 – a) UV-Vis spectra of Krasol® at three different concentrations, between 250 and 350 nm wavelength; b) Beer-Lambert plot of the absorbance at 291 nm of Krasol®

Summary of Pre-Polymer Characterisation

In conclusion, Krasol® was found to be a better define, bifunctional polybutadiene containing a lower proportion of the elastomeric *cis*/*trans*-1,4 isomer within its backbone, when compared to Polyvest®, used in all results obtained until this chapter. With a notably lower molecular weight, the hard to soft-block ratio will be greater. Compounding this information with the lower proportion of elastomeric microstructure within Krasol®'s composition, materials produced using Krasol® are expected to display stiffer, less elastomeric behaviours than their Polyvest®-based alternatives.

A summary of all of the physical parameters, along with those found for Polyvest® are tabulated; the physical parameters that were used when calculating molar ratios for the synthesis of materials in this chapter, is given in the right-most column.

5.2.2 Synthesis of Thermoplastic Elastomers

The synthetic procedures used to produce the synthons **Molecules 5, 6 and 7** with which Krasol® and amine-modified Krasol® were co-polymerised, are detailed in Chapter 3. The post-polymerisation modification of Krasol®, for the preparation of amine-functionalised polybutadiene, with which all aldehyde-functionalised synthons were co-polymerised, followed the same methodology used to produce modified Polyvest®, also detailed in Chapter 3.

*Synthesis of No Dynamic Control (**PBD TP CTL0**)*

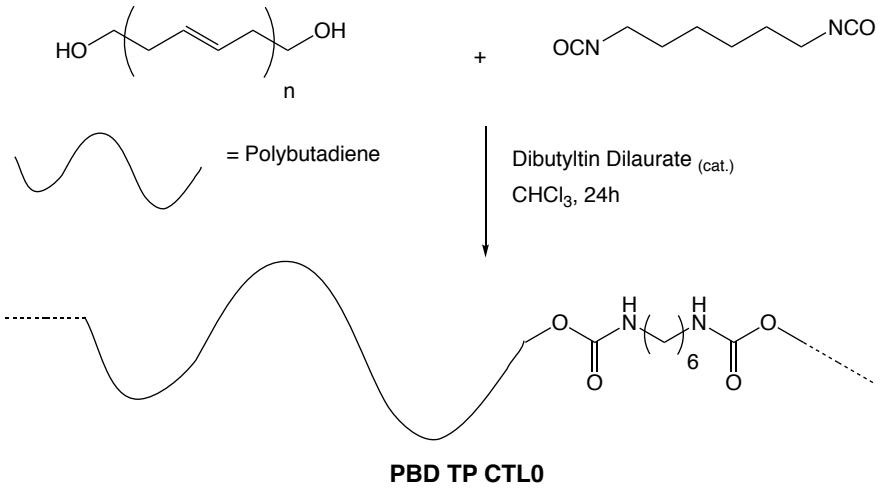

*Scheme 44 – Synthesis of **PBD TP CTL0** from Krasol® and HDI*

Taking influence from the synthetic procedure developed for **PBD CTL0**, the synthesis of **PBD TP CTL0** was first attempted by mixing of solutions of HDI and Krasol® in a 1/1 stoichiometric ratio, in chloroform, before addition of dibutyltin dilaurate, and pipetting the resultant solution into a mould for polycondensation (Scheme 44). The resultant materials possessed significantly poorer structural integrity, with a tacky surface that crumbled at the touch. A series of new stoichiometries (with an increased proportion of isocyanate) were tested, with NCO/OH ratios of 1.1/1, 1.2/1, 1.35/1 and 1.65/1. In all cases, the materials were again found to possess poor elasticity, a weak structural integrity and tackiness on the surface.

To optimise the conditions for the chain-extension, the solution of HDI was introduced into the solution of Krasol® and dibutyltin dilaurate (NCO/OH 1.1/1), as before, but instead this solution was allowed to react with stirring in the round-bottom flask, under argon, at room temperature overnight. The colourless solution was then pipetted into the mould and allowed

to slowly evaporate in an atmosphere of chloroform, before post-curing at 50 ºC under vacuum for 5 hours. The resulting material was a strong, elastic sample, with no tackiness on the surface.

*Synthesis of Control UPy (**PBD TP CTL1 UPy**)*

Following on from the successful synthesis of **PBD TP CTL0**, this same methodology was extended to the synthesis of **PBD TP CTL1 UPy**, using a 1.1/1 NCO/OH ratio reacted in the round-bottom flask at room temperature, under argon, overnight (Scheme 45). Unlike **PBD TP CTL0**, however, this method resulted in a swollen polymer network, which could not be transferred into a mould for re-shaping. This difference can only be attributed to the hydrogen-bonding association of the ureidopyrimidinone producing a polymeric network.

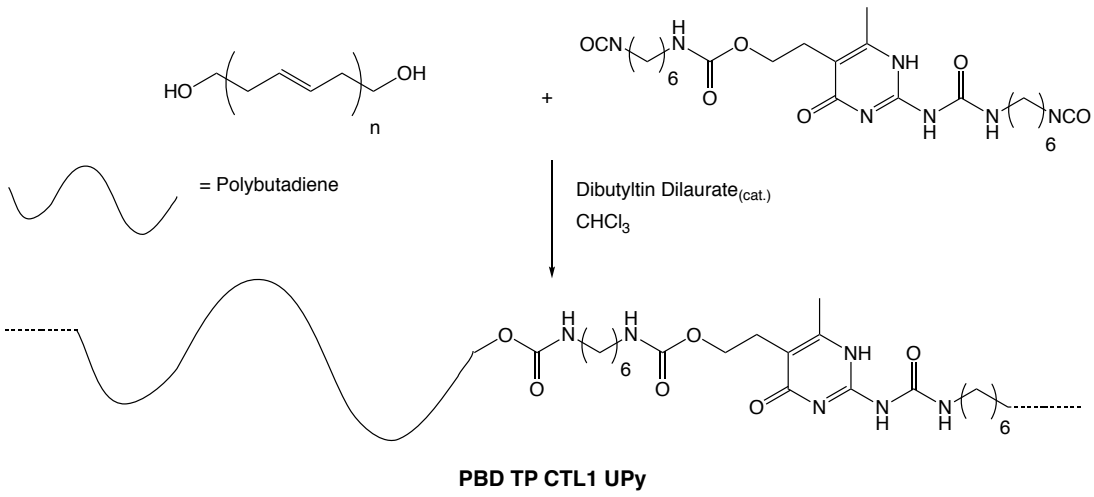

*Scheme 45 – Synthesis of **PBD TP CTL1 UPy** from Krasol® and **5***

Reverting to the methodology used to produce the thermoset materials in Chapter 3, the solutions of **Molecule 5**, Krasol® and dibutyltin dilaurate, were mixed before immediate transfer to the Teflon® moulds, where polycondensation and slow evaporation could proceed in a controlled shape. After post-curing at 50 ºC under vacuum for 5 hours, the produced materials were found to be solid elastic materials that were dry to touch with a slightly yellow colour.

*Synthesis of Control Imine (**PBD TP CTL1 IMI**)*

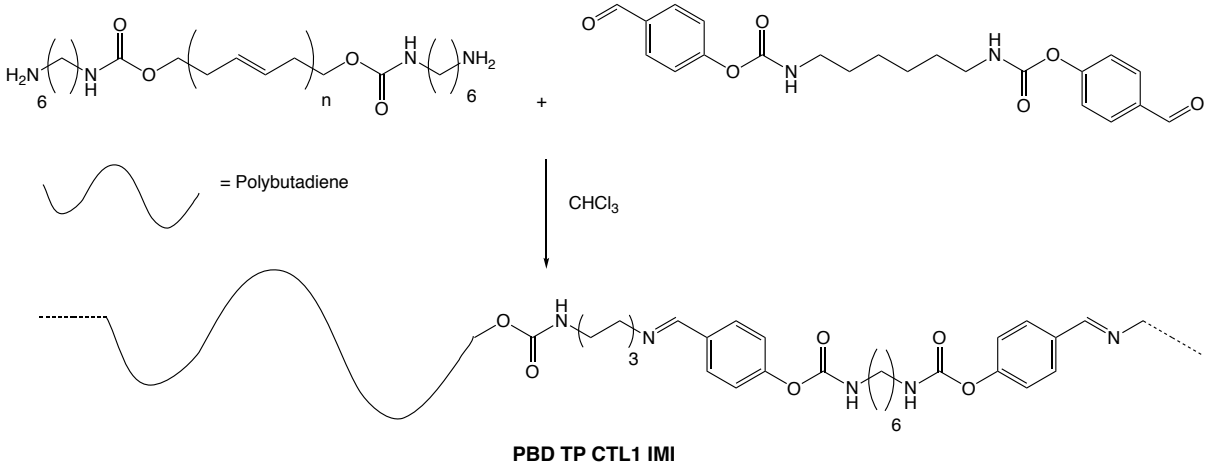

*Scheme 46 – Synthesis of **PBD TP CTL1 IMI** from amine-modified Krasol® and 7*

Using the same method used to produce **PBD TP CTL0**, a mixture of **Molecule 7** and amine-functionalised Krasol®, in chloroform in a 1.1/1 CHO/NH_2 ratio, were stirred overnight before transfer and evaporation in a Teflon® mould, in an atmosphere of chloroform, and the resulting material was post-cured at 50 ºC under vacuum for 5 hours. As with **PBD CTL1 IMI**, no catalyst was needed to produce materials displaying a good degree of structural robustness that were dry to the touch.

*Synthesis of Double Dynamic (**DOUBLE DYNAMIC TP**)*

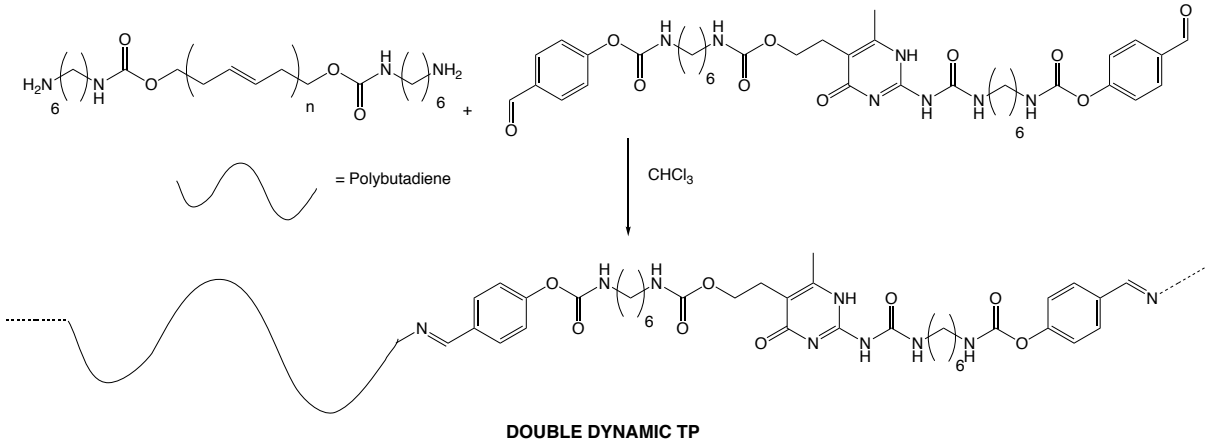

*Scheme 47 – Synthesis of **DOUBLE DYNAMIC TP** from amine-modified Krasol® and **6***

The same methodology used to produce **DOUBLE DYNAMIC** was used for the synthesis of **DOUBLE DYNAMIC TP**, whereby solutions of **Molecule 6** and amine-functionalised Krasol® in chloroform were mixed, without addition of catalyst, before transfer to a Teflon® mould in which curing and evaporation was allowed to proceed. Post-curing at 50 ºC under vacuum for 5 hours yielded structurally robust, dry and homogeneous materials.

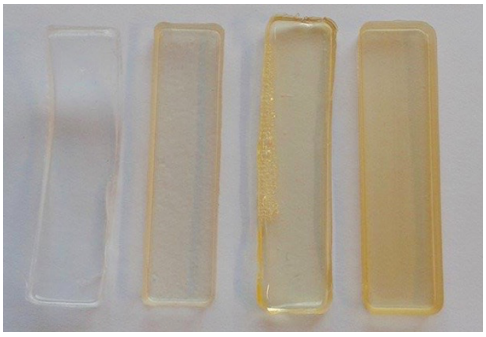

Figure 87 – Image of the four materials synthesised – left-to-right: ***PBD TP CTL0, PBD TP CTL1 UPy, PBD TP CTL1 IMI, DOUBLE DYNAMIC TP***

5.2.3 Chemical Characterisation

Infrared Analysis

In order to follow the chemical change occurring after the chain-extension reaction of each material, FTIR spectrophotometry with the ATR accessory was conducted on both the starting materials and solid products.

A comparison of the FTIR spectra of un-modified and amine-functionalised Krasol® is shown in Figure 88. As observed from the analysis of Polyvest®, no prominent peaks attributable to the presence of alcohol or amine were found. This absence means that it was unfortunately not possible to follow the formation of imines by the expected decrease in the presence of aldehydes within the system. One prominent difference between the two spectra was the occurrence of a peak at 1726 cm^{-1} after modification with amine, resulting from the C=O stretch of the urethane carbonyl moiety.

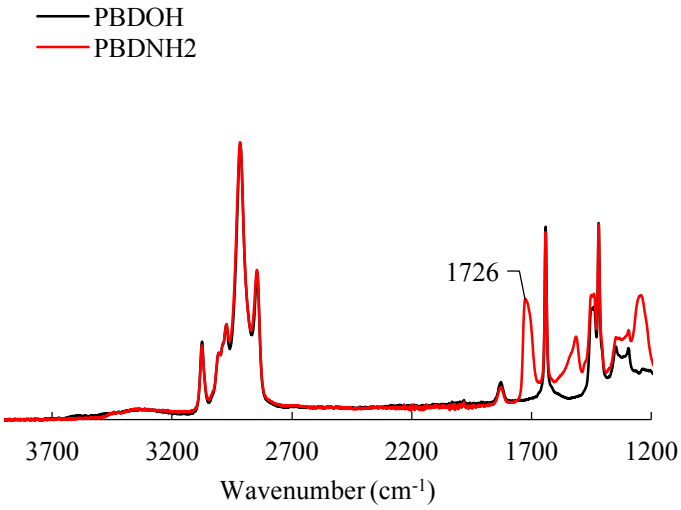

Figure 88 – FTIR spectra of Krasol® and amine-modified Krasol®

Instead, following the formation of imines was attempted by observing any change in the presence of the aldehyde. Disappointingly, as observed with the materials based on Polyvest®, a large number of peaks overlap between the wavenumbers of 1775 cm^{-1} – 1600 cm^{-1} (Figure 89a and b), causing difficulties in deciphering the exact change in chemical functionality from the starting materials.

An absorbance peak was observed in both **Molecules 6** and **7**, at ~1700 cm^{-1}, attributed to the C=O stretch of the aldehyde. When co-polymerised with amine-functionalised polybutadiene, this peak was observed to decrease in intensity, compared to all surrounding absorbance peaks; this is good evidence of the consumption of aldehyde on imine formation. Again, due to the overlapping absorbance peaks around wavenumbers that imine were expected to absorb (1700 – 1650 cm^{-1}), it was not possible to find any specific evidence of imine formation by FTIR.

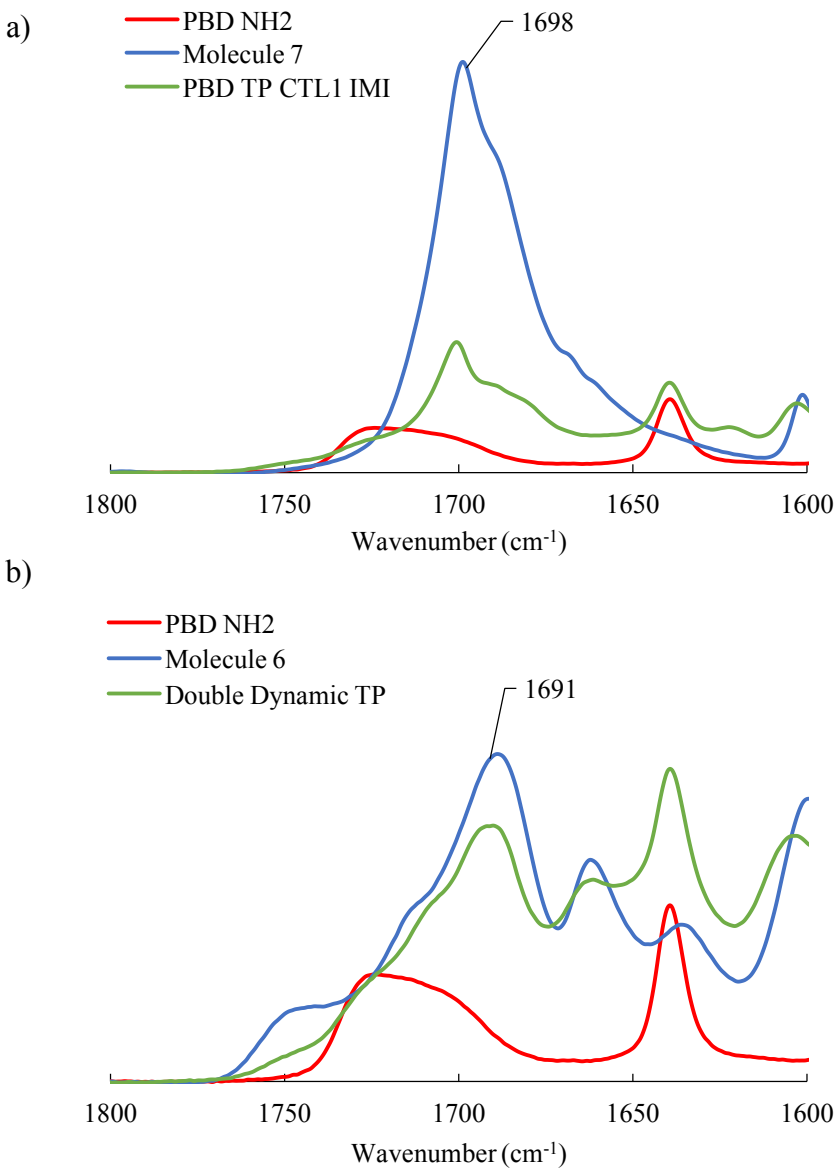

*Figure 89 – Partial FTIR spectra of a) amine-modified Krasol® (red), **7** (blue) and **PBD TP CTL1 IMI** (green) between wavenumbers 1800 and 1600 cm^{-1}; b) amine-modified Krasol® (red), **6** (blue), **DOUBLE DYNAMIC TP** (green) between 1800 and 1600 cm^{-1}*

5.2.4 Physical Characterisation

Differential Scanning Calorimetry

The effect of temperature on the heat capacitance of each material was analysed by DSC, between a temperature range between -100 and 250 ºC in a nitrogen atmosphere (Figure 90).

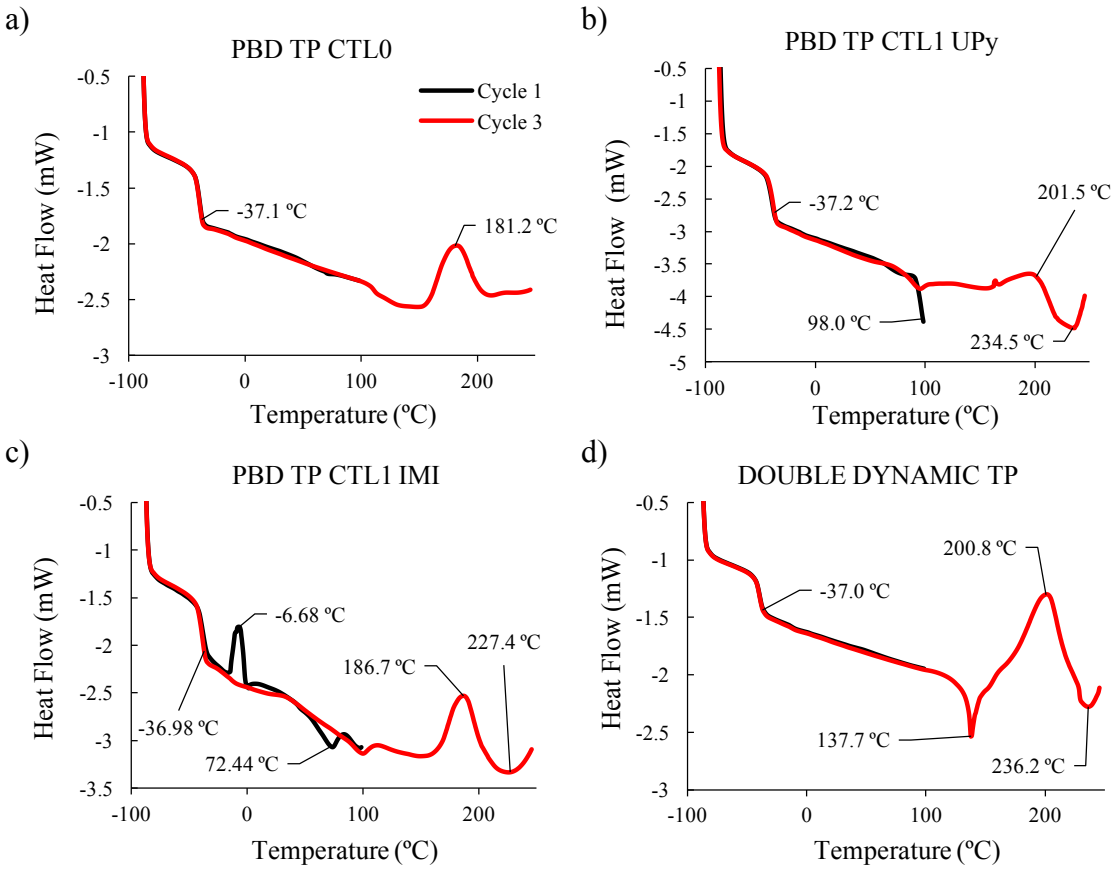

*Figure 90 – Differential Scanning Calorimetry spectra of a) **PBD TP CTL0**, b) **PBD TP CTL1 UPy**, c) **PBD TP CTL1 IMI**, d) **DOUBLE DYNAMIC TP**, for temperatures between -100 and 250 ºC. Three cycles, cycle two not depicted.*

A large exothermic event at ~–37 ºC was observed in each material, indicating the glass transition temperature (T_g). The fact that this observation was made in both thermoset and thermoplastic materials, confirms that the main factor influencing the T_g, of either material, is the nature of the soft block. In the case of materials based on Krasol®, a T_g of almost 40 ºC higher than materials based on Polyvest® observed. It is likely that the higher temperature observed is due to the higher content of the 1,2 microstructure present in Krasol®.

Observations between -20 ºC and 140 ºC show some differences between each of the materials containing dynamic groups (**PBD TP CTL1 UPy**, **PBD TP CTL1 IMI** and

DOUBLE DYNAMIC TP). **PBD TP CTL1 UPy** shows an endothermic event at 98 ºC which is erased upon subsequent cycling; **PBD TP CTL1 IMI** shows a similar endothermic event but at 25 ºC lower in temperature, this peak is also observed with an exothermic event at ~–7 ºC. Both of these events could be attributed to the loss of residual water trapped within the material, either as a result of incomplete curing, or from absorption of atmospheric water. This explanation fits well with **PBD TP CTL1 IMI** as the exothermic event at lower temperatures may be attributed to the melting point of water, and the higher temperatures its boiling. Another possible explanation for the event observed in **PBD TP CTL1 UPy** at 98 ºC, which could also explain the exothermic event observed at 137 ºC when analysing **DOUBLE DYNAMIC TP**, could be the dissociation of soft segment hydrogen bonding, as introduced in Chapter 4.

The endothermic events observed at ~230 ºC in all materials containing dynamic moieties, also observed in the ureidopyrimidinone-containing materials in Chapter 4, may result from the breakage of hard-block inter-urethane, or UPy-UPy hydrogen-bonding, aggregates.

Thermogravimetric Analysis (TGA)

The effect of temperature on the mass of each material was analysed by TGA for a temperature range between 100 – 600 ºC in a nitrogen atmosphere, and is displayed as the derivative of the weight in Figure 91.

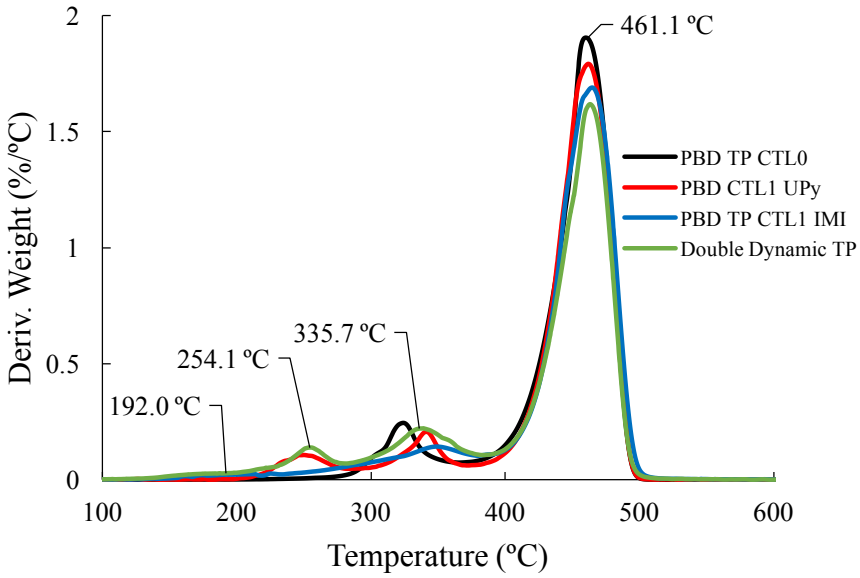

Figure 91 – Thermograviametric spectra of each thermoset material between the temperature range 100 – 600 ºC

Similarly to observations made when analysing the thermoset materials by TGA, **PBD TP CTL0** is observed to lose mass in three distinct phases, corresponding to: degradation of urea/urethane groups at ~330 ºC, followed by the degradation of the polybutadiene backbone in two phases from 350 ºC – 500 ºC.

Co-polymerisation with the ureidopyrimidinone, in **PBD TP CTL1 UPy** and **DOUBLE DYNAMIC TP** results in an additional mass loss peak at 254 ºC, similarly to observations made with **PBD CTL1 UPy**.

Chain-extension with imine-containing monomers had an almost negligible effect on the materials, with the peak observed at ~190 ºC in thermosets (Chapter 4) almost undetected. This interesting difference may be attributed to absence of imine cross-links, and that imine bonds in the main-chain of the polymer backbone are less susceptible to degradation by heat than imines at cross-linking points.

DOUBLE DYNAMIC TP was again observed to have the additive behaviour of each of the control materials, with all mass loss peaks present at very similar temperatures. The precise chemical cause for each of these mass loss events may be characterised by extension of this experiment with online gas chromatography. It is likely, due to the relative sizes of the mass loss peaks, however, that all peaks below temperatures of 390 ºC are a consequence of some chemical change in the hard blocks of the materials. The mass loss peaks and their corresponding hard and soft block contents are given in Table 13.

	Hard Block Weight %	1st Phase Mass Loss %	Soft Block Weight %	2nd/3rd/4th Phase Mass Loss %
PBD TP CTL0	5.5	10.5	94.5	89
PBD TP CTL1 UPy	15	5	85	8.5 / 86
PBD TP CTL1 IMI	12.5	13.5	87.5	85.5
Double Dynamic TP	14	8	86	15 / 75.5

*Table 13 – Tabulated data of hard/soft block mass fraction vs mass loss observed by TGA for **PBD TP CTL0**, **PBD TP CTL1 UPy**, **PBD TP CTL1 IMI**, and **DOUBLE DYMAMIC TP***

X-Ray Scattering

To probe how hard and soft blocks are aggregated within the thermoplastic materials, and to investigate the presence of micro-phase separation, if any was present at all, wide and small-angle X-ray scattering (WAXS and SAXS) was conducted (Figure 92a and b). All analysis was performed at room temperature on solid samples with varying thicknesses; **PBD TP CTL1 IMI** is still, as yet, uncharacterised.

WAXS analysis of all samples gave observations very similar to those of the materials based on Polyvest®. A single reflection corresponding to objects with a 1.378 $Å^{-1}$ size (4.56 Å) indicative of the presence of hydrogen-bonding accounting for hydrogen bonding present in urethane hard block aggregation and also the ureidopyrimidinone self-complementary pairs.

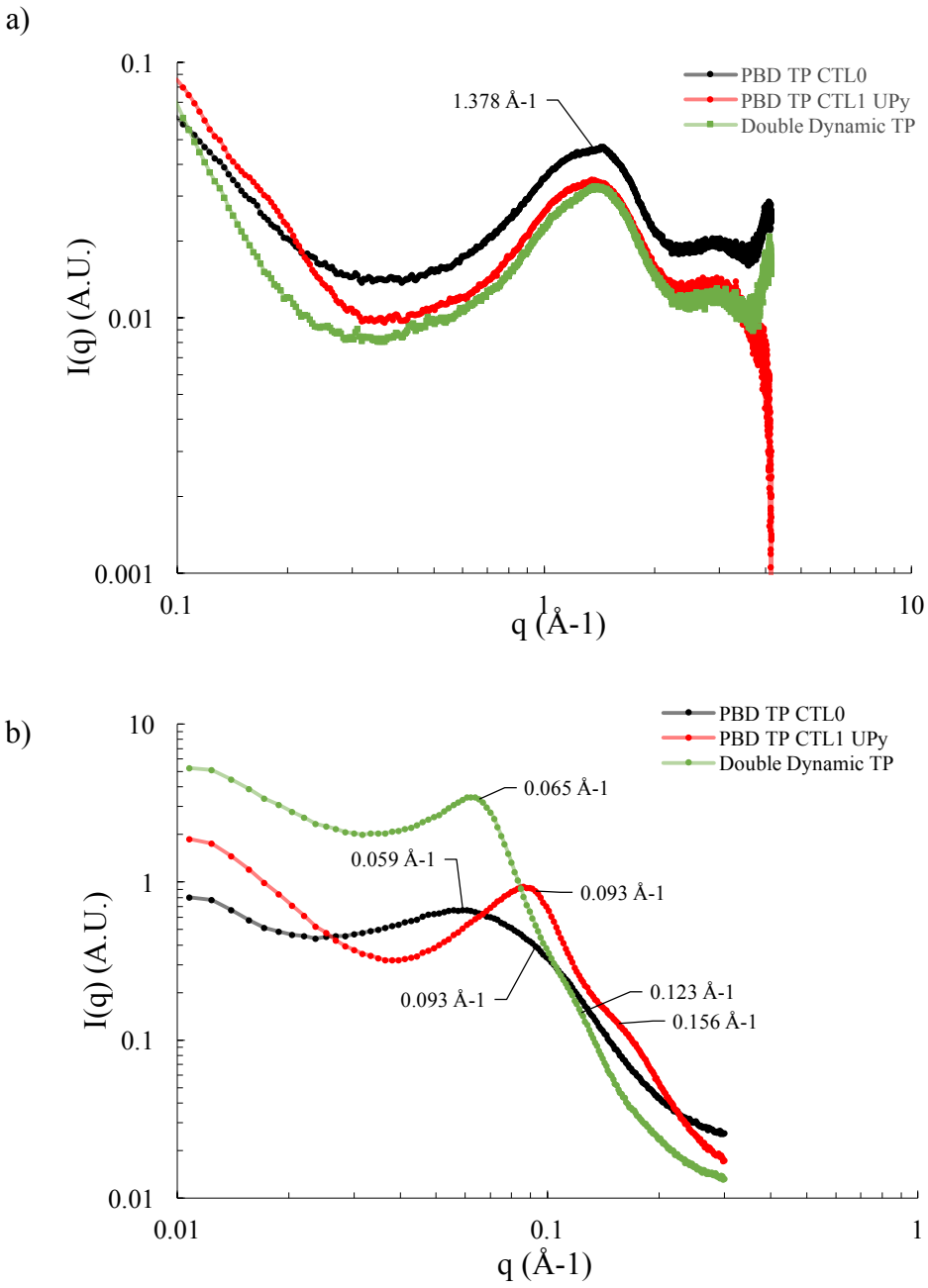

Figure 92 – a) Wide Angle X-Ray Scattering(WAXS) spectra of each thermoplastic material; b) Small Angle X-Ray Scattering (SAXS) spectra of each thermoplastic material

Measurement of larger objects, using SAXS, gave surprisingly different results to those obtained from the analysis of samples in Chapter 4. **PBD TP CTL1 UPy** appeared to be composed of a considerably different range of larger objects compared to **PBD TP CTL0**,

contrary to what was found in Chapter 4. These new reflections at 0.156 $Å^{-1}$ (40.27 Å) correspond closely to the previously published literature detailed in Chapter 4, whereby planar stacking of ureidopyrimidinones have been observed to form nanofibers of this size.[3] Reflections of this size are also weakly observed as a broad shoulder in **PBD TP CTL1 UPy**. The reflections of larger objects in both **PBD TP CTL0** and **DOUBLE DYNAMIC TP**, at 0.059 $Å^{-1}$ and 0.065 $Å^{-1}$ (~100 Å), may be attributed to the more typical hard block sizes from polyurethanes synthesised from HDI hard blocks.[4]

In light of these conflicting results between Polyvest® and Krasol®-based materials, two future studies are proposed: repetition of all materials described so far, as well as both SAXS and WAXS analysis of **PBD TP CTL1 IMI**, followed by variable-temperature X-ray scattering to follow the evolution of these micro-scale objects with temperature. Neutron scattering would probably not be useful, as analysis of objects on this scale can be disrupted by the presence of micro-bubbles and micro-defects within the bulk material.

	WAXS		SAXS			
	q Value (Å-1)	*D-Spacing (Å)*	*q Value (Å-1)*	*D-Spacing (Å)*	*q Value (Å-1)*	*D-Spacing (Å)*
PBD TP CTL0	1.378	4.56	0.093	67.56	0.059	106.49
PBD TP CTL1 UPy	1.378	4.56	0.156	40.28	0.093	67.56
Double Dynamic TP	1.378	4.56	0.123	51.08	0.065	96.66

Table 14 – X-Ray reflections observed by both WAXS and SAXS and the respective d-spacings

Dynamic Mechanical (Thermal) Analysis (DMTA)

The physical behaviour of the materials was first tested by DMTA, with the application of low stresses and observation of their subsequent physical response. The same testing parameters were used as described in Chapter 4, with a sinusoidal force between 0.4 and 0.8% strain, for a temperature range between –50 ºC and 150 ºC, and for a frequency range between 0.1 Hz and 15 Hz. **PBD TP CTL1 IMI** is still, as yet, uncharacterised.

From the plot of storage modulus (E') vs temperature at 1 Hz, displayed in Figure 93, the same T_g across all materials can be observed at ~–40 ºC. This observation is in line with the results obtained from DSC, as well as the conclusion that the T_g is governed by the composition of the soft block, and substitution of the hard block and chain-extension/cross-linking chemistries has no effect.

The global storage modulus is different in each material. A distinctly decreased storage modulus is observed in **PBD TP CTL1 UPy**, when compared to **PBD TP CTL0**. This is most likely explained by the different synthetic methodologies used to make the materials: chain-

extension in solution versus chain-extension in the mould. It is likely that allowing chain-extension to proceed by simple diffusion (and not aided by stirring) decreases the efficiency of the reaction yielding a lower M_w material, and therefore a lower E'. The increased E' of **DOUBLE DYNAMIC TP** would likely be increased further still by using reaction conditions that would allow for a more efficient chain-extension reaction.

At higher temperatures, **PBD TP CTL0** was observed to maintain better structural rigidity at higher temperatures than both **PBD TP CTL1 UPy** and **DOUBLE DYNAMIC TP**, with the rubbery plateau extending beyond 110 ºC. This is also reflected in a consistently low tangent delta to over 100 ºC (Figure 93). The dynamic exchange between ureidopyrimidinone cross-links, and imine bonds within the polymer backbone, are likely activated at these elevated temperatures, causing their decreased thermal durability.

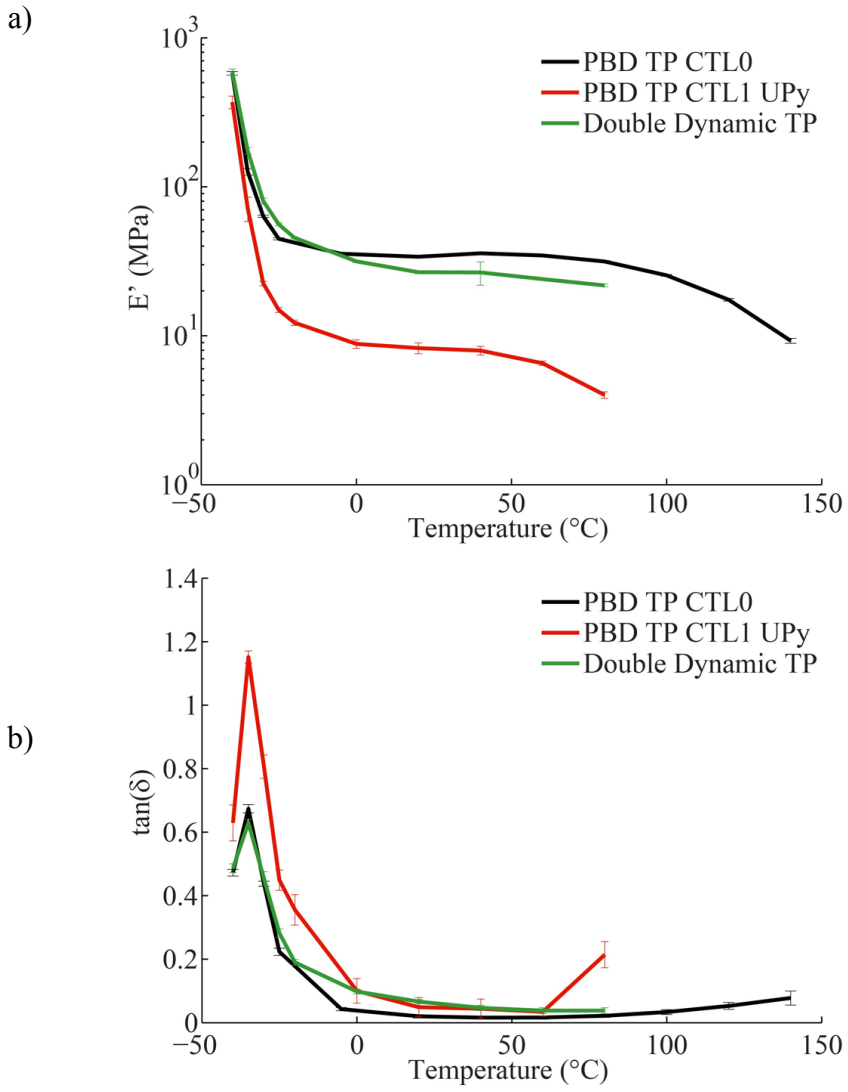

Figure 93 – Evolution of the storage modulus vs temperature, obtained by dynamic mechanical analysis, for each thermoplastic material between a frequancy of 1Hz –70 and 150 ºC; b) Evolution of tan(δ) vs temperature, obtained by DMTA, for each thermoplastic material at a frequency of 1 Hz between –70 and 150 ºC

Stress/Strain Cycles

The stress response, when being consecutively cycled to 20% strain ten times, with a frequency of 1 Hz, was measured for each material at room temperature (Figure 94).

Two main observations were made from this analysis: both linear thermoplastics **PBD TP CTL0** and **PBD TP CTL1 IMI** displayed classical viscoelastic behaviour – the introduction of the ureidopyrimidinone moiety within the co-polymer markedly increased the elastic behaviour of the materials; and, materials containing ureidopyrimidinone moieties reached a lower maximum stress at 20% strain.

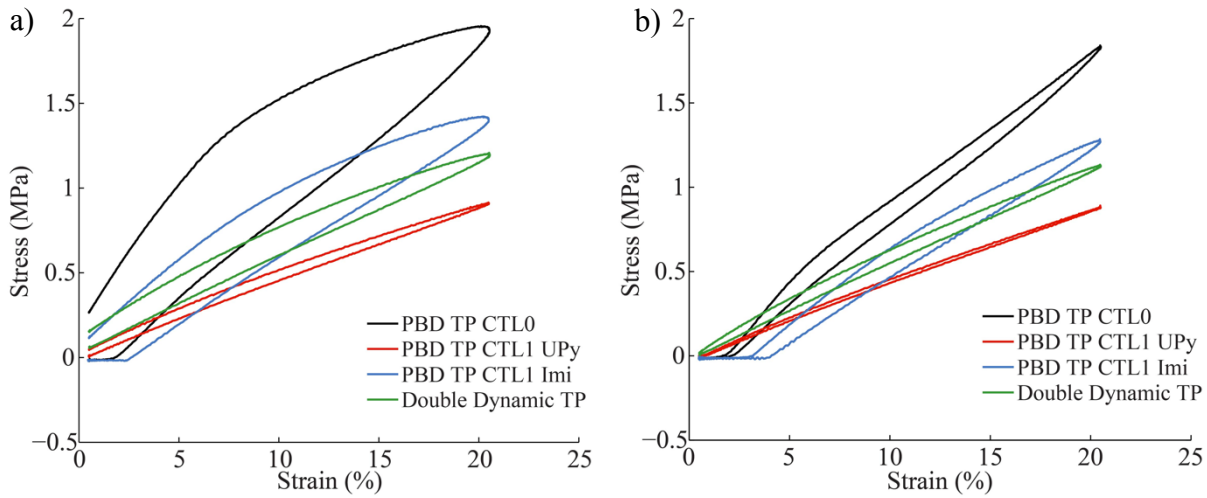

Figure 94 – Stress/strain curves of each thermoplastic material at a frequency of 100 mHz, a) first and b) tenth cycles.

Both materials made from the linear chain-extension of polybutadiene, without the presence of ureidopyrimidinone (i.e. **PBD TP CTL0** and **PBD TP CTL1 IMI**) displayed typical viscoelastic behaviour, with a large hysteresis on the first cycling, which decreased with each subsequent cycle. The presence of the ureidopyrimidinone moiety caused a large change in behaviour, with a considerably decreased hysteresis and a purer elastic behaviour. It is likely that the presence of the strong self-complementary dimerisation between ureidopyrimidinone moieties causes some degree of cross-linking and hence a more thermoset elastomeric behaviour. The difference in sample preparation, i.e. chain extension with stirring vs chain-extension in the mould with simultaneous evaporation, could also be the cause for these significantly different observations.

Similarly to the behaviour observed with **DOUBLE DYNAMIC** and **PBD CTL1 IMI**, detailed in Chapter 4, a ‘lag strain’ (where no immediate stress response is observed at low

strains) was observed for **PBD TP CTL0** and **PBD TP CTL1 IMI**. This is, again, a typical example of viscoelastic behaviour that is expected from such thermoplastic elastomers. Observation of this behaviour in the cross-linked materials, from Chapter 4, could be due to dynamic exchange between imine bonds causing an increased thermoplastic character.

Introduction of the ureidopyrimidinone, within polybutadiene-based materials that were chain-extended with the urethane chemical function, showed a significant decrease in the maximum stress reached at 20% strain. The same behaviour was observed when introducing the ureidopyrimidinone moiety to materials based on chain-extension with the imine chemical function (i.e. **DOUBLE DYNAMIC TP**). It may be that this is caused by the strain-induced dissociation of the ureidopyrimidinone dimers, or higher order aggregates (nanofibers). It is very likely, as mentioned above, that the sample preparation has a significant impact on decreasing the maximum stress at 20% strain, due to the possibly incomplete chain-extension and as a consequence of a lower molecular weight.

5.2.5 Recyclability

Solubility and Re-Moulding

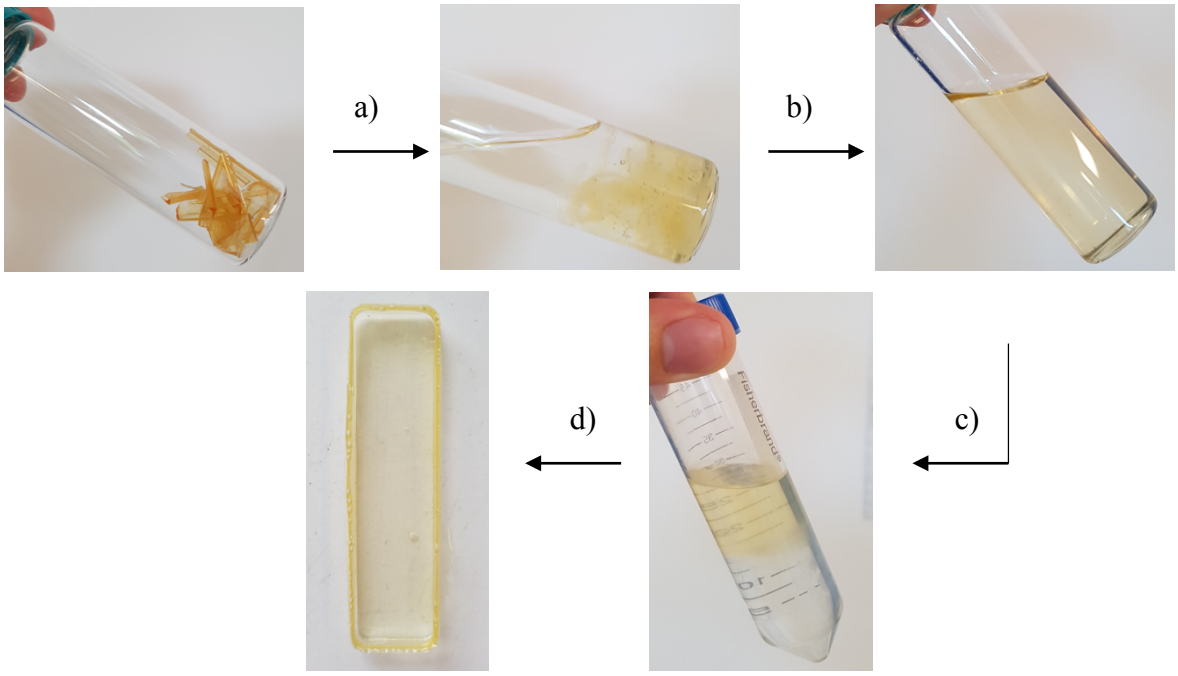

*Figure 95 – Images detailing the solubility of **DOUBLE DYNAMIC TP** in acidified organic solvent, and the ability to reform bulk elastomers after neutralisation and evaporation: a) add THF, b) add 10 wt% $TFA_{(aq)}$, c) neutralise with addition of $NaHCO_{3(aq)}$, d) evaporate in air*

The method described in Chapter 4, for the dissolution and recycling of **DOUBLE DYNAMIC** was extended in a similar way to **DOUBLE DYNAMIC TP**, this time with greater success. The four-step reprocessing method, illustrated in Figure 95, involves the swelling of off-cut pieces of **DOUBLE DYNAMIC TP** in THF; the dissolution of these pieces by addition of 10 weight percent TFA in a small amount of water (~0.3 mL) and shaking; neutralisation of the solution by addition of sodium hydrogen carbonate and separation of the aqueous layer; re-moulding of the neutralised solution with evaporation in ambient conditions. The produced material qualitatively appeared to maintain the same elastomeric characteristics as the starting material.

Quantification of the change in physical performance of **DOUBLE DYNAMIC TP** after recycling was conducted by DMTA (Figure 96). As before, the stress strain behaviour of the sample was tested at both high and low temperatures. At low temperatures, the glass transition temperature was found at the same temperature (~–45ºC), with a slight increase in both E' and tan(δ). A steeper transition from the glassy to the rubbery state was observed in recycled materials (~–30 to 20 ºC), followed by a slightly decreased E' at the rubbery plateau (–20 to +75 ºC). In both the pristine and the recycled materials, viscous flow was found to occur at temperatures above 75 ºC, with the increase in standard deviation of the results rendering them unreliable.

Analysis of the physical behaviour stress/strain cycles and elongation until break studies on both pristine and recycled materials, are currently under way.

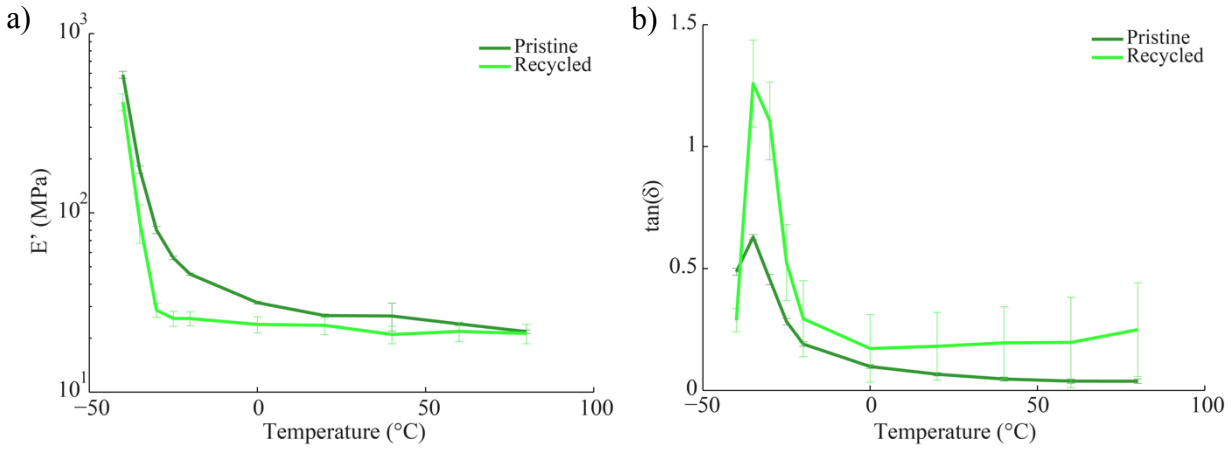

*Figure 96 – Evolution of the a) storage modulus and b) tangent delta versus temperature for **DOUBLE DYNAMIC TP** before and after recycling by the aforementioned process. Pristine sample (dark green), recycled samples (recycled). Tested at frequency of 1 Hz between –45 and 75 ºC*

Self-Healing

Finally, the ability of each material to repair after being damaged, on exposure to either heat or solvent, was evaluated by optical microscopy (Figure 97).

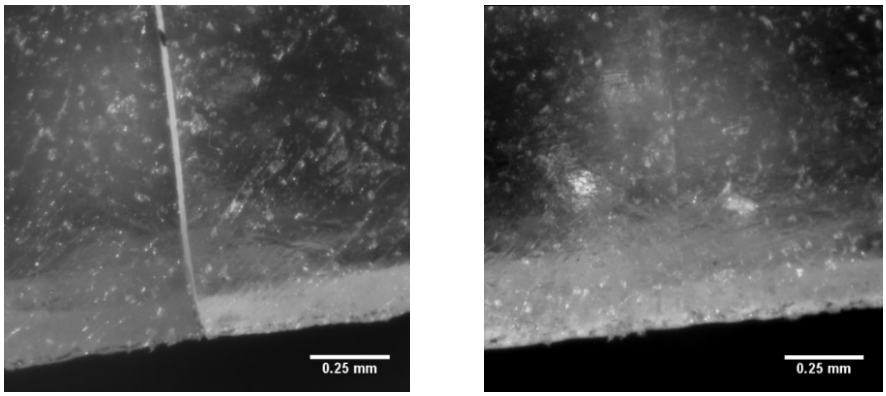

*Figure 97 – Microscope images of **DOUBLE DYNAMIC TP** before (left) and after (right) self-healing, after exposure to heat (70 ºC) using an ironing procedure*

Following the same procedure as described in Chapter 4, a piece of each material was partially cut through its full thickness before the application of heat in an ironing-like fashion. Contrary to the observation made for the materials based on Polyvest®, whereby all materials containing dynamic groups were found to have a similar ability to self-heal, with the exception of **PBD CTL0**, all materials, including **PBD TP CTL0**, were observed to self-heal to some degree. **PBD TP CTL1 UPy** and **DOUBLE DYNAMIC TP** displayed healing after ironing at just 70 ºC (40 ºC cooler than for the thermoset materials), while **PBD CTL1 IMI** required heating to ~120 ºC. These observations could be a macroscopic display of the different kinetic rates at which dynamic exchange occurs within the materials, with **PBD CTL1 IMI**, containing only imine bonds as dynamic moieties, requiring higher temperatures to achieve the activation energy. As the ureidopyrimidinone is anticipated to exchange at a faster rate than imines (but produce a weaker bond), the observed self-healing at lower temperatures in both **PBD TP CTL1 UPy** and **DOUBLE DYNAMIC TP** could be as a consequence of this kinetic difference. As expected with thermoplastic materials, **PBD TP CTL0** also displayed healing characteristics, requiring temperatures ~120 ºC for the partial melt-state to be achieved. Quantitative comparison to determine, and compare, the strength of the self-healed materials would be necessary to draw any firm conclusions; this quantitative analysis is normally achieved by comparing the stress at break of pristine materials, to that of their self-healed counterparts.

5.3 Conclusions and Perspectives

The chain-extension co-polymerisation of bi-functional polybutadiene, with a functionality of ≤2, with two dynamic chemical functions yielded a thermoplastic material, which was recyclable and self-healable, with a strongly elastic character.

Co-polymerisation with monomers containing the ureidopyrimidinone chemical moiety caused a cross-linking behaviour, reflected in the tendency toward more elastic behaviour when stretched, due to the formation of strong UPy dimers between polymer chains. Objects with an even larger size were also detected, by X-ray scattering, likely due to a second degree of UPy stacking forming inter-hard-block nanofibers.

Replacement of the urethane functionality with the imine chemical bond gave the material solubility in acidic conditions. A methodology was successfully devised whereby broken material was dissolved and re-casted to yield homogenous elastomeric material of a qualitatively similar appearance to the pristine material. Quantification of the double-dynamic material after dissolution and re-moulding also gave strong evidence of the retention of similar physical behaviour of the material.

Upon ironing a broken sample containing both hydrogen-bonding and imine chemical functionalities, at a temperature of just 70 ºC for five heating cycles, significant recovery of the polymer could be observed by optical microscopy. The chemical exchange between the dynamic chemical moieties is suggested to be the cause of this self-healing characteristic. Further analysis with regards to quantifying the degree of self-healing will be necessary to determine any difference caused by the inclusion of two, kinetically distinct dynamic chemical groups.

Direct comparison between the chemically cross-linked materials produced in Chapters 3 and 4 and the thermoplastic materials in this chapter, is made more difficult due to the differing methodologies used to produce the materials. A distinct loss in thermal stability, on removal of the chemical cross-links, can, however, be clearly observed. Lower stresses are observed in materials without cross-links (i.e. based on Krasol®), when 20% strain is applied.

5.4 References

1. Tanaka, Y., Takeuchi, Y., Kobayashi, M. & Tadokoro, H. Characterization of diene polymers. I. Infrared and NMR studies: Nonadditive behavior of characteristic infrared bands. *J. Polym. Sci. Part A-2 Polym. Phys.* **9,** 43–57 (1971).
2. Vilar, W. D., Menezes, S. M. C. & Seidl, P. R. Hydroxyl-terminated polybutadiene. *Polym. Bull.* **38,** 327–332 (1997).
3. Appel, W. P. J., Portale, G., Wisse, E., Dankers, P. Y. W. & Meijer, E. W. Aggregation of ureido-pyrimidinone supramolecular thermoplastic elastomers into nanofibers: A kinetic analysis. *Macromolecules* **44,** 6776–6784 (2011).
4. Spírková, M., Matejka, L., Hlavatá, D., Meissner, B. & Pytela, J. Polybutadiene-based polyurethanes with controlled properties: preparation and characterization. *J. Appl. Polym. Sci.* **77,** 381–389 (2000).

General Conclusions and Perspectives

From the work completed in this thesis, a series of elastic thermoplastic and thermoset materials, containing dynamic covalent and non-covalent chemical moieties, were synthesised and characterised. The incorporation of two dynamic chemical functionalities (the hydrogen-bonding ureidopyrimidinone and reversible and exchangeable covalent imine bond) was aimed at gaining better control over the kinetic rates of reversibility, which may then be used as a handle with which the degree and rate of self-healing may be controlled.

In chapter 2, the incorporation of two dynamic chemical moieties onto one polymeric backbone was attempted by the synthesis of a main-chain supramolecular polymer. Bi-functional α,ω-alkyne-functionalised polyisoprene was synthesised by modification of α,ω-hydroxyl-functionalised polyisoprene; this polymer backbone was then coupled by CuAAc 'click' chemistry with an azide-functionalised ureidopyrimidinone. Despite clear analytical confirmation of the success of the functionalisation, no distinct change in the physical properties was observed.

In a renewed approach, detailed in chapters 3 and 4, multi-functional polybutadiene was co-polymerised with a ureidopyrimidinone derivative to form double-dynamic thermoset elastomers. The synthesis of the materials was achieved by the polycondensation of amine-functionalised polybutadiene and aldehyde-functionalised ureidopyrimidinone, forming an elastomeric polyimine. The role of each dynamic chemical function (the ureidopyrimidinone and imine) on the physical behaviour of the materials was probed by comparison with appropriate control materials. Rubbery behaviour (E = ~15 MPa) was observed at temperatures between -30 and +70 ºC. At temperatures above 120 ºC, stress relaxation was observed resulting from the thermally-activated dynamic exchange between both the ureidopyrimidinone dimers and transimination. Cut or damaged double-dynamic materials were qualitatively observed to self-heal in the bulk after short exposure to elevated temperatures (~120 ºC), as well as in a semi-swollen state at room temperature. Adhesiveness to two pieces of the same material was investigated, with preliminary results of adhesive strength a promising prospect for further study.

In the final chapter (chapter 5), the established chemistry was extended onto better-defined bifunctional polybutadienes, with the formation of thermoplastic dynamic materials. In this material, the supramolecular hydrogen-bonding interactions between ureido-pyrimidinones drove the formation of supramolecular polymer networks. As with the thermoset

elastomers, the thermoplastic materials were also found to display elastic behaviour, although within a smaller temperature range (–10–+60 ºC). At elevated temperatures (>60 ºC), a melting transition was observed. As with the thermoset materials, self-healing was observed, however, considerably lower temperatures (70 ºC) could be used to achieve qualitatively fully-healed samples.

Development of this work may focus on a number of different areas: primarily, a detailed study into the orthogonality of the two dynamic groups should be conducted, best achieved by the synthesis and physical analysis of materials containing different proportions of the aldehyde-ureidopyrimidinone derivative and aldehyde-hexane derivative; investigation into the use of different diisocyanates, to form the ureidopyrimidinone derivative, in order to produce different hard-block interactions, and thus potentially changing the physical characteristics of the resulting materials; investigation into the use of different polymer backbones, with the same goal of changing the physical behaviour of the materials; investigation into the formation of similar dynamic materials from unmodified, commercially-available (hydroxyl-functionalised) polymer backbones, via alternative dynamic covalent chemistries, may also be of interest.

Appendix

Solvents, Chemical Reagents and Chromatographic Methods

All reactions were performed under an atmosphere of argon unless otherwise indicated. All reagents and solvents were purchased at the highest commercial quality and used without further purification unless otherwise noted. Dry solvents were obtained using a double column SolvTech purification system. Water was deionized by using a milli-gradient system (Millipore, Molsheim, France). Yields refer to purified spectroscopically (^{1}H NMR) homogeneous materials. Thin Layer Chromatography was performed with TLC silica on aluminium foil (Silica Gel/UV254, Aldrich). In most cases, irradiation using a Bioblock VL-4C UV-Lamp (6 W, 254 nm and/or 365 nm) was used for visualization.

Apparatus

Kinematic Viscosity

Viscosity measurements were conducted using a Schott Capillary Viscometer CT52 and a Schott Ostwald Capillary viscometer (k = 0.0294). The sample solution was loaded into the viscometer and allowed to equilibrate to 25 ºC for 5 minutes before each measurement was taken.

Thermogravimetric Analysis (TGA)

Thermogravimetric analysis (TGA) was performed using the TGA Q50 V20.10 Build 36 (TA Instruments) instrument. A heating ramp from 25 ºC to 900 ºC at a rate of 25 ºC/mol

in an atmosphere of nitrogen, under a nitrogen flow of 40 mL/min, was subjected to ~7 mg of each material.

Differential Scanning Calorimetry (DSC)

Differential scanning calorimetry (DSC) was performed using a DSC Q20 V24.9 Build 121 (TA Instruments) instrument. The samples were prepared using hermetic aluminium pans and the experiments conducted under a flow of nitrogen 50 mL/min using ~7 mg of each material. The samples were cooled to –90 ºC and heated to 100 ºC, for the first cycle, followed by cooling to –90 ºC, for the second cycle, and heating from –90 ºC to 250 ºC, for the third and final cycle. All heating ramps were executed at a rate of 10 ºC/min. Glass transition temperatures were obtained using automated TA Instruments software.

Size Exclusion Chromatography (SEC) / Light Scattering (LS)

SEC experiments were performed at the Institut Charles Sadron at the Plateforme de caractérisation des polymers, on three PLgel-B columns (granulometry: 10 μm, length: 30 cm, internal diameter: 7.5 mm, separation in the 10^3–10^7 g.mol^{-1}). A triple detector from Viscotek was used (light scattering, viscometer, refractometer). All samples were analysed in THF solution. Rate of flow: 1 mL/min. The samples were dissolved in the solvent 24 h prior to experiment and heated up to 50°C before being filtered on a 0.45 μm PTFE and injected.

X-Ray Scattering

SAXS experiments were performed using a RIGAKU (Elexience, France) diffractometer. This diffractometer operates using pinhole collimation of the X-ray beam and a two-dimensional gas-filled multi-wire detector. A monochromatic (λ = 1.54 Å with $\Delta/ < 4\%$) and focussed X-ray beam is obtained through a multilayer optic designed and fabricated osmic.

The size of the incident beam on the sample was ~700 μm. The sample-to-detector distance was set at 0.80 m, allowing to explore scattering vectors ranging from q = 0.01 $Å^{-1}$ to 0.3 $Å^{-1}$. The magnitude of the scattering vector is defined by $q = 4\pi\sin(\theta/2)/\lambda$, where λ and θ are the wavelength of the incident beam and the scattering angle, respectively. The q-resolution, related to the beam size on the same and the beam divergence, was close to 0.0025 $Å^{-1}$ Measurements were performed at room temperature.

WAXS experiments were performed using a RIGAKU (Elexience, France) diffractometer. This diffractometer operates using pinhole collimation of the X-ray beam and a two-dimensional storage phosphor screen (Imaging Plate) detector. The sample-to-detector distance was set at 0.05 m, allowing to explore scattering vectors ranging from q = 1 $Å^{-1}$ to 3 $Å^{-1}$.

Ultraviolet-Visible light Spectrophotometry (UV-VIS)

UV-Vis spectra were recorded using a Varian Cary 5000 spectrophotometer using a quartz glass cuvette of 1 cm optical path under ambient conditions in cyclohexane.

Mass Spectrometry

ESI-MS mass spectra were recorded on a SQD apparatus from Waters. MALDI-TOF mass spectra were recorded on a Bruker Daltonics AutoflexII TOF spectrometer. HRMS mass spectra were recorded on a Micro-Q-TOF apparatus from Bruker.

Nuclear Magnetic Resonance Spectroscopy (NMR)

^{1}H NMR spectra were recorded on a Bruker Avance 400 spectrometer at 400 MHz and ^{13}C spectra at 100 MHz and at 25°C. The spectra were internally referenced to the residual

proton solvent signal ($CDCl_3$: 7.26 ppm and DMSO-d_6: 2.50 ppm) for ^1H spectrum, and $CDCl_3$: 77.16 ppm for ^{13}C spectrum). For ^1H NMR assignments, the chemical shifts are given in ppm. The following notation is used for the ^1H NMR spectral splitting patterns: singlet (s), doublet (d), triplet (t), multiplet (m), broad (b).

The rate of formation of hemiacetal and imine, and loss of aldehyde was followed by ^1H NMR spectroscopy at concentrations of ~5 μM in DMSO-d^6: resonances at 8.31, 8.17 and 9.95 ppm were followed, respectively.

Fourier Transform Infrared Spectrophotometry (FTIR)

Infrared spectrophotometry was performed on solid elastomeric and neat polymeric samples using a Bruker Vertex 70 FTIR spectrophotometer with an ATR accessory provided by Smiths.

Transmission Electron Microscopy (TEM)

TEM experiments were performed using a CM12 Philips microscope equipped with a MVIII (SoftImaging System) CCD camera. Samples were analyzed in Bright Field Mode with a LaB_6 cathode and 120 kV tension. Image treatments were performed by using analySIS (Soft Imaging System) software. For the sample preparation, a carbon-coated copper grid was placed on a Whatman filter paper, before addition of one drop of the gel dissolved in DMF. The grid was then allowed to dry in air.

Dynamic Mechanical Thermal Analysis (DMTA)

Dynamic mechanical thermal analysis (DMTA) was conducted using an Instron E3000 instrument in tension mode. Rectangular samples of the dimensions ~10 mm x 1 mm cross-section and ~30 mm length were tested in the frequency range of 0.1 Hz to 15 Hz

(logarithmically spaces) and for a temperature range between –75 ºC to 140 ºC. Heating increments of 15 ºC with a 15 minute equilibration time were used for each temperature transition; at temperatures approaching T_g smaller 5 ºC increments were used. Stress was applied on the sample between a range of 0.4 and 0.8%, oscillated in a sinusoidal manner. At frequencies below 1 Hz, 10 cycles were recorded for each frequency, while above 1 Hz 100 cycles were recorded for each frequency.

Wavematrix software (V 1.9.398) was used for all programming of the machine and acquisition of the data.

Data were treated using MATLAB®, with calculation of the mean and standard deviations for E', E" and tan(δ). Due to unreliably large standard deviations at the highest frequencies, only frequencies ~10 Hz were considered to be valid.

Stress/Strain Experiments

Stress/strain cycling was performed using the Instron E3000 in tension mode. Rectangular samples of the dimensions ~10 mm x 1 mm cross-section and ~30 mm length were tested at three frequencies: 10 mHz, 100 mHz and 1 Hz, at room temperature, with a maximum strain of 20%. Each sample was cycled ten times. On analysis of the strain recovery, samples were left under no strain for between 1 and 3 days, at room temperature.

Data were collected and treated using Instorn Wavematrix software (V 1.9.398).

Elongation Until Break Experiments

Elongation until break measurements were performed using an Instron E3000 instrument (with the AVE videoextensiometer attachment) at ambient temperature (~25 ºC), with a strain rate of 0.4%/s. Samples of the dimensions ~10 mm x 1 mm cross-section and ~30

mm length were tested (sandwiched between PDMS films between the clamp and the sample to avoid slippage) between 3–6 times (single use).

Data were recorded and analysed using Bluehill 3 software, with the Young's modulus calculated from the initial slope of the resulting curve. True strain was calculated using the Bluehill 3 software.

Stress Relaxation Experiments

Stress relaxation experiments were performed using an Instron E3000 instrument in tension mode, using rectangular samples with a ~10 mm x 1 mm cross-section and ~30 mm length. Samples were stretched to achieve 1 N of tensile force, which required strain levels according to temperature.

Data were collected and treated using Instron Wavematrix software (V 1.9.398).

Experimental Protocols

Polyisoprenes

Synthesis of Secondary Butyllithium

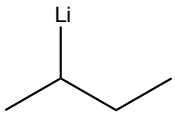

Lithium metal (5.1 g, 0.735 mol) was removed from oil and washed with cyclohexane, before being stirred in a solution of cyclohexane (130 mL). 2-chlorobutane (13 mL, 0.160 mol) was added *via* a dropping funnel directly attached to the reaction vessel, to maintain the air-tight atmosphere. The solution was stirred for 2 hours with colour change from colourless to deep purple observed. The concentration of *sec*-butyllithium was determined, by titration from

acetanilide in dimethylsulfoxide with addition of triphenylmethane as a colour indicator, to be 0.51 M.

*Synthesis of Polyisoprene (**PI1 CTL**)*

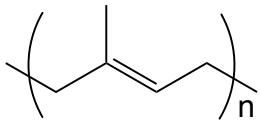

Titration of impurities from the reaction vessel was first performed by introduction of cyclohexane (100 mL), isoprene monomer (2 drops) and *sec*-BuLi (a few drops until clear yellow colour was observed at solution surface). The solution was stirred for 20 minutes to allow for complete reaction of butyllithium and impurities. *Sec*-BuLi (2 mL, 0.51 M) and isoprene monomer (14.7 mL) were added to the flask and stirred for 20 minutes to allow initiation to complete. The reaction mixture was then heated at 50 ºC for 3 hours to allow propagation maximum to occur. Reaction mixture was allowed to cool to room temperature and polymerisation was terminated by addition of methanol (3 drops). A white solid precipitate in a viscous colourless solution was produced, which was then concentrated *in vacuo* to produce an oily cloudy white residue.

After drying overnight under vacuum, the residue was precipitated by drop wise addition into methanol (1 L) with continuous stirring. The white, viscous precipitate was allowed to decant, liquid poured-off and the resulting solid was dissolved in toluene. Removal of toluene *in vacuo* produced **PI1 CTL** as a viscous residue product which was then oven-dried under vacuum for 3 days, and stored in a refrigerator in an argon atmosphere. **PI1 CTL** (9.95 g, 100%, PDI 1.04, M_w 10,310 g/mol)

*Synthesis of Monohydroxyl-Functionalised Polyisoprene (**PI1 OH**)*

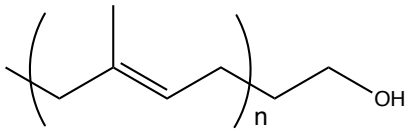

Titration of impurities from the reaction vessel was first performed by introduction of toluene (100 mL), 1,1-diphenylethylene (5 drops) and *sec*-BuLi (5 drops until orange colour persisted). This solution was stirred for 20 minutes to allow for complete reaction of butyllithium and impurities. *Sec*-BuLi (2 mL, 0.5 M) and isoprene monomer (14.7 mL) were added to the flask and stirred for 20 minutes with cooling in a water ice bath (5 ºC), to allow initiation to complete. The reaction mixture was then heated to 45 ℃ for 2 hours to allow propagation maximum to occur. Reaction mixture was allowed to cool to room temperature, and then further cooled to -85 ℃ (bath of isopropyl alcohol and solid carbon dioxide). Ethylene oxide (11 drops) was added and the solution allowed to warm to room temperature with stirring overnight. Methanol (1 mL) was added to terminate the reaction. The reaction mixture was concentrated *in vacuo* to produce a colourless viscous residue, which was then re-dissolved in toluene (~200 mL), centrifuged and precipitated in methanol (1 L). The white, viscous precipitate was allowed to decant, the liquid was poured-off and the residue dissolved in cyclohexane before being evaporated *in vacuo* and dried under vacuum overnight to yield **PI1 OH** (10.46 g, quantitative, PDI 1.03, M_w 10,012 g/mol).

*Synthesis of Monoalkyne-Functionalised Polyisoprene (**PI1 ALK**)*

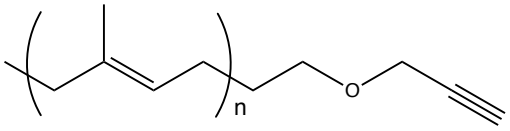

Hydroxyl-functionalised polyisoprene (**PI1 OH**, 10,120 g/mol) (7.04 g, 0.7 mmol) was dissolved in THF (70 mL) under an atmosphere of argon. Diphenylmethyl potassium (1.5 mL) was then added until brown colouration persisted. After stirring for 30 minutes, propargyl bromide (~2 mL) was added changing colouration to colourless and then quickly to brown/yellow. The solution was allowed to stir overnight at room temperature.

The solution was then evaporated *in vacuo* and redissolved in cyclohexane (~200 mL) before being centrifuged. The solution was precipitated into stirred methanol (700 mL) and allowed to decant before pouring off the liquid to isolate the precipitate, to yield **PI1 ALK** as a viscous clear yellow liquid (6.27 g, 89%, PDI 1.03, M_w 10,074 g/mol).

*Synthesis of Polyisoprene with Bis-Functional Initiator (**PI2 CTL**)*

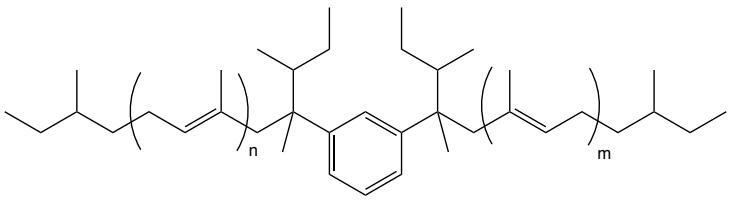

Titration of impurities from the reaction vessel was first performed by introduction of toluene (100 mL), 1,3-diisopropenyl benzene (2 drops) and *sec*-BuLi (8 drops until red colour persisted). This solution was stirred for 1 hour to allow for complete reaction of butyllithium and impurities. 1,3-diisopropenyl benzene (0.5 mL) and s*ec*-BuLi (4.3 mL, 0.5 M) were added to the flask and stirred for 1.5 hours at 60 ºC, to allow complete deprotonation (and therefore

activation) of 1,3-diisopropenyl benzene. The reaction mixture was then cooled to 5 ºC in an ice bath, isoprene monomer (14.7 mL) added, and the solution was stirred for 20 minutes to allow completion of initiation. The reaction mixture was then heated to 45 ℃ for 2 hours to allow propagation maximum to occur. The reaction mixture was allowed to cool to room temperature, before addition of methanol (1 mL).

The reaction mixture was centrifuged and precipitated in methanol (1 L). The white, viscous precipitate was allowed to decant, the liquid was poured-off and the resulting solid was dissolved in cyclohexane (~100 mL) before being evaporated *in vacuo* and dried under vacuum overnight to yield **PI2 CTL** as a viscous liquid (9.65 g, 97%, PDI 1.31, M_w 31,171 g/mol).

*Synthesis of α,ω-Dihydroxyl-Functionalised Polyisoprene (**PI2 OH**)*

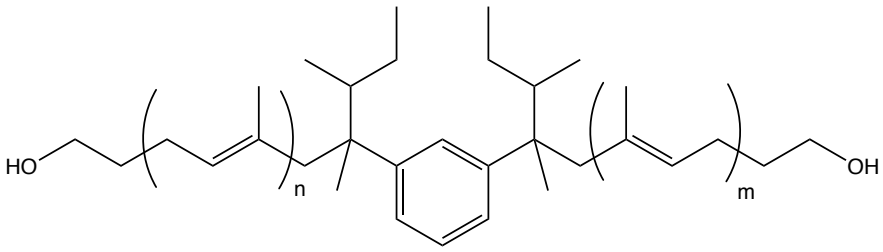

Titration of impurities from the reaction vessel was first performed by introduction of toluene (100 mL), 1,3-diisopropenyl benzene (2 drops) and *sec*-BuLi (12 drops until red colour persisted). This solution was stirred for half an hour to allow for complete reaction of butyllithium and impurities. 1,3-Diisopropenyl benzene (0.5 mL) and s*ec*-BuLi (4.3 mL, 0.5 M) were added to the flask and stirred for 4 hours at 40 ºC, to allow complete deprotonation (and therefore activation) of 1,3-diisopropenyl benzene. The reaction mixture was then cooled to 5 ºC in an ice bath, isoprene monomer (14.7 mL) added, and the solution was stirred for 20 minutes to allow completion of initiation. The reaction mixture was then heated to 45 ℃ for 2

hours to allow propagation maximum to occur. The red/brown solution lost colour to a pale yellow. The reaction mixture was cooled to -20 ºC in an alcohol/$CO_{2(s)}$ bath before addition of ethylene oxide (11 drops) and allowed to stir overnight at room temperature. The pale yellow solution became a colourless gel. Methanol (0.5 mL) was added, changing the gel into a colourless solution.

The reaction mixture was centrifuged and precipitated in methanol (1 L). The white, viscous precipitate was allowed to decant, the liquid was poured-off and the resulting solid was dissolved in cyclohexane (~200 mL) before being evaporated *in vacuo* and dried under vacuum overnight to yield **PI2 OH** (9.72 g, 98%, PDI: 1.07, M_w 26140 g/mol) as a viscous liquid.

*Synthesis of α,ω-Dialkyne-Functionalised Polyisoprene (**PI2 ALK**)*

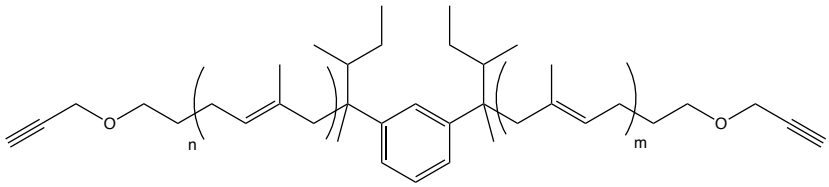

PI2 OH (27,450 g/mol) (3.10 g, 0.11 mmol) was dissolved in THF (30 mL) under an atmosphere of argon. Diphenylmethyl potassium (13 drops) was added to the stirred solution, until red/brown coloration persisted. Gel formation was observed. After allowing the gel to stir for 30 minutes, propargyl bromide (1 mL, 13.2 mmol) was introduced. The gel was observed to re-dissolve to form a clear pale yellow solution. This solution was allowed to stir at room temperature for 4 hours. Small amounts of a dark brown precipitate formed.

The solution was then evaporated *in vacuo* and the residue was redissolved in cyclohexane (~200 mL) before being centrifuged. The solution was precipitated into stirred methanol (300 mL) and allowed to decant before pouring off the liquid to isolate the precipitate.

The precipitate was dissolved in cyclohexane and evaporated *in vacuo* to yield **PI2 ALK** as a viscous clear yellow liquid. (3g, 95%, PDI 1.37, M_w 28,260 g/mol)

Ureidopyrimidinone Synthons

*Synthesis of 2-amino-6-(heptan-3-yl)pyrimidin-4(3H)-one (**1**)*

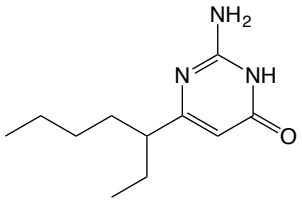

In a round-bottomed flask purged of air with three vacuum/argon cycles, 2-ethylhexanoic acid (3.3 mL, 21 mmol), ethyl acetate (20 mL) and dimethylformamide (6 drops) were added; the solution was then cooled to 0 ℃ and oxalyl chloride (2.7 mL, 31.5 mmol) added drop wise. The colourless solution was observed to turn very pale yellow. The solution was then stirred, at room temperature, overnight. In a separate round-bottomed flask, purged of air by three vacuum/argon cycles, potassium ethyl malonate (5.36 g, 31.5 mmol), magnesium chloride (3.60 g, 37.8 mmol) and ethyl acetate (35 mL) were added; the solution was cooled to 0 ℃ and triethylamine (10.8 mL, 77.7 mmol) was added dropwise. This white suspension was left to stir overnight at 35 ℃. The acyl chloride, cooled to 0 ºC in an ice bath, was added to the malonate solution *via* cannula, and the resulting solution was allowed to stir for 1 day. The white suspension of the malonate turned into an orange colour, on introduction of the clear yellow acyl chloride solution.

The coagulated orange solution was cooled to 0 ℃ and 13% HCl (~30 mL) was added dropwise. The solution was allowed to stir for 1 hour before being transferred to a separating funnel. The aqueous layer was isolated and washed with ethyl acetate (30 mL). The organic

portions were combined and washed with 13% HCl (40 mL), water (40 mL) and 5% $NaCO_3$ (40 mL). The solvent was then evaporated *in vacuo* to leave a orange/brown residue (4.25 g, 20 mmol, 94%). This compound was used in the next step without further purification or characterisation.

In a round-bottomed flask purged of air by three vacuum/argon cycles, ethyl 4-ethyl-3-oxooctanoate, from the previous step, (3.59 g, 16.8 mmol), ethanol (75 mL), guanidine carbonate (1.96 g, 21.8 mmol) and potassium *tert*-butoxide (1.84, 16.8 mmol) were heated under reflux (80 ℃) for 3 days. The orange/brown solution was observed to turn dark brown/green and then brown/red. The solvent was then evaporated *in vacuo* to produce an orange/brown residue, which was then re-dissolved in chloroform (100 mL). The organic layer was washed with water (3 x 50 mL) and brine (50 mL). The organic phase was then evaporated *in vacuo* to leave an orange solid product. Further purification by column chromatography (SiO_2 $CHCl_3$:MeOH 98:2 → 96:4) yielded compound **1** as an orange powder product (1.06 g, 30%).

^{1}H NMR ($CDCl_3$, 400 MHz, 25 °C): δ = 5.60 (s, 1H, —NHC(O)C***H***—), 2.20 (dt, *J* = 7.2 Hz 1H, —NCC***H***—), 1.60—1.49 (m, 4H, —CH(C***H***$_2$CH$_3$)— and —CH((CH$_2$)$_2$C***H***$_2$CH$_3$)), 1.31—1.14 (m, 4H, —CH((C***H***$_2$)$_2$CH$_2$CH$_3$), 0.82 (t, *J* = 7.4 Hz, 3H, —CH(CH$_2$C***H***$_3$), 0.81 (t, *J* = 7.2 Hz, 3H, —CH((CH$_2$)$_2$CH$_2$C***H***$_3$)).

^{13}C NMR ($CDCl_3$, 100 MHz, 25 ºC): δ= 175.6, 156.4, 101.4, 47.4, 33.3, 29.5, 27.0, 22.6, 13.9, 11.8

HRMS (ESI-MS): m/z calcd. for $C_{11}H_{20}N_3O$: 210.16 [M+H]+, found: 210.162

*Synthesis of 1-(6-((tert-butyldiphenylsilyl)oxy)hexyl-3-6-(heptan-3-yl)-4-oxo-1,4dihydropyrimidin-2-yl)urea (**2**)*

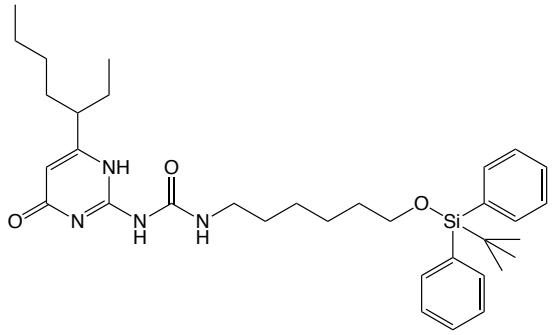

In a round-bottomed flask, 2-ethylpentynyl isocytosine (**1**) (126 mg, 0.6 mmol) and N-{6-[(tert-butyldiphenylsilyl)oxy]hexyl}-1H-imidazole-1-carboxamide (kindly donated by Dr Antoine Goujon) (523 mg, 1.2 mmol) were dissolved in DMF (10 mL). The clear green/yellow solution was heated to 80 ºC with stirring for 2 hours before addition of triethylamine (~1 mL). Heating was continued overnight, before being stopped, the solution was then cooled to room temperature and the solvent evaporated *in vacuo*. The crude product was purified by column chromatography (SiO_2, cyclohexane:ethyl acetate 100→80%) to yield compound **2** as a pale yellow oil (258 mg, 72%).

^{1}H NMR ($CDCl_3$, 400 MHz, 25 °C): 13.26 (bs, 1H, –NHC(O)N***H***CH_2–), 11.91 (bs, 1H, –N***H***C(O)NHCH$_2$—), 10.19 (bs, 1H, –NHC(O)NHCN***H***C)—), 7.68–7.63 (m, 4H, –SiC(C***H***)(C***H***)), 7.43 – 7.34 (m, 6H, –SiC(CH)(CH)(C***H***)(C***H***)(C***H***), 5.81 (s, 1H, —NC(O)CH—), 3.65 (t, *J* = 6.4 Hz, 2H, —C***H***$_2$Si), 3.25 (t, *J* = 7.2 Hz, 1H, —NHC(O)NHC***H***$_2$—), 3.23 (t, *J* = 7.2 Hz, 1H, —NHC(O)NHC***H***$_2$—), 2.29 (m, 1H, —CC***H***(CH$_2$CH$_3$)((CH$_2$)$_3$CH$_3$)), 1.70—1.50 (m, 8H, —NHCH$_2$(C***H***$_2$)$_4$CH$_2$OH), 1.43 (m, 4H, —CH(C***H***$_2$CH$_3$)— and —CH(((CH$_2$)$_2$C***H***$_2$CH$_3$)), 1.31—1.2 (m, 4H, —CH(((C***H***$_2$)$_2$CH$_2$CH$_3$)), 1.04 (s, 9H, –Si((C***H***$_3$)$_3$), 0.89 (t, *J* = 7.6 Hz, 3H, —C***H***$_3$) 0.87 (t, *J* = 7.6 Hz, 3H, —C***H***$_3$)

*Synthesis of 1-(6-(heptan-3-yl)-4-oxo-1,4-dihydropyrimidin-2-yl)-3-(6-hydroxyhexyl)urea (**3**)*

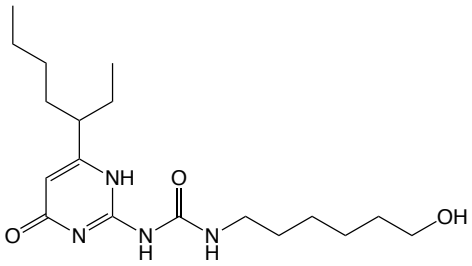

Compound **2** (258 mg, 0.43 mmol) and TBAF (2.1 mL, 2.1 mmol) were added to a round bottomed flask and purged of air with three vacuum/argon cycles. THF (5 mL) was added and the solution heated under reflux (60 ºC) with stirring for 2 days. The solution was then cooled to room temperature and evaporated *in vacuo* and the residue was re-dissolved in dicloromethane (10 mL). The organic layer was then washed with water (2 x 10 mL), dried over sodium sulphate and evaporated *in vacuo* to yield a pale yellow residue. This residue was then purified by column chromatography (SiO_2, CH_2Cl_2/MeOH 98/2→95/5) to yield Compound **3** as a pale yellow powder (91 mg, 60%).

^{1}H NMR ($CDCl_3$, 400 MHz, 25 °C): δ= 13.27 (bs, 1H, –NHC(O)N***H***CH_2–), 11.90 (bs, 1H, –N***H***C(O)NHCH$_2$—), 10.12 (bs, 1H, –NHC(O)NHCN***H***C)—), 5.85 (s, 1H, —NC(O)CH—), 3.63 (t, *J* = 6.4, 2H, —C***H***$_2$OH), 3.26 (t, *J* = 7.2 Hz, 1H, —NHC(O)NHC***H***$_2$—), 3.25 (t, *J* = 6.8 Hz, 1H, —NHC(O)NHC***H***$_2$—), 2.32–2.25 (m, 1H, —CC***H***(CH_2CH_3)((CH_2)$_3$$CH_3$)), 1.70—1.50 (m, 8H, —NHCH$_2$(C***H***$_2$)$_4$CH$_2$OH), 1.45–1.35 (m, 4H, —CH(C***H***$_2$CH$_3$)— and —CH(((CH$_2$)$_2$C***H***$_2$CH$_3$)), 1.31—1.20 (m, 4H, —CH(((C***H***$_2$)$_2$CH$_2$CH$_3$)), 0.87 (t, *J* = 7.6 Hz 3H, —C***H***$_3$), 0.85 (t, *J* = 6.8 Hz, 3H, —C***H***$_3$)

^{13}C NMR ($CDCl_3$, 100 MHz, 25 ºC): δ= 173.5, 156.7, 155.7, 154.9, 106.2, 62.1, 45.4, 39.4, 32.9, 32.5, 30.3, 29.4, 26.6, 25.9, 24.7, 22.5, 13.9, 11.7.

HRMS (ESI-MS): m/z calcd. for $C_{18}H_{32}LiN_4O_3$: 359.263 [M+H]+, found: 359.263

*Synthesis of 1-(6-azidohexyl(-3-(6-(heptan-3-yl)-4-oxo-1,4-dihydropyrimidin-2-yl)urea (**4**)*

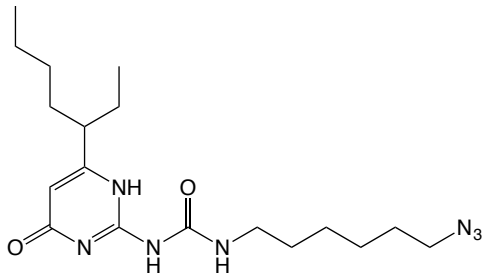

Hydroxyl-functionalised ureidopyrimidinone (**3**) (126 mg, 0.36 mmol), was dissolved in THF (5 mL) in an atmosphere of argon. Triethylamine (10 drops) was added and the solution cooled with an ice bath. Methanesulfonyl chloride (10 drops, ~0.5 mL, ~6.5 mmol) was added resulting in the formation of a yellow precipitate. The solution was stirred at room temperature for four hours before the solvent was evaporated *in vacuo* and the resulting yellow residue redissolved in dichloromethane (~10 mL). The organic layer was washed with water (2 x 20 mL) and dried over sodium sulfate. After evaporating *in vacuo*, the product was taken in to the next step without further purification or characterisation.

Methanesulfonylated ureido-pyrimidinone (~126 mg, 0.29 mmol) was dissolved in DMF (5 mL) before addition of sodium azide (189 mg, 2.9 mmol) and the solution stirred solution and heated at 50 ºC overnight. DMF was evaporated *in vacuo* and the brown residue redissolved in dichloromethane (~50 mL). The organic layer was washed with water (2 x 50 mL) and brine (50 mL) dried on sodium sulphate and evaporated *in vacuo* to yield a brown/red oily residue. The product was further purified by column chromatography (SiO_2, CH_2Cl_2/MeOH 100/0→95/5), to yield compound **4** (69 mg, 0.18 mmol, 51%) as a viscous brown liquid.

^{1}H NMR ($CDCl_3$, 400 MHz, 25 °C): δ= 13.23 (bs, 1H, –NHC(O)N***H***CH_2–), 11.90 (bs, 1H, –N***H***C(O)NHCH_2—), 10.20 (bs, 1H, –NHC(O)NHCN***H***C)—), 5.80 (s, 1H, —NC(O)CH—), 3.25 (m, 4H, —NHC(O)NHC***H***$_2$— and —C***H***$_2N_3$), 2.30 (m, 1H, —CC***H***(CH_2CH_3)((CH_2)$_3CH_3$)), 1.70—1.50 (m, 8H, —NHCH_2(C***H***$_2$)$_4CH_2N_3$), 1.44–1.36 (m, 4H, —CH(C***H***$_2CH_3$)— and —CH(((CH_2)$_2$C***H***$_2CH_3$)), 1.31—1.20 (m, 4H, —CH(((C***H***$_2$)$_2CH_2CH_3$)), 0.89 (t, *J* = 7.2 Hz, 3H, —C***H***$_3$), 0.86 (t, *J* = 6.8 Hz, 3H —C***H***$_3$).

^{13}C NMR ($CDCl_3$, 100 MHz, 25 ºC): δ= 173.2, 156.7, 155.6, 154.9, 106.2, 51.4, 50.8, 45.4, 39.9, 32.9, 29.3, 28.8, 26.6, 26.5, 26.4, 22.5, 13.9, 11.7

MS (MALDI-TOF): m/z calcd. for $C_{18}H_{31}N_7O_2$: 377.490 [M+H], found: 378.236 [M+H]

Click Reaction of Monoalkyne-Functionalised Polyisoprene and Azido-Urediopyrimidinone

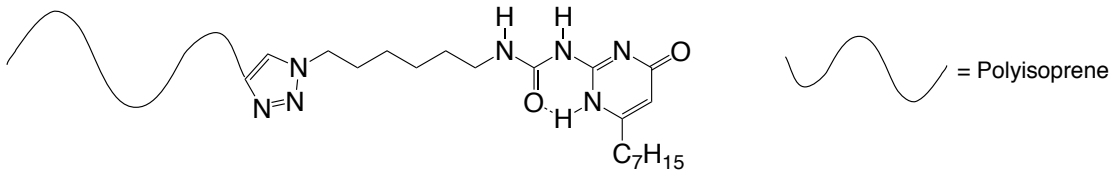

Alkyne-functionalised polyisoprene (**PI1 ALK**) (100 mg, 0.01 mmol) was added to a Schlenck flask, which was then purged with argon, and then dissolved in THF (600 µL). A solution of azide-functionalised urediopyrimidinone (**4**) (3.77 mg, 0.01 mmol) in THF (200 µL) was added to the stirred solution of **PI1 ALK**.

In a separate flask THF (200 µL) was added to copper(I)bromide (4.3 mg, 0.03 mmol). To this suspension PMDETA (6 µL) was added and the suspension stirred and sonicated. This suspension was then added to the previously prepared solution with vigorous stirring. The solution was allowed to stir overnight at room temperature, producing a clear green solution.

The solution was the concentrated *in vacuo* and the residue redissolved in toluene (~50 mL). The solution was then washed with $EDTA_{(aq)}$ (3 x ~25 mL) by vigorously stirring the two layers until the organic layer appeared colourless. The toluene was then evaporated *in vacuo* to yield a colourless viscous liquid **PI1 UPy**.

*Click Reaction of Bisalkyne-Functionalised Polyisoprene and Azido-Urediopyrimidinone (**PI2 UPy**)*

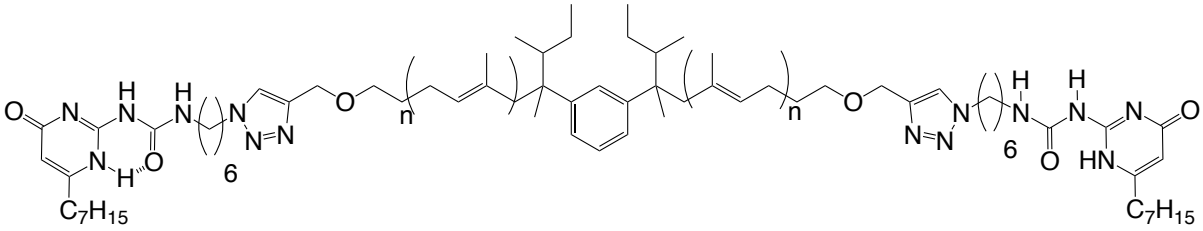

Alkyne-functionalised polyisoprene (**PI1 ALK**) (500 mg, 0.019 mmol) was added to a Schlenck flask, which was then purged with argon, and then dissolved in THF (600 μL). A solution of azide-functionalised urediopyrimidinone (**4**) (14.8 mg, 0.040 mmol) in THF (400 μL) was added to the stirred solution of **PI1 ALK**.

In a separate flask THF (400 μL) was added to copper(I)bromide (8.6 mg, 0.06 mmol). To this suspension PMDETA (12 μL) was added and the suspension stirred and sonicated. This suspension was then added to the previously prepared solution with vigorous stirring. The solution was allowed to stir overnight at room temperature, producing a clear green solution.

The solution was then concentrated *in vacuo* and the residue re-dissolved in toluene (~100 mL). The solution was then washed with $EDTA_{(aq)}$ (3 x 75 mL) by vigorously stirring the two layers until the organic layer appeared colourless. The toluene was then evaporated *in vacuo* to yield a colourless viscous liquid **PI1 UPy**.

Synthesis of 2-amino-5-(2-hydroxyethyl)-6-methylpyrimidin-4(1H)-one

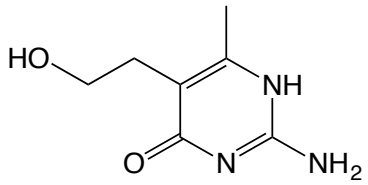

An adapted protocol from the literature was used to synthesise this molecule.[1]

Triethylamine (26 mL, 0.186 mol), ethanol (150 mL), 2-acetyl butyrolactone (8.4 mL, 0.078 mol), guanidine carbonate salt (14.05 g, 0.156 mol) were heated under reflux (80 ºC) for 20 hours. The white suspension was observed to dissolve to a clear yellow solution before a yellow clouded solution was observed after 3 hours. The solution was then cooled to room temperature, the white precipitate filtered and washed with ethanol (2 x 200 mL) before being suspended in water (~50 mL) and neutralised to pH 7 with 1 N HCl and allowed to stir for 1 hour. The white precipitate was then filtered, washed with water and ethanol and dried (7.98 g, 60%).

^{1}H NMR (DMSO d_6, 400 MHz, 25 °C): δ= 10.95 (bs, 1H, —$CH_2O\boldsymbol{H}$), 6.43 (bs, 2H, —$N\boldsymbol{H}_2$), 4.50 (bs, 1H, —N***H***), 3.35 (t, *J* = 7.2 Hz, 2H, —$CH_2C\boldsymbol{H}_2OH$), 2.44 (t, *J* = 7.2 Hz, 2H, —$C\boldsymbol{H}_2CH_2OH$), 2.06 (s, 3H, —$C\boldsymbol{H}_3$).

^{13}C NMR (DMSO D_6, 100 MHz, 25 ºC): δ= 164.5, 160.7, 153.4, 108.2, 60.0, 28.8, 20.7

[1] Fang, X. *et al.* Biomimetic Modular Polymer with Tough and Stress Sensing Properties. *Macromolecules* **46,** 6566–6574 (2013).

*Synthesis of 2-(2-(3-(6-isocyanatohexyl)ureido)-6-methyl-4-oxo-1,4-dihydropyrimidin-5-yl)ethyl (6-isocyanatohexyl)carbamate (**5**)*

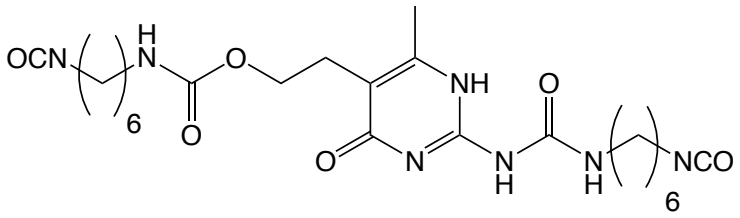

An adapted protocol from the literature was used to synthesise this molecule.[2]

2-amino-5-(2-hydroxyethyl)-6-methylpyrimidin-4(1H)-one (2.25 g, 13.3 mmol) was added to a 2-neck round bottomed flask, which was then purged of air with three vacuum/argon cycles and filled with DMF (10 mL). To this stirred suspension, cold HDI (20 mL, 124.9 mmol) and pyridine (2 mL) was added; the resulting white suspension was then heated overnight at 90 ºC. Complete dissolution of the white precipitate was observed after 2 hours at heat and the clear colourless solution turned clear yellow overnight. The solution was then added drop wise to cold diethyl ether (300 mL) producing an off-white precipitate and a clear yellow liquid, which was decanted. The solid was then washed again and decanted from cold diethyl ether (2 x 300 mL) before being isolated by filtration, washed with diethyl ether (2 x 100 mL) and dried to leave compound **5** as an off-white powder (4.5 g, 67%).

^{1}H NMR ($CDCl_3$, 400 MHz, 25 ºC) δ = 12.95 (s, 1H, –NHC(O)N***H***CH_2–), 11.92 (s, 1H, –N***H***C(O)NHCH_2), 10.17 (s, 1H, –NHC(O)NHCN***H***C(CH_3)–), 4.70 (s, 1H, –CH_2CH_2OC(O)N***H***CH_2–), 4.19 (t, *J* = 6.2 Hz, 2H, –CH_2OC(O)NHC***H***$_2$–), 3.32 (t, *J* = 7.2 Hz, 4H, –CH_2C***H***$_2$NCO), 3.29 (t, *J* = 6.8 Hz, 2H, –CH_2C***H***$_2$OC(O)NHCH_2–), 3.18–3.13 (m, 2H, –

[2] Guo, M. *et al.* Tough stimuli-responsive supramolecular hydrogels with hydrogen-bonding network junctions. *J. Am. Chem. Soc.* **136,** 6969–6977 (2014).

C***H***$_2$NHC(O)NH–), 2.77 (t, *J* = 6.6 Hz, 2H, –C***H***$_2$CH$_2$OC(O)NHCH$_2$–), 2.27 (s, 3H, –CH$_3$), 1.70–1.30 (m, 16H, CH$_2$(C***H***$_2$)$_4$CH$_2$NCO).

^{13}C NMR (CDCl$_3$, 100 MHz, 25 ºC): δ= 172.2, 156.7, 156.5, 153.5, 144.9, 113.8, 62.9, 43.0, 42.9, 40.9, 39.8, 31.14, 31.09, 29.9, 29.1, 26.2, 26.1, 26.0, 25.6, 17.2.

*Synthesis of 2-(2-(3-(6-(((4-formylphenoxy)carbonyl)amino)hexyl)ureido)-6-methyl-4-oxo-1,4-dihydropyrimidin-5-yl)ethyl (4-formylphenyl) hexane-1,6-diyldicarbamate (**6**)*

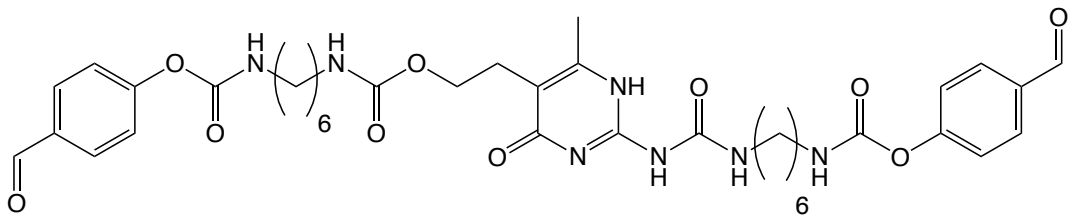

Compound **5** (1.44 g, 2.8 mmol) and 4-hydroxybenzaldehyde (1.71 g, 14 mmol) were added to a 2-necked round-bottomed flask, and purged of air by three vacuum/argon cycles. Distilled chloroform (15mL) was added via an addition funnel and dibutyltin dilaurate (2 drops) added by syringe, via the septum, and the resulting solution stirred with heating (60 ºC) overnight. The turbid orange suspension was observed to fully dissolve after 2 hours. The solution was then added drop wise to stirred diethyl ether (100 mL), the solid was then washed with ethanol (2 x 100 mL) and diethyl ether (2 x 100 mL), before drying to yield compound **6** as a white powder. (1.82 g, 87%).

^{1}H NMR (DMSO d$_6$, 400 MHz, 25 ºC) δ = 11.53 (bs, 1H, –NHC(O)N***H***CH$_2$–), 9.97 (s, 2H, –Ar–C***H***O), 9.51 (bs, 1H, –N***H***C(O)NHCH$_2$–), 7.93 (d, *J* = 8.2 Hz, 4H, (–(C***H***$_2$)CHO)$_2$), 7.33 (d, *J* = 8.2 Hz, 4H, (–(C***H***)$_2$(CH)$_2$CHO–)$_2$), 7.04 (t, *J* = 5.9 Hz, 1H, –NHC(O)NHCNHC(CH$_3$)), 3.96 (t, *J* = 6.6 Hz, 2H, –NHC(O)OC***H***$_2$CH$_2$–), 3.17–3.12 (m, 2H, –C***H***$_2$NHC(O)OCH$_2$–),

3.11–3.05 (m, 4H, –C***H***$_2$NHC(O)OAr–), 2.98–2.93 (m, 2H, –NHC(O)NHC***H***$_2$–), 2.61 (bt, *J* = 6.5 Hz, 2H, –NHC(O)OCH$_2$C***H***$_2$–), 2.16 (s, 3H, –C***H***$_3$), 1.50–1.20 (m, 16H, –NHCH$_2$(C***H***$_2$)$_8$CH$_2$NH–).

^{13}C NMR (DMSO D^6, 100 MHz, 25 ºC): δ= 191.9, 156.1, 155.9, 153.4, 132.9, 130.9, 122.2, 115.8, 29.3, 29.3, 29.2, 29.1, 29.0, 29.0, 25.9, 25.9, 25.8.

Synthesis of bis(4-formylphenyl) hexane-1,6-diyldicarbamate (7)

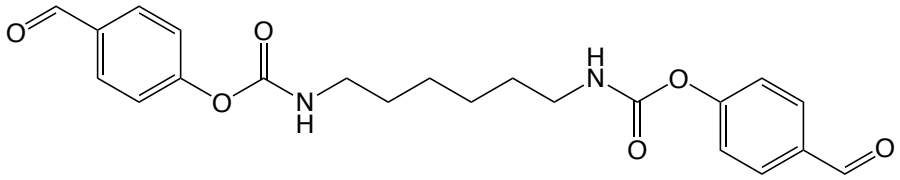

In a 100 mL round-bottomed flask, 4-hydroxybenzaldehyde (7.95 g, 0.065 mol) was suspended in dichloromethane (15 mL). To this stirred suspension, hexamethylene1,6-diisocyanate (5 mL, 0.031 mol) and pyridine (1 mL) were added and the suspension stirred with heating at 50 ºC for 7 hours. The off-white suspension was then precipitated into diethyl ether (300 mL) and stirred for 1 hour. The solvent was decanted and the precipitate washed again with diethyl ether (2 x 300 mL), before the off-white powder was isolated by vacuum filtration and further washed with diethyl ether (2 x 100 mL) to yield compound **7** as a white powder (11.89 g, 93%).

^{1}H NMR (CDCl$_3$, 400 MHz, 25 °C): δ= 9.97 (s, 2H, O***H***C(C$_2$H$_2$)(C$_2$H$_2$)O—), 7.89 (d, *J* = 8.4 Hz, 4H, OHC(C$_2$H$_2$)(C$_2$***H***$_2$), 7.33 (d, *J* = 8.4 Hz, 4H, OHC(C$_2$***H***$_2$)(C$_2$H$_2$)), 5.16 (t, *J* = 6.7 Hz, 2H, (—C(O)N***H***CH$_2$—)), 3.27 (q, *J* = 6.7 Hz 4H, (—C(O)NHC***H***$_2$CH$_2$—)), 1.66–1.59 (m, 4H, (—NHCH$_2$C***H***$_2$CH$_2$—)), 1.47–1.42 (m, 4H, (—NHCH$_2$CH$_2$C***H***$_2$—)).

^{13}C NMR ($CDCl_3$, 100 MHz, 25 ºC): δ= 191.0, 155.7, 153.8, 133.4, 131.2, 122.0, 41.1, 29.7, 26.1

HRMS (ESI-MS): m/z calcd. for $C_{22}H_{24}N_2O_6$: 413.1713 $[M+H]^+$, found: 413.184

Modification of Polybutadienes

Amine-Modification of Polybutadiene

Identical experimental procedures were used to produce amine-functionalised polybutadienes from both Polyvest® and Krasol® commercial materials. An example of the procedure, using Polyvest® is given below.

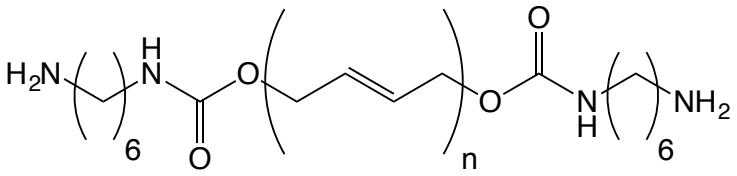

In a 2-neck round bottomed flask (with an addition funnel containing distilled chloroform and a septum attached), polybutadiene Polyvest® (3.97 g, 0.79 mmol) was added and dried under vacuum for 1 hour. The flask was then filled with argon and the polymer dissolved in chloroform (20 mL). In a separate 2-neck round bottomed flask (with a burette of distilled chloroform and a septum attached), carbonyl diimidazole (1.29 g, 8.0 mmol) was added and purged of air with three vacuum/air cycles before being dissolved in chloroform. (10 mL). The solution of polybutadiene was added drop wise to the solution of CDI and the resulting colourless solution allowed to stir overnight at room temperature. The solvent was then evaporated *in vacuo* and cyclohexane (30 mL) was added leading to the formation of a white suspension. The suspension was then filtered, washed with cyclohexane (3 x 30 mL) and

the solution evaporated *in vacuo*. The resulting viscous liquid polymer was then reacted, without further purification, with 1,6-diaminohexane:

In a 2-neck round bottomed flask (with an addition funnel of distilled chloroform and a septum attached) the polymer from the previous step was purged of air by three vacuum/argon cycles. Chloroform (30 mL) was then added and the solution stirred to homogeneity before addition to of 1,6-diaminohexane (1.2 g, 10 mmol) in a chloroform solution (50 mL). The resulting solution was then stirred overnight at room temperature. The solution was then precipitated in methanol (500 mL) and the solid residue was dried *in vacuo* to yield **PBD NH_2** as a pale green viscous liquid polymer (3.5 g, 85%).

Polyvest®-based Materials

^{1}H NMR ($CDCl_3$, 400 MHz, 25 °C): δ = 5.64–5.51 (br, 1,2-polyisoprene), 5.47–5.29 (br, *cis*/*trans*-1,4-polyisoprene), 5.02–4.89 (br, 1,2-polyisoprene), 4.71–4.56 (br, –C***H***$_2$OC(O)NHCH$_2$–), 3.21–3.09 (br, –CH$_2$OC(O)NHC***H***$_2$–), 2.69 (t, *J* = 7.0 Hz, –C***H***$_2$NH$_2$), 2.11–1.98 (br, 1,2-polyisoprene), 1.52–1.22 (br, *cis*/*trans*-1,4-polyisoprene)

Krasol®-based Materials

^{1}H NMR ($CDCl_3$, 400 MHz, 25 °C): δ = 5.57–5.30 (br, 1,2 and *cis*/*trans*-1,4-polyisoprene), 5.01–4.87 (br, 1,2-polyisoprene), 4.66–4.57 (br, –C***H***$_2$OC(O)NHCH$_2$–), 3.20–3.10 (br, –CH$_2$OC(O)NHC***H***$_2$–), 2.69 (t, *J* = 7.0 Hz –C***H***$_2$NH$_2$), 2.20–1.84 (br, 1,2-polyisoprene), 1.50–1.12 (br, *cis*/*trans*-1,4-polyisoprene)

Synthesis of Double-Dynamic Materials

Polyurethane Polyaddition of Polybutadiene and Hexamethylene-1,6-diisocyanate ***(PBD CTL0)***

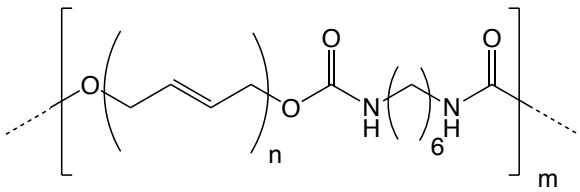

In a 2-neck round bottomed flask, hydroxyl-functionalised polybutadiene Polyvest™ (4.0 g, 0.8 mmol) was purged of air by three vacuum/argon cycles. Chloroform (20 mL) was then added and the solution stirred to homogeneity. To the stirred solution, 1,6-hexamethylene diisocyanate (0.26 mL, 1.6 mmol) and dibutyltin dilaurate (2 drops) were added and the resulting solution stirred to homogeneity. The solution was then pipetted into a Teflon® mould and allowed to evaporate in an atmosphere of chloroform overnight, before post-curing at 50 ºC under vacuum for 5 hours.

*Polyurethane Polyaddition of Polybutadiene and Diisocyanate-Funcitonalised Ureidopyrimidinone (**PBD CTL1 UPy**)*

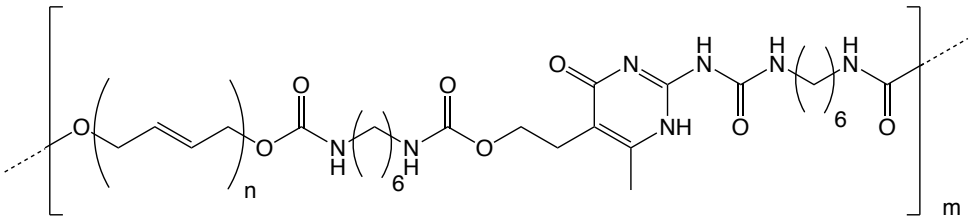

In a 2-neck round-bottom flask, hydroxyl-functionalised polybutadiene Polyvest® (2.0 g, 0.4 mmol) was purged of air, by three vacuum/argon cycles before dissolution in chloroform (10 mL). In a separate flask, diisocyanate-functionalised ureidopyrimidinone (**5**) (404 mg, 0.8 mmol) was added and purged of air by three vacuum/argon cycles before dissolution in chloroform (10 mL). The solution of **5** was then added to the polymer solution and the resulting mixture was stirred to homogeneity before addition of dibutyltin dilaurate (2 drops).

The solution was then pipetted into a Teflon® mould and allowed to evaporate in an atmosphere of chloroform overnight, before post-curing at 50 ºC under vacuum for 5 hours.

*Polyimine Polycondensation of Amine-Functionalised Polybutadiene and Diialdehyde-Funcitonalised Hexane (**PBD CTL1 IMI**)*

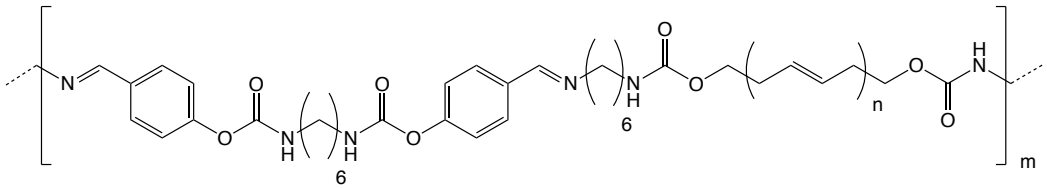

In a 2-neck round-bottom flask, amine-functionalised polybutadiene Polyvest® (2.5 g, 0.5 mmol) was purged of air, by three vacuum/argon cycles before dissolution in chloroform (10 mL). In a separate flask, the dialdehyde-functionalised hexane derivative (**6**) (412 mg, 1.0 mmol) was added and purged of air by three vacuum/argon cycles before dissolution in chloroform (10 mL). The solution of **6** was then added to the polymer solution the resulting mixture was and stirred to homogeneity.

The solution was then pipetted into a Teflon® mould and allowed to evaporate in an atmosphere of chloroform overnight, before post-curing at 50 ºC under vacuum for 5 hours.

*Polyimine Polycondensation of Amine-Functionalised Polybutadiene and Diialdehyde-Funcitonalised Ureidopyrimidinone (**DOUBLE DYNAMIC**)*

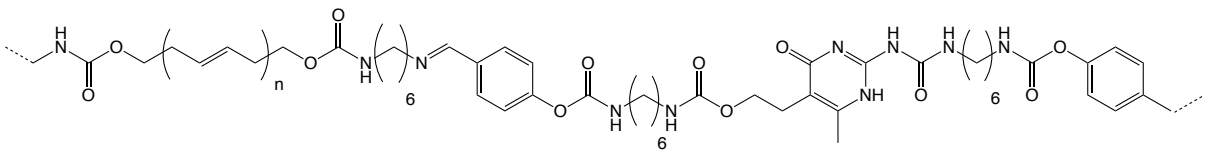

In a three-necked round bottom flask, amine-modified polybutadiene (2 g, 0.4 mmol) was added and purged of air by three vacuum/argon cycles, before addition of chloroform (5

mL). In a separate flask, dialdehyde-functionalised ureidopyrimidinone (**5**) (600 mg, 0.8 mmol) was dissolved in chloroform (5 mL) and added *via* syringe to the stirred polybutadiene solution.

The resulting solution was then pipetted into a Teflon® mould and allowed to evaporate in a saturated atmosphere of chloroform, before post-curing at 50 ºC under vacuum for 5 hours.

Polyurethane Polyaddition of Polybutadiene and Hexamethylene-1,6-diisocyanate ***(PBD TP CTL0)***

A similar procedure as was used to produce **PBD CTL0**, at the same scale, was used to produce **PBD TP CTL0**. The procedures differed in the time between mixing of the reagents and pipetting into the mould. For **PBD TP CTL0** the reaction solution was stirred overnight at room temperature, before pipetting into the Teflon® mould.

*Polyurethane Polyaddition of Polybutadiene and Diisocyanate-Functionalised Ureidopyrimidinone (**PBD TP CTL1 UPy**)*

The same procedure and scale as was used to produce **PBD CTL1 UPy** was used to produce **PBD TP CTL1 UPy**.

*Polyimine Polycondensation of Amine-Functionalised Polybutadiene and Diialdehyde-Funcitonalised Hexane (**PBD TP CTL1 IMI**)*

A similar procedure as was used to produce **PBD CTL1 IMI**, at the same scale, was used to produce **PBD TP CTL1 IMI**. The procedures differed in the time between mixing of the reagents and pipetting into the mould. For **PBD TP CTL1 IMI** the reaction solution was stirred overnight at room temperature, before pipetting into the Teflon® mould.

*Polyimine Polycondensation of Amine-Functionalised Polybutadiene and Diialdehyde-Functionalised Ureidopyrimidinone (**DOUBLE DYNAMIC TP**)*

The same procedure and scale as was used to produce **PBD CTL1 UPy**, was used to produce **PBD TP CTL1 UPy**.

Supplementary Data

Stress/Strain

PBD CTL0

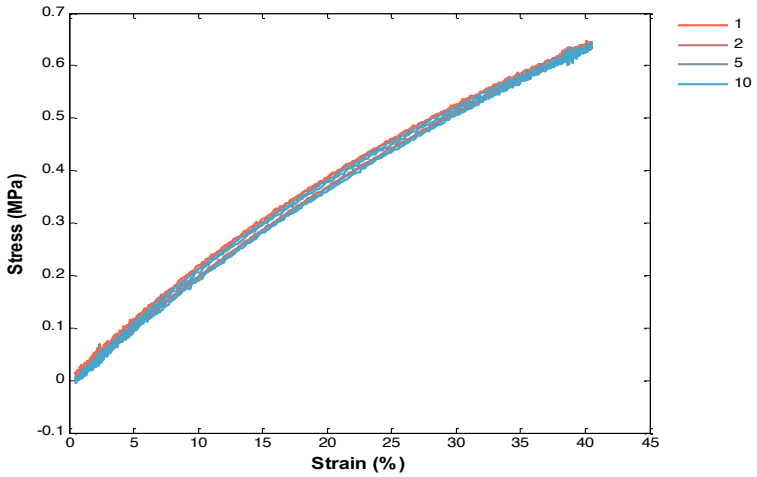

*Figure 98 – Stress/strain cycles for **PBD CTL0** 10 mHz - 1st, 2nd, 5th and 10th cycle*

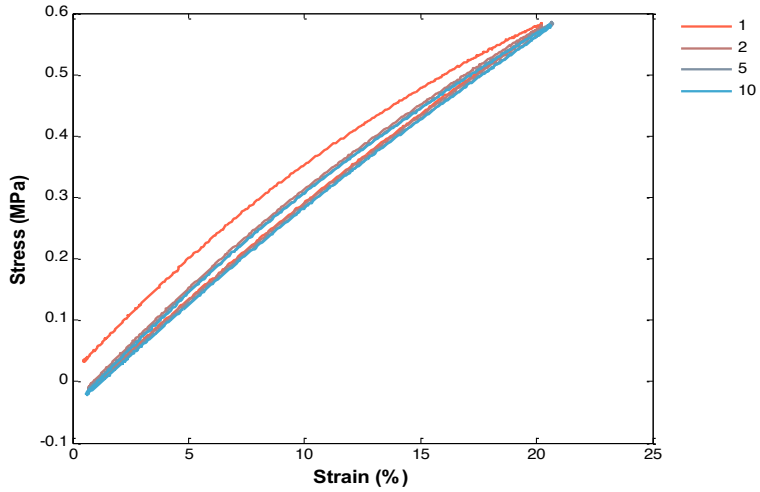

*Figure 99 – Stress/strain cycles for **PBD CTL0** 100 mHz - 1st, 2nd, 5th and 10th cycle*

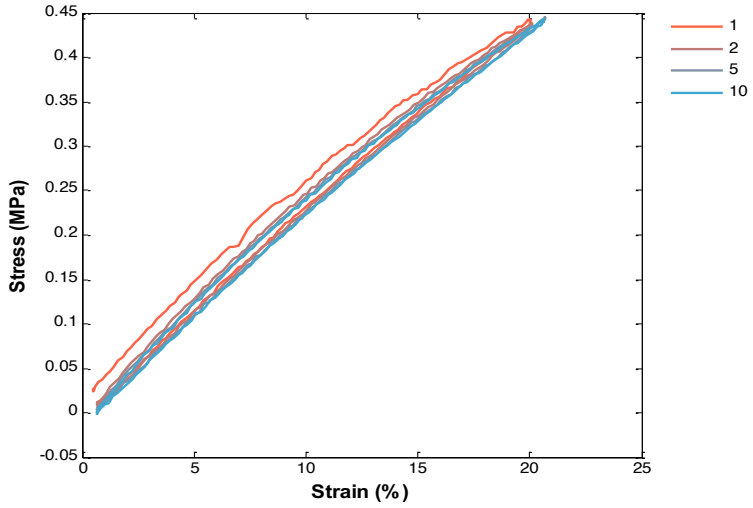

*Figure 100 – Stress/strain cycles for **PBD CTL0** 1000 mHz - 1st, 2nd, 5th and 10th cycle*

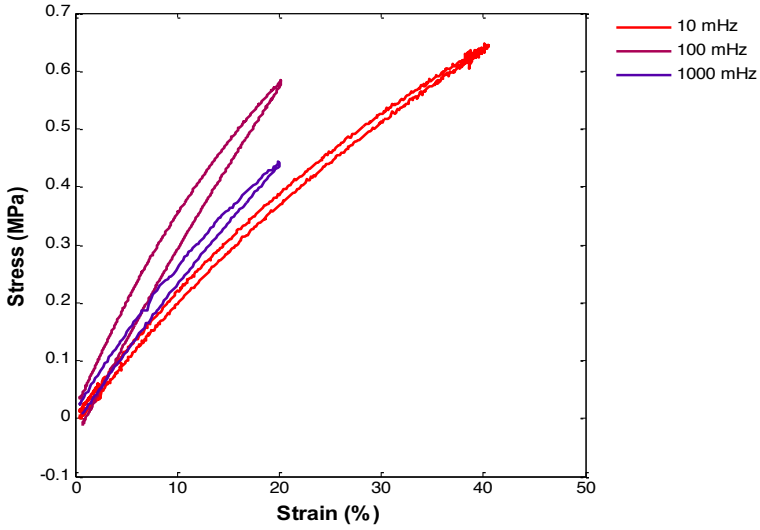

*Figure 101 – Stress/strain cycles for **PBD CTL0** at 10, 100 and 1000 mHz – 1st cycle*

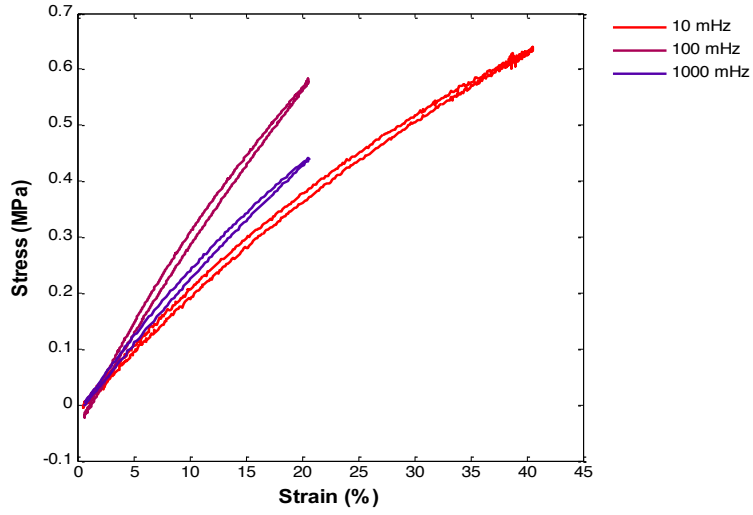

*Figure 102 – Stress/strain cycles for **PBD CTL0** at 10, 100 and 1000 mHz – 10th cycle*

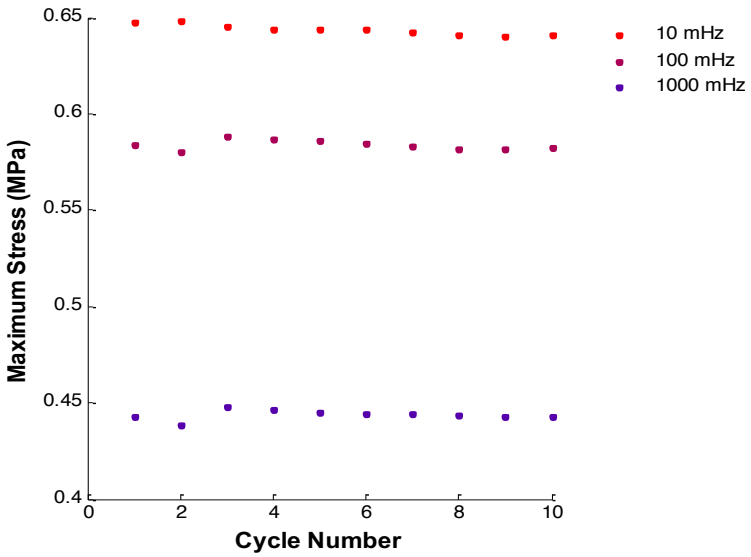

*Figure 103 – Maximum stress from stress/strain cycles of **PBD CTL0** at 10, 100 and 1000 mHz*

PBD CTL1 UPy

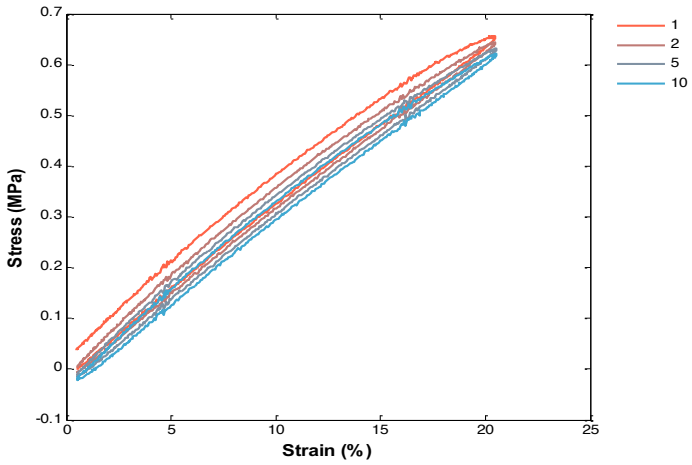

*Figure 104– Stress/strain cycles for **PBD CTL1 UPy** 10 mHz - 1st, 2nd, 5th and 10th cycle*

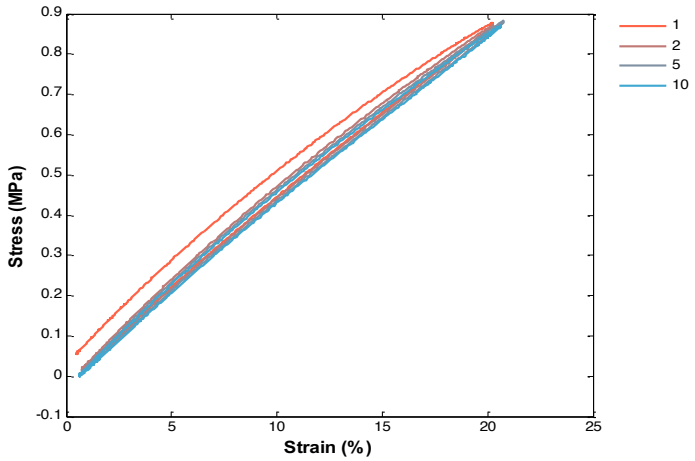

*Figure 105 –Stress/strain cycles for **PBD CTL1 UPy** 100 mHz - 1st, 2nd, 5th and 10th cycle*

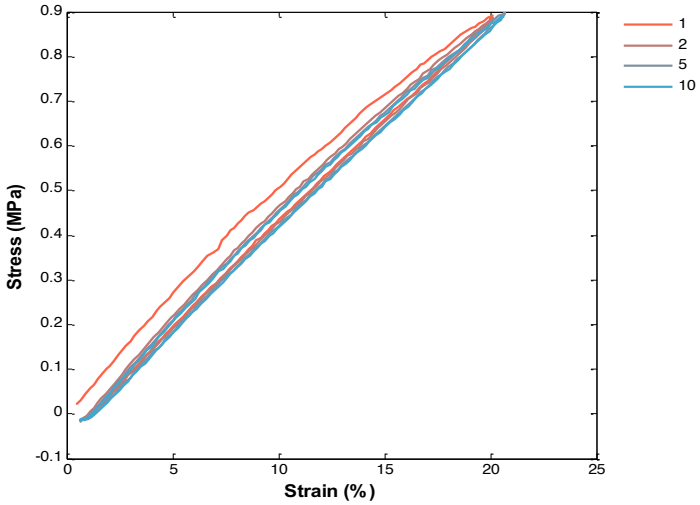

*Figure 106 – Stress/strain cycles for **PBD CTL1 UPy** 1000 mHz - 1st, 2nd, 5th and 10th cycle*

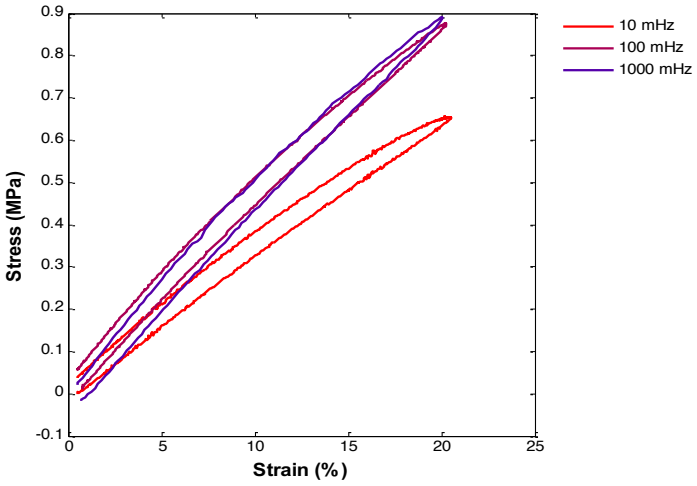

*Figure 107 – Stress/strain cycles for **PBD CTL1 UPy** at 10, 100 and 1000 mHz – 1st cycle*

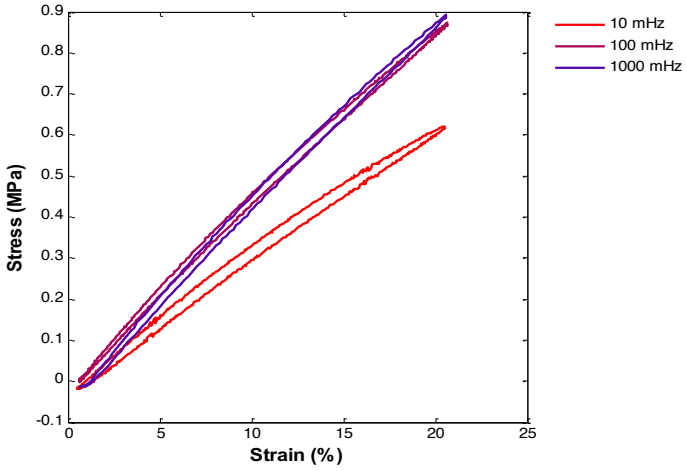

*Figure 108 – Stress/strain cycles for **PBD CTL1 UPy** at 10, 100 and 1000 mHz – 10th cycle*

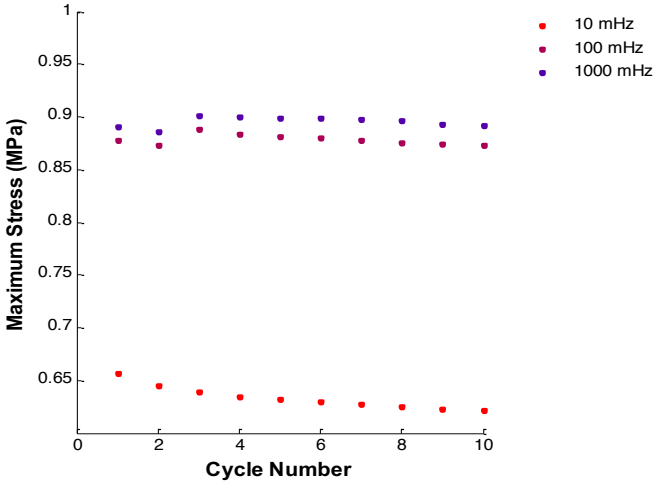

*Figure 109 – Maximum stress from stress/strain cycles of **PBD CTL1 UPy** at 10, 100 and 1000 mHz*

PBD CTL1 IMI

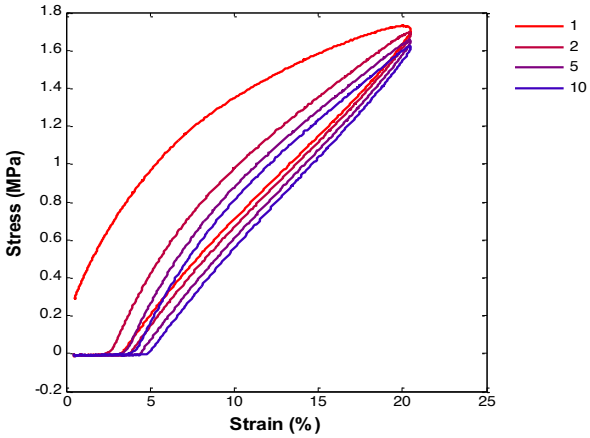

*Figure 110 – Stress/strain cycles for **PBD CTL1 IMI** 100 mHz - 1st, 2nd, 5th and 10th cycle*

DOUBLE DYNAMIC

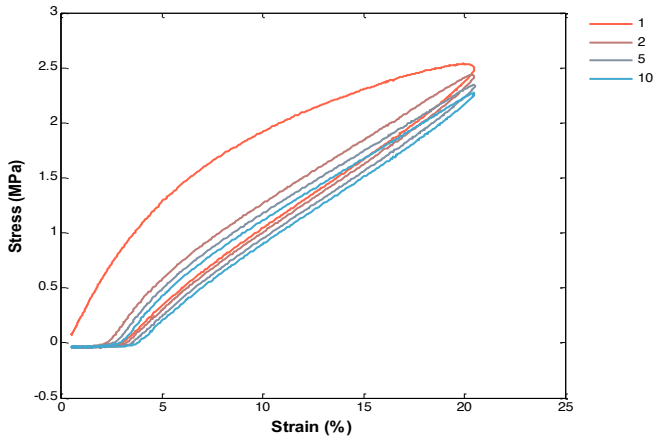

*Figure 111 – Stress/strain cycles for **DOUBLE DYNAMIC** 10 mHz - 1st, 2nd, 5th and 10th cycle*

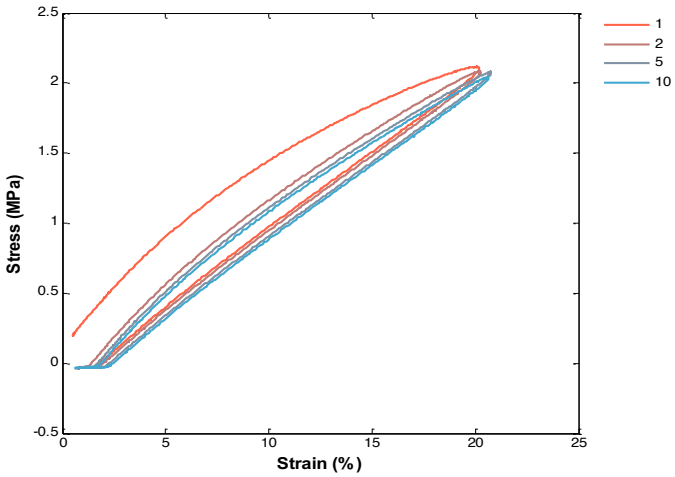

*Figure 112 – Stress/strain cycles for **DOUBLE DYNAMIC** 100 mHz - 1st, 2nd, 5th and 10th cycle*

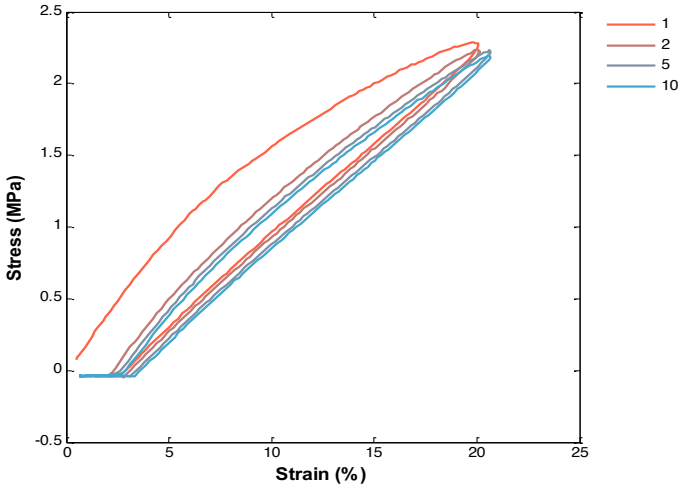

*Figure 113 – Stress/strain cycles for **DOUBLE DYNAMIC** 1000 mHz - 1st, 2nd, 5th and 10th cycle*

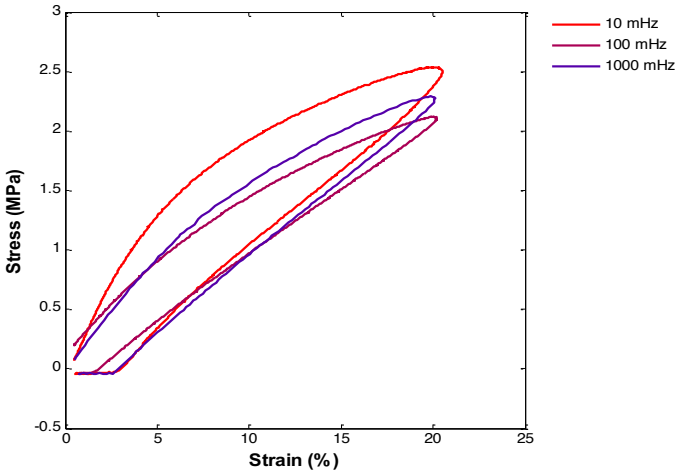

*Figure 114 – Stress/strain cycles for **DOUBLE DYMAMIC** at 10, 100 and 1000 mHz – 1st cycle*

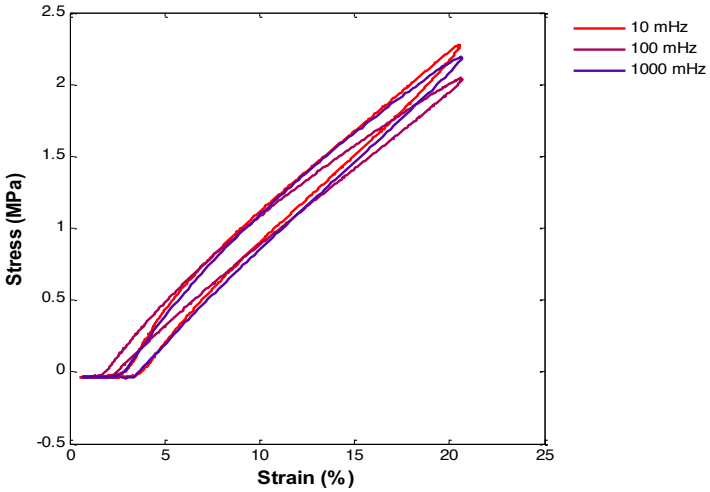

*Figure 115 – Stress/strain cycles for **DOUBLE DYNAMIC** at 10, 100 and 1000 mHz – 10th cycle*

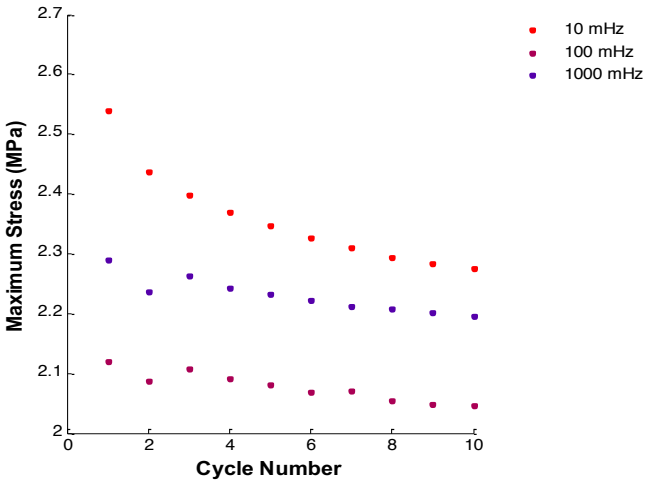

*Figure 116 – Maximum stress from stress/strain cycles of **DOUBLE DYNAMIC** at 10, 100 and 1000 mHz*

Stress/Strain Comparisons

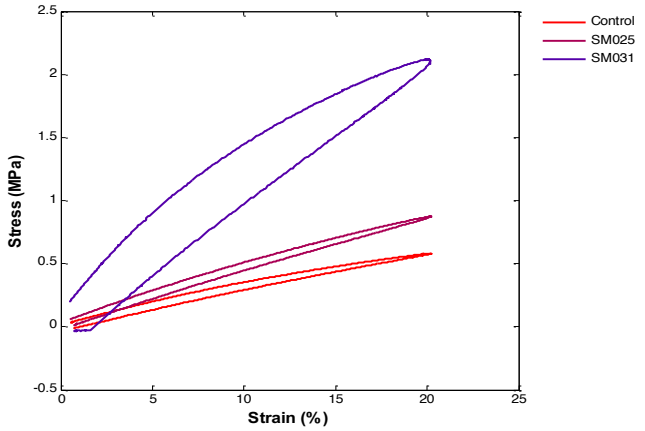

*Figure 117 – Stress/strain cycle comparisons for **PBD CTL0** (red-control), **PBD CTL1 UPy** (pruple-SM025) and **DOUBLE DYNAMIC** (blue-SM031) – 1st cycle at 100 mHz*

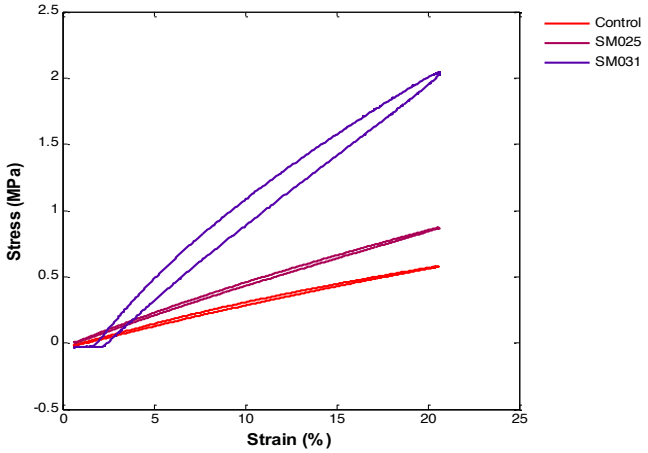

*Figure 118 – Stress/strain cycle comparisons for **PBD CTL0** (red-control), **PBD CTL1 UPy** (pruple-SM025) and **DOUBLE DYNAMIC** (blue-SM031) – 10th cycle at 100 mHz*

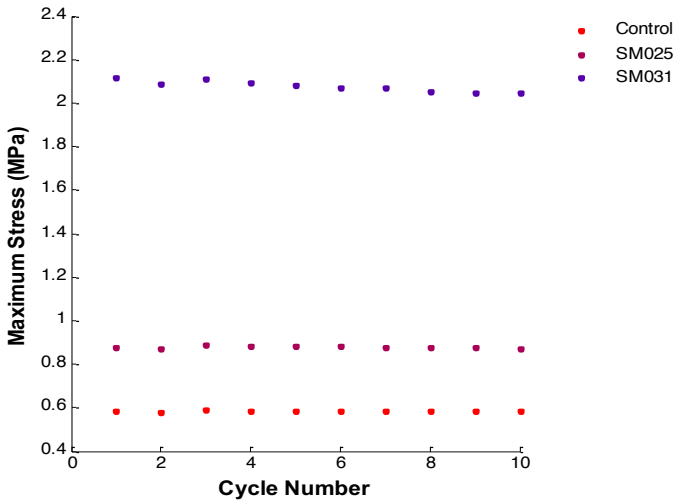

*Figure 119 – Maximum stress from stress/strain cycles versus cycle number for 10 cycles for **PBD CTL0** (red-control), **PBD CTL1 UPy** (pruple-SM025) and **DOUBLE DYNAMIC** (blue-SM031) at 100 mHz*

Elongation Until Break

PBD CTL0

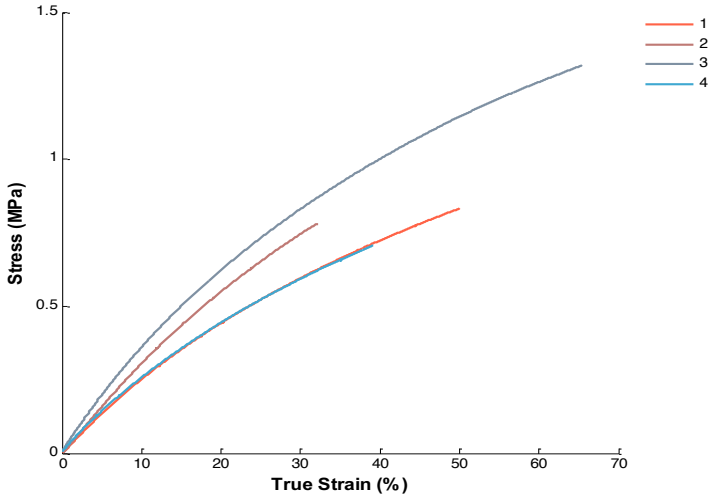

*Figure 120 – Stress versus True Strain for **PBD CTL0***

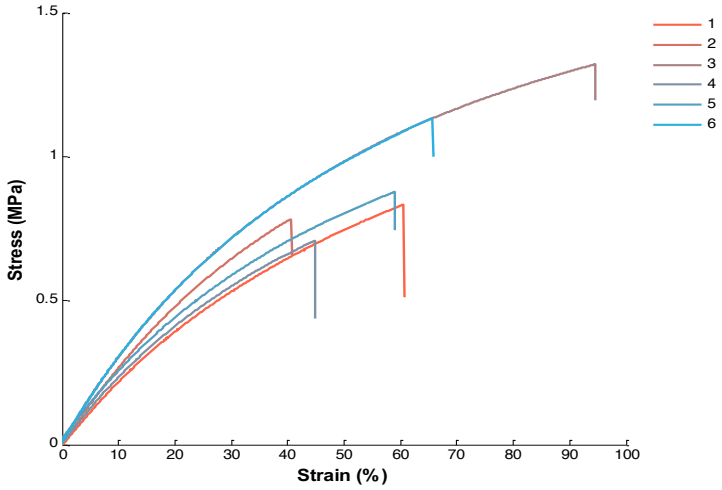

*Figure 121 -– Stress versus engineering strain for **PBD CTL0***

PBD CTL1 UPy

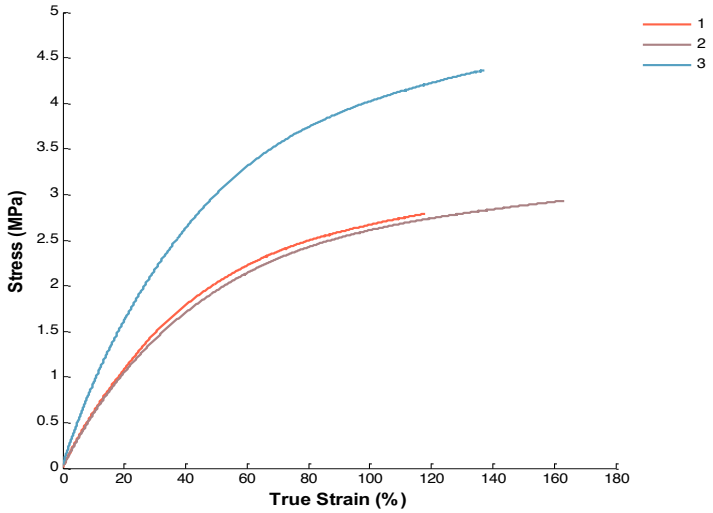

*Figure 122 –Stress versus True Strain for **PBD CTL1 UPy***

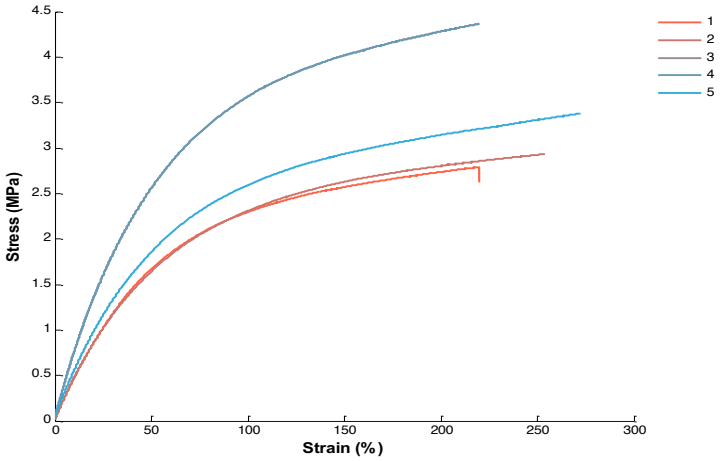

*Figure 123 – Stress versus engineering strain for **PBD CTL1 UPy***

DOUBLE DYNAMIC

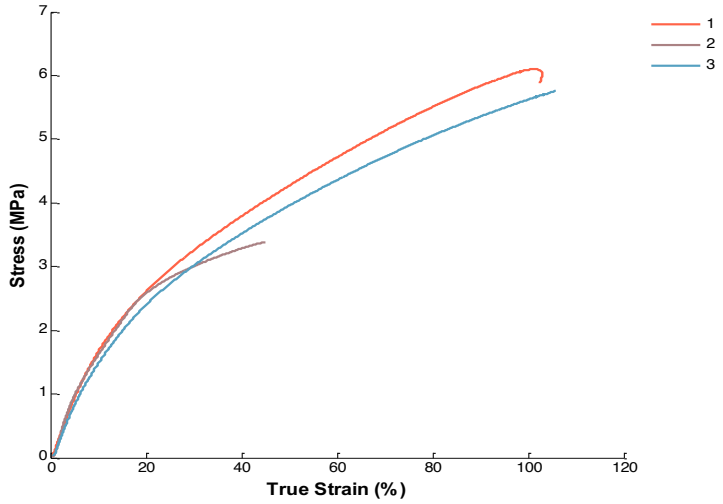

*Figure 124 – Stress versus True Strain for **DOUBLE DYNAMIC***

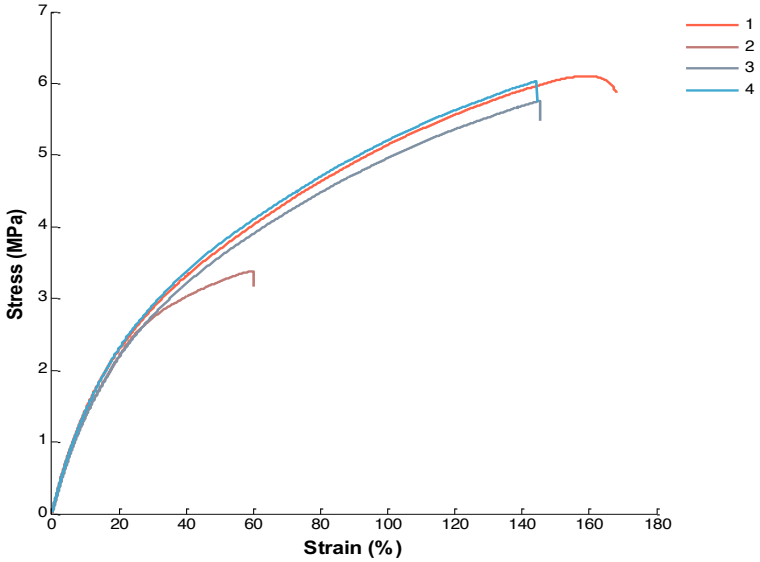

*Figure 125 – Stress versus engineering strain for **DOUBLE DYNAMIC***

Stress Relaxation

PBD CTL1 UPy

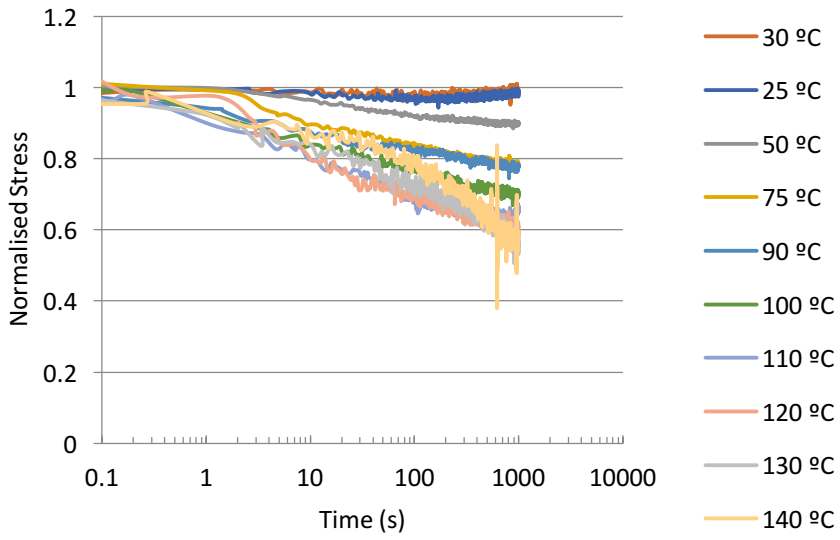

*Figure 126 – Stress relaxation of **PBD CTL1 UPy** between a temperature range of 30 to 140 ºC*

PBD CTL1 IMI

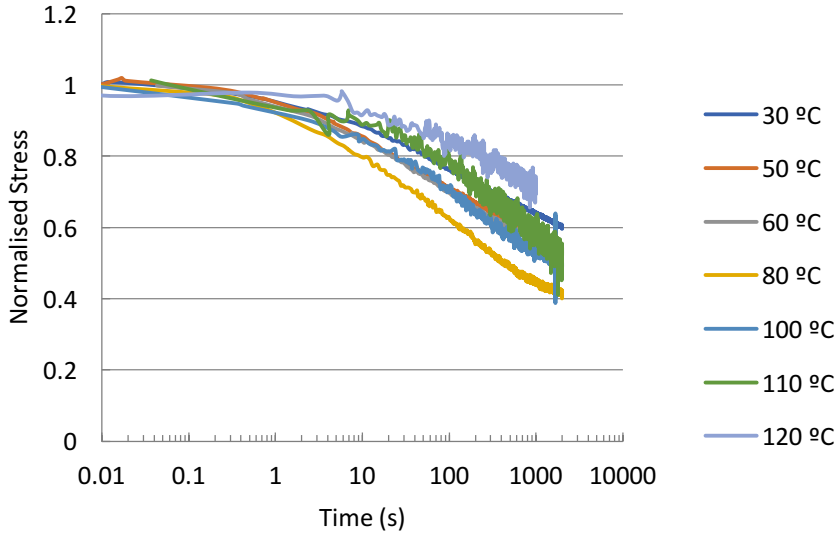

*Figure 127 – Stress relaxation of **PBD CTL2 IMI** between a temperature range of 30 to 120 ºC*

Résumé en Français

Introduction

Les propriétés physiques des matériaux sont déterminées par leur composition chimique. Pour les polymères, les propriétés physiques des plastiques produits sont régies par les facteurs clés suivants : composition du squelette polymère, degrés de polymérisation et de réticulation, cristallinité. Au cours des dernières années, des liaisons de réticulations covalentes dynamiques ont été envisagées comme alternative aux liaisons covalentes irréversibles rencontrées dans les matériaux thermodurcissables classiques.[1] Idéalement, ces matériaux réticulés de manière réversible (Réseaux Covalents Dynamiques ou RCD) pourraient présenter une robustesse aux contraintes physiques similaire aux thermodurcissables conventionnels, mais avec des avantages de réajustement, de recyclage et de réparation, et pouvant surmonter ainsi des problèmes industriels majeurs dans ce domaine (Figure 1).[2–4]

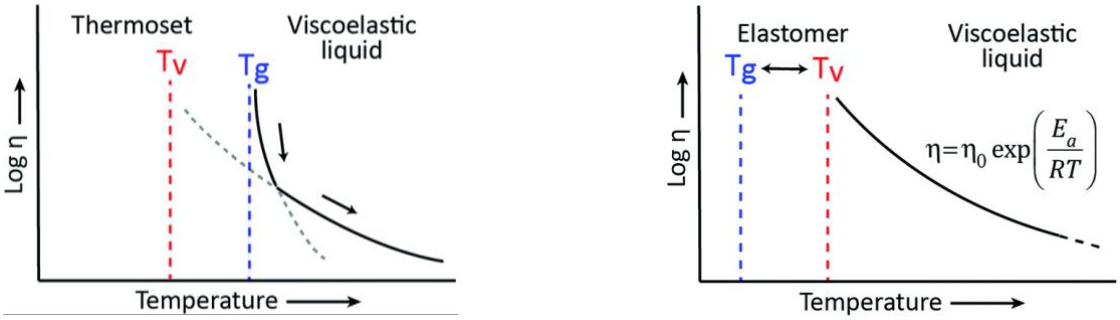

Figure 1 – Graphes illustrant l'évolution de la viscosité de réseaux covalents dynamiques suivant le modèle a) Arrhenius ou b) WLF.

Un inconvénient toujours observé jusqu'ici dans ces RCD est la cinétique lente de l'échange dynamique qui doit donner lieu à ces nouvelles propriétés plastiques et, par conséquent, le chimiste n'a qu'une capacité limitée à contrôler et adapter ces nouvelles propriétés aux applications. Le contrôle cinétique de la dynamique du réseau a déjà été permis par dopage avec un catalyseur supplémentaire ou en utilisant des réactions d'échange qui sont rapides à température ambiante[5]. Cependant, ces solutions ne sont pas idéales car elles nécessitent l'utilisation d'une quantité importante de catalyseur et des températures élevées et/ou, dans certains cas, une déformation peut se produire aux températures d'utilisation. Pour accélérer les processus d'échange, l'utilisation de liaisons supramoléculaires peut également être envisagée. Dans ce cas des phénomènes d'autoréparation rapides sont observés. Cependant, les matériaux mettant en jeu ces liaisons comme unités de réticulation ont tendance à ne pas résister aux contraintes physiques, tout en se comportant comme des thermoplastiques et, par conséquent, à rapidement perdre leur intégrité structurelle.[6]

Dans notre travail de thèse, nous nous sommes proposé d'élaborer un nouveau type de matériau polyuréthane pour les revêtements d'étanchéité incorporant des fragments de reconnaissance supramoléculaire au sein d'un réseau covalent dynamique, combinant ainsi les avantages de l'échange cinétique rapide entre les liaisons supramoléculaires et la force d'un réseau covalent. Nous avons postulé que l'introduction de fragments associés par reconnaissance supramoléculaire dans ce matériau permettrait un échange chimique initial rapide, fournissant une structure potentiellement adhésive et autoréparable, renforcée par des échanges covalents plus forts permettant de conservé une intégrité mécanique jusqu'à de hautes température. Nous avons ainsi envisagé que les nouveaux matériaux soient élastomères à température ambiante, affichant un comportement élastique malléable caractéristique, qu'ils soient auto-cicatrisant après un dommage, et qu'ils puissent être solubles et recyclables dans des conditions appropriées tout en restant stables dans les conditions d'utilisation. La réactivité au stimuli nécessaires pour activer les dynamiques caractéristiques (ici exposition à la chaleur ou à un milieu acide) a été évaluée, ainsi que la caractérisation physique des matériaux dans une large gamme de températures.

Le nouveau réseau à double dynamique a été conçu avec trois caractéristiques principales : 1) un long bloc mou de polymères téléchéliques présentant des propriétés d'élastomère, 2) un bloc dur contenant un fragment permettant l'auto-assemblage supramoléculaire et contenu dans 3) un réseau de nœuds de réticulation covalents réversibles (Figure 2). Pour le bloc mou, le polybutadiène a été sélectionné en raison de sa grande élasticité, de sa disponibilité commerciale et de son coût très faible. Pour le bloc dur, un motif à liaisons hydrogène basé sur l'unité ureidopyrimidinone a été sélectionné en raison des constantes d'association élevées associées ($K \approx 10^6\ M^{-1}$)[7] et de sa nature auto-complémentaire. Enfin, la liaison imine a été choisie afin de permettre la création d'un réseau covalent dynamique pouvant être formé sans catalyseur, et dont l'échange ne peut se produire qu'à des températures suffisamment éloignées des températures d'utilisation.

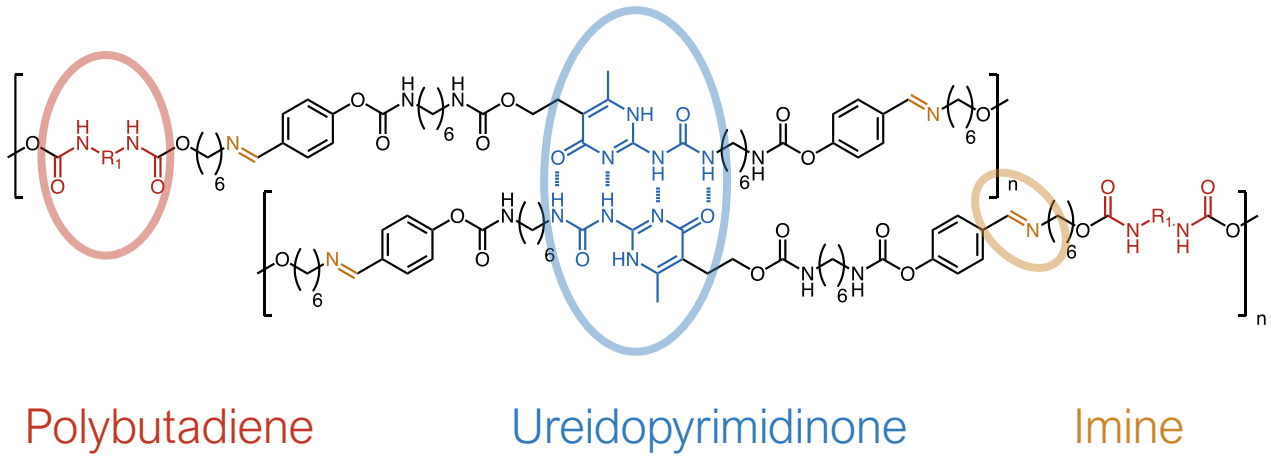

*Figure 2 – Schéma conduisant au polymère **1** qui comprend un bloc mou (rouge), un bloc dur (bleu) et un agent de réticulation covalent dynamique (jaune)*

Résultats et Discussions

Synthèse

La synthèse du polymère **1** a été réalisée à l'échelle de la dizaine de grammes à partir de composés commerciaux et a nécessité la formation de deux composés intermédiaires (Figure 3).

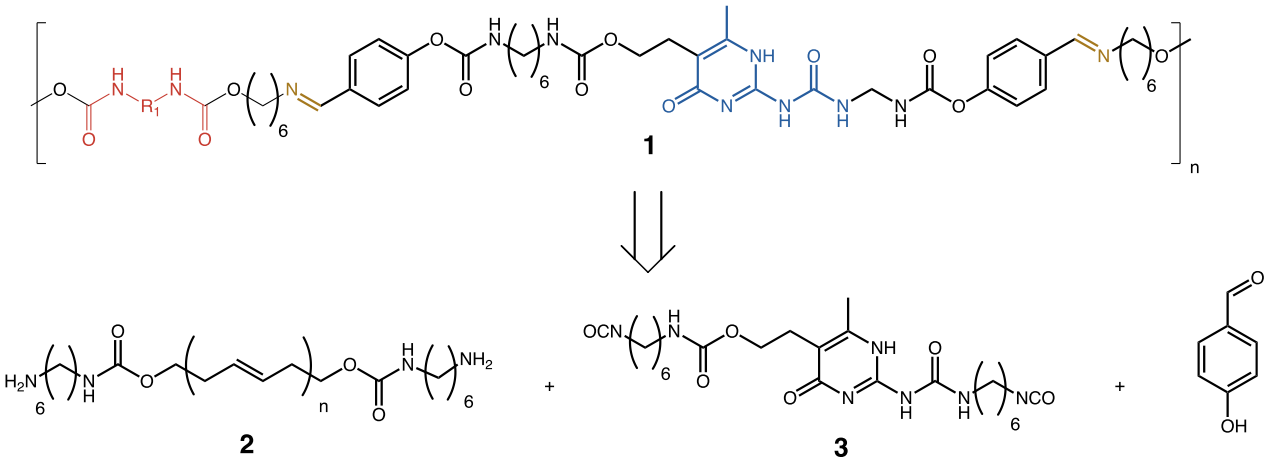

*Figure 3 – Schéma rétrosynthétique conduisant au polymère **1** qui comprend un bloc mou (rouge), un bloc dur (bleu) et un agent de réticulation covalent dynamique (jaune), à partir du polybutadiène bis-amine **2**, d'une uréidopyrimidinone bis-isocyanate **3** et du 4-hydroxybenzaldehyde.*

Le polybutadiène fonctionnalisé par des amines (Pré-Polymère **2**) a été obtenu en deux étapes à partir de polybutadiène bis-alcool (Polyvest EP HT®, M_n ~ 5000, PDI ~ 2, DF ~ 2,4). Ce pré-polymère a ensuite été couplé avec une nouvelle uréidopyrimidinone fonctionnalisée par des aldéhydes et obtenue en une étape à partir de la molécule **3** et du 4-hydroxybenzaldehyde.[8] Cette réaction de polymérisation par polycondensation a été effectuée sur des pré-polymères de masse 2K, comme cela est fréquemment réalisé dans le cas de la polymérisation du polyuréthane. Le pré-polymère **2** et l'agent de réticulation ont été séparément dissous dans des solvants organiques avant d'être mélangés. La solution résultante a été directement transférée dans un moule puis laissée à évaporer lentement avant d'être post-durcie à 50 °C sous vide. Trois matériaux de contrôle ont également été synthétisés afin d'évaluer avec précision l'origine chimique des propriétés physiques de **1**, comme cela est discuté plus en détail dans la suite de ce résumé (Figure 4). Tout d'abord, un polymère de contrôle **4** à base de polyuréthane et ne comprenant pas de fragments dynamiques a été obtenu en une étape à partir du polybutadiène bis-alcool (Polyvest EP HT®) et du 1,6-hexaméthylènediisocyanate (HDI), en présence d'un catalyseur organométallique, le dilaurate de di-*n*-butylétain (DBDTL). Ensuite, un polymère témoin **5** contenant uniquement l'unité de reconnaissance supramoléculaire a été synthétisé à partir du polybutadiène bis-alcool (Polyvest EP HT®) et de la molécule **3**. Enfin, le polymère de contrôle **6** ne contenant que des liaisons imines covalentes dynamiques a été synthétisé par polycondensation de pré-polymère **2** avec un agent de

réticulation fonctionnalisé par deux aldéhydes et obtenu en une étape à partir du 1,6-hexaméthylènediisocyanate et du 4-hydroxybenzaldéhyde.

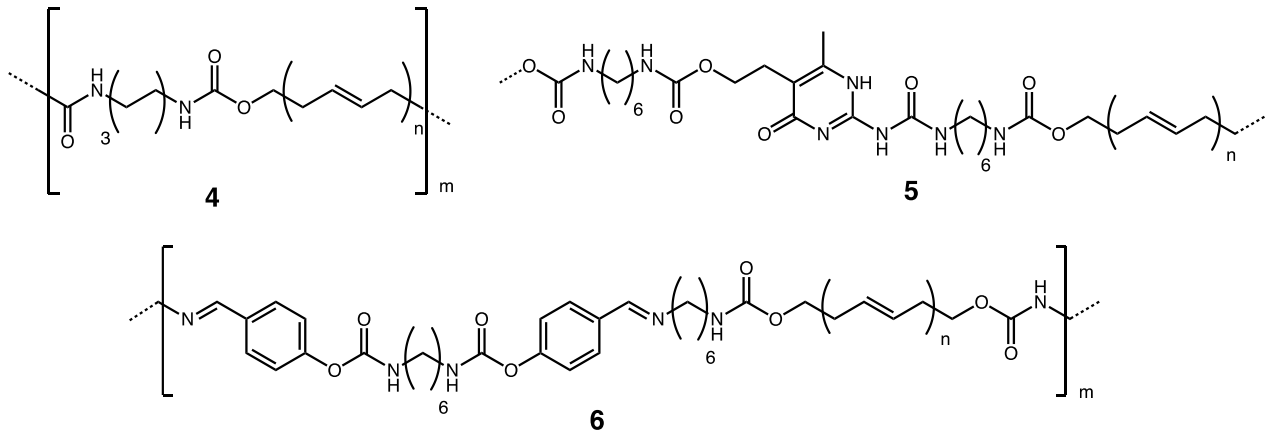

Figure 4 – Polymères de contrôle 4 ne contenant aucune unité dynamique, 5 ne contenant que les unites uréidopyrimidinone et 6 ne contenant que les liaisons imines covalentes dynamiques.

Caractérisations Physiques

En vue de leur utilisation dans des conditions extérieures extrêmes, la caractérisation physique de chaque matériau a été effectuée à des températures allant de -100 ºC à +150 ºC. Par calorimétrie différentielle à balayage (DSC, Figure 5a) et analyse thermomécanique dynamique (DMTA, Figure 9a), la température de transition vitreuse (T_v) mesurée pour tous les polymères est similaire (~–74 ºC), indiquant que le composant déterminant pour ce paramètre est le bloc mou. Tous les échantillons ont également montré une bonne stabilité thermique: au-dessus de 200 ºC, l'analyse thermogravimétrique ATG (Figure 5b) montre un léger phénomène de perte de masse pour les matériaux **1**, **5** et **6** avant l'événement principal de perte de masse commun à tous les matériaux et apparaissant vers 465 °C. Le premier phénomène pourrait être considéré comme une conséquence de la présence de fragments dynamiques alors que le dernier pourrait être dû à la dégradation du squelette du polybutadiène.

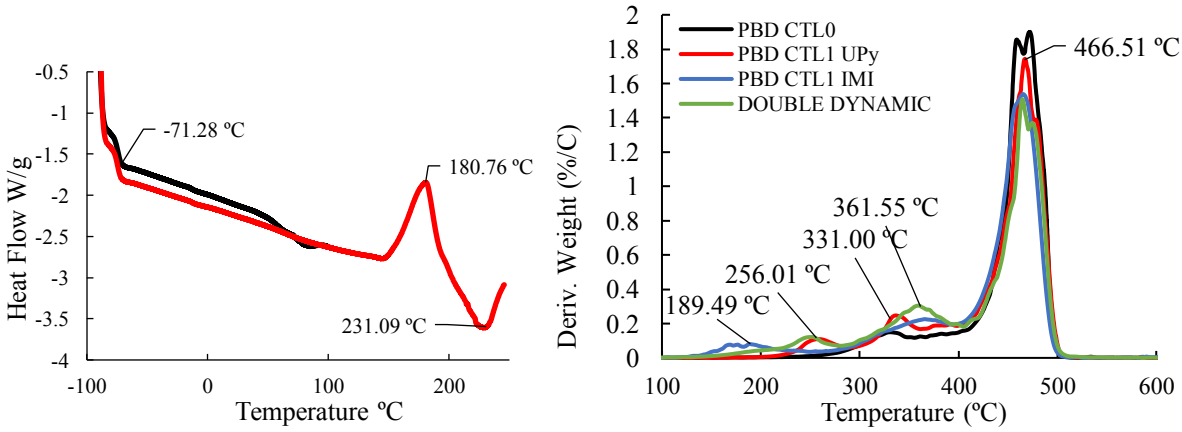

Figure 5 – a) Spectre DSC du polymère 1, (Tg at~ -74 ºC); b) Spectre ATG du polymère 1

L'analyse de la composition microstructurale des matériaux a été réalisée par l'utilisation de la diffraction des rayons X aux petits et grands angles. Avec WAXS (Figure 6a), des réflexions correspondant à des objets à l'échelle de 1,045 Å-1 (3,5 Å) ont été observées, probablement en raison de la présence de liaisons hydrogène dans les matériaux. Comme tous les matériaux comprennent des liaisons uréthane dans le squelette du polymère, l'observation d'objets à cette échelle était attendue. Des interactions de liaison hydrogène entre les fragments d'uréidopyrimidinone sont également susceptibles d'être observées dans les réflexions à cette échelle. Des objets légèrement plus grands à 0,546 $Å^{-1}$ et 0,467 $Å^{-1}$ (11,51 Å et 13,45 Å, respectivement) ont également été observés dans les matériaux à base d'imine, probablement en raison de la présence d'agrégations des fragments imine aromatiques. Avec SAXS (Figure 6b), une large réflexion à 0,046 $Å^{-1}$ avec un épaulement à 0,102 $Å^{-1}$ (137 Å et 62 Å, respectivement) a été observée, en accord étroit avec la littérature, résultant de l'agrégation de blocs durs de polyuréthane d'ordre supérieur. Les réflexions observées à partir des matériaux à base d'imine étaient différentes de 0,049 $Å^{-1}$ et 0,067 $Å^{-1}$ (128 Å et 49 Å, respectivement), probablement en raison de l'agrégation de blocs durs différents. Il est postulé que les matériaux à base d'imine peuvent comprendre des blocs durs ordonnés en nanofibres.

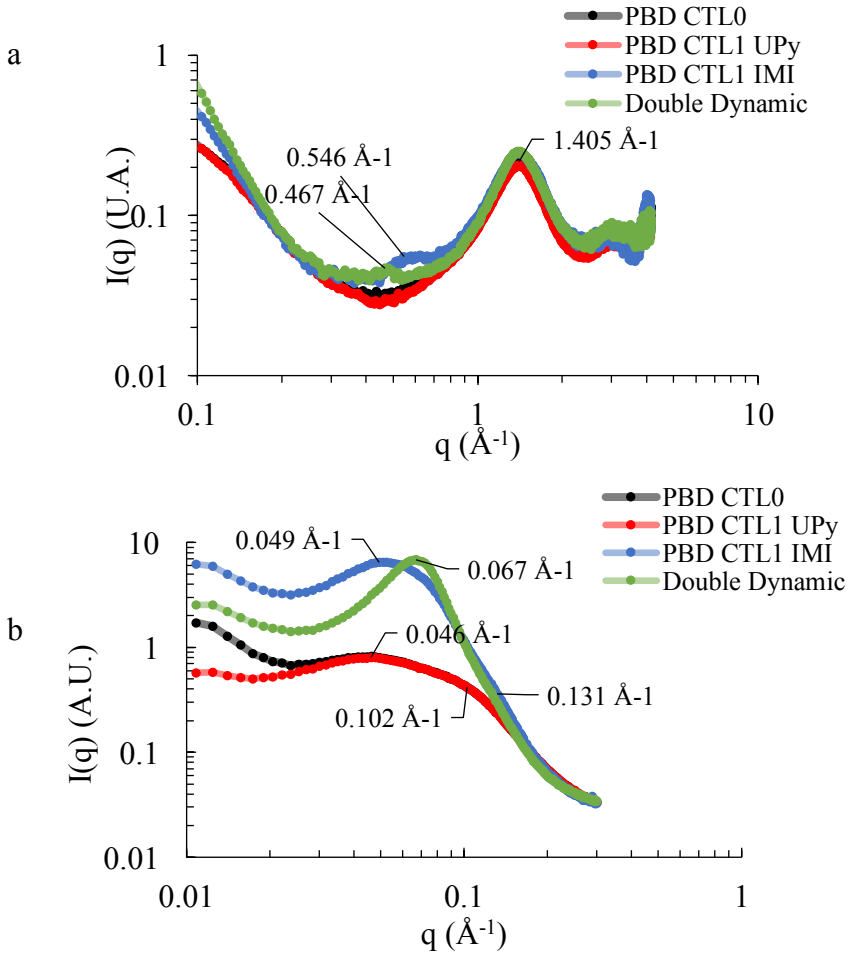

Figure 6 – a) Spectres de diffusion de rayons X à grand angle (WAXS) de chaque matériau thermodurcissable pour une gamme q comprise entre 0,1 et 4 $Å^{-1}$; b) Spectres de diffraction des rayons X aux petits angles (SAXS) de chaque matériau pour une gamme q comprise entre 0,01 et 0,20 $Å^{-1}$

La présence de microcristallinité dans les blocs durs des matériaux **1** et **5**, comme proposé ci-dessus, pourrait également expliquer la valeur supérieure de E' à toutes les températures par rapport à **4** et **6**. Les uréthanes aromatiques (en **4** et **6**) présentent une ressemblance frappante avec d'autres blocs durs cristallisables reportés par Hayes *et al* (Figure 7a).[9]

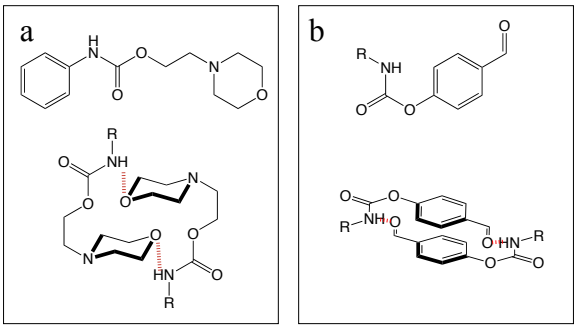

Figure 7 – a) Représentation schématique de l'empilement cristallin des groupements uréthane/morpholine ;[9] b. Représentation schématique de l'empilement cristallin proposé pour le bloc dur

Nous proposons que deux ordres de cristallinité soient présents: un ordre lié à l'auto-assemblage des uréidopyrimidinones provoqué par les liaisons H complémentaires et un second ordre lié à l'empilement aromatique assisté par liaisons H (Figure 7b). Les tentatives de cristallisation du composé **6** n'ont pas encore donné de monocristaux de qualité suffisante pour la diffraction des rayons X, mais la dissolution de **4** dans le DMF conduit à la formation d'un gel (Figure 8a). Ce gel a été analysé par microscopie électronique à transmission (TEM, Figure 8b) révélant la présence de longues fibres supramoléculaires, probablement en raison de cette cristallinité de second ordre.

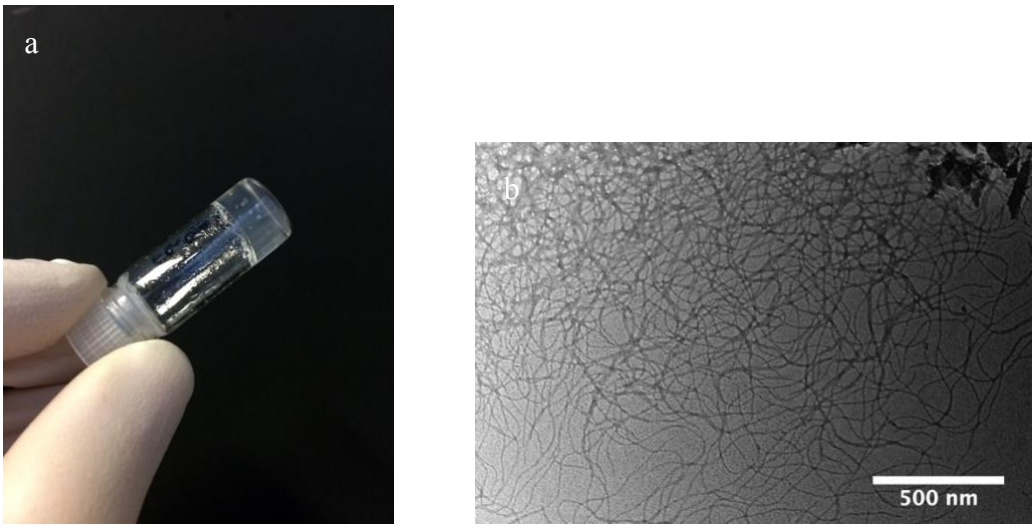

Figure 8 – a) Image du gel formé par la molécule 4 dans la DMF; b) Image TEM de ce gel.

Lorsque la température augmente depuis la T_v (–74 ºC) jusqu'à température ambiante (Figure 9a), une diminution nette du module de stockage (E ') (mesuré par DMTA) est observée pour les matériaux **4** et **5**, qui atteint alors un plateau entre –20 °C et 80 °C. Une diminution beaucoup plus linéaire de E' est observée pour les matériaux **1** et **6**, avec un plateau plus difficilement définissable. Le plateau observé pour **4** et **5** correspond au plateau caoutchoutique couramment observé dans les matériaux élastomères. Le comportement linéaire qui n'était pas forcément attendu pour **1** et **6** pourrait s'expliquer par les réactions d'échange entre les nœuds de réticulation de l'imine, perturbant ainsi le plateau caoutchoutique. Une autre explication pourrait être la présence d'une certaine microcristallinité (Figure 7a and b), induite par la présence de liaisons uréthanes aromatiques qui pourraient se rompre lorsque la température augmente. Au-delà de ~110 ºC, cependant, un comportement plus visqueux a été observé pour les matériaux **1**, **5** et **6**, ce qui est probablement dû à l'échange dynamique entre les unités réversibles covalentes ou entre les motifs supramoléculaires, qui doivent être activés à ces températures.

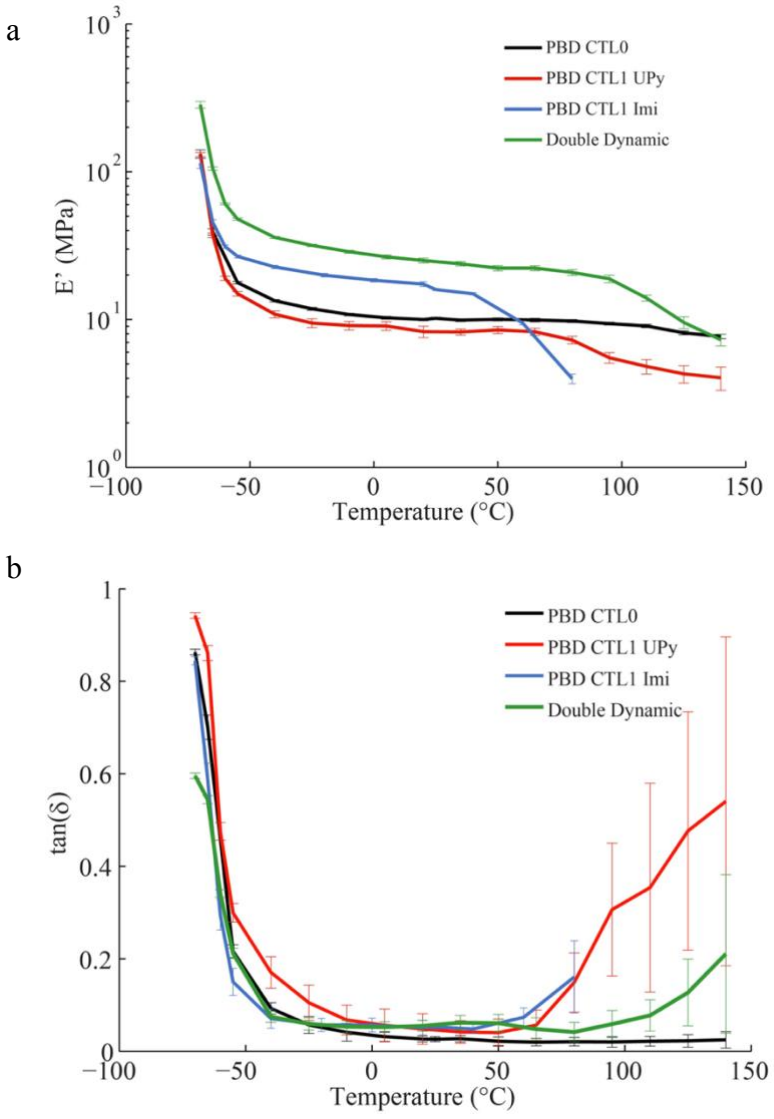

*Figure 9 – a) Evolution du module de stockage (MPa) en fonction de la température pour les polymères **1**, **4**, **5** et **6** (mesures par DMTA);b) Evolution de la tangente delta en fonction de la température pour les polymères **1**, **4**, **5** et **6** (mesures par DMTA)*

Les limites physiques des matériaux ont également été testées à température ambiante en allongement jusqu'à la rupture (0.4 $\%s^{-1}$) (Figure 10a). Les matériaux contenant des chimies dynamiques (**1** et **5**) ont résisté en étirement jusqu'à 100% de plus et jusqu'à 6 fois plus de stress que le contrôle ne contenant aucune fonctionnalité dynamique (matériau **4**). La présence de groupements aromatiques au niveau des blocs durs des matériaux **1** et **5** par rapport aux blocs aliphatiques du matériau **4** pourrait être responsable d'une meilleure répartition de ces blocs durs, augmentant ainsi la résistance au stress. Des cycles de 20% de tension (à une fréquence de 1 Hz) ont été appliqués aux matériaux pour évaluer leur réponse à des charges de forte contrainte successives (Figure 10b). La plasticité du matériau **1** est évidente et importante, ce qui est un comportement rare pour un matériau thermodurcissable chimiquement réticulé. On peut raisonnablement penser que ce comportement se produit en raison de la rupture de la cristallinité du second ordre liée à l'uréthane aromatique (comme suggéré ci-dessus) et qui n'est pas récupéré lors des cycles de stress ultérieurs.

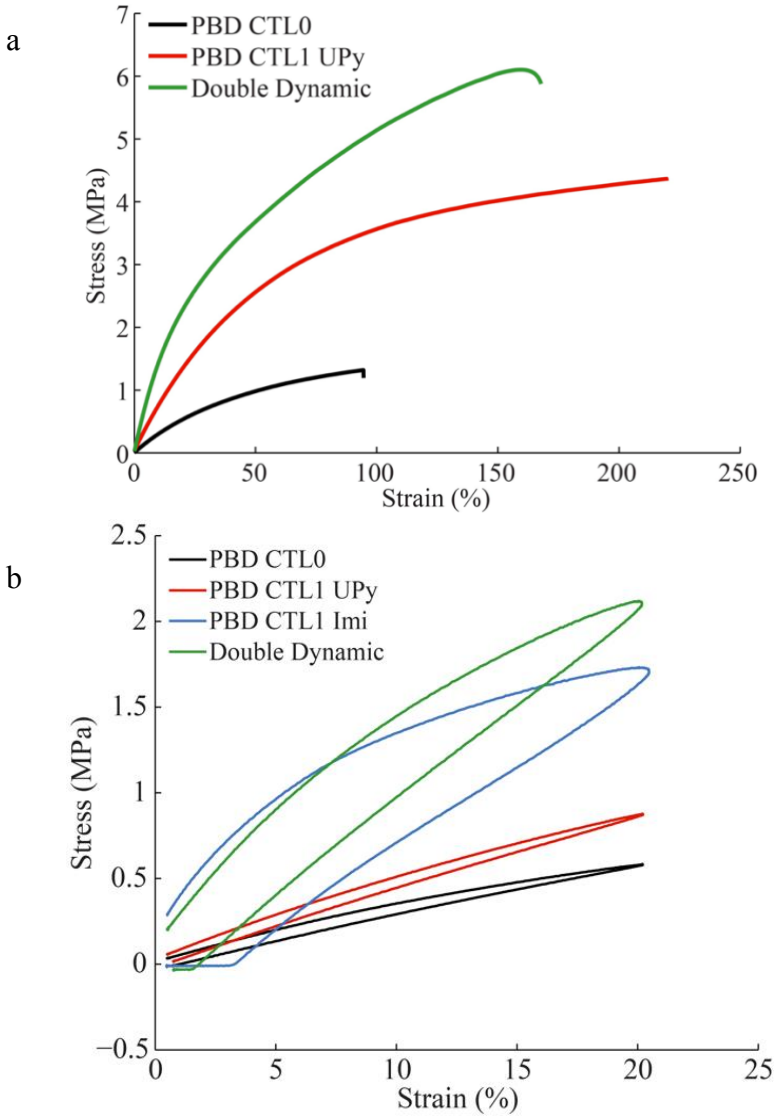

Figure 10 – a) Etudes d'élongation jusqu'à la rupture de matériaux obtenus à partir des polymères 4, 5 et 1 (0.4 %s-1); b) Cycles Stress/Contrainte pour les matériaux obtenus à partir des polymères 4, 5 et 1 (1 Hz)

Le comportement dynamique à des températures élevées a été étudié par microscopie optique. Le matériau **1** a été partiellement entaillé, puis un bref chauffage (5 minutes) localisé sur la coupe a été appliqué, conduisant à la réparation de celle-ci (Figure 11). Cette réponse aux dommages, induite par la chaleur, n'a été observée que dans les réseaux covalents dynamiques **1** et **6**, ce qui suggère fortement que la présence des liaisons imines aux points de réticulation est responsable de cet effet auto-cicatrisant. L'auto-cicatrisation des matériaux n'est pas observée à température ambiante, l'échange dynamique entre les liaisons imine dépendant fortement de la température.

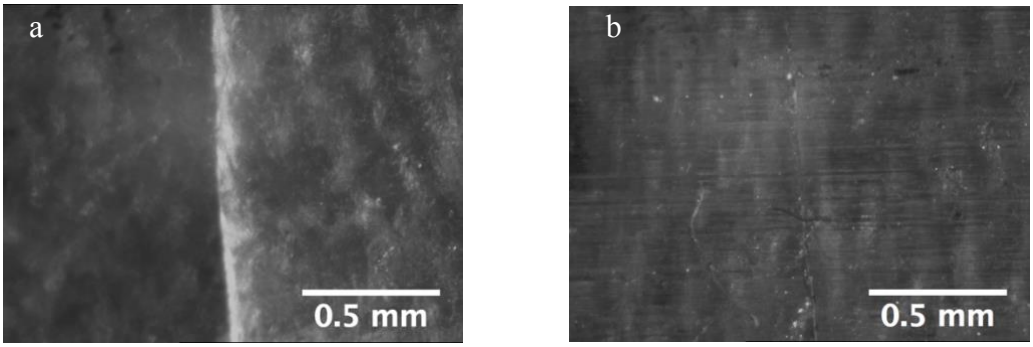

Figure 11 – Images de microscopie optique démontrant le caractère auto-réparant du polymère 1

Enfin, la recyclabilité et la réutilisation des matériaux ont été étudiées. En raison de la nature labile de la liaison imine dans des conditions acides aqueuses, le matériau **1** a d'abord été immergé dans du THF avant l'ajout de 5% en masse de TFA dans l'eau (Figure 12a–d). En présence de THF, un gonflement de **1** est observé, tout en maintenant son intégrité structurelle. Après l'ajout de TFA, le matériau commence immédiatement à se dissoudre puis, après 20 minutes d'agitation, il ne reste qu'une solution visqueuse. La solution a ensuite été pipetée dans un moule ouvert et laissée à sécher à température ambiante puis sous vide à 50 ºC (4 heures), résultant en un matériau élastomère transparent et d'apparence identique à l'original. Les études poussées concernant les propriétés mécaniques de ce matériau recyclé sont actuellement en cours.

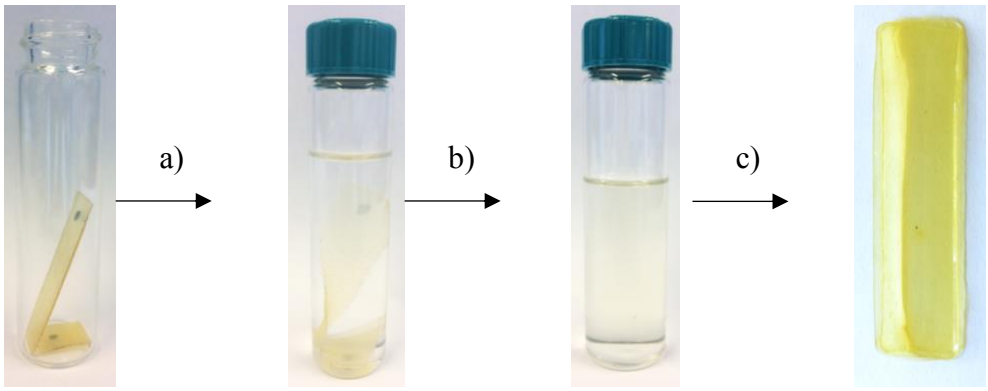

Figure 12 – a) Matériau obtenu à partir du polymère 1; b) Gonflement dans le THF; c) Dissolution de ce matériau après l'ajout de 5 wt% de TFA dans 0.2 mL d'eau; d) Reformation du matériau 1 après évaporation

Extension aux Thermoplastiques

Afin de mieux comprendre comment la réticulation par liaison hydrogène influence les propriétés physiques du matériau résultant, un squelette de polybutadiène mieux défini a été utilisé. Dans ce polybutadiène, le degré de fonctionnalité était ≤ 2, garantissant que les matériaux résultants n'étaient pas réticulés chimiquement (mais seulement physiquement).

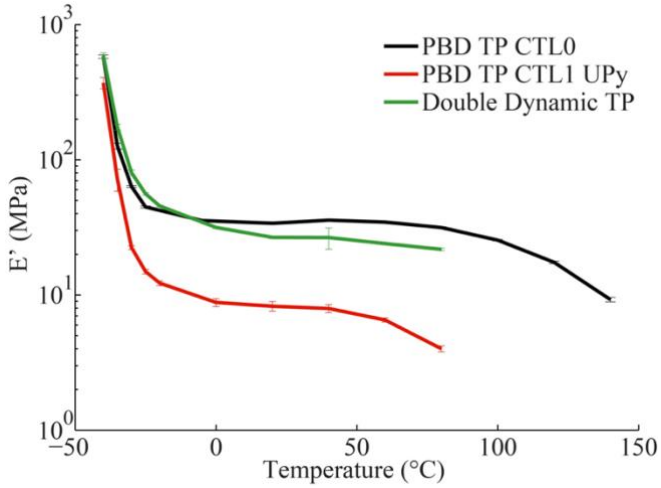

Figure 13 – Evolution du module de stockage en fonction de la température, obtenue par analyse mécanique dynamique, pour chaque matériau thermoplastique entre une fréquence de 1Hz –70 et 150 ºC

En raison de la nature thermoplastique des matériaux, une transition de fusion distincte a été observée, par DMTA (Figure 13), à des températures supérieures à 80 ºC. Cette transition de masse fondue observée dans les matériaux thermoplastiques résultait de la rupture induite par la chaleur des liaisons H, et s'est révélée se produire à des températures considérablement plus basses par rapport aux matériaux thermodurcissables renforcés par des liaisons imines.

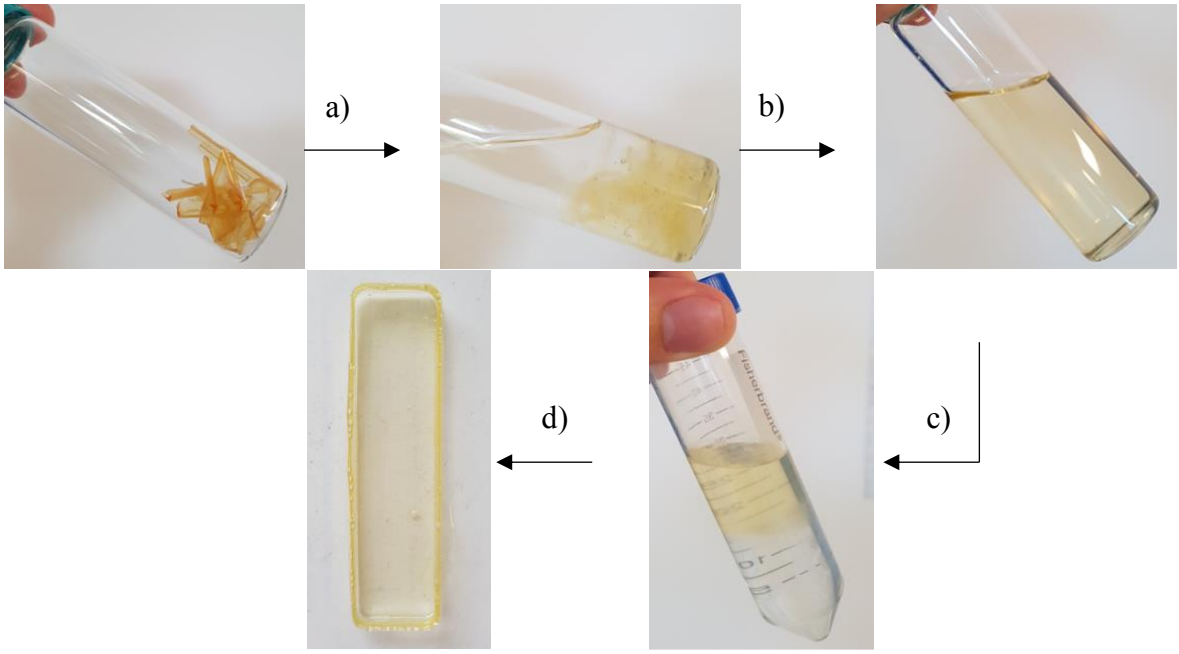

Figure 14 – Images détaillant la solubilité de TP DOUBLE DYNAMIQUE dans un solvant organique acidifié, et la capacité de reformer les élastomères en vrac après neutralisation et évaporation: a) ajouter du THF, b) ajouter 10% en poids de TFA (aq), c) neutraliser avec $NaHCO_3$ (aq), d) s'évaporer dans l'air

La recyclabilité du solvant du matériau thermoplastique a été évaluée avec une approche légèrement modifiée. Dans cette approche, le matériau thermoplastique à double dynamique est gonflé dans du THF, comme précédemment (Figure 14a). Cela a ensuite été suivi de l'addition d'acide organique, en dissolvant complètement le matériau (Figure 14b). Le THF a ensuite été neutralisé avec $NaHCO_3$, après séparation de phase induite par addition de saumure (Figure 14c). La phase organique neutralisée a ensuite été pipetée et évaporée dans un moule (Figure 14d), en formant un matériau ayant des propriétés physiques qualitativement similaires à celles de la matière vierge.

Conclusion générale

En conclusion, un matériau contenant deux fonctionnalités dynamiques (ureido-pyrimidinone et imine) a été synthétisé et ses caractéristiques physiques par rapport à des matériaux analogues avec des quantités variables ou même en l'absence de composants dynamiques ont été étudiées. Il a été constaté que le matériau à double dynamique était plus rigide, avec un module d'élasticité considérablement plus élevé, et qu'il pouvait supporter des charges de contraintes jusqu'à six fois plus élevées que les matériaux témoins. Avec une exposition à des températures plus élevées, le matériau présente des propriétés plus visqueuses et peut se guérir automatiquement en cas de rupture. Le matériau peut être dissous dans un mélange THF/H_2O contenant 5% en masse de TFA pour être recyclé et reformé. La combinaison de l'ensemble de ces propriétés au sein d'un même matériau nous semble unique dans la littérature à ce jour.

Ce travail fait en ce moment l'objet d'un dépôt de brevet avec la SATT Conectus et son contenu doit pour l'instant rester confidentiel.

Références

1. Montarnal, D., Capelot, M., Tournilhac, F. & Leibler, L. Silica-Like Malleable Materials from Permanent Organic Networks. *Science (80-.).* **334,** 965–968 (2011).
2. Denissen, W., Winne, J. M. & Du Prez, F. E. Vitrimers: permanent organic networks with glass-like fluidity. *Chem. Sci.* **7,** 30–38 (2016).
3. Kloxin, C. J. & Bowman, C. N. Covalent adaptable networks: smart, reconfigurable and responsive network systems. *Chem. Soc. Rev.* **42,** 7161–73 (2013).
4. Imbernon, L. & Norvez, S. From landfilling to vitrimer chemistry in rubber life cycle. *Eur. Polym. J.* **82,** 347–376 (2015).
5. Denissen, W. *et al.* Chemical control of the viscoelastic properties of vinylogous urethane vitrimers. *Nat. Commun.* **8,** 14857 (2017).
6. Herbst, F., Döhler, D., Michael, P. & Binder, W. H. Self-healing polymers via supramolecular forces. *Macromolecular Rapid Communications* **34,** 203–220 (2013).
7. Sijbesma, R. P. Reversible Polymers Formed from Self-Complementary Monomers Using Quadruple Hydrogen Bonding. *Science (80-.).* **278,** 1601–1604 (1997).
8. Guo, M. *et al.* Tough stimuli-responsive supramolecular hydrogels with hydrogen-bonding network junctions. *J. Am. Chem. Soc.* **136,** 6969–6977 (2014).
9. Merino, D. H. *et al.* A systematic study of the effect of the hard end-group composition on the microphase separation, thermal and mechanical properties of supramolecular polyurethanes. *Polym. (United Kingdom)* **107,** 368–378 (2016).